

Universiteit
Leiden
The Netherlands

# The ins and outs of ligand binding to CCR2

Zweemer, A.J.M.

**Citation**
Zweemer, A. J. M. (2014, November 20). *The ins and outs of ligand binding to CCR2*. Retrieved from https://hdl.handle.net/1887/29763

| | |
|---|---|
| Version: | Corrected Publisher's Version |
| License: | Licence agreement concerning inclusion of doctoral thesis in the Institutional Repository of the University of Leiden |
| Downloaded from: | https://hdl.handle.net/1887/29763 |

**Note:** To cite this publication please use the final published version (if applicable).

Cover Page



Universiteit Leiden




The handle http://hdl.handle.net/1887/29763 holds various files of this Leiden University dissertation

**Author:** Zweemer, Annelien
**Title:** The ins and outs of ligand binding to CCR2
**Issue Date:** 2014-11-20

# The INS and OUTS of ligand binding to CCR2

**Annelien Jacomina Maria Zweemer**

The research described in this thesis was performed at the Division of Medicinal Chemistry of the Leiden Academic Centre for Drug Research, Leiden University (Leiden, The Netherlands). The research was part of the TI-Pharma initiative "Target residence time in translational drug research: the CCR2 chemokine receptor as a case in point" (Project number D1-301), in collaboration with Vertex Pharmaceuticals (San Diego, CA, USA) and the Vrije Universiteit Amsterdam (Amsterdam, The Netherlands).

This thesis was printed by Gildeprint (Enschede, The Netherlands).

The printing of this thesis was financially supported by PeproTech.

Cover design: Esmee Gramberg- www.annageemag.com

© Annelien Zweemer 2014. All rights reserved.
No part of this thesis may be reproduced in any form without the prior written permission of the holder of copyright.

# The INS and OUTS of ligand binding to CCR2

**Proefschrift**

ter verkrijging van
de graad van Doctor aan de Universiteit Leiden,
op gezag van Rector Magnificus prof. mr. C.J.J.M. Stolker,
volgens besluit van het College voor Promoties
te verdedigen op 20 november 2014
klokke 16:15 uur

door

**Annelien Jacomina Maria Zweemer**
geboren te Goes
in 1985

**Promotiecommissie**

| | |
|---|---|
| Promotor: | Prof. Dr. A.P. IJzerman |
| Co-Promotor: | Dr. L.H. Heitman |
| Overige Leden: | Prof. Dr. M.M. Rosenkilde |
| | Prof. Dr. B. van de Water |
| | Prof. Dr. J. Kuiper |
| | Prof. Dr. P.H. van de Graaf |

## Contents


| | | |
|---|---|---|
| Chapter 1 | General introduction | 7 |
| Chapter 2 | Bias in chemokine receptor signalling | 23 |
| Chapter 3 | Multiple binding sites for small molecule antagonists at the chemokine receptor CCR2 | 45 |
| Chapter 4 | Discovery and mapping of an intracellular antagonist binding site at the chemokine receptor CCR2 | 71 |
| Chapter 5 | Allosteric modulation of the chemokine receptor CCR2 by amiloride analogues and sodium ions | 97 |
| Chapter 6 | Structure-kinetics relationships – an overlooked parameter in hit-to-lead optimization: a case of cyclopentylamines as CCR2 antagonists | 121 |
| Chapter 7 | Conclusions and future perspectives | 143 |
| | Summary | 159 |
| | Samenvatting | 163 |
| | List of publications | 169 |
| | Curriculum Vitae | 173 |
| | Acknowledgements | 177 |

# Chapter 1

**General Introduction**

As long as human beings have recognized and suffered from disease, there has been a quest for cures and therapies. Historically, natural product extracts served as the main source of drugs. In the second half of the nineteenth century, the first isolation of biologically active molecules from these extracts succeeded, and soon after that the first synthesis of the pharmaceutical drug aspirin took place [1]. Due to enormous progress in all fields related to pharmaceutical sciences, the art of drug discovery has evolved greatly in the 20$^{th}$ and 21$^{st}$ century. We are now able to synthesize large chemical libraries of up to millions of synthetic small molecules, which can be screened against the target of interest in order to identify potential drug candidates [2]. As a consequence, it is not a surprise that for one particular target many different drug-like molecules are discovered. This is also the case for the chemokine receptor CCR2, a receptor that is involved in a large variety of diseases ranging from autoimmune and metabolic diseases to atherosclerosis and pain. Despite major efforts of the pharmaceutical industry and synthesis of many inhibitors, there is at this moment no clinically effective drug available that targets this receptor. In order to improve current drug candidates, one would benefit from understanding their mechanism of action at a molecular level, which is often incomplete in the current process of drug discovery. In this thesis we therefore zoom in at the molecular level of CCR2, and reveal novel insights in mechanisms of action of existing as well as novel drug-like molecules. These findings serve as a fundament for future drug discovery programs, and will be equally relevant for understanding the outcomes of current drug candidates in later stages of development.

In order to grasp the relevance of the research and the concepts that will be discussed in this thesis, first of all the world of G protein-coupled receptors (GPCRs) will be introduced, the protein family to which CCR2 belongs. The activation and inhibition of GPCRs will be outlined, as well as their role in physiology and disease. This brings us to the receptor of interest, CCR2, a member of the GPCR subfamily of chemokine receptors. Finally the current status of drug discovery targeting CCR2 will be addressed, followed by the outline of the aim and contents of this thesis.

## G protein-coupled receptors

### Classification and structure

GPCRs comprise the largest family of membrane receptors in mammalian cells; the human genome has been estimated to encode approximately 800 GPCRs [3]. GPCRs are located at the cell surface and transduce an extracellular signal into an intracellular response. They are

expressed in nearly all organs and tissues of the human body, and therefore they regulate a broad range of physiological processes. The structure of a GPCR consists of an extracellular N-terminus and an intracellular C-terminus with seven transmembrane-spanning α-helices, resulting in three extra- and intracellular loops (Fig. 1) [4]. The understanding of the 3D-conformational structure has substantially increased since attempts to crystallize GPCRs became more successful; we now have snapshots of at least 23 different GPCRs available at the time of writing of this introduction, including those for the chemokine receptors CXCR4 and CCR5 [5, 6]. According to the IUPHAR Committee on Receptor Nomenclature and Drug Classification, the superfamily of GPCRs is divided in six classes based on their functional similarity and sequence homology [7]. Each family generally shares over 25% sequence identity in the transmembrane core region, with specific sets of highly conserved residues and motifs. The largest and most studied subfamily is formed by the class A rhodopsin-like receptors, to which the chemokine receptors belong. The remaining classes are the class B secretin receptor family, class C metabotropic glutamate/pheromone receptors, class D fungal mating pheromone receptors, class E cyclic AMP receptors and class F frizzled/smoothened like receptors. In addition, for ~15% of all GPCRs the endogenous ligand is at present unknown, and therefore these receptors are accordingly named orphan GPCRs [7].

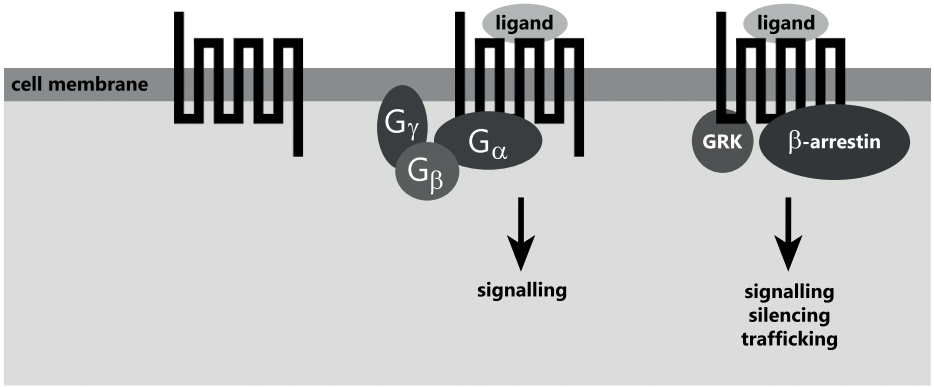



**Fig. 1**. Schematic representation of GPCRs embedded in the cell membrane. Upon ligand binding and receptor activation, signal transducing proteins like G proteins, GRKs and β-arrestins can bind at the intracellular side.

## GPCR signalling in health and disease

Upon activation due to ligand binding at the extracellular side of the GPCR, the receptor undergoes conformational changes that allow recruitment of intracellular signalling proteins (Fig. 1) [8]. These signalling proteins subsequently become activated and start a downstream

signal transduction cascade. Multiple types of signalling proteins have been associated with GPCRs, among which the family of G proteins is most ubiquitous and best characterised [9].

There are four members of the family of heterotrimeric G proteins, being $G_s$, $G_i$, $G_q$, $G_{12/13}$, which individually consist of a $G_\alpha$, $G_\beta$ and $G_\gamma$ subunit (Fig. 1) [10]. Activation of G proteins results in an exchange of guanosine diphosphate (GDP) for guanosine triphosphate (GTP) in the alpha subunit, which is followed by dissociation of the activated $G_\alpha$ and $G_{\beta\gamma}$ subunits. These subunits can activate a wide variety of signalling molecules, of which adenylyl cyclase (AC), the MAP kinase pathways and phospholipase C (PLC) are most prominent [11]. Second messengers, including cyclic AMP, inositol triphosphate and calcium ions, then turn on a range of effector systems to change the behavior of the cell, ranging from morphological changes and secretion of molecules, to the regulation of gene transcription.

Besides G proteins, GPCRs can bind and activate other cytosolic proteins such as G protein-coupled receptor kinases (GRKs) and β-arrestins (Fig. 1) [9]. GRKs and β-arrestins orchestrate GPCR activities at three different levels [12]. First of all they induce *silencing*, which is the functional uncoupling of the receptor from its G protein by a mechanism known as desensitisation. In addition they mediate receptor *trafficking*, characterized by receptor internalization, resensitisation and/or degradation. Finally, they can induce *signalling*, via the activation or inhibition of intracellular signalling pathways independently of heterotrimeric G proteins.

Together, these signalling proteins determine the response of a cell to an extracellular stimulant. Due to the great divergence in GPCRs this can vary from the regulation of the heart rate to the perception of odors and flavors. All of these processes are carefully fine-tuned, and therefore malfunctioning of any GPCR can result in severe diseases. Since GPCRs comprise a large protein-family, and are involved in the most prevalent disease areas including cancer, obesity, diabetes and cardiac dysfunction, approximately one third of the pharmaceuticals on the market today target these proteins [13].

## Ligands for G protein-coupled receptors

### Activation and inhibition of GPCRs

GPCRs are very flexible membrane proteins and their conformation varies from an inactive state (R) to several active states (R*) [14, 15]. The ratio between active and inactive states is dependent on the type of GPCR and its cellular environment. Some are naturally present with high proportions in an active state; these GPCRs signal without any ligand binding, a

phenomenon that is named 'constitutive activity' or 'basal activity' [16, 17]. The ratio between active and inactive states is affected by binding of ligands at the extracellular face of the GPCR. Agonist ligands preferentially bind to and stabilize the active state R* of a receptor, resulting in an increase in receptor activity and signalling (Fig. 2A+B). Some ligands behave as partial agonists; these ligands activate the receptor, but cannot elicit the maximum possible response that is induced by a full agonist (Fig. 2B). These partial agonists have been reported to stabilize a distinct conformational state of the receptor compared to full agonists [18, 19]. Others propose that partial agonists are able to dynamically bind with multiple orientations to a receptor, which results in active and inactive populations of receptors of which the ratio determines the level of the response [20]. Inverse agonists preferentially bind to the inactive state R and reduce the receptor activity (Fig. 2A+B) [21]. Again, a distinction can be made between full and partial inverse agonists [22, 23]. Neutral antagonists prevent GPCR activation, but bind equally well to active as well as inactive conformations, and therefore these ligands do not affect the basal activity of the receptor (Fig. 2A+B) [21].

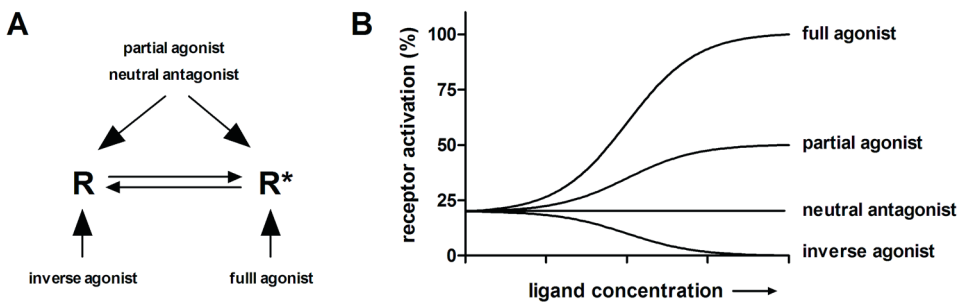



**Fig. 2.** (A) The preference of different ligands to bind to the inactive (R) and/or active (R*) receptor state. (B) Receptor activation upon binding of a full agonist, partial agonist, neutral antagonist or inverse agonist.

This classical view of receptor signalling has been refined during the past couple of years, since we began to appreciate that one GPCR is able to activate multiple signalling proteins, via different active states [15]. It is now evident that certain ligands are able to stabilize a specific active state of a GPCR, and the first structural basis for this phenomenon was recently reported for the serotonin 5-$HT_{1B/2B}$ and the $\beta_2$-adrenergic receptors [24, 25]. This can result in ligand-directed signalling via one specific pathway, named 'functional selectivity' or 'biased signalling' [26]. In extreme cases it might occur that a certain ligand for one GPCR is an agonist for signalling pathway A, while it behaves as an antagonist for signalling pathway B. This concept is also applicable to chemokine receptors and is therefore important to take into account during drug discovery, as will be further discussed in Chapter 2.

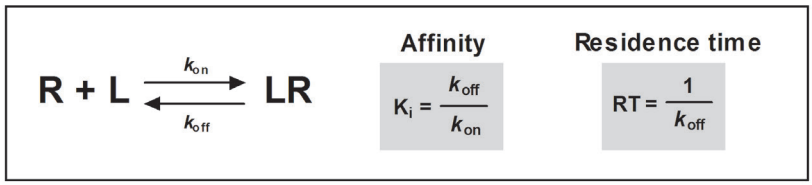
**Orthosteric and allosteric ligands**

The endogenous ligands for the GPCR superfamily are very diverse, ranging from peptide hormones, lipids and nucleotides to odorants and ions [7]. The binding site of these endogenous ligands is called the "orthosteric" binding site. Especially since the introduction of small molecule and peptide drugs, it was discovered that multiple ligand binding sites are present on GPCRs. If a ligand binds to the same binding site as the endogenous ligand, it is named an orthosteric ligand. In contrast, when it binds to a topographically distinct site from where the endogenous ligand binds, it is named an 'allosteric' ligand [27]. This term has been derived from the Greek word 'allo', which means 'other'. Allosteric ligands can exert a variety of effects at a functional level [28]. Allosteric agonists can activate GPCRs by themselves without the presence of any orthosteric ligand. In addition, since the allosteric site is different from the orthosteric site, a GPCR is in some cases able to simultaneously bind both orthosteric and allosteric ligands. Allosteric ligands are thereby able to alter the binding and/or signalling properties induced by the ligand at the orthosteric site and are accordingly named allosteric modulators, which can be further classified as allosteric enhancers (or positive allosteric modulators- PAMs) and allosteric inhibitors (or negative allosteric modulators – NAMs). Since the binding pocket of chemokine receptors is quite large and the size of synthetic drugs very small compared to the endogenous chemokine protein ligand, allosteric modes of action are often observed for this family of GPCRs [5, 29]. In this thesis two novel allosteric binding pockets were discovered, located within the core domain and at the intracellular side of CCR2, as described in Chapters 4 and 5.

**Ligand-receptor binding kinetics**

In order to activate or inhibit signalling events via a GPCR, a ligand first needs to bind to the receptor [30]. Both agonists and antagonists bind to the receptor with a certain association rate ($k_{on}$), followed by their release of binding from the receptor with dissociation rate $k_{off}$ (Scheme 1). The strength of binding is represented by the parameter $K_i$, which stands for the affinity of a ligand for its receptor, and is determined by the ratio $k_{off}/k_{on}$ (Scheme 1). This affinity can be easily measured in pharmacological assays, and drug discovery programs classically optimize this equilibrium parameter to end with high affinity ligands that are put forward in the drug development cycle. The affinity of a ligand is a very important measure, but next to that the concept of individually optimizing $k_{on}$ and $k_{off}$ has gained more and more attention during the last decade [31, 32]. Importantly, affinity is measured in a closed system (*in vitro*) at equilibrium, whereas in open systems like the human body (*in vivo*) the drug and target can have fluctuating concentrations [33]. This discrepancy may make equilibrium

measurements less appropriate to predict the effect of a drug *in vivo*. It would be better suited to additionally measure the lifetime of the drug-target complex, represented by the term 'residence time' that can be calculated as the reciprocal of $k_{off}$ (Scheme 1) [34].




**Scheme 1**. Binding of a ligand (L) to the receptor (R) with association rate $k_{on}$, and dissociation of L from R with dissociation rate $k_{off}$. The affinity ($K_i$) and residence time (RT) can be derived from these rate constants.

Several studies have indicated that long residence time ligands can contribute to improved efficacy, reduced side effects and a longer duration of action. The latter would enable once-daily dosage forms as opposed to multiple doses and thus increases patient compliance [35-39]. Examples are the angiotensin II subtype-1 ($AT_1$) receptor antagonist olmesartan for treatment of hypertension [40, 41], and the neurokinin-1 ($NK_1$) receptor antagonist aprepitant for prevention of acute and delayed chemotherapy-induced nausea and vomiting [42]. In addition, the rate at which a drug binds to a target receptor is crucial to the onset of the drug effect, therefore quick binding of a drug to its target is preferred [43].

The residence time of a ligand can be measured in kinetic binding assays upon radiolabelling the compound of interest [44]. However, this is labor intensive and cost-inefficient, and therefore a method to determine the residence time of unlabelled ligands was invented in 1984 by Motulsky and Mahan [45]. It took twenty years before this competition association assay was picked up by a larger audience, but nowadays it is applied to assess ligand binding kinetics at many GPCRs [32, 36, 39, 46]. Based on this method a higher throughput screening assay was developed in our laboratory, named the 'dual point kinetic assay', which facilitates the screening for long residence time ligands [47]. In Chapter 6 we applied both of these assays to study the residence time of antagonists for CCR2, to stimulate drug discovery based on kinetic profiles next to affinity in order to eventually improve clinical efficacy.

## Chemokine receptors and their ligands

### The chemokine receptor family

The chemokine receptor CCR2 belongs to the GPCR subfamily of chemokine receptors. They are predominantly expressed on immune cells and serve an important role in the host immune response against invading pathogens [48, 49]. Approximately 23 different chemokine receptors are known to date, and these can be activated by one or several of the 48 different chemokine ligands. Chemokines are small peptides of 70 to 120 amino acid residues, which are classified into four families according to the interaction pattern of the cysteine residues in their N-terminus: XC, CC, CXC and CX3C, where C represents a cysteine bridge and X/X3 stands for one or three non-cysteine residues (Fig. 4) [50].

Chemokine receptor binding and activation are generally thought to occur via a two-step process in which the first step is governed by binding of the large peptide ligand to the N-terminus and extracellular loops of the GPCR protein [51]. Subsequently, the N-terminus of the chemokine is well-positioned to interact with the transmembrane (TM) domains, leading to activation of the receptor [52].

Chemokines can be divided into two functional groups: homeostatic chemokines that are involved in leukocyte homing, and inflammatory chemokines that are produced in inflamed tissue by resident and infiltrating cells [53]. Several chemokines have both a homeostatic and inflammatory function. The secretion of chemokines evokes a chemokine gradient that results in chemotaxis: direct migration of cells expressing the appropriate chemokine receptor towards the chemokine ligand [54]. More details of the functions and the regulation of the chemokine receptor system are described in Chapter 2.

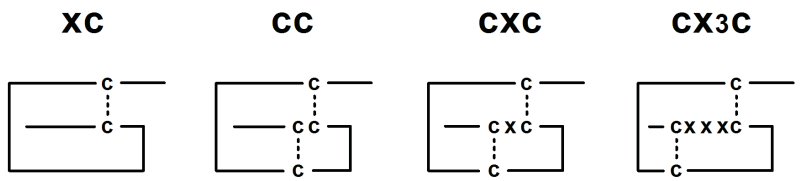



**Fig. 3.** The structure of chemokine families XC, CC, CXC and CX3C. Disulfide bridges are represented by the dotted lines.

### The chemokine receptor CCR2

In 1994 CCR2 was fully cloned and characterized by Charo and co-workers [55]. It exists in two alternatively spliced forms: CCR2a and CCR2b [56]. CCR2b is the predominantly expressed variant on which the current study was focussed, therefore I refer to this variant as “CCR2” in

this thesis. CCR2 is abundantly expressed on immune cells such as monocytes, natural killer cells and T-lymphocytes and can be bound by eight different inflammatory chemokines, being CCL2, CCL7, CCL8, CCL11, CCL13, CCL16, CCL24 and CCL26 [57-60]. CCL2 is the most studied chemokine for CCR2, and is unique among the seven CCR2 chemokines since it is the only ligand that binds exclusively to CCR2. Intracellular signalling pathways that are activated by CCR2 are mainly driven by $G_i$ proteins and β-arrestins [61]. Further downstream the activation of kinase cascades including extracellular signal-regulated kinase (ERK) 1/2 and Akt, as well as calcium signalling have been reported. Notably, the different chemokines have been reported to preferentially activate specific signalling pathways over others, implying that the concept of biased-signalling is applicable to this receptor, as discussed in Chapter 2 [61-63].

**CCR2 as drug target**

CCR2 is involved in a variety of diseases characterized by inflammation. Increased levels of CCL2 have been found associated to atherosclerosis, and CCR2 knock-out mice show a reduction in lesion size in the arterial wall [64, 65]. Several studies have shown that CCR2 on monocytes and macrophages mediates their recruitment to the atherosclerotic lesion and thereby contributes to plaque formation [66]. In addition, CCL2 and CCR2 are both highly expressed in the dorsal root ganglion (DRG) and on astrocytes and microglial cells in the peripheral and central nervous system during chronic pain states [67]. Knock-out of CCR2 in mice was found to diminish development of chronic pain states like neuropathic pain, and therefore many companies search for CCR2 antagonists as pain-reducing agents since no therapies are currently available for this disease [68]. Rheumatoid arthritis is characterized by inflammation in the joints, and again increased expression of CCL2 and CCR2-expressing macrophages has been found at these sites [69]. From these examples it seems that both CCR2 and its ligands are associated to different disease states through a common mechanism of action, which is a combination of direct activation of CCR2 in the cells of the target tissue and recruitment of circulating inflammatory cells into the tissue. Other diseases for which an important role of CCR2 and its chemokines has been reported include cancer [70], asthma [71], fibrosis [72], diabetes [73] and multiple sclerosis [74].

CCR2 inhibition by small molecule antagonists or monoclonal antibodies has been evaluated in a number of clinical trials targeting all the diseases mentioned above [75]. Unfortunately the majority of these trials failed, with the predominant reason being a lack of efficacy in Phase II. On-going trials include studies with the antagonists CCX140 and PF-04634817 for diabetic nephropathy [76, 77], and PF-04136309 for pancreatic adenocarcinoma [78]. The only marketed drugs for chemokine receptors at this moment are the CCR5 antagonist maraviroc and the CXCR4 antagonist AMD3100 [79, 80]. Maraviroc

inhibits entry of human immunodeficiency virus (HIV) into CCR5-positive cells, and AMD3100 is used to mobilize human hematopoietic stem cells from the bone marrow. Notably, both these conditions are not related to inflammatory diseases, highlighting the difficulty to intervene in those pathologies.

## This thesis

### Aim

The aim of the study was to provide a detailed insight in the molecular mechanism of action of CCR2 antagonists in order to improve drug discovery targeting this receptor. Three separate binding pockets via which CCR2 can be modulated were discovered, and different routes that lead to insurmountable antagonism of this receptor were revealed. In this thesis these results will be discussed in view of the complexity of the chemokine system. They should provide the reader with insights that will hopefully lead to the development of clinically effective drugs in the long term.

### Outline

The family of chemokine receptors and their endogenous chemokines will be more extensively introduced and discussed in **Chapter 2**. This chapter is particularly devoted to the so-called biased-signalling of chemokines and its implications for drug discovery.

**Chapter 3** is focused on small molecule antagonists for CCR2, for which multiple binding sites were discovered. This chapter presents four orthosteric antagonists, including INCB3344, and two allosteric antagonists, including CCR2-RA-[R].

The binding site of the allosteric antagonist CCR2-RA-[R] was discovered to be located at the intracellular side of the receptor. **Chapter 4** presents the amino acid residues in the receptor involved in binding of CCR2-RA-[R], which were revealed by means of an experimental and computational approach.

Besides the orthosteric and allosteric binding sites of the antagonists in Chapters 3 and 4, yet another binding site for CCR2 small molecule inhibitors was discovered. Modulation of CCR2 via this site by amiloride analogues as well as sodium ions is described in **Chapter 5**.

**Chapter 6** is focused on the discovery of novel orthosteric antagonists. This chapter describes how the residence time of CCR2 antagonists was increased by specific and small structural changes. This type of structure-kinetics relationships (SKR) should be incorporated in hit-to-lead optimization in order to increase the discovery of clinically effective CCR2 antagonists.

The research presented in these chapters reveals that binding sites for small molecule ligands are present throughout the entire transmembrane domain of CCR2. Therefore this thesis literally presents the *ins* and *outs* of ligand binding to CCR2. These results and its forthcoming opportunities for drug discovery are concluded and discussed in **Chapter 7**.

## References


1. Schroder, A., Prinzhorn, A., Kraut, K., *Uber salicylverbindungen.* Annalen der Chemie und Pharmacie, 1869. 150(1): p. 1-20.
2. Mayr, L.M. and Bojanic, D., *Novel trends in high-throughput screening.* Curr Opin Pharmacol, 2009. 9(5): p. 580-8.
3. Lagerstrom, M.C. and Schioth, H.B., *Structural diversity of G protein-coupled receptors and significance for drug discovery.* Nat Rev Drug Discov, 2008. 7(4): p. 339-57.
4. Venkatakrishnan, A.J., et al., *Molecular signatures of G-protein-coupled receptors.* Nature, 2013. 494(7436): p. 185-94.
5. Wu, B., et al., *Structures of the CXCR4 chemokine GPCR with small-molecule and cyclic peptide antagonists.* Science, 2010. 330(6007): p. 1066-71.
6. Tan, Q., et al., *Structure of the CCR5 chemokine receptor-HIV entry inhibitor maraviroc complex.* Science, 2013. 341(6152): p. 1387-90.
7. Davenport, A.P., et al., *International Union of Basic and Clinical Pharmacology. LXXXVIII. G protein-coupled receptor list: recommendations for new pairings with cognate ligands.* Pharmacol Rev, 2013. 65(3): p. 967-86.
8. Preininger, A.M., J. Meiler, and H.E. Hamm, *Conformational flexibility and structural dynamics in GPCR-mediated G protein activation: a perspective.* J Mol Biol, 2013. 425(13): p. 2288-98.
9. Ritter, S.L. and R.A. Hall, *Fine-tuning of GPCR activity by receptor-interacting proteins.* Nat Rev Mol Cell Biol, 2009. 10(12): p. 819-30.
10. Downes, G.B. and N. Gautam, *The G protein subunit gene families.* Genomics, 1999. 62(3): p. 544-52.
11. Hamm, H.E., *The many faces of G protein signaling.* J Biol Chem, 1998. 273(2): p. 669-72.
12. Reiter, E. and R.J. Lefkowitz, *GRKs and beta-arrestins: roles in receptor silencing, trafficking and signaling.* Trends Endocrinol Metab, 2006. 17(4): p. 159-65.
13. Rask-Andersen, M., M.S. Almen, and H.B. Schioth, *Trends in the exploitation of novel drug targets.* Nat Rev Drug Discov, 2011. 10(8): p. 579-90.
14. Leff, P., *The two-state model of receptor activation.* Trends Pharmacol Sci, 1995. 16(3): p. 89-97.
15. Bouvier, M., *Unraveling the structural basis of GPCR activation and inactivation.* Nat Struct Mol Biol, 2013. 20(5): p. 539-41.
16. Cotecchia, S., et al., *Regions of the alpha 1-adrenergic receptor involved in coupling to phosphatidylinositol hydrolysis and enhanced sensitivity of biological function.* Proc Natl Acad Sci U S A, 1990. 87(8): p. 2896-900.
17. Costa, T. and S. Cotecchia, *Historical review: Negative efficacy and the constitutive activity of G-protein-coupled receptors.* Trends Pharmacol Sci, 2005. 26(12): p. 618-24.
18. Kobilka, B.K. and X. Deupi, *Conformational complexity of G-protein-coupled receptors.* Trends Pharmacol Sci, 2007. 28(8): p. 397-406.
19. Bhattacharya, S., et al., *Ligand-stabilized conformational states of human beta(2) adrenergic receptor: insight into G-protein-coupled receptor activation.* Biophys J, 2008. 94(6): p. 2027-42.
20. Bock, A., et al., *Dynamic ligand binding dictates partial agonism at a G protein-coupled receptor.* Nat Chem Biol, 2014. 10(1): p. 18-20.
21. Kenakin, T., *Efficacy as a vector: the relative prevalence and paucity of inverse agonism.* Mol Pharmacol, 2004. 65(1): p. 2-11.

22. Labarre, M., et al., *Inverse agonism by Dmt-Tic analogues and HS 378, a naltrindole analogue.* Eur J Pharmacol, 2000. 406(1): p. R1-3.

23. Yanagawa, M., T. Yamashita, and Y. Shichida, *Glutamate acts as a partial inverse agonist to metabotropic glutamate receptor with a single amino acid mutation in the transmembrane domain.* J Biol Chem, 2013. 288(14): p. 9593-601.

24. Wacker, D., et al., *Structural features for functional selectivity at serotonin receptors.* Science, 2013. 340(6132): p. 615-9.

25. Liu, J.J., et al., *Biased signaling pathways in beta2-adrenergic receptor characterized by 19F-NMR.* Science, 2012. 335(6072): p. 1106-10.

26. Stallaert, W., A. Christopoulos, and M. Bouvier, *Ligand functional selectivity and quantitative pharmacology at G protein-coupled receptors.* Exp Opin Drug Discov, 2011. 6(8): p. 811-25.

27. May, L.T., et al., *Allosteric modulation of G protein-coupled receptors.* Annu Rev Pharmacol Toxicol, 2007. 47: p. 1-51.

28. Christopoulos, A. and T. Kenakin, *G protein-coupled receptor allosterism and complexing.* Pharmacol Rev, 2002. 54(2): p. 323-74.

29. Scholten, D.J., et al., *Pharmacological modulation of chemokine receptor function.* Br J Pharmacol, 2012. 165(6): p. 1617-43.

30. Kenakin, T., *Principles: receptor theory in pharmacology.* Trends Pharmacol Sci, 2004. 25(4): p. 186-92.

31. Vauquelin, G. and S.J. Charlton, *Long-lasting target binding and rebinding as mechanisms to prolong in vivo drug action.* Br J Pharmacol, 2010. 161(3): p. 488-508.

32. Dowling, M.R. and S.J. Charlton, *Quantifying the association and dissociation rates of unlabelled antagonists at the muscarinic M3 receptor.* Br J Pharmacol, 2006. 148(7): p. 927-37.

33. Hulme, E.C. and M.A. Trevethick, *Ligand binding assays at equilibrium: validation and interpretation.* Br J Pharmacol, 2010. 161(6): p. 1219-37.

34. Copeland, R.A., D.L. Pompliano, and T.D. Meek, *Drug-target residence time and its implications for lead optimization.* Nat Rev Drug Discov, 2006. 5(9): p. 730-9.

35. Tummino, P.J. and R.A. Copeland, *Residence time of receptor-ligand complexes and its effect on biological function.* Biochemistry, 2008. 47(20): p. 5481-92.

36. Slack, R.J., et al., *Pharmacological characterization of GSK1004723, a novel, long-acting antagonist at histamine H(1) and H(3) receptors.* Br J Pharmacol, 2011. 164(6): p. 1627-41.

37. Sykes, D.A., M.R. Dowling, and S.J. Charlton, *Exploring the mechanism of agonist efficacy: a relationship between efficacy and agonist dissociation rate at the muscarinic M3 receptor.* Mol Pharmacol, 2009. 76(3): p. 543-51.

38. Casarosa, P., et al., *Preclinical evaluation of long-acting muscarinic antagonists: comparison of tiotropium and investigational drugs.* J Pharmacol Exp Ther, 2009. 330(2): p. 660-8.

39. Fleck, B.A., et al., *Binding kinetics redefine the antagonist pharmacology of the corticotropin-releasing factor type 1 receptor.* J Pharmacol Exp Ther, 2012. 341(2): p. 518-31.

40. Oparil, S., et al., *Comparative efficacy of olmesartan, losartan, valsartan, and irbesartan in the control of essential hypertension.* J Clin Hypertens, 2001. 3(5): p. 283-91, 318.

41. Le, M.T., et al., *Molecular characterisation of the interactions between olmesartan and telmisartan and the human angiotensin II AT1 receptor.* Br J Pharmacol, 2007. 151(7): p. 952-62.

42. Lindstrom, E., et al., *Neurokinin 1 receptor antagonists: correlation between in vitro receptor interaction and in vivo efficacy.* J Pharmacol Exp Ther, 2007. 322(3): p. 1286-93.

43. Zhang, R. and F. Monsma, *Binding kinetics and mechanism of action: toward the discovery and development of better and best in class drugs.* Exp Opin Drug Discov, 2010. 5(11): p. 1023-9.

44. Maguire, J.J., R.E. Kuc, and A.P. Davenport, *Radioligand binding assays and their analysis.* Methods Mol Biol, 2012. 897: p. 31-77.

45. Motulsky, H.J. and L.C. Mahan, *The kinetics of competitive radioligand binding predicted by the law of mass action.* Mol Pharmacol, 1984. 25(1): p. 1-9.

46. Guo, D., et al., *Functional efficacy of adenosine A(2)A receptor agonists is positively correlated to their receptor residence time.* Br J Pharmacol, 2012. 166(6): p. 1846-59.

47. Guo, D., et al., *Dual-point competition association assay: a fast and high-throughput kinetic screening method for assessing ligand-receptor binding kinetics.* J Biomol Screen, 2013. 18(3): p. 309-20.

48. Zlotnik, A. and O. Yoshie, *The chemokine superfamily revisited.* Immunity, 2012. 36(5): p. 705-16.

49. Esche, C., C. Stellato, and L.A. Beck, *Chemokines: key players in innate and adaptive immunity.* J Invest Dermatol, 2005. 125(4): p. 615-28.

50. Alexander, S.P., A. Mathie, and J.A. Peters, *Guide to Receptors and Channels (GRAC), 5th edition.* Br J Pharmacol, 2011. 164 Suppl 1: p. S1-324.

51. Monteclaro, F.S. and I.F. Charo, *The amino-terminal domain of CCR2 is both necessary and sufficient for high affinity binding of monocyte chemoattractant protein 1. Receptor activation by a pseudo-tethered ligand.* J Biol Chem, 1997. 272(37): p. 23186-90.

52. Pease, J.E., et al., *The N-terminal extracellular segments of the chemokine receptors CCR1 and CCR3 are determinants for MIP-1alpha and eotaxin binding, respectively, but a second domain is essential for efficient receptor activation.* J Biol Chem, 1998. 273(32): p. 19972-6.

53. Moser, B., et al., *Chemokines: multiple levels of leukocyte migration control.* Trends Immunol, 2004. 25(2): p. 75-84.

54. Tanino, Y., et al., *Kinetics of chemokine-glycosaminoglycan interactions control neutrophil migration into the airspaces of the lungs.* J Immunol, 2010. 184(5): p. 2677-85.

55. Charo, I.F., et al., *Molecular cloning and functional expression of two monocyte chemoattractant protein 1 receptors reveals alternative splicing of the carboxyl-terminal tails.* Proc Natl Acad Sci U S A, 1994. 91(7): p. 2752-6.

56. Wong, L.M., et al., *Organization and differential expression of the human monocyte chemoattractant protein 1 receptor gene. Evidence for the role of the carboxyl-terminal tail in receptor trafficking.* J Biol Chem, 1997. 272(2): p. 1038-45.

57. Berkhout, T.A., et al., *Cloning, in vitro expression, and functional characterization of a novel human CC chemokine of the monocyte chemotactic protein (MCP) family (MCP-4) that binds and signals through the CC chemokine receptor 2B.* J Biol Chem, 1997. 272(26): p. 16404-13.

58. Combadiere, C., et al., *Monocyte chemoattractant protein-3 is a functional ligand for CC chemokine receptors 1 and 2B.* J Biol Chem, 1995. 270(50): p. 29671-5.

59. Ogilvie, P., et al., *Eotaxin is a natural antagonist for CCR2 and an agonist for CCR5.* Blood, 2001. 97(7): p. 1920-4.

60. Myers, S.J., L.M. Wong, and I.F. Charo, *Signal transduction and ligand specificity of the human monocyte chemoattractant protein-1 receptor in transfected embryonic kidney cells.* J Biol Chem, 1995. 270(11): p. 5786-92.

61. Berchiche, Y.A., et al., *Different effects of the different natural CC chemokine receptor 2b ligands on beta-arrestin recruitment, Galphai signaling, and receptor internalization.* Mol Pharmacol, 2011. 79(3): p. 488-98.

62. O'Boyle, G., et al., *Chemokine-mediated inflammation: Identification of a possible regulatory role for CCR2.* Mol Immunol, 2007. 44(8): p. 1944-53.

63. Ogilvie, P., et al., *Unusual chemokine receptor antagonism involving a mitogen-activated protein kinase pathway.* J Immunol, 2004. 172(11): p. 6715-22.

64. Boring, L., et al., *Decreased lesion formation in CCR2-/- mice reveals a role for chemokines in the initiation of atherosclerosis.* Nature, 1998. 394(6696): p. 894-7.

65. Szalai, C., et al., *Involvement of polymorphisms in the chemokine system in the susceptibility for coronary artery disease (CAD). Coincidence of elevated Lp(a) and MCP-1 -2518 G/G genotype in CAD patients.* Atherosclerosis, 2001. 158(1): p. 233-9.

66. Gautier, E.L., C. Jakubzick, and G.J. Randolph, *Regulation of the migration and survival of monocyte subsets by chemokine receptors and its relevance to atherosclerosis.* Arterioscler Thromb Vasc Biol, 2009. 29(10): p. 1412-8.

67. Abbadie, C., *Chemokines, chemokine receptors and pain.* T Immunol, 2005. 26(10): p. 529-34.

68. Abbadie, C., et al., *Impaired neuropathic pain responses in mice lacking the chemokine receptor CCR2.* Proc Natl Acad Sci U S A, 2003. 100(13): p. 7947-52.

69. Gaffo, A., K.G. Saag, and J.R. Curtis, *Treatment of rheumatoid arthritis.* Am J Health Syst Pharm, 2006. 63(24): p. 2451-65.

70. Conti, I. and B.J. Rollins, *CCL2 (monocyte chemoattractant protein-1) and cancer.* Semin Cancer Biol, 2004. 14(3): p. 149-54.

71. Batra, J. and B. Ghosh, *Genetic contribution of chemokine receptor 2 (CCR2) polymorphisms towards increased serum total IgE levels in Indian asthmatics.* Genomics, 2009. 94(3): p. 161-8.

72. Seki, E., et al., *CCR2 promotes hepatic fibrosis in mice.* Hepatology, 2009. 50(1): p. 185-97.

73. Weisberg, S.P., et al., *CCR2 modulates inflammatory and metabolic effects of high-fat feeding.* J Clin Invest, 2006. 116(1): p. 115-24.

74. Mahad, D.J. and R.M. Ransohoff, *The role of MCP-1 (CCL2) and CCR2 in multiple sclerosis and experimental autoimmune encephalomyelitis (EAE).* Semin Immunol, 2003. 15(1): p. 23-32.

75. Struthers, M. and A. Pasternak, *CCR2 antagonists.* Curr Top Med Chem, 2010. 10(13): p. 1278-98.

76. *Chemocentryx product pipeline.* Available from: http://www.chemocentryx.com/product/overview.html.

77. *Pfizer product pipeline as of Nov 2013*. Available from: http://www.pfizer.com/research/science_and_technology/product_pipeline.

78. *ClinicalTrials.gov*. Available from: http://clinicaltrials.gov/show/NCT01413022.

79. Lieberman-Blum, S.S., H.B. Fung, and J.C. Bandres, *Maraviroc: a CCR5-receptor antagonist for the treatment of HIV-1 infection.* Clin Ther, 2008. 30(7): p. 1228-50.

80. De Clercq, E., *Recent advances on the use of the CXCR4 antagonist plerixafor (AMD3100, Mozobil) and potential of other CXCR4 antagonists as stem cell mobilizers.* Pharmacol Ther, 2010. 128(3): p. 509-18.

# Chapter 2

## Bias in chemokine receptor signalling

Annelien J.M. Zweemer
Jimita Toraskar
Laura H. Heitman
Adriaan P. IJzerman

*Trends in Immunology* ***2014*** *35(6):243-252*

## Abstract

Chemokine receptors are widely expressed on a variety of immune cells and play a crucial role in normal physiology as well as in inflammatory and infectious diseases. The existence of 23 chemokine receptors and 48 chemokine ligands guarantees a tight control and fine-tuning of the immune system. Here, we discuss the multiple regulatory mechanisms of chemokine signalling at a systemic, cellular, and molecular level. In particular, we focus on the impact of biased signalling at the receptor level; an emerging concept in molecular pharmacology. An improved understanding of these mechanisms may provide a framework for more effective drug discovery and development at a target class that is so relevant for immune function.

## Regulation of the chemokine system

Chemokines are the most important regulators of leukocyte trafficking and play a central role in the immune system [1]. They act via abundantly expressed chemokine receptors, which belong to the family of G protein-coupled receptors (GPCRs) (Box 1), on a wide variety of immune cells. Activation of these chemokine receptors induces migration and differentiation of immune cells, which both are essential processes during innate and adaptive immune responses [2].



**Box 1.** Chemokine receptors as GPCRs

*GPCRs*

- With >800 members, GPCRs are the largest family and most diverse group of cell surface receptors and the most common target for therapeutic drugs [8].
- The GPCR structure consists of an extracellular N-terminus, an intracellular C-terminus and seven transmembrane (TM) helices, connected by three cytoplasmic and three extracellular loops [9].
- Ligand binding mostly takes place in a pocket formed by the seven helices close to the extracellular side of the receptor; it induces a conformational change at the intracellular side of the receptor that results in receptor activation and subsequent signalling [10].
- At the intracellular side different effector proteins can bind and transduce signals, among which are G proteins and β-arrestins [11].

*Chemokine receptors*

- Chemokine receptors belong to the class A Rhodopsin-like family of GPCRs.
- 23 different chemokine receptors have been identified that can be activated by ~48 chemokine ligands [IUPHAR/BPS Guide to Pharmacology, http://www.guidetopharmacology.org, accessed on 07-02-2014].
- Four subclasses of chemokine ligands have been identified on the basis of the pattern of conserved cysteine residues (C, CC, CXC and $CX_3C$) [12].
- Chemokine receptors have been classified as C, CC, CXC and $CX_3C$ receptors based on the chemokine subclass ligand that they bind.
- Most chemokine receptors bind multiple chemokines, and most chemokines can bind to and activate multiple chemokine receptors.
- The chemokine receptors ACKR1 (DARC), ACKR2 (D6), ACKR3 (CXCR7) and ACKR4 (CCX-CKR) are so-called decoy receptors that predominantly scavenge chemokine ligands from the extracellular environment, although some of these also couple to β-arrestins [13].

The chemokine-directed immune response involves a complex network of reactions that are carefully fine-tuned at multiple levels throughout the body (Fig. 1). At the systems level this involves spatiotemporal and tissue-specific expression of chemokine receptors and their ligands. At the cellular level the chemokine receptor signal can be modulated by coexpression of many differentially expressed proteins on immune cells. Finally, there is growing evidence of biased signalling at the molecular level for chemokine receptors, which implies that different chemokine ligands activate different intracellular pathways although binding to the same receptor.

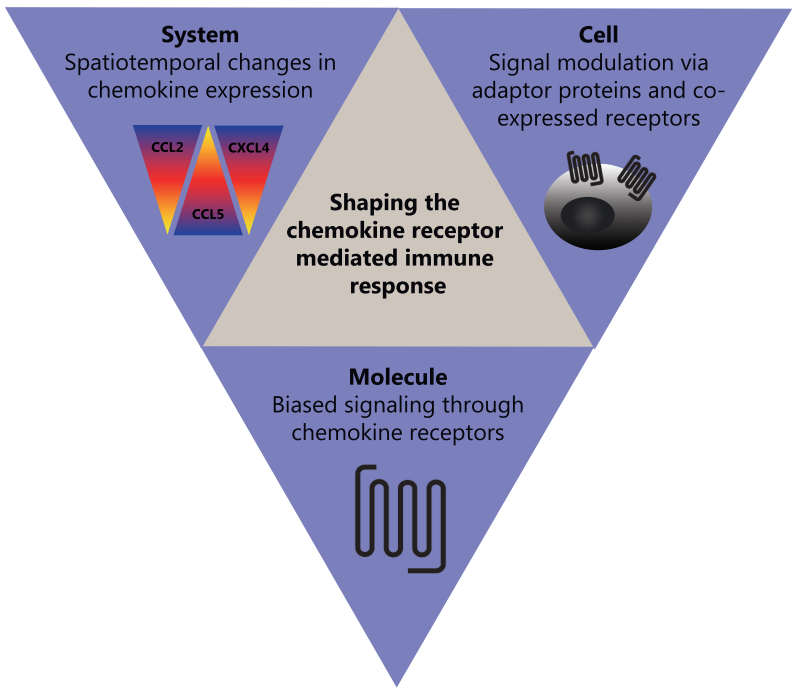



**Fig. 1.** Schematic representation of the structure of this review. The chemokine receptor-mediated immune response is discussed at a systems, cellular and molecular level.

With regard to this bias at the receptor level, novel mechanistic insights have been attained lately due to the advances in X-ray crystallography and NMR methods to resolve the structure of membrane proteins, such as GPCRs. Several structures of chemokine receptors have been elucidated now, among which are chemokine CXC receptor (CXCR)1, CXCR4 and chemokine CC receptor (CCR)5 [3-5]. In addition, for the serotonin 5-hydroxytryptamine $(HT)_{1B/2B}$ and the $\beta_2$-adrenergic receptors a structural basis for biased signalling was reported

[6, 7]. Similar mechanisms for ligand bias are likely to be present for the family of chemokine receptors, since these are particularly prone to biased signalling due to the presence of multiple endogenous chemokine ligands.

So far there has only been limited success in clinical trials targeting chemokine receptors. We propose therefore to consider chemokine regulation and bias at multiple levels in order to better understand their intricacies. Thus, in this review we present a summary of chemokine receptor signalling at a systems, cellular, and molecular level. Immunologists should be aware of the bias that can be introduced at a molecular level, whereas pharmacologists need to keep in mind that their target molecule could be modulated or expressed differently at a systems level.



## Regulation of chemokine expression and receptor activation

The human chemokine system consists of approximately ~23 receptors and 48 ligands [IUPHAR/BPS Guide to Pharmacology, http://www.guidetopharmacology.org, accessed on 07-02-2014], of which the classically signalling chemokine receptors are presented in Fig. 2. Most chemokine receptors can be activated by multiple chemokines, and one chemokine often has the ability to activate multiple receptors. Although previously regarded as redundant, the unique expression patterns of the various chemokines suggest that they form the basis for a specific and fine-tuned functioning of the immune system [1]. This is not only important in normal physiology, but also during certain immunopathological disease states, as illustrated by the CCR2 receptor and its ligands. CCR2 can be activated by the chemokine ligands chemokine CC ligand (CCL)2/monocyte chemotactic protein (MCP)-1, CCL7/MCP-3, CCL8/MCP-2, CCL11/eotaxin, CCL13/MCP-4, and CCL16/human CC chemokine (HCC)-4. Most studies have been focused on the CCL2–CCR2 interaction because CCL2 is the endogenous ligand with the highest affinity for CCR2. Nevertheless, in infectious diseases, CCL7 has been found to be crucial for monocyte recruitment to inflammatory sites mediated through CCR2 [14]. An example of distinct expression patterns observed in immunopathology is the regulation of the CCR4 ligands CCL17/thymus- and activation-regulated chemokine (TARC) and CCL22/macrophage-derived chemokine (MDC), which are not expressed in healthy skin tissue [15]. However, in inflamed skin lesions, CCL17 is detected on endothelial cells, whereas CCL22 is only presented by dendritic cells [15]. This distinct chemokine expression pattern has been demonstrated in diseases ranging from psoriasis to atopic dermatitis, therefore, this could be a general feature underlying the disease state. In general the balance, timing, and

pattern of chemokine expression appears to regulate the generation of immune-cell-specific responses in health and disease [16].

In addition to the difference in release and production of chemokines among various tissues, their *in vivo* availability also depends on the interaction of chemokines with specific glycosaminoglycan (GAG) chains that are presented at the cell surface as part of membrane proteoglycans. The binding of chemokines to GAGs allows immobilization, accumulation, and retention of chemokines on cell surfaces near their sites of production in order to provide directional signals to migrating cells [17]. In addition, GAG interactions are involved in the transport of chemokines across cell surfaces. GAGs may selectively bind chemokines and therefore fine-tune the immune response, because they display varying affinities for specific chemokines and are differentially expressed in time and location on specific cell types and tissues [18]. Furthermore, cells and tissues can alter the expression of GAGs in pathophysiology. This has been observed upon inflammatory stimuli in diseases of the gastrointestinal tract as well as in multiple different tumours [19, 20]. GAGs might even be directly involved in signalling, since their attached core proteins that span the membrane can undergo tyrosine phosphorylation and thereby contribute to signal transduction, as reported for CXCL12/SDF-1 and the proteoglycan syndecan-4 [21]. Although they are a crucial factor for chemokine signalling, the exact functional consequences of chemokine-GAG interactions and the level of specificity are still largely speculative.

Not only GAGs can alter the availability of chemokines, but also chemokine receptors themselves. A certain group of chemokine receptors, known as atypical chemokine receptors (ACKRs) [13], have been proposed to act mainly as chemokine ligand scavengers [22, 23]. Furthermore, under certain circumstances the G protein-coupled chemokine receptors have been demonstrated to become uncoupled from G protein signalling. For example, dendritic cells and monocytes treated with anti-inflammatory interleukin (IL)-10 express 'uncoupled' or 'nonsignalling' CCR1, CCR2 and CCR5, which can scavenge their corresponding inflammatory chemokines *in vitro* as well as in mice [24]. Another study demonstrated both *in vitro* and *in vivo* that apoptotic leukocytes express 'silent' CCR5 receptors, scavenging CCR5 ligands, and thereby contributing to the resolution of inflammation in a mouse model of peritonitis [25]. Therefore expression of a certain chemokine receptor does not always imply a contribution to the disease state. In fact, one might speculate that a pharmacological blockade of these receptors can increase free chemokine levels and therefore result in enhanced pathology.

Altogether the examples above illustrate that the expression of chemokines and their receptors varies over time and between different conditions, and studies of mechanisms and outcomes associated with this differential expression in a number of disease states have been

reviewed previously [26, 27]. As noted above, it is clear that expression of chemokines and their receptors does not necessarily imply a role as stimulator or enhancer of a pathophysiological state, which is an important factor to consider while developing antagonists targeting the chemokine system. Besides the regulation of chemokines and their receptors throughout the body, there is substantial evidence that chemokine receptors modulate each other within a particular immune cell. This is discussed in the following section.

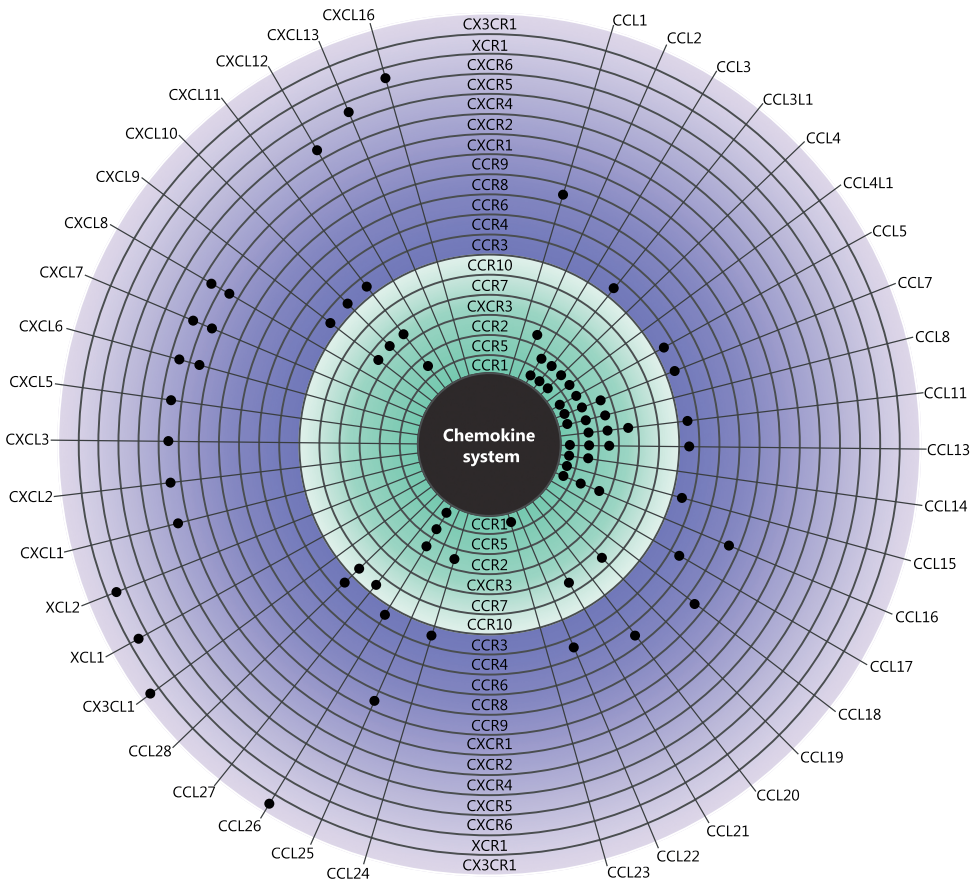



**Fig. 2**. Overview of the family of chemokines and chemokine receptors. The green inner circle represents those chemokine receptors for which some form of biased signalling has been documented. This is not (yet) the case for the chemokine receptors in the blue outer circle. The black dots represent the chemokine ligands that have been shown to bind to a given chemokine receptor. The group of atypical chemokine receptors (ACKRs) is not depicted in this figure.

## Regulation of chemokine receptor signalling in immune cells

Chemokine receptors are expressed by immune cells in both the innate and adaptive compartments, including B and T lymphocytes, monocytes and neutrophils [28]. Distinct expression profiles characterize the different leukocyte subtypes. For example in T helper (Th) cells, several chemokine receptors are associated with the Th1 phenotype (including CXCR3 and CCR5), whereas others are associated with the Th2 phenotype (including CCR4 and CCR8). This phenomenon is likely related to their discriminate functions in response to viral and bacterial pathogens or during allergic reactions [29, 30]. In the case of monocytes, a different repertoire of chemokine receptors can be expressed depending on environmental factors and stimuli. Lipopolysaccharide (LPS) downregulates CCR1, CCR2, and CCR5 expression in monocytes, whereas IL-2 stimulates CCR2 expression [31]. In addition, CCR7 is upregulated upon immunogenic stimulation, possibly to facilitate lymph-node homing [32, 33]. Tight regulation of the different chemokine receptors on immune cells therefore shapes the immune cell response.

The majority of immune cells express multiple chemokine receptors simultaneously. At a cellular level, chemokines can counteract each other or display synergy, thereby reducing the inflammatory response or increasing the selectivity of cell recruitment [34, 35]. For example, via heterologous receptor desensitization or internalization one chemokine can lower the responsiveness of a cell to other chemokines binding to a distinct chemokine receptor [36]. This phenomenon has been studied in human peripheral blood T cells, which express CCR5 and CXCR4 [37]. Upon simultaneous addition of their chemokines CCL4/macrophage inflammatory protein (MIP)-1β, CCL5/regulated on activation, normal T cell expressed and secreted (RANTES), and CXCL12, the capacity of CXCL12 to induce chemotaxis *in vitro* is suppressed. This crosstalk does not involve the internalization of the receptor, but rather a cross-desensitization via a decrease in phosphorylation of downstream signalling proteins. The rich chemokine environment surrounding the leukocytes during inflammatory conditions can therefore induce different cellular responses than determined in assays that only reflect the behaviour of one particular chemokine receptor and ligand [38].

Chemokines can also modulate signalling responses through other chemokine receptors due to the presence of heterodimeric or hetero-oligomeric receptor complexes [39]. This has been demonstrated for several chemokine receptors, among which CCR2, CCR5, and CXCR4 [40-42]. In CCR2-CCR5 heterodimers, the CCR5 ligands CCL3/MIP-1α, CCL4, and CCL5 were able to displace CCL2 from CCR2 [42]. This so-called negative cooperativity was further analysed in different *in vitro* assays to confirm the allosteric nature of this displacement via

heterodimers [41]. The relevance for immune cell functioning has been demonstrated as well, because negative binding cooperativity takes place in hetero-oligomeric complexes between the binding pockets of CCR2, CCR5, and CXCR4 in T cells and monocytes that endogenously express these receptors [40]. As a result, the recruitment of these cells mediated by the CXCR4 agonist CXCL12 in mice could be inhibited by antagonists of CCR2 and CCR5.



Within immune cells, the magnitude and duration of the signal depends on the exposed chemokine concentration and on (subsequent) chemokine receptor desensitization, phosphorylation, and internalization. These processes are regulated via G protein-coupled receptor kinases (GRKs) and β-arrestins [43]. On the intracellular side of the cell, the different repertoires of these adaptor proteins regulate the eventual cellular effects. In RBL-2H3 cells stably expressing both receptors, it has been shown that CXCR1 and CXCR2 couple to distinct GRK isoforms [44]. CXCR1 predominantly couples to GRK2, whereas CXCR2 interacts with GRK6 to negatively regulate receptor sensitization and trafficking, eventually affecting cell signalling [44, 45]. The role of GRK6 in neutrophil recruitment was further demonstrated in studies using wild type and GRK6$^{-/-}$ knockout mice [44]. In addition, different types of immune cells express different types of GRKs and β-arrestins; the levels of which may also vary, adding another layer of bias and fine-tuning of the response of chemokines and their receptors [46, 47].

Thus, there are multiple co-receptors and adaptor proteins that define the eventual chemokine receptor signal. In order to study the effect of a chemokine or potential drug candidate, it is important to include cell types and tissues that reflect the *in vivo* situation more so than cell lines, devoid of physiological context, with heterologous receptor expression.

## Biased signalling through chemokine receptors

At the molecular level yet another type of bias is present in the chemokine system, because chemokine receptors are capable of differentially signalling in a ligand-specific manner. This biased signalling, also called functional selectivity, refers to agonist ligands that favour the activation of a certain intracellular signalling pathway over another [48]. The following sections discuss the multiple intracellular signalling routes that can be activated by chemokines. The aim is to give a comprehensive overview of the biased signalling events that have been reported for chemokine receptors so far, illustrating that the chemokine system is extensively fine-tuned at the receptor level already.

*GPCR signalling*

GPCRs transduce the effects of many extracellular signals/ligands (whether those are chemokines or other hormones and neurotransmitters) to intracellular pathways and signalling routes (Fig. 3). They bind to and activate heterotrimeric G proteins that consist of a $G_{\alpha}$, $G_{\beta}$, and $G_{\gamma}$ subunit, for which 21, 6, and 12 different types are present in humans, respectively [49]. Activation of these G proteins modulates the production of second messenger molecules such as cyclic AMP (cAMP), intracellular calcium ($Ca^{2+}$) and inositol phosphates (IPs), which control further downstream effectors like protein kinase (PK)C and Akt. GPCR activation and consequently G protein-mediated signalling are terminated via phosphorylation of the GPCR by GRKs. The phosphorylated receptor recruits β-arrestins, of which various subtypes exist. This association often results eventually in receptor internalization to the cytosol, effectively impeding further signalling from the receptor. After receptor coupling, β-arrestins are also able to transduce signals themselves, for example via subsequent activation of the extracellular signal-regulated kinase (ERK) pathway [50]. For the purpose of the present discussion, we focus on the major signalling pathways via G proteins and β-arrestins to illustrate the phenomenon of biased signalling through chemokine receptors in functions of the immune system.

In case of extreme signal bias through GPCRs, one ligand may mainly activate G proteins, whereas another ligand only activates β-arrestins. This results in different cellular effects ('texture') although both ligands act via the same receptor; a process which has been extensively studied and discussed for GPCRs in general, as reviewed by Kenakin and Christopoulos [51]. Biased signalling does not only comprise distinct signalling via either G proteins or β-arrestins, but also includes more subtle differences in the activation of other downstream signalling proteins. For example, ligands can discriminate between different types of G proteins, whereas others differently affect signalling events like ERK activation or $Ca^{2+}$ mobilization. It is important to note that pathway activation depends also on the expression level of the receptor as well as the cellular expression and availability of signalling molecules, which result in cell-specific differences (Fig. 3).

Advances in structural biology have led to an accumulating understanding of the underlying mechanisms. The first structural features in a GPCR crystal structure that are responsible for biased signalling were recently revealed for the serotonin receptors $5\text{-}HT_{1B}$ and $5\text{-}HT_{2B}$ [6]. Conformational changes at the intracellular side in their helix VI and helix VII were reported to be responsible for G protein signalling or β-arrestin signalling, respectively [6, 52, 53]. In addition to the 'snapshots' of bias in crystal structures, the emerging field of protein molecular dynamics further contributes to our understanding of ligand bias. Such

studies have simulated at the atomic level how small perturbations at the more extracellularly located ligand binding site can lead to large conformational changes at the intracellular side of the receptor [54]. Importantly, not only do we start to understand the molecular features of biased signalling, we now also recognize its implications as it may lead to the development of therapeutics that have selective efficacy and fewer side effects [55].



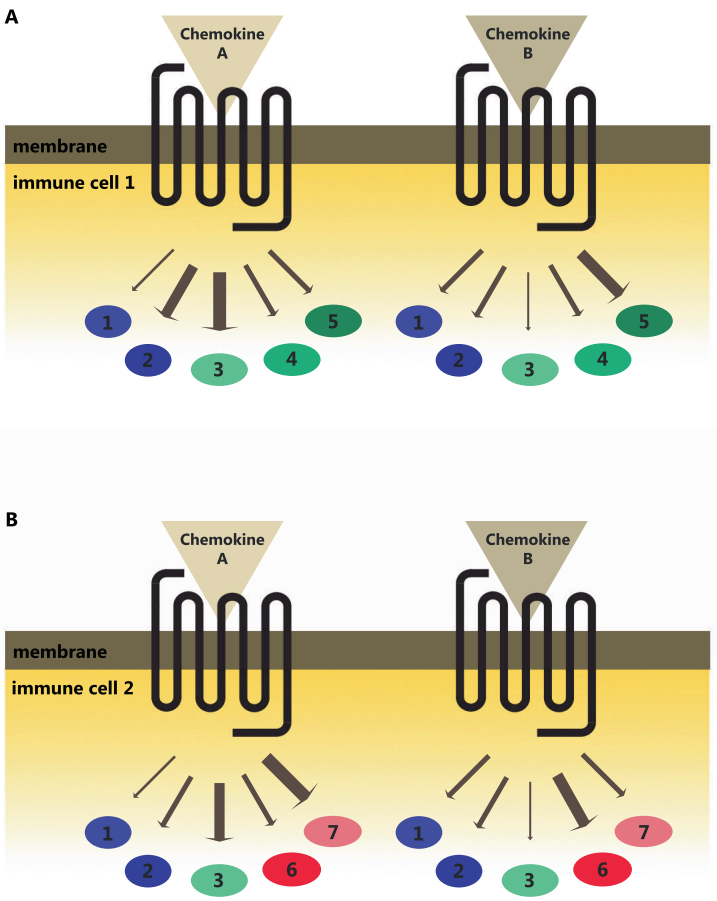



**Fig. 3.** Schematic representation of biased signalling through chemokine receptors. The extent of signalling via signalling proteins 1-7 is represented by the thickness of the arrows. (A) Chemokines A and B bind to the same chemokine receptor in immune cell 1, but activate distinct signalling pathways. A signals predominantly via proteins 2 and 3, whereas B signals mainly via protein 5. (B) Immune cell 2 expresses signalling proteins different from immune cell 1, which results in differential signalling profiles for chemokines A and B.

The chemokine receptor family is prone to ligand-induced biased signalling, because most chemokine receptors can be activated by multiple chemokines. Interestingly, this is different from many other GPCRs with only one endogenous ligand, where ligand bias has largely been observed for synthetic agonists only. In several studies the activation of multiple pathways has been compared among the different chemokines, and for certain chemokine receptors a biased signalling pattern was discovered (Fig. 2 and 3). These receptors include CCR1 [56-59], CCR2 [60-62], CCR5 [63-65], CCR7 [66-68], CCR10 [57] and CXCR3 [57, 69]. With the exception of the homeostatic chemokine receptor CCR7, all are inflammatory chemokine receptors that bind multiple chemokines. The following sections discuss the biased signalling through each of these receptors individually.

*Biased signalling through CC chemokine receptors*

*CCR1*. The expression of CCR1 is known to coincide with the G protein subtypes $G_{i/o}$, $G_{14}$ and $G_{16}$ [70]. Four chemokines, CCL3, CCL5, CCL7, and CCL15/HCC-2, were found to differentially activate these G protein subtypes in COS-7 cells or HEK293 cells transfected with CCR1, resulting in different intracellular levels of cAMP, ERK, and IP [56]. More specifically, CCL15 was discovered to be the only chemokine ligand that did not signal via $G_{14}$ and $G_{16}$. The inability of CCL15 to activate CCR1 as effectively as the others could potentially be caused by its long N-terminal region. The N-terminal region is responsible for receptor activation, whereas the N-loop region is responsible for receptor binding. CCL15 can bind the receptor with high affinity due to its structural homology to other CC chemokines in the N-loop region, but its extended N-terminal region largely precludes subsequent receptor activation [58]. Further support comes from the finding that neither CCL14/HCC-1 nor CCL23/myeloid progenitor inhibitory factor (MPIF)-1, both having a long N-terminal region, can activate CCR1 despite sufficient binding affinity [56]. Another study on CCR1 agonism examined a total of eight different chemokine ligands, and reported that CCL8 was a poor G protein-activator whereas CCL4 was proposed to act as an *in vivo* inhibitor of CCR1 in the leukaemia cell line HL-60 because it showed only marginal receptor activation in functional assays [59]. In CCR1-transfected HEK293 cells, CCL5 and CCL23 have been identified as G protein-biased chemokines compared to CCL3, while CCL5, CCL15, and CCL23 display bias for internalization following β-arrestin recruitment [57]. All these different studies illustrate that CCR1 is heavily prone to biased signalling.

*CCR2*. The CCR2 receptor has been reported to bind eight chemokines, namely CCL2, CCL7, CCL8, CCL11, CCL13, CCL16, CCL24/eotaxin-2 and CCL26/eotaxin-3. Berchiche *et al.* studied the $G_i$ activation and β-arrestin recruitment profiles of these different ligands in

HEK293 cells transfected with CCR2 [60]. Overall, the potency and efficacy rank orders of G protein activation and β-arrestin recruitment were comparable. However, when the β-arrestin subtypes 1 and 2 were compared, the weak arrestin recruiters CCL8 and CCL13 were found to show bias towards β-arrestin 2. Interestingly, the study also reported the kinetics of the CCR2-β-arrestin complexes. CCL7 had a high potency to recruit β-arrestin, but with a short half-life of the signal, whereas CCL8 and CCL13 induced weak but stable signals over time. These differences in kinetic patterns are additional factors leading to signal bias that deserve more attention; it has been reported for other GPCRs that this can be an underlying factor for differential signalling as well as signal termination [71]. Besides the signalling properties of the different CCR2 ligands, it was reported that CCL2, CCL7 and CCL13 induce homodimer formation of CCR2, whereas the other chemokines do not [60]. The formation of dimers, hetero- or homo-, is yet another mechanism to create bias in signalling and should therefore be taken into account when interpreting signal bias of any chemokine receptor.



*CCR5*. The signalling properties of CCL3, CCL4, CCL5, CCL8, and CCL13 via CCR5 have been investigated in cAMP accumulation and $Ca^{2+}$ mobilisation assays in CHO cells stably expressing CCR5. The potency rank order of chemokine ligands was similar between the two assays, however, CCL13 was completely unable to affect cAMP concentrations [63]. The $Ca^{2+}$ responses were G protein-dependent, except for CCL3 that produced a $Ca^{2+}$ signal in a partly G protein-independent manner. These results illustrate that the CCR5 chemokines act differently. Interestingly, other groups that used different cell systems, including RBL-2H3 and COS-7 cells expressing CCR5, reported different rank orders of signalling efficiencies [65, 72]. This indicates cell-type specific effects or differential activation of the various intracellular effectors by these chemokines (Fig. 3). It further emphasizes that the choice of cell lines must be an important parameter; primary cell lines and immune cells may better represent an *in vivo* relevant bias in signalling. The underlying mechanism for the differential effects of CCR5 ligands has been addressed in studies that focused on the structural determinants at the receptor level. Biased signalling could be a result of ligand-specific induction of phosphorylation sites and thereby specific recruitment of GRKs, which differs among the CCR5 chemokine ligands [65]. A mutagenesis study further explored molecular determinants of CCR5-induced signalling. Residues in helix VI and VII were identified that are responsible for causing biased signalling [64]. In the crystal structures of the serotonin receptors it was the orientation of these same helices that was found to induce biased signalling [6]. It would be very interesting to determine if these structural features can be translated to other chemokine receptors as well, which would be helpful for drug development targeting these receptors.

*CCR7*. CCL19/Epstein-Barr virus-induced molecule 1 ligand chemokine (ELC) and CCL21/secondary lymphoid tissue chemokine (SLC) are the endogenous agonists for CCR7. They are equally active in promoting G protein activation, $Ca^{2+}$ mobilization, and chemotaxis [67, 68]. However, in terms of β-arrestin recruitment and subsequent internalization of the receptor they behave differently. It was found that β-arrestin 3 was responsible for CCR7 internalization in the T cell lymphoma cell line HuT78 after stimulation with CCL19, which was not the case for CCL21-induced internalization [66]. Although both ligands allowed recruitment of β-arrestin 2, only CCL19 led to redistribution of β-arrestin-2 into endocytotic vesicles and classical receptor desensitization in HEK293 cells stably expressing CCR7 [67]. The underlying mechanism for this difference in β-arrestin recruitment was found to be a differential recruitment of GRKs that phosphorylate CCR7. CCL19 activates both GRK3 and GRK6 whereas CCL21 activates GRK6 only. Kohout and co-workers have reported findings that support this differential recruitment of GRKs, revealing that CCL19 induces specific phosphorylation sites on CCR7 in HEK293 cells [68].

*CCR10*. CCL27/cutaneous T cell-attracting chemokine (CTACK) and CCL28/mucosae-associated epithelial chemokine (MEC) are the two endogenous chemokines for CCR10. Both ligands are capable of G protein signalling measured by cAMP accumulation, but only CCL27 is capable of recruiting β-arrestin and internalizing the receptor [57]. In the same study it was assessed that CCL28 displayed a higher efficacy for migration of peripheral blood mononuclear cells (PBMCs). The biased signalling of CCL28 was speculated to be causal for this effect, explained by the lack of β-arrestin signalling and internalization that could result in prolonged and unopposed G protein activation [57].

*Biased signalling through CXC chemokine receptors and ACKRs*

*CXCR3*. CXCR1, CXCR2 and CXCR3 are the three CXC chemokine receptors that can each bind to multiple chemokines, but thus far biased signalling has only been reported for CXCR3. The activation of CXCR3 by CXCL9/monokine induced by gamma-interferon (MIG), CXCL10/IP-10 and CXCL11/interferon-inducible T cell alpha chemoattractant (I-TAC) has been investigated in a label-free impedance-based cellular assay [69]. For this technique, low-voltage currents run through microelectrode sensors at the bottom of a plate to which cells are attached. Changes in impedance upon ligand addition are continuously measured, and reflect receptor activation in the absence of a chemical or biological biosensor within the cell. Using this technique Watts *et al.* showed that CXCL9 behaved as a biased CXCR3 agonist in HEK293 cells stably expressing CXCR3, stimulating solely G protein-dependent pathways [69]. However, another study compared cAMP accumulation, β-arrestin recruitment and internalization

in classical functional assays with HEK293 cells transfected with CXCR3, and reported the opposite finding of CXCL9 being β-arrestin biased [57]. In addition CXCL11 was biased towards internalization. Apparently, CXCR3 is subject to biased signalling, of which the extent and nature may be determined by the different receptor expression levels and cellular assays used (Fig. 3). Although future studies will ascertain whether biased signalling through other CXC receptors exists, we would hypothesize that this is likely, because, for example, CXCR2 binds seven different chemokine ligands.



*ACKRs*. It should be noted that the ACKRs [13] such as ACKR1 (Duffy antigen/receptor for chemokines (DARC)), ACKR2 (D6), ACKR3 (CXCR7) and ACKR4 (chemocentryx chemokine receptor (CCX-CKR)) can bind a wide variety of chemokine ligands, with up to 18 ligands for ACKR1. These receptors were initially regarded as non-signalling decoy receptors because of their inability to activate typical G protein-signalling pathways, and therefore ACKRs were proposed to only scavenge ligands or function as co-receptors [22]. However, some recent studies have shown that these ACKRs can signal predominantly through β-arrestins. The chemokines CXCL11 and CXCL12 induce β-arrestin-2 recruitment to ACKR3 transfected in CHO cells, and a small molecule ACKR3 ligand has been reported to induce this β-arrestin-2 recruitment with even higher potency and efficacy [73]. Another study also reported that CXCL12 induces β-arrestin-2 recruitment to ACKR3 in HEK293 cells transfected with ACKR3, as well as rat vascular smooth muscle cells (VSMCs), which results in downstream activation of ERK [74]. These signalling properties were discovered to be important in physiologically relevant cell lines, since the ACKR3-mediated migration of rat VSMCs was found to be a β-arrestin-mediated process [74]. Besides ACKR3, ACKR2 can also recruit β-arrestins, however, further evidence of subsequent signalling remains to be elucidated for this receptor [75]. Given these reports of β-arrestin recruitment and signalling through ACKRs, it has been proposed that these receptors should be regarded as a subfamily of β-arrestin-biased GPCRs. However, there is now one case reported of ACKR3 signalling via $G_{i/o}$ in primary rodent astrocytes and human glioma cells [76]. This finding reveals the presence of thus far hidden properties of ACKRs, and the exact role and significance of ACKR-mediated signalling remains an open question for future research. ACKRs serve homeostatic functions by clearing chemokines from circulation and tissues [77], and in addition viruses and parasites are capable of modulating the expression of ACKRs to elude chemokines [78]. These receptors are therefore important for innate and adaptive immunity, emphasizing the necessity to resolve their functioning.

**Concluding remarks**

Here, we have discussed the regulation and bias in chemokine expression and signalling at a systems, cellular and molecular level. The presented evidence implies that the focus on only one natural ligand of a chemokine receptor as a prototype agonist is insufficient; neither should we focus on one single chemokine receptor *in vitro* because there might be several other receptors that determine the fate of the immune cell *in vivo*.

Over the past few years the 'drugability' of chemokine receptors has been reviewed and questioned [79]. The family of chemokine receptors is involved in a wide variety of diseases, mostly characterized by chronic inflammation. Although >50% of these receptors have been examined in clinical trials in the past decade, only two drugs targeting chemokine receptors have been approved by the regulatory authorities. The CCR5 antagonist maraviroc inhibits entry of HIV into CCR5-positive cells [80], and the CXCR4 antagonist AMD3100 is used to mobilize human haematopoietic stem cells from the bone marrow [81]. Notably, neither of these conditions is an inflammatory disease, nor is biased signalling involved. Possible reasons for the failure of other drug candidates targeting chemokine receptors are: i) lack of efficacy due to inappropriate disease models; ii) lack of efficacy due to poor pharmacokinetics such as binding to serum components; and iii) off-target (side) effects. The complexity at multiple levels of the chemokine system is another factor that introduces challenges for effective intervention in disease states (Box 2). Integration of these issues in early stages of drug discovery and development programs is necessary in order to develop clinically effective drugs with an acceptable benefit/risk profile. The clinical relevance of biased ligands is illustrated by the μ-opioid receptor agonist TRV130, which has recently been tested in Phase I studies and is entering Phase II in 2014 for the treatment of acute pain [82]. TRV130 causes G protein signalling with similar potency and efficacy as morphine, but with far less β-arrestin recruitment and receptor internalization [83]. Subsequent studies in mice have demonstrated that this bias results in higher analgesic efficacy, less gastrointestinal dysfunction, and less respiratory suppression than morphine.

In summary we have reviewed the regulation of and bias in chemokine receptor signalling that should be taken into account by immunologists as well as pharmacologists (Fig. 1). The expression profile of chemokine ligands at the target tissue should be determined and considered in order to design appropriate *in vitro* studies, taking into account the differential expression profiles in health and disease. This is important given the aforementioned data that reported crucial and different roles between chemokine ligands that bind to one chemokine receptor. In addition, the growing evidence of biased signalling through chemokine receptors shows that we cannot restrict ourselves to incorporate one chemokine ligand only, because

the effect of drug candidates in the presence of other chemokine ligands might be different. Although heterologous cell systems can be used at the start of a project, the function of the chemokine receptor and impact of a drug should be studied in physiologically relevant cells as early as possible, because coexpressed proteins and receptors can modulate the behaviour and response of a chemokine receptor. It is hoped that this review will help in designing such experiments.



**Box 2.** Chemokine signalling: implications for drug discovery in immunology

The complexity of the chemokine receptor family and its ligands should be considered during drug discovery. Most chemokine receptors are activated by multiple chemokine ligands, which should be taken into account upon developing small molecule antagonists. This can be illustrated by research on the chemokine receptor CCR1. For this receptor it has been shown that small molecule ligands can both act as allosteric enhancers for CCL3 and at the same time as a competitive blockers of the binding of CCL5 [84]. This drug-induced bias is important, since chemokines are differentially expressed and regulated during immunopathology.

Not only small molecule ligand, but also short lipidated peptide sequences named pepducins have been found to be candidate drugs targeting chemokine receptors. The pepducin ATI-2341 selectively targets CXCR4 and is an allosteric agonist *in vitro* as well as *in vivo* [85]. In a recent study it was discovered that ATI-2341 revealed functional selectivity for $G_i$ pathways over $G_{13}$ and β-arrestin [86]. In comparison to the CXCR4 antagonist AMD-3100, which is used in the clinic to mobilize haematopoietic stem cells from the bone marrow for transplantation of leukaemia patients [81], the pepducin ATI-2341 does not induce the additional undesired mobilization of lymphocytes [85]. Whether CXCR4-mediated biased signalling of ATI-2341 with respect to AMD-3100 is causal for this difference remains a question for further research.

Besides the pepducins, small molecule ligands can also induce biased signalling upon binding to chemokine receptors [64, 69, 87, 88]. For CCR5, the small molecule agonists YM-370749 and ESN-196 are able to induce G protein-coupling and activation of $Ca^{2+}$ responses [87, 88]. However, they do not stimulate chemotactic activity but instead induce internalization of CCR5 from the cell surface [87, 88]. These ligands are therefore functionally selective CCR5 ligands that act differently from the chemokine CCL5. This biased profile of small molecules acting via CCR5 could be of use as a novel class of anti-HIV-1 therapeutics, for which internalization of the receptor has been found to inhibit viral entry to the cell.

In conclusion, it is important to consider that drugs might differently affect one chemokine receptor depending on the chemokine that binds this receptor. In addition, these drugs can exert biased signalling via chemokine receptors themselves.

## References


1. Zlotnik, A. and O. Yoshie, *The chemokine superfamily revisited.* Immunity, 2012. 36(5): p. 705-16.
2. Esche, C., C. Stellato, and L.A. Beck, *Chemokines: key players in innate and adaptive immunity.* J Invest Dermatol, 2005. 125(4): p. 615-28.
3. Wu, B., et al., *Structures of the CXCR4 chemokine GPCR with small-molecule and cyclic peptide antagonists.* Science, 2010. 330(6007): p. 1066-71.
4. Tan, Q., et al., *Structure of the CCR5 chemokine receptor-HIV entry inhibitor maraviroc complex.* Science, 2013. 341(6152): p. 1387-90.
5. Park, S.H., et al., *Structure of the chemokine receptor CXCR1 in phospholipid bilayers.* Nature, 2012. 491(7426): p. 779-83.
6. Wacker, D., et al., *Structural features for functional selectivity at serotonin receptors.* Science, 2013. 340(6132): p. 615-9.
7. Liu, J.J., et al., *Biased signaling pathways in beta2-adrenergic receptor characterized by 19F-NMR.* Science, 2012. 335(6072): p. 1106-10.
8. Pierce, K.L., R.T. Premont, and R.J. Lefkowitz, *Seven-transmembrane receptors.* Nat Rev Mol Cell Biol, 2002. 3(9): p. 639-50.
9. Venkatakrishnan, A.J., et al., *Molecular signatures of G-protein-coupled receptors.* Nature, 2013. 494(7436): p. 185-94.
10. Preininger, A.M., J. Meiler, and H.E. Hamm, *Conformational flexibility and structural dynamics in GPCR-mediated G protein activation: a perspective.* J Mol Biol, 2013. 425(13): p. 2288-98.
11. Ritter, S.L. and R.A. Hall, *Fine-tuning of GPCR activity by receptor-interacting proteins.* Nat Rev Mol Cell Biol, 2009. 10(12): p. 819-30.
12. Alexander, S.P., A. Mathie, and J.A. Peters, *Guide to Receptors and Channels (GRAC), 5th edition.* Br J Pharmacol, 2011. 164 Suppl 1: p. S1-324.
13. Bachelerie, F., et al., *International Union of Pharmacology. LXXXIX. Update on the extended family of chemokine receptors and introducing a new nomenclature for atypical chemokine receptors.* Pharmacol Rev, 2013. 66(1): p. 1-79.
14. Tsou, C.L., et al., *Critical roles for CCR2 and MCP-3 in monocyte mobilization from bone marrow and recruitment to inflammatory sites.* J Clin Invest, 2007. 117(4): p. 902-9.
15. D'Ambrosio, D., et al., *Quantitative differences in chemokine receptor engagement generate diversity in integrin-dependent lymphocyte adhesion.* J Immunol, 2002. 169(5): p. 2303-12.
16. Groom, J.R. and A.D. Luster, *CXCR3 ligands: redundant, collaborative and antagonistic functions.* Immunol Celll Biol, 2011. 89(2): p. 207-15.
17. Tanino, Y., et al., *Kinetics of chemokine-glycosaminoglycan interactions control neutrophil migration into the airspaces of the lungs.* J Immunol, 2010. 184(5): p. 2677-85.
18. Lortat-Jacob, H., *The molecular basis and functional implications of chemokine interactions with heparan sulphate.* Curr Opin Struct Biol, 2009. 19(5): p. 543-8.
19. Sasisekharan, R., et al., *Roles of heparan-sulphate glycosaminoglycans in cancer.* Nat Rev Cancer, 2002. 2(7): p. 521-8.
20. Gotte, M., *Syndecans in inflammation.* FASEB J, 2003. 17(6): p. 575-91.
21. Charnaux, N., et al., *Syndecan-4 is a signaling molecule for stromal cell-derived factor-1 (SDF-1)/ CXCL12.* FEBS J, 2005. 272(8): p. 1937-51.
22. Bonecchi, R., et al., *Regulation of D6 chemokine scavenging activity by ligand- and Rab11-dependent surface up-regulation.* Blood, 2008. 112(3): p. 493-503.

23. Nibbs, R.J. and G.J. Graham, *Immune regulation by atypical chemokine receptors.* Nat Rev Immunol, 2013. 13(11): p. 815-29.
24. D'Amico, G., et al., *Uncoupling of inflammatory chemokine receptors by IL-10: generation of functional decoys.* Nat Immunol, 2000. 1(5): p. 387-91.
25. Ariel, A., et al., *Apoptotic neutrophils and T cells sequester chemokines during immune response resolution through modulation of CCR5 expression.* Nat Immunol, 2006. 7(11): p. 1209-16.
26. Mabuchi, T., et al., *Chemokine receptors in the pathogenesis and therapy of psoriasis.* J Dermatol Sci, 2012. 65(1): p. 4-11.
27. Mortier, A., J. Van Damme, and P. Proost, *Overview of the mechanisms regulating chemokine activity and availability.* Immunol Lett, 2012. 145(1-2): p. 2-9.
28. Ebert, L.M., P. Schaerli, and B. Moser, *Chemokine-mediated control of T cell traffic in lymphoid and peripheral tissues.* Mol Immunol, 2005. 42(7): p. 799-809.
29. Tsuchiya, T., et al., *Th1, Th2, and activated T-cell marker and clinical prognosis in peripheral T-cell lymphoma, unspecified: comparison with AILD, ALCL, lymphoblastic lymphoma, and ATLL.* Blood, 2004. 103(1): p. 236-41.
30. Panina-Bordignon, P., et al., *The C-C chemokine receptors CCR4 and CCR8 identify airway T cells of allergen-challenged atopic asthmatics.* J Clin Invest, 2001. 107(11): p. 1357-64.
31. Sica, A., et al., *Bacterial lipopolysaccharide rapidly inhibits expression of C-C chemokine receptors in human monocytes.* J Exp Med, 1997. 185(5): p. 969-74.
32. Jeannin, P., et al., *Outer membrane protein A renders dendritic cells and macrophages responsive to CCL21 and triggers dendritic cell migration to secondary lymphoid organs.* Eur J Immunol, 2003. 33(2): p. 326-33.
33. Forster, R., A.C. Davalos-Misslitz, and A. Rot, *CCR7 and its ligands: balancing immunity and tolerance.* Nat Rev Immunol, 2008. 8(5): p. 362-71.
34. Gouwy, M., et al., *Synergy between proinflammatory ligands of G protein-coupled receptors in neutrophil activation and migration.* J Leukoc Biol, 2004. 76(1): p. 185-94.
35. Gouwy, M., et al., *Synergy between coproduced CC and CXC chemokines in monocyte chemotaxis through receptor-mediated events.* Mol Pharmacol, 2008. 74(2): p. 485-95.
36. Ali, S., et al., *An apparent paradox: chemokine receptor agonists can be used for anti-inflammatory therapy.* Mol Immunol, 2007. 44(7): p. 1477-82.
37. Hecht, I., et al., *Heterologous desensitization of T cell functions by CCR5 and CXCR4 ligands: inhibition of cellular signaling, adhesion and chemotaxis.* Int Immunol, 2003. 15(1): p. 29-38.
38. Paoletti, S., et al., *A rich chemokine environment strongly enhances leukocyte migration and activities.* Blood, 2005. 105(9): p. 3405-12.
39. Salanga, C.L., M. O'Hayre, and T. Handel, *Modulation of chemokine receptor activity through dimerization and crosstalk.* Cell Mol Life Sci, 2009. 66(8): p. 1370-86.
40. Sohy, D., et al., *Hetero-oligomerization of CCR2, CCR5, and CXCR4 and the protean effects of "selective" antagonists.* J Biol Chem, 2009. 284(45): p. 31270-9.
41. Springael, J.Y., et al., *Allosteric modulation of binding properties between units of chemokine receptor homo- and hetero-oligomers.* Mol Pharmacol, 2006. 69(5): p. 1652-61.
42. El-Asmar, L., et al., *Evidence for negative binding cooperativity within CCR5-CCR2b heterodimers.* Mol Pharmacol, 2005. 67(2): p. 460-9.
43. Reiter, E. and R.J. Lefkowitz, *GRKs and beta-arrestins: roles in receptor silencing, trafficking and signaling.* Trends Endocrin Metab, 2006. 17(4): p. 159-65.
44. Raghuwanshi, S.K., et al., *The chemokine receptors CXCR1 and CXCR2 couple to distinct G protein-coupled receptor kinases to mediate and regulate leukocyte functions.* J Immunol, 2012. 189(6): p. 2824-32.

45. Richardson, R.M., et al., *Role of the cytoplasmic tails of CXCR1 and CXCR2 in mediating leukocyte migration, activation, and regulation.* J Immunol, 2003. 170(6): p. 2904-11.

46. Lombardi, M.S., et al., *Adjuvant arthritis induces down-regulation of G protein-coupled receptor kinases in the immune system.* J Immunol, 2001. 166(3): p. 1635-40.

47. Vroon, A., C.J. Heijnen, and A. Kavelaars, *GRKs and arrestins: regulators of migration and inflammation.* J Leukoc Biol, 2006. 80(6): p. 1214-21.

48. Luttrell, L.M. and T.P. Kenakin, *Refining efficacy: allosterism and bias in G protein-coupled receptor signaling.* Methods Mol Biol, 756: p. 3-35.

49. Downes, G.B. and N. Gautam, *The G protein subunit gene families.* Genomics, 1999. 62(3): p. 544-52.

50. Shenoy, S.K., et al., *beta-arrestin-dependent, G protein-independent ERK1/2 activation by the beta2 adrenergic receptor.* J Biol Chem, 2006. 281(2): p. 1261-73.

51. Kenakin, T. and A. Christopoulos, *Signalling bias in new drug discovery: detection, quantification and therapeutic impact.* Nat Rev Drug Discov, 2013. 12(3): p. 205-16.

52. Rasmussen, S.G., et al., *Crystal structure of the beta2 adrenergic receptor-Gs protein complex.* Nature, 2011. 477(7366): p. 549-55.

53. Rahmeh, R., et al., *Structural insights into biased G protein-coupled receptor signaling revealed by fluorescence spectroscopy.* Proc Natl Acad Sci U S A, 2012. 109(17): p. 6733-8.

54. Dror, R.O., et al., *Activation mechanism of the beta2-adrenergic receptor.* Proc Natl Acad Sci U S A, 2011. 108(46): p. 18684-9.

55. Whalen, E.J., S. Rajagopal, and R.J. Lefkowitz, *Therapeutic potential of beta-arrestin- and G protein-biased agonists.* Trends Mol Med, 2011. 17(3): p. 126-39.

56. Tian, Y., et al., *Differential chemokine activation of CC chemokine receptor 1-regulated pathways: ligand selective activation of Galpha 14-coupled pathways.* Eur J Immunol, 2004. 34(3): p. 785-95.

57. Rajagopal, S., et al., *Biased Agonism as a Mechanism for Differential Signaling by Chemokine Receptors.* J Biol Chem, 2013. 288(49): p. 35039-48.

58. Crump, M.P., et al., *Solution structure of eotaxin, a chemokine that selectively recruits eosinophils in allergic inflammation.* J Biol Chem, 1998. 273(35): p. 22471-9.

59. Chou, C.C., et al., *Pharmacological characterization of the chemokine receptor, hCCR1 in a stable transfectant and differentiated HL-60 cells: antagonism of hCCR1 activation by MIP-1beta.* Br J Pharmacol, 2002. 137(5): p. 663-75.

60. Berchiche, Y.A., et al., *Different effects of the different natural CC chemokine receptor 2b ligands on beta-arrestin recruitment, Galphai signaling, and receptor internalization.* Mol Pharmacol, 2011. 79(3): p. 488-98.

61. O'Boyle, G., et al., *Chemokine-mediated inflammation: Identification of a possible regulatory role for CCR2.* Mol Immunol, 2007. 44(8): p. 1944-53.

62. Ogilvie, P., et al., *Unusual chemokine receptor antagonism involving a mitogen-activated protein kinase pathway.* J Immunol, 2004. 172(11): p. 6715-22.

63. Leach, K., S.J. Charlton, and P.G. Strange, *Analysis of second messenger pathways stimulated by different chemokines acting at the chemokine receptor CCR5.* Biochem Pharmacol, 2007. 74(6): p. 881-90.

64. Steen, A., et al., *Biased and constitutive signaling in the CC-chemokine receptor CCR5 by manipulating the interface between transmembrane helices 6 and 7.* J Biol Chem, 2013. 288(18): p. 12511-21.

65. Oppermann, M., et al., *Differential effects of CC chemokines on CC chemokine receptor 5 (CCR5) phosphorylation and identification of phosphorylation sites on the CCR5 carboxyl terminus.* J Biol Chem, 1999. 274(13): p. 8875-85.

66. Byers, M.A., et al., *Arrestin 3 mediates endocytosis of CCR7 following ligation of CCL19 but not CCL21.* J Immunol, 2008. 181(7): p. 4723-32.

67. Zidar, D.A., et al., *Selective engagement of G protein coupled receptor kinases (GRKs) encodes distinct functions of biased ligands.* Proc Natl Acad Sci U S A, 2009. 106(24): p. 9649-54.

68. Kohout, T.A., et al., *Differential desensitization, receptor phosphorylation, beta-arrestin recruitment, and ERK1/2 activation by the two endogenous ligands for the CC chemokine receptor 7.* J Biol Chem, 2004. 279(22): p. 23214-22.

69. Watts, A.O., et al., *Label-free impedance responses of endogenous and synthetic chemokine receptor CXCR3 agonists correlate with Gi-protein pathway activation.* Biochem Biophys Res Comm, 2012. 419(2): p. 412-8.

70. Wilkie, T.M., et al., *Characterization of G-protein alpha subunits in the Gq class: expression in murine tissues and in stromal and hematopoietic cell lines.*Proc Natl Acad Sci U S A, 1991. 88(22): p. 10049-53.

71. Ahn, S., et al., *Differential kinetic and spatial patterns of beta-arrestin and G protein-mediated ERK activation by the angiotensin II receptor.* J Biol Chem, 2004. 279(34): p. 35518-25.

72. Samson, M., et al., *Molecular cloning and functional expression of a new human CC-chemokine receptor gene.* Biochemistry, 1996. 35(11): p. 3362-7.

73. Zabel, B.A., et al., *Elucidation of CXCR7-mediated signaling events and inhibition of CXCR4-mediated tumor cell transendothelial migration by CXCR7 ligands.* J Immunol, 2009. 183(5): p. 3204-11.

74. Rajagopal, S., et al., *Beta-arrestin- but not G protein-mediated signaling by the "decoy" receptor CXCR7.* Proc Natl Acad Sci U S A, 2010. 107(2): p. 628-32.

75. McCulloch, C.V., et al., *Multiple roles for the C-terminal tail of the chemokine scavenger D6.* J Biol Chem, 2008. 283(12): p. 7972-82.

76. Odemis, V., et al., *The presumed atypical chemokine receptor CXCR7 signals through G(i/o) proteins in primary rodent astrocytes and human glioma cells.* Glia, 2012. 60(3): p. 372-81.

77. Cardona, A.E., et al., *Scavenging roles of chemokine receptors: chemokine receptor deficiency is associated with increased levels of ligand in circulation and tissues.* Blood, 2008. 112(2): p. 256-63.

78. Mantovani, A., R. Bonecchi, and M. Locati, *Tuning inflammation and immunity by chemokine sequestration: decoys and more.* Nat Rev Immunol, 2006. 6(12): p. 907-18.

79. Schall, T.J. and A.E. Proudfoot, *Overcoming hurdles in developing successful drugs targeting chemokine receptors.* Nat Rev Immunol, 2011. 11(5): p. 355-63.

80. Lieberman-Blum, S.S., H.B. Fung, and J.C. Bandres, *Maraviroc: a CCR5-receptor antagonist for the treatment of HIV-1 infection.* Clin Ther, 2008. 30(7): p. 1228-50.

81. De Clercq, E., *Recent advances on the use of the CXCR4 antagonist plerixafor (AMD3100, Mozobil) and potential of other CXCR4 antagonists as stem cell mobilizers.* Pharmacol Ther, 2010. 128(3): p. 509-18.

82. Soergel, D.G., et al., *First clinical experience with TRV130: Pharmacokinetics and pharmacodynamics in healthy volunteers.* J Clin Pharmacol, 2013.

83. DeWire, S.M., et al., *A G protein-biased ligand at the mu-opioid receptor is potently analgesic with reduced gastrointestinal and respiratory dysfunction compared with morphine* J Pharmacol Exp Ther, 2013. 344(3): p. 708-17.

84. Jensen, P.C., et al., *Positive versus negative modulation of different endogenous chemokines for CC-chemokine receptor 1 by small molecule agonists through allosteric versus orthosteric binding.* J Biol Chem, 2008. 283(34): p. 23121-8.

85. Tchernychev, B., et al., *Discovery of a CXCR4 agonist pepducin that mobilizes bone marrow hematopoietic cells.* Proc Natl Acad Sci U S A, 2010. 107(51): p. 22255-9.

86. Quoyer, J., et al., *Pepducin targeting the C-X-C chemokine receptor type 4 acts as a biased agonist favoring activation of the inhibitory G protein.* Proc Natl Acad Sci U S A, 2013. 110(52): p. 5088-97.

87. Saita, Y., et al., *Structural basis for the interaction of CCR5 with a small molecule, functionally selective CCR5 agonist.* J Immunol, 2006. 177(5): p. 3116-22.

88. Ferain, T., et al., *Agonist-induced internalization of CC chemokine receptor 5 as a mechanism to inhibit HIV replication.* J Pharmacol Exp Ther, 2011. 337(3): p. 655-62.

# Chapter 3

## Multiple binding sites for small molecule antagonists at the chemokine receptor CCR2

Annelien J.M. Zweemer
Indira Nederpelt
Hilde Vrieling
Sarah Hafith
Maarten L. J. Doornbos
Henk de Vries
Jeffrey Abt
Raymond Gross
Dean Stamos
John Saunders
Martine J. Smit
Adriaan P. IJzerman
Laura H. Heitman

*Molecular Pharmacology* ***2013*** *84(4):551-561*

## Abstract

The chemokine receptor CCR2 is a G protein–coupled receptor that is activated primarily by the endogenous CC chemokine ligand 2 (CCL2). Many different small-molecule antagonists have been developed to inhibit this receptor, as it is involved in a variety of diseases characterized by chronic inflammation. Unfortunately, all these antagonists lack clinical efficacy, and therefore a better understanding of their mechanism of action is warranted. In this study, we examined the pharmacological properties of small-molecule CCR2 antagonists in radioligand binding and functional assays. Six structurally different antagonists were selected for this study, all of which displaced the endogenous agonist $^{125}$I-CCL2 from CCR2 with nanomolar affinity. Two of these antagonists, INCB3344 [*N*-(2-(((3*S*,4*S*)-1-((1*r*,4*S*)-4-(benzo[d][1,3]dioxol-5-yl)-4-hydroxycyclohexyl)-4-ethoxypyrrolidin-3-yl)amino)-2-oxoethyl)-3-(trifluoromethyl)benzamide] and CCR2-RA, were radiolabeled to study the binding site in greater detail. We discovered that [$^{3}$H]-INCB3344 and [$^{3}$H]-CCR2-RA bind to distinct binding sites at CCR2, the latter being the first allosteric radioligand for CCR2. Besides the binding properties of the antagonists, we examined CCR2 inhibition in multiple functional assays, including a novel label-free whole-cell assay. INCB3344 competitively inhibited CCL2-induced G protein activation, whereas CCR2-RA showed a noncompetitive or allosteric mode of inhibition. These findings demonstrated that the CCR2 antagonists examined in this study can be classified into two groups with different binding sites and thereby different modes of inhibition. We have provided further insights in CCR2 antagonism, and these insights are important for the development of novel CCR2 inhibitors.

## Introduction

The CC chemokine receptor 2 (CCR2) is a G protein–coupled receptor that can be activated by the endogenous CC chemokine ligands CCL2, CCL7, CCL8, CCL11, and CCL13. CCR2 is expressed on monocytes, dendritic cells, activated T lymphocytes, and basophils and plays an important role in the immune system [1-3]. These immune cells migrate to increasing concentrations of chemokines at sites of inflammation as part of the immune response, also known as chemotaxis. Besides this important role in physiology, increased levels of CCR2 and its ligands can induce severe tissue damage, resulting in a variety of diseases, such as multiple sclerosis [4], atherosclerosis [5], rheumatoid arthritis [6] and neuropathic pain [7], which makes CCR2 an attractive target for the pharmaceutical industry.



Chemokines are thought to bind to their receptors in a two-step manner. First, they interact with the extracellular side of the receptor, after which the N terminus of the chemokine can enter the interhelical binding pocket in the transmembrane (TM) domain to activate the receptor [8, 9]. This binding pocket of chemokine receptors has been divided into a major binding pocket (TM helices 3, 4, 5, 6 and 7) and a minor binding pocket (TM helices 1, 2, 3 and 7) [10]. Small-molecule antagonists (~600 Da) are at least 10-fold smaller than the endogenous chemokines (~8600 Da), and therefore at best their binding sites can only partly overlap. For CCR2, several mutagenesis studies have provided evidence for the binding of small-molecule antagonists in the major and minor pocket [11-13]. These ligands often contain a positively charged basic nitrogen that interacts with the conserved negatively charged glutamic acid residue (E291) in TM7, which is directly located between the major and minor binding pocket [14]. In addition several other CCR2 antagonists have been developed that do not possess such a basic nitrogen, and their binding site remains to be elucidated [15]. As there is growing evidence of multiple ligand binding sites for other chemokine receptors, we sought to determine if CCR2 contains several binding sites as well.

To gain a better understanding of the interaction of CCR2 and its ligands, we examined the binding sites and pharmacological properties of six chemically distinct CCR2 antagonists. These antagonists are RS504393 (6-methyl-1′-[2-(5-methyl-2-phenyl-4-oxazolyl)ethyl]-spiro[4*H*-3,1-benzoxazine-4,4′-piperidin]-2(1*H*)-one) [11], BMS22 (2-[(isopropylaminocarbonyl)amino]-*N*-[2-[[*cis*-2-[[4-(methylthio)benzoyl]amino]cyclohexyl]amino]-2-oxoethyl]-5-(trifluoromethyl)benzamide) [16], Teijin compound 1 (*N*-[2-[[(3*R*)-1-[(4-chlorophenyl)methyl]-3-pyrrolidinyl]amino]-2-oxoethyl]-3-(trifluoromethyl)benzamide) [17], INCB3344 [*N*-(2-(((3*S*,4*S*)-1-((1*r*,4*S*)-4-(benzo[d][1,3]dioxol-5-yl)-4-hydroxycyclohexyl)-4-ethoxypyrrolidin-3-yl)amino)-2-oxoethyl)-3-(trifluoromethyl)benzamide] [18], the (R)

isomer CCR2-RA-[R] [19] and JNJ-27141491 [(*S*)-3-[3,4-difluorophenyl)-propyl]-5-isoxazol-5-yl-2-thioxo-2,3-dihydro-1*H*-imidazole-4-carboxyl acid methyl ester] [20] (Fig. 1). In this study, for the first time, we provide evidence for two distinct binding sites of small-molecule antagonists at the CCR2 receptor. We also discuss the possible biased antagonism of some of the compounds. This work contributes to a better understanding of the nature of the interactions of diverse ligands at the CCR2 receptor.

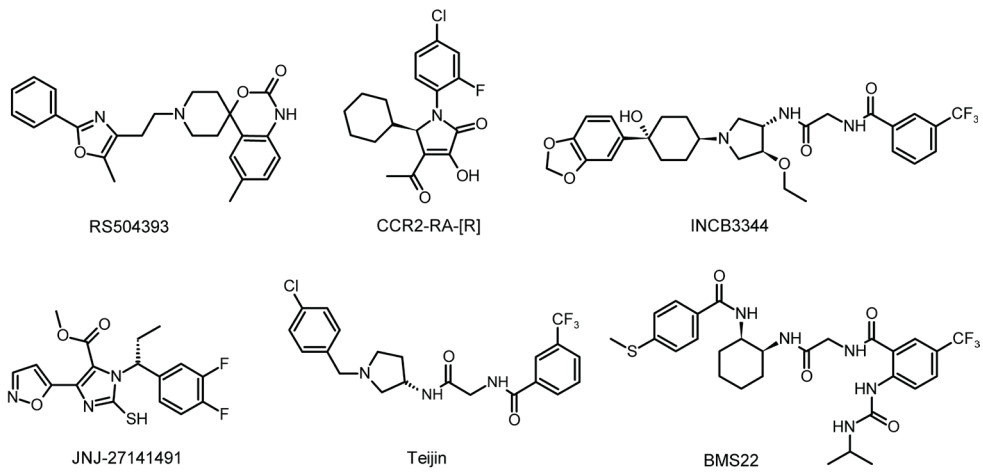



**Fig. 1.** Chemical structures of reference CCR2 small-molecule antagonists.

## Materials and Methods

**Chemicals and reagents.** CCL2 was purchased from PeproTech (Rocky Hill, NJ) and the CCR2 antagonists BMS22 [16], RS504393 [11] and Teijin compound 1 [17] were obtained from Tocris Bioscience (Bristol, UK). INCB3344, JNJ-27141491 and CCR2-RA-[R] were synthesized in-house as described previously [18, 21-23]. [$^3$H]-INCB3344 (specific activity 32 Ci mmol$^{-1}$) was custom-labeled by ViTrax (Placentia, CA), by means of direct titration of the parent ligand. Notably, INCB3344 was labeled as a racemic mixture of the two isomers *N*-(2-(((3*S*,4*S*)-1-((1*r*,4*S*)-4-(benzo[d][1,3]dioxol-5-yl)-4-hydroxycyclohexyl)-4-ethoxypyrrolidin-3-yl)amino)-2-oxoethyl)-3-(trifluoromethyl)benzamide and *N*-(2-(((3*R*,4*R*)-1-((1*r*,4*R*)-4-(benzo[d][1,3]dioxol-5-yl)-4-hydroxycyclohexyl)-4-ethoxypyrrolidin-3-yl)amino)-2-oxoethyl)-3-(trifluoromethyl)benzamide, but only the first isomer had sufficient affinity to label CCR2 in our experiments (see later discussion herein). The racemic radioligand [$^3$H]-CCR2-RA (specific

activity 63 Ci $mmol^{-1}$) was custom-labeled by ViTrax, for which a dehydrogenated precursor of CCR2-RA was provided. CCR2-RA was labeled as a racemic mixture of the two isomers (*R*)-4-acetyl-1-(4-chloro-2-fluorophenyl)-5-cyclohexyl-3-hydroxy-1,5-dihydro-2*H*-pyrrol-2-one and (*S*)-4-acetyl-1-(4-chloro-2-fluorophenyl)-5-cyclohexyl-3-hydroxy-1,5-dihydro-2*H*-pyrrol-2-one. $^{125}$I-CCL2 (2200 Ci/mmol) and guanosine 5′-*O*-(3-[$^{35}$S]thio)triphosphate ([$^{35}$S]GTPγS) (1250 Ci/mmol) were purchased from PerkinElmer (Waltham, MA). Bovine serum albumin (fraction V) was purchased from Sigma-Aldrich (St. Louis, MO). Bicinchoninic acid (BCA) and BCA protein assay reagent were obtained from Pierce Chemical Company (Rockford, IL). Tango CCR2-*bla* U2OS cells stably expressing human CCR2 (U2OS-CCR2) were obtained from Invitrogen (Carlsbad, CA). All other chemicals were obtained from standard commercial sources.



**Cell cultures.** U2OS-CCR2 cells were cultured in McCoy's 5a medium supplemented with 10% fetal calf serum, 2 mM glutamine, 0.1 mM nonessential amino acids, 25 mM HEPES, 1 mM sodium pyruvate, 100 IU/ml penicillin, 100 µg/ml streptomycin, 100µg/ml G418, 50 µg/ml hygromycin, and 125 µg/ml zeocin in a humidified atmosphere at 37 °C and 5% $CO_2$. Cells were subcultured twice weekly at a ratio of 1:6 on 10-cm ø or 15-cm ø plates by trypsinization.

**Cell membrane preparation.** Cells were detached from 15-cm ø plates by scraping into 5 ml of phosphate-buffered saline and subsequently centrifuged for 5 minutes at 3000g. The pellets were resuspended in ice-cold 50 mM Tris-HCl buffer and 5 mM $MgCl_2$, pH 7.4, and homogenized with an Ultra Turrax homogenizer (IKA-Werke GmbH & Co. KG, Staufen, Germany). Membranes and the cytosolic fraction were separated by centrifugation at 31,000g in an Optima LE-80 K ultracentrifuge (Beckman Coulter, Inc., Fullerton, CA) at 4 °C for 20 minutes. The pellet was resuspended in 10 ml of Tris-HCl buffer, and the homogenization and centrifugation steps were repeated. Finally, the membrane pellet was resuspended in 50 mM Tris-HCl buffer and 5 mM $MgCl_2$, pH 7.4, and aliquots of 250 µl were stored at −80 °C. Membrane protein concentrations were measured using a BCA protein determination [24].

**$^{125}$I-CCL2 binding assays.** Binding assays were performed in a 100-µl reaction volume containing 50 mM Tris-HCl buffer (pH 7.4), 5 mM $MgCl_2$, 0.1% 3-[(3-cholamidopropyl)-dimethylammonio]-1-propanesulfonic acid (CHAPS) and 15 µg of membrane protein at 37 °C. For homologous competition experiments, increasing concentrations of CCL2 were incubated with 0.1 nM or 0.05 nM $^{125}$I-CCL2 for 150 minutes. At this concentration, total radioligand binding did not exceed 10% of the amount added to prevent ligand depletion. Nonspecific

binding was determined with 10 µM INCB3344. Displacement assays were performed with 0.1 nM $^{125}$I-CCL2 using 10 concentrations of competing ligand for 150 minutes of incubation. Association experiments were performed with 0.1 nM $^{125}$I-CCL2 at different time intervals of incubation for 3 hours. Nonspecific binding was determined for every time point with 10 µM INCB3344. For dissociation experiments, the membranes were first incubated with 0.1 nM $^{125}$I-CCL2 for 2 hours. Dissociation was initiated by the addition of 10 µM INCB3344 at different time points. For all experiments, incubations were terminated by dilution with ice-cold 50 mM Tris-HCl buffer supplemented with 0.05% CHAPS and 0.5 M NaCl. Separation of bound from free radioligand was performed by rapid filtration through a 96-well GF/B filter plate precoated with 0.25% polyethyleneimine using a PerkinElmer Filtermate-harvester (PerkinElmer, Groningen, The Netherlands). Filters were washed 10 times with ice-cold wash buffer, and 25 µl of Microscint scintillation cocktail (PerkinElmer) was added to each well; the filter-bound radioactivity was determined by scintillation spectrometry using the P-E 1450 Microbeta Wallac Trilux scintillation counter (PerkinElmer).

**[$^3$H]-INCB3344 binding assays.** Binding assays were performed in 100-µl reaction volume containing 50 mM Tris-HCl buffer (pH 7.4), 5 mM $MgCl_2$, 0.1% CHAPS, and 10 µg of membrane protein at 25°C. Saturation experiments were carried out using nine different concentrations of radioligand from 0.5 to 45 nM for 120 minutes of incubation. Nonspecific binding was determined at three concentrations of radioligand with 10 µM BMS22. Displacement assays were carried out with 1.8 nM [$^3$H]-INCB3344 using 10 concentrations of competing ligand for 120 minutes of incubation. Association experiments were performed with 1.8 nM [$^3$H]-INCB3344 at different time intervals of incubation for 150 minutes. For dissociation experiments, the membranes were first incubated with 1.8 nM [$^3$H]-INCB3344 for 90 minutes. Dissociation was initiated by adding 10 µM of BMS22 at different time points. In all cases, total radioligand binding did not exceed 10% of the amount added to prevent ligand depletion. For all experiments, incubations were terminated by dilution with ice-cold 50 mM Tris-HCl buffer supplemented with 0.05% CHAPS. Separation of bound from free radioligand was performed as described in the section entitled "$^{125}$I-CCL2 Binding Assays" using uncoated 96-well GF/B filter plates.

**[$^3$H]-CCR2-RA binding assays.** Assay conditions were similar to those described for [$^3$H]-INCB3344 binding assays. Saturation experiments were carried out using 12 different concentrations of 0.1–75 nM radioligand for 120 minutes of incubation. Nonspecific binding was determined at three concentrations of radioligand with 10 µM JNJ-27141491.

Displacement assays were carried out with 3 nM [$^3$H]-CCR2-RA using six concentrations of competing ligand for 120 minutes of incubation. Association experiments were performed with 3 nM [$^3$H]-CCR2-RA at different time intervals of incubation for 180 minutes. For dissociation experiments, the membranes were first incubated with 3 nM [$^3$H]-CCR2-RA for 90 minutes. Dissociation was initiated by the addition of 10 µM of JNJ-27141491 at different time points. In all cases, total radioligand binding did not exceed 10% of the amount added to prevent ligand depletion. All experiments were terminated as described in "[$^3$H]-INCB3344 Binding Assays."



**Tango** β-arrestin recruitment assay. The assay was performed using the Tango CCR2-*bla* U2OS *β*-arrestin recruitment assay kit (Invitrogen), following the kit protocol. Tango CCR2-*bla* U2OS (U2OS-CCR2) cells were cultured in medium supplemented with 10% dialyzed fetal calf serum (Invitrogen) instead of normal serum for two passages prior to the assay. Briefly, cells were seeded at a density of 40,000 cells per well in Freestyle Expression Medium (Invitrogen) into a black-wall clear-bottom 96-well plate (PerkinElmer). Cells were stimulated with increasing concentrations of CCL2 and incubated for 16 hours at 37 °C and 5% $CO_2$. For antagonist assays, the cells were exposed to increasing concentrations of compound for 30 minutes before stimulation with an $EC_{80}$ concentration (5 nM) of CCL2 for 16 hours at 37 °C and 5% $CO_2$. The final dimethylsulfoxide concentration was 0.1% for all assay points. After agonist exposure, the cells were loaded with 16 µl LiveBLAzer FRET B/G substrate (Invitrogen) for 2 hours at room temperature. After excitation at 400 nm, fluorescence emission values at 460 and 535 nm were measured in an EnVision multilabel plate reader (PerkinElmer). The ratio of the emission at 460 and 535 nm was calculated for each well.

**Label-free whole-cell impedance assay.** The xCELLigence RTCA system (Roche Applied Science, Mannheim, Germany) was used to perform whole-cell assays [25, 26]. Tango CCR2-*bla* U2OS (U2OS-CCR2) cells were cultured in medium supplemented with 10% dialyzed fetal calf serum (Invitrogen) instead of normal serum for two passages before the assay. Initially, 50 µl of culture medium was added to wells in E-plates 96 to obtain background readings, followed by the addition of 50 µl of cell suspension containing 20,000 cells per well. The E-plate containing the cells was left at room temperature for 30 minutes before insertion into the xCELLigence station in the incubator at 37 °C and 5% $CO_2$. The cell index (CI) was monitored overnight every 15 minutes, during which time the cells grew to near confluence. After 16–18 hours, the cells were stimulated with increasing concentrations of CCL2. For the antagonist assays, cells were first preincubated for 30 minutes with increasing concentrations of antagonist or vehicle control that was added in 5 µl of compound solution

(final concentration of 0.25% dimethylsulfoxide). Subsequently, cells were stimulated with an $EC_{80}$ concentration (3 nM) of CCL2. Directly after stimulation, the measurement frequency was increased to 15-second intervals, followed by 30-second, 1-minute, and 5-minute intervals. For data analysis, the CI values were normalized to CI values before ligand addition, and baseline was corrected with CI traces obtained from vehicle control-treated cells.

**[$^{35}$S]GTP$\gamma$S binding assay.** Ten micrograms of membranes were diluted in 100 µl of assay buffer containing 50 mM Tris-HCl buffer (pH 7.4), 5 mM $MgCl_2$, 100 mM NaCl, 1 mM EDTA, 0.05% bovine serum albumin, 10 µM GDP, and 10 µg of saponin per assay point. To determine the $IC_{50}$ values of antagonists, the membranes were preincubated with varying concentrations of antagonist for 30 minutes at 25 °C. Then CCL2 (10 nM) was added, followed by another incubation of 30 minutes; finally, the mixture was incubated for 90 minutes after the addition of [$^{35}$S]GTP$\gamma$S (0.3 nM). To determine the $EC_{50}$ value of CCL2, the membranes were preincubated with varying concentrations of CCL2 in the absence (control) or presence of fixed concentrations of antagonist for 30 minutes at 25 °C. Then [$^{35}$S]GTP$\gamma$S (0.3 nM) was added, and the mixture was incubated for 90 minutes. For all experiments, the incubation was terminated by dilution with ice-cold 50 mM Tris-HCl buffer supplemented with 5 mM $MgCl_2$. Separation of bound from free radioligand was performed as described under "$^{125}$I-CCL2 Binding Assays" using uncoated 96-well GF/B filter plates.

**Data analysis.** All experiments were analyzed using the nonlinear regression curve fitting program Prism 5 (GraphPad, San Diego, CA). The $K_D$ values of [$^3$H]-INCB3344 and [$^3$H]-CCR2-RA were obtained by computer analysis of saturation curves according to the equation bound = $(B_{max}*[L])/([L] + K_D)$, where $B_{max}$ is the maximal number of binding sites (pmol/mg) and $K_D$ is the concentration of radioligand required to reach half-maximal binding. The $K_D$ value of $^{125}$I-CCL2 was calculated from homologous competition experiments using the Cheng-Prusoff equation, assuming that unlabeled and labeled CCL2 had identical affinities [27]. The dissociation rate constant ($k_{off}$) was obtained by computer analysis of the exponential decay of radioligand binding to the receptor. Association rate constants ($k_{on}$) were calculated according to the equation $k_{on} = (k_{obs} - k_{off})/[L]$, where $k_{obs}$, the observed rate constant to approach equilibrium, was obtained by computer analysis of the exponential association, and [$L$] is the amount of radioligand used for the association experiments. All experiments were fit according to monophasic equations except for dissociation of [$^3$H]-CCR2-RA, which occurred in a biphasic manner. From radioligand displacement data, $K_i$ values were calculated from $IC_{50}$ values using the Cheng-Prusoff equation [27]. [$^{35}$S]GTP$\gamma$S, $\beta$-arrestin recruitment and xCELLigence curves were analyzed by nonlinear regression to obtain $IC_{50}$ or $EC_{50}$ values, where xCELLigence peak

responses were obtained within 5 minutes after the addition of compound using the RTCA software 1.2 (ACEA Biosciences, Inc., San Diego, CA). Data shown are the mean ± S.E.M. of at least three separate experiments performed in duplicate. Statistical analysis was performed with a two-tailed unpaired Student's *t* test. Comparison of the means of multiple data sets was performed by one-way analysis of variance, followed by a Tukey's multiple comparison test.



## Results

### Radioligand binding assays

**Characterization of $^{125}$I-CCL2.** In this study, we performed radioligand binding assays for CCR2 with the labeled endogenous agonist $^{125}$I-CCL2 as a tracer ligand. To determine the affinity of $^{125}$I-CCL2 for CCR2, homologous displacement assays were performed on membranes of U2OS cells stably expressing CCR2 (U2OS-CCR2). This resulted in a $K_D$ of 0.068 ± 0.014 nM and a $B_{max}$ of 0.31 ± 0.03 pmol/mg (Fig. 2A; Table 1). Kinetic association and dissociation experiments were performed to determine the rate constants $k_{on}$ and $k_{off}$ (Fig. 2B). Both the association and dissociation of $^{125}$I-CCL2 were best fit by monophasic curves, yielding a $k_{on}$ of 0.29 ± 0.06 $nM^{-1}$ $min^{-1}$ and a $k_{off}$ of 0.033 ± 0.003 $min^{-1}$. The calculated kinetic $K_D$ value ($k_{off}/k_{on}$) of 0.12 nM thus agreed fairly well with the affinity obtained in the homologous competition assay.

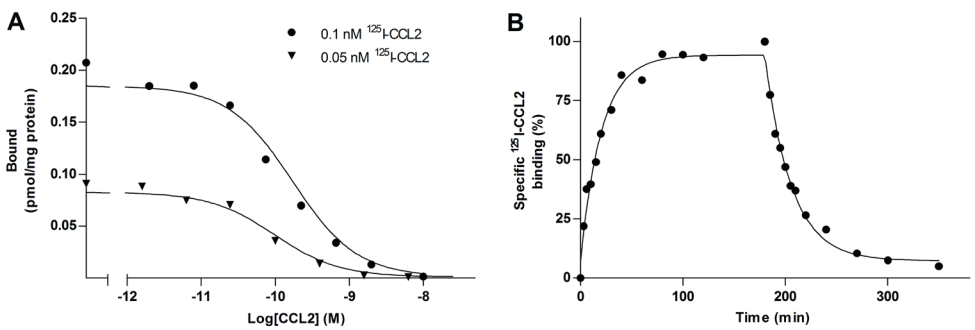



**Fig. 2.** Characterization of $^{125}$I-CCL2 binding to membranes of U2OS cells stably expressing CCR2. (A) Homologous competition assay of 0.1 nM and 0.05 nM $^{125}$I-CCL2 in the presence of increasing concentrations of unlabeled CCL2. Nonspecific binding was determined in the presence of 10 µM INCB3344. (B) Association and dissociation kinetics of 0.1 nM $^{125}$I-CCL2 binding to CCR2 at 37 °C. Dissociation was initiated by the addition of 10 µM INCB3344. Association and dissociation rate constants were 0.29 ± 0.06 $nM^{-1}$ $min^{-1}$ and 0.033 ± 0.003 $min^{-1}$, respectively. Data were best fitted using a one-phase association and one-phase exponential decay function. For all experiments a representative graph of one experiment performed in duplicate is shown (see Table 1 for $K_D$, $B_{max}$ values).

**Table 1.** Equilibrium binding parameters of $^{125}$I-CCL2, [$^3$H]-INCB3344 and [$^3$H]-CCR2-RA, determined on U2OS membranes expressing CCR2.

| | $^{125}$I-CCL2 | [$^3$H]-INCB3344 | [$^3$H]-CCR2-RA |
|---|---|---|---|
| $K_D$ (nM) | 0.068 ± 0.014[a] | 0.90 ± 0.03[b] | 5.8 ± 0.2[c] |
| $B_{max}$ (pmol/mg) | 0.31 ± 0.03[a] | 7.1 ± 0.2[b] | 9.7 ± 0.2[c] |

Data are presented as mean ± S.E.M. of three experiments performed in duplicate.
[a]Homologous displacement of $^{125}$I-CCL2 from CCR2 at 37 ºC.
[b]Saturation binding of 0.5- 45 nM [$^3$H]-INCB3344 to CCR2 at 25 ºC.
[c]Saturation binding of 0.2- 75 nM [$^3$H]-CCR2-RA to CCR2 at 25 ºC.

**Displacement of $^{125}$I-CCL2 from CCR2.** A panel of reference CCR2 antagonists (Fig. 1) was selected for analysis in radioligand displacement assays. U2OS-CCR2 membranes were incubated with$^{125}$I-CCL2 and increasing concentrations of antagonist (Fig. 3A). All antagonists fully displaced $^{125}$I-CCL2 from the CCR2 receptor, with $IC_{50}$ values reported in Table 2. INCB3344 had the highest affinity for CCR2 ($IC_{50}$ = 5.4 nM), followed by BMS22 ($IC_{50}$ = 27 nM), CCR2-RA-[R] ($IC_{50}$ = 103 nM), RS504393 ($IC_{50}$ = 132 nM), JNJ-27141491 ($IC_{50}$ = 172 nM), and Teijin compound 1 ($IC_{50}$ = 220 nM).

**Table 2.** Displacement of $^{125}$I-CCL2, [$^3$H]-INCB3344 and [$^3$H]-CCR2-RA from U2OS membranes expressing CCR2.

| Compound | $^{125}$I-CCL2 displacement $IC_{50}$ ± S.E.M. | [$^3$H]-INCB3344 displacement $K_i$ ± S.E.M. | [$^3$H]-CCR2-RA displacement $K_i$ ± S.E.M. |
|---|---|---|---|
| | *nM* | *nM or % binding* | |
| CCL2 | 0.19 ± 0.04 | 79 ± 2%[a] | 77 ± 4%[a] |
| INCB3344 | 5.4 ± 0.8 | 1.2 ± 0.1 | 169 ± 17%[b]* |
| BMS22 | 27 ± 4 | 5.1 ± 1.3 | 164 ± 16%[b]* |
| RS504393 | 132 ± 25 | 62 ± 3 | 157 ± 16%[b]* |
| Teijin | 220 ± 26 | 107 ± 10 | 159 ± 17%[b]* |
| JNJ-27141491 | 172 ± 15 | 112 ± 3%[b]* | 12 ± 3 |
| CCR2-RA-[R] | 103 ± 18 | 109 ± 1%[b]* | 5.0 ± 0.8 |

Data are presented as mean ± S.E.M. of at least three experiments performed in duplicate.
[a]Percentage of radioligand binding in presence of 100 nM CCL2. 100% was determined in the presence of buffer and therefore values < 100% represent displacement.
[b]Percentage of radioligand binding in presence of 1 μM antagonist. 100% was determined in the presence of buffer and therefore values >100% represent enhancement
*p< 0.05, Student's *t*-test.

The antagonists INCB3344, BMS22, RS504393, and Teijin share structural similarities, whereas JNJ-27141491 and CCR2-RA-[R] form a different set of molecules (Fig. 1). We decided to tritium-label the two high-affinity racemic compounds INCB3344 and CCR2-RA within the two classes, for which we used two unsaturated precursor molecules that we synthesized in-

house. We anticipated that these two molecules would help us to characterize in more detail the binding sites of low-molecular-weight antagonists targeting CCR2.

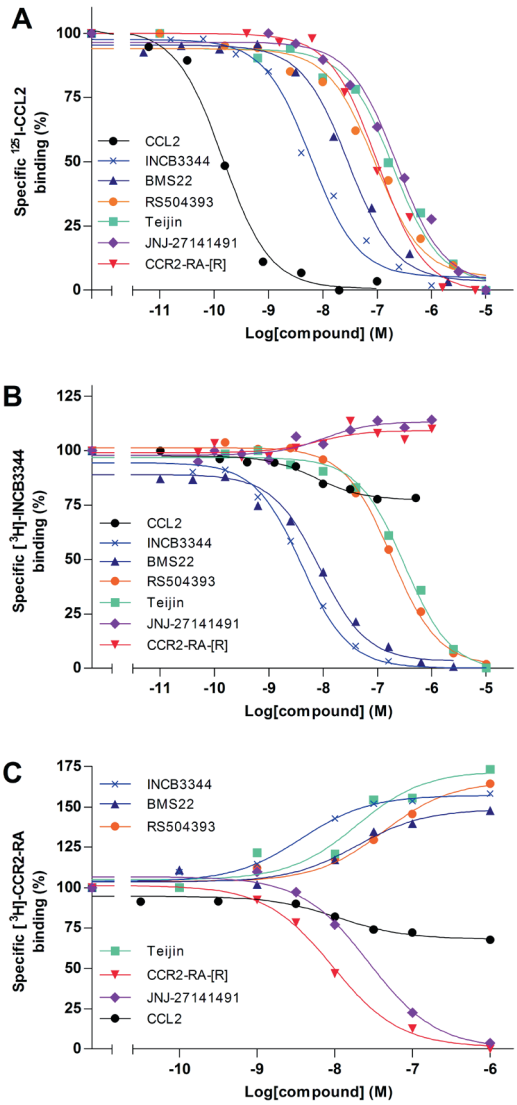



**Fig. 3.** Displacement of (A) $^{125}$I-CCL2 binding, (B) [$^{3}$H]-INCB3344 binding and (C) [$^{3}$H]-CCR2-RA binding to U2OS membranes stably expressing CCR2 by increasing concentrations of CCL2 and six reference CCR2 antagonists. Results are presented as percentage of bound radioligand for one representative experiment performed in duplicate (see Table 2 for affinity values).

**Characterization of [$^3$H]-INCB3344.** Tritium-labeled INCB3344 is a racemic mixture of two isomers. In $^{125}$I-CCL2 displacement experiments with the isolated unlabeled isomers, we had found that the (3*S*,4*S*) isomer had an $IC_{50}$ of 3.8 ± 0.5 nM, whereas the affinity of the other isomer was at least 1000-fold lower ($IC_{50}$ = 4.3 ± 0.9 $\mu$M). Since we used low nanomolar concentrations (1.8 nM) of [$^3$H]-INCB3344 in the binding studies, we concluded that CCR2 was solely labeled by the high affinity (3*S*,4*S*) isomer.

Saturation binding experiments yielded a $K_D$ of 0.90 ± 0.03 nM with a $B_{max}$ of 7.1 ± 0.2 pmol/mg (Fig. 4; Table 1). Equilibrium binding of [$^3$H]-INCB3344 to U2OS-CCR2 membranes was reached within 1 hour at 25 °C as assessed with kinetic association experiments (Fig. 4B). This radioligand was specifically bound to CCR2 as no binding was detected in U2OS membranes that do not express CCR2 (data not shown). Dissociation of [$^3$H]-INCB3344 was initiated by 10 $\mu$M BMS22 and resulted in a dissociation half-life of 53 minutes at 25 °C (Fig. 4B). Both kinetic studies were best fit by monophasic curves, which confirmed that CCR2 was labeled by only one of the isomers. From these data, we calculated the association and dissociation rate constants, 0.054 ± 0.002 $nM^{-1}$ $min^{-1}$ and 0.013 ± 0.002 $min^{-1}$, respectively, which resulted in a kinetic $K_D$ of 0.23 nM, in fair agreement with the equilibrium value of 0.90 nM.

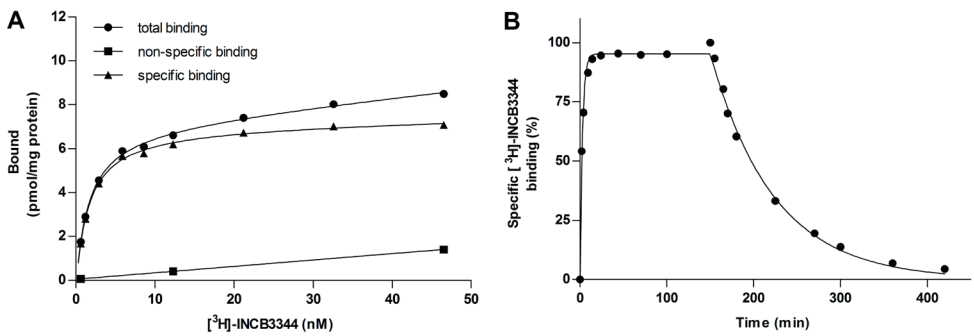



**Fig. 4.** Characterization of [$^3$H]-INCB3344 binding to membranes of U2OS cells stably expressing CCR2. (A) Saturation binding of [$^3$H]-INCB3344 to CCR2. Different concentrations of [$^3$H]-INCB3344 were incubated in the presence (nonspecific binding) or absence (total binding) of 10 µM BMS22. Specific binding was determined by subtracting the nonspecific binding from the total binding. (B) Association and dissociation kinetics of 1.8 nM [$^3$H]-INCB3344 to CCR2 at 25 °C. Dissociation was initiated by the addition of 10 µM BMS22. Association and dissociation rate constants were 0.054 ± 0.002 $nM^{-1}$ $min^{-1}$ and 0.013 ± 0.002 $min^{-1}$, respectively. Data were best fitted using a one-phase association and one-phase exponential decay function. For all experiments a representative graph of one experiment performed in duplicate is shown (see Table 1 for $K_D$, $B_{max}$ values).

**Displacement of [$^3$H]-INCB3344 from CCR2.** Homologous displacement by INCB3344 yielded a $K_i$ of 1.2 ± 0.2 nM (Fig. 3B;Table 2), which corresponded to the $K_D$ that was obtained from saturation binding experiments. CCL2 displaced only 21% of bound [$^3$H]-INCB3344 from the receptor. The antagonists BMS22, RS504393, and Teijin were able to displace fully [$^3$H]-INCB3344 from CCR2 with nanomolar affinities, whereas JNJ-27141491 and CCR2-RA-[R] did not displace [$^3$H]-INCB3344, which indicates that they bind at different sites at the CCR2 receptor. At a concentration of 1 $\mu$M, JNJ-27141491 and CCR2-RA-[R] rather significantly increased [$^3$H]-INCB3344 binding, with 12 and 9% (Student's *t* test $p < 0.01$; Table 2), respectively.



**Characterization of [$^3$H]-CCR2-RA.** CCR2-RA was also tritium-labeled as a racemic mixture of two isomers. In $^{125}$I-CCL2 displacement experiments, the unlabeled (*R*) and (*S*) isomers had $IC_{50}$ values of 103 ± 18 and 216 ± 21 nM, respectively. We therefore cannot exclude that CCR2 was labeled to some extent by the lower-affinity isomer, too, although we took care to use a low concentration of 3 nM in the displacement assays. Saturation binding experiments yielded a $K_D$ of 5.8 ± 0.2 nM with a $B_{max}$ of 9.7 ± 0.2 pmol/mg (Fig. 5A; Table 1). Equilibrium binding of [$^3$H]-CCR2-RA to U2OS-CCR2 membranes was reached within 2 hours at 25 °C as assessed with kinetic association experiments after a monophasic fit (Fig. 5B). This radioligand was specifically bound to CCR2 as no binding was detected in U2OS membranes that do not express CCR2 (data not shown). Dissociation of [$^3$H]-CCR2-RA was initiated by 10 $\mu$M of JNJ-27141491 and resulted in a biphasic dissociation pattern with $k_{off1}$ and $k_{off2}$ of 0.24 ± 0.02 $min^{-1}$ and 0.029 ± 0.005 $min^{-1}$, respectively (Fig. 5C).

**Displacement of [$^3$H]-CCR2-RA from CCR2.** CCL2 displaced only 23% of bound [$^3$H]-CCR2-RA from the receptor (Fig. 3C; Table 2). The antagonists JNJ-27141491 and the unlabeled (R) isomer CCR2-RA-[R] were able to displace fully [$^3$H]-CCR2-RA from CCR2 with nanomolar affinities, whereas antagonists INCB3344, BMS22, RS504393, and Teijin did not displace [$^3$H]-CCR2-RA, suggesting that they bind at a different site at the CCR2 receptor. In contrast, INCB3344, BMS22, RS504393, and Teijin significantly increased [$^3$H]-CCR2-RA binding with 69, 64, 57, and 59% at a concentration of 1 $\mu$M, respectively (Student's *t* test $p < 0.05$; Table 2).

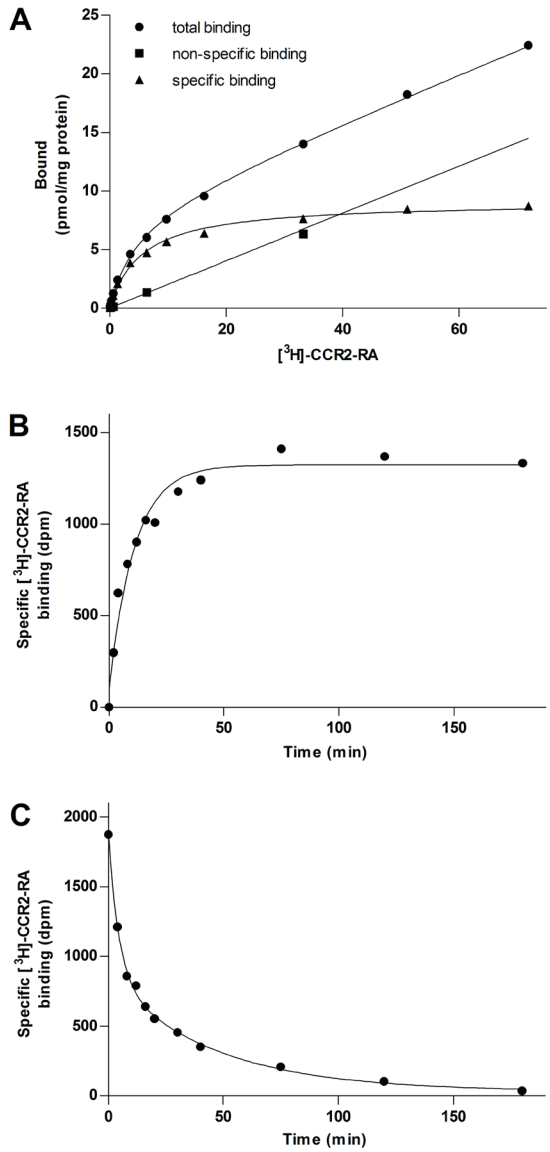



**Fig. 5.** Characterization of [$^3$H]-CCR2-RA binding to membranes of U2OS cells stably expressing CCR2. (A) Saturation binding of [$^3$H]-CCR2-RA to CCR2. Different concentrations of [$^3$H]-CCR2-RA were incubated in the presence (nonspecific binding) or absence (total binding) of 10 µM JNJ-27141491. Specific binding was determined by subtracting the nonspecific binding from the total binding. (B) Association kinetics of 3 nM [$^3$H]-CCR2-RA to CCR2 at 25 °C. Data were best fitted using a one-phase association function resulting in a $k_{obs}$ of 0.089 ± 0.005 min$^{-1}$. (C) Dissociation kinetics of 3 nM [$^3$H]-CCR2-RA to CCR2 at 25 °C. Dissociation was initiated by the addition of 10 µM JNJ-27141491. Data were best fitted using a two-phase exponential decay function, resulting in a $k_{off1}$ of 0.24 ± 0.02 min$^{-1}$ and a $k_{off2}$ of 0.029 ± 0.005 min$^{-1}$. For all experiments a representative graph of one experiment performed in duplicate is shown (see Table 1 for $K_D$, $B_{max}$ values).

## Functional assays

In addition to radioligand binding experiments, we performed a number of functional assays, both G protein–dependent and –independent.

**Inhibition of beta-arrestin recruitment to CCR2.** We first performed beta-arrestin recruitment assays (G protein–independent) to assess the inhibitory potency of all six antagonists. CCL2 induced beta-arrestin recruitment to CCR2 with an $EC_{50}$ of 1.4 ± 0.4 nM (n = 4) (Fig. 6A). All antagonists were able to inhibit beta-arrestin recruitment induced by 5 nM CCL2 (Fig. 6B; Table 3). Interestingly, JNJ-27141491 and CCR2-RA-[R] were more potent inhibitors of *β*-arrestin recruitment than were Teijin and RS504393, whereas these antagonists showed equal affinities in the $^{125}$I-CCL2 displacement assay.

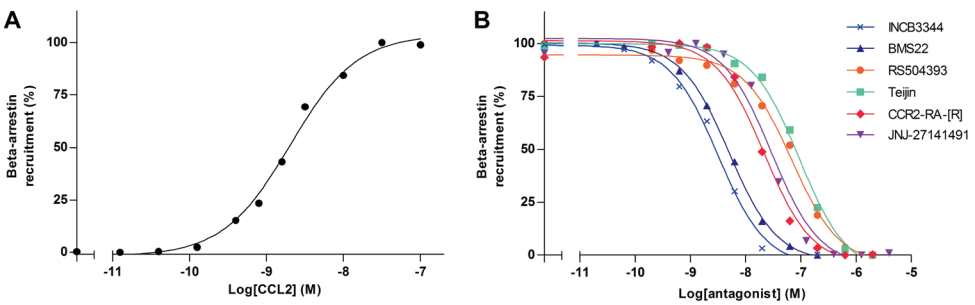



**Fig. 6.** (A) CCL2-induced beta-arrestin recruitment to U2OS cells stably expressing CCR2. (B) Inhibition of CCL2-induced beta-arrestin recruitment to CCR2. Cells were incubated with a concentration of CCL2 that evoked 80% of the maximum response (5 nM). Increasing concentrations of the antagonists were added to determine their $IC_{50}$ value. For all experiments, basal activity was set at 0%, and the maximum response at 100%. Results are presented for one representative experiment performed in duplicate (see Table 3 for $IC_{50}$ values).

**Table 3.** Inhibition of CCL2 induced cellular responses measured in [$^{35}$S]GTPγS membrane binding assays as well as beta-arrestin recruitment and xCELLigence label free whole cell assays.

| Compound | [$^{35}$S]GTPγS binding inhibition $IC_{50}$ ± S.E.M. (nM) | Beta-arrestin recruitment inhibition $IC_{50}$ ± S.E.M. (nM) | xCELLigence[a] $IC_{50}$ ± S.E.M. (nM) |
|---|---|---|---|
| INCB3344 | 2.8 ± 0.8 | 3.2 ± 0.2 | 2.0 ± 0.5 |
| BMS22 | 5.5 ± 1.8 | 4.8 ± 0.4 | 21 ± 6* |
| RS504393 | 19 ± 7** | 68 ± 3 | 87 ± 15 |
| Teijin | 183 ± 48 | 67 ± 13 | 292 ± 66* |
| JNJ-27141491 | 3.9 ± 1.0** | 29 ± 1 | 25 ± 4 |
| CCR2-RA-[R] | 24 ± 3 | 25 ± 4 | 64 ± 14*** |

Data are presented as mean ± S.E.M. of three experiments performed in duplicate.
[a]Inhibition of CCL2 was calculated from concentration-response curves derived from peak-analysis of CI changes.
*p<0.05, vs. beta-arrestin data; ANOVA, Tukey's MCT.
**p<0.05, vs. beta-arrestin and xCELLigence data; ANOVA, Tukey's MCT.
***p<0.05, vs. [$^{35}$S]GTPγS and beta-arrestin data; ANOVA, Tukey's MCT.

**Analysis of CCR2 inhibition in an impedance-based label-free whole-cell assay.** The xCELLigence RTCA system was used to study the activation and inhibition of CCR2 in a label-free whole-cell assay. Typically, the addition of CCL2 resulted in an immediate dose-dependent increase in the CI to a peak level within 5 minutes, followed by a second peak after approximately 20 minutes, which then returned to baseline after 1 hour of incubation (Fig. 7A). Concentration-effect curves were obtained by analysis of the peak level that appeared within 5 minutes after stimulation and resulted in an $EC_{50}$ value of 1.1 ± 0.1 nM for CCL2 (n = 5) (Fig. 7B). Preincubation with all antagonists resulted in inhibition of the CCL2-induced response (Fig. 7C; Table 3). The antagonists were equally potent as inhibitors of CCL2-induced impedance effects as they were able to inhibit *β*-arrestin recruitment, except for Teijin and CCR2-RA-[R], which were less potent as inhibitors of the impedance response with $IC_{50}$ values of 292 ± 66 nM and 64 ± 14 nM, respectively.

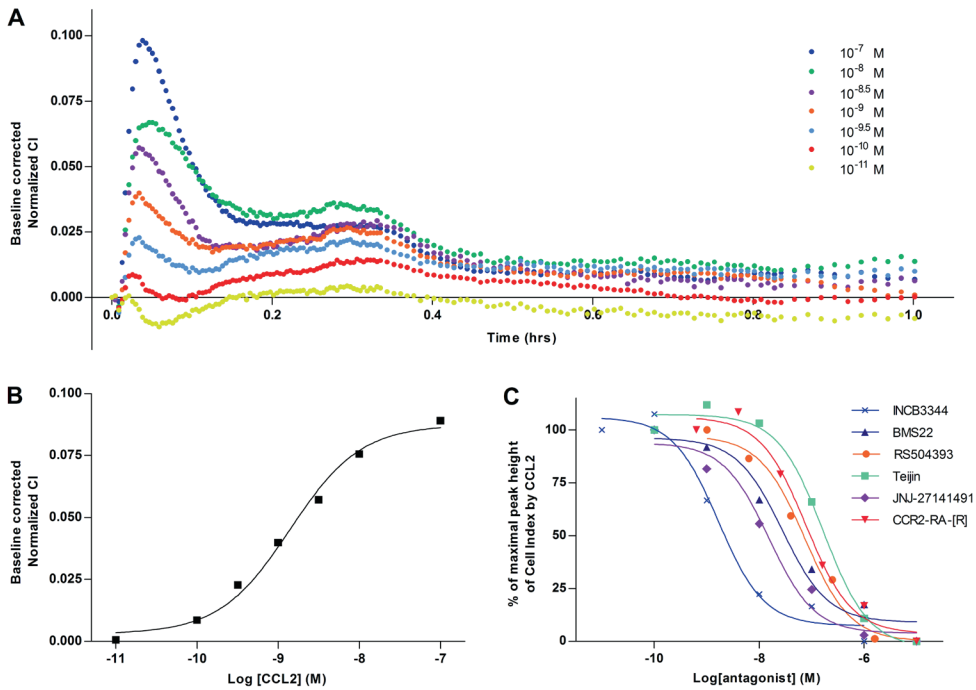



**Fig. 7.** Impedance measurements in the xCELLigence label-free assay for U2OS cells stably expressing CCR2. (A) Representative graph of baseline-corrected normalized CI after the addition of different concentrations of CCL2. (B) Concentration-response curve for CCL2 derived from peak-height analysis of CI changes for the 5-minute interval after application. (C) Inhibition of CCL2-induced impedance measurements. Cells were incubated with a concentration of CCL2 that evoked 80% of the maximum response (3 nM). Increasing concentrations of the antagonists were added 30 min before agonist stimulation to determine their $IC_{50}$ value, derived from peak-height analysis of CI changes for the 5-minute interval after the application of CCL2. Results are presented for one representative experiment performed in duplicate (see Table 3 for $IC_{50}$ values).

**[$^{35}$S]GTPγS binding to CCR2.** We also performed a G protein–dependent functional assay. For this purpose, we used a [$^{35}$S]GTP*γ*S binding assay on U2OS-CCR2 membranes, where we measured G protein activation by CCL2 in the absence or presence of different antagonists (Fig. 8). CCL2 stimulated [$^{35}$S]GTP*γ*S binding with an $EC_{50}$ value of 5.7 ± 0.9 nM (n = 8; see also, Fig. 8, B and C). All antagonists were able to inhibit CCL2-induced G protein activation (Fig. 8A; Table 3). Notably, RS504393 and JNJ-27141491 were more potent inhibitors of G protein activation than of *β*-arrestin recruitment or the impedance response evoked by CCL2, their $IC_{50}$ values being 19 ± 7 nM and 3.9 ± 1.0 nM, respectively.

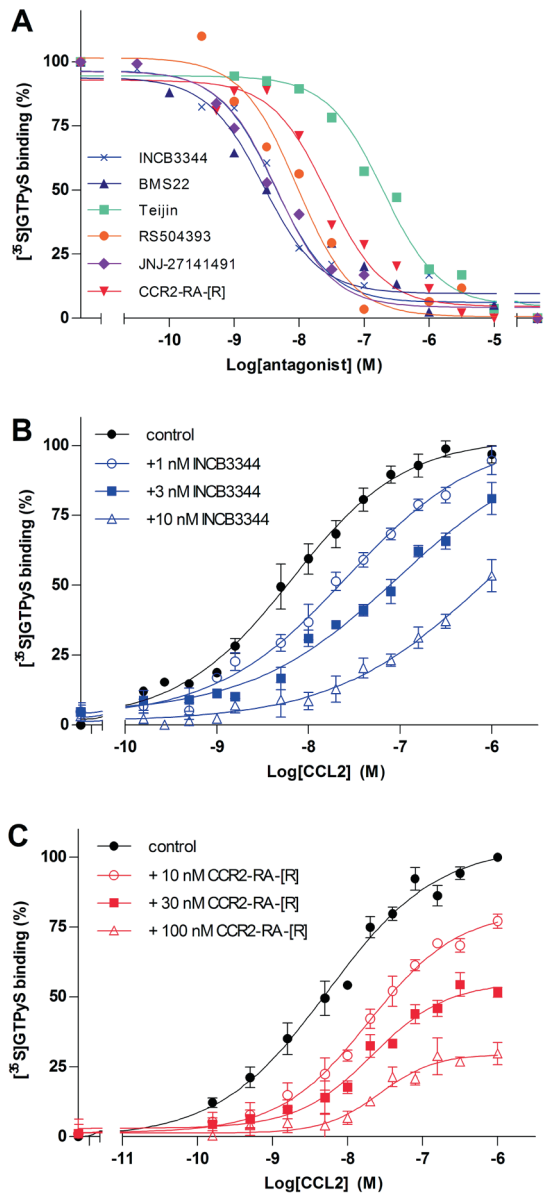



**Fig. 8.** [$^{35}$S]GTPγS binding to membranes of U2OS cells stably expressing CCR2. (A) Inhibition of CCL2-induced [$^{35}$S]GTPγS binding by six small molecule antagonists. Membranes were incubated with a concentration of CCL2 that evoked 80% of the maximum response (10 nM). Increasing concentrations of the antagonists were added to determine their $IC_{50}$ value. (B,C) Concentration-effect curves of CCL2-induced [$^{35}$S]GTPγS binding. Increasing concentrations of CCL2 were added simultaneously with indicated concentrations of INCB3344 (B) or CCR2-RA-[R] (C). For all experiments basal activity was set at 0% and the maximum response at 100%. Results are presented as mean percentage ± S.E.M. of three experiments performed in duplicate (see Table 4 for $pEC_{50}$ and $E_{max}$ values).

Based on the displacement data obtained with [$^3$H]-INCB3344 and [$^3$H]-CCR2-RA, INCB3344 and CCR2-RA-[R] were selected as representative antagonists for the two putative distinct binding sites. To examine their mechanism of inhibition in more detail, we analyzed the shift of CCL2-induced [$^{35}$S]GTPγS binding in the presence of fixed concentrations of antagonist. The maximal effect of CCL2 in the presence of CCR2-RA-[R] was significantly reduced, whereas CCL2's potency was slightly, but similarly, decreased at all three antagonist concentrations (Fig. 8C; Table 4). In contrast, the addition of INCB3344 markedly decreased the $EC_{50}$ value of CCL2, whereas the efficacy of CCL2 was unaffected (Fig. 8B; Table 4). A Schild plot analysis of the INCB3344 data yielded a $K_B$ value of 0.4 nM, which is in close agreement with the $K_D$ value of 0.9 nM determined in the saturation binding assay. Overall, these data indicate that INCB3344 behaved as a competitive antagonist, whereas CCR2-RA-[R] clearly showed noncompetitive antagonism for CCR2 with respect to CCL2, as indicated by a decrease in CCL2's efficacy in the presence of increasing concentrations of CCR2-RA-[R].



**Table 4.** G protein activation by CCL2 measured by [$^{35}$S]GTPγS binding. Potency and maximum effect of CCL2 in the absence or presence of different concentrations of CCR2-RA-[R].

| | **$pEC_{50}$ ± S.E.M.** | **$E_{max}$ ± S.E.M. (%)** |
|---|---|---|
| control | 8.3 ± 0.1 | 104 ± 4 |
| + 1 nM INCB3344 | 7.6 ± 0.1* | 103 ± 7 |
| + 3 nM INCB3344 | 7.0 ± 0.3* | 102 ± 14 |
| + 10 nM INCB3344 | 6.2 ± 0.9 | ND[a] |
| + 10 nM CCR2-RA-[R] | 7.7 ± 0.1* | 81 ± 6** |
| + 30 nM CCR2-RA-[R] | 7.7 ± 0.1* | 55 ± 4*** |
| + 100 nM CCR2-RA-[R] | 7.6 ± 0.1* | 30 ± 3*** |

[a]Not determined.
Data are presented as mean ± S.E.M. of at least three experiments (*p<0.05,** p< 0.001, *** p< 0.0001 vs. control, Student's *t*-test)

## Discussion

Previous studies reported CCR2 and its endogenous ligand CCL2 as major players in a variety of diseases [4, 5, 7]. Given this potential role as a drug target, the pharmaceutical industry has developed many CCR2 antagonists [15], although without much clinical success. Given the variety in chemical scaffolds, it is surprising that little attention, if any, has been paid to the binding mode of these ligands to the receptor. Therefore, the present study was designed to compare the binding site and mechanism of inhibition for a selection of these antagonists.

To study the binding of these antagonists to CCR2, we used the radioligand $^{125}$I-CCL2 and the custom-labeled small-molecule radioligands [$^3$H]-INCB3344 and [$^3$H]-CCR2-RA. We

found an affinity constant of 0.068 nM for $^{125}$I-CCL2, which corresponds to reported data in literature ($K_D$ 0.05 nM) [28, 29]. In addition, the dissociation rate constant of $^{125}$I-CCL2 from U2OS-CCR2 membranes of 0.033 $min^{-1}$ is in agreement with the previously reported $k_{off}$ of 0.036 $min^{-1}$ [28]. [$^3$H]-INCB3344 was previously published and characterized as a radioligand for CCR2 [30]. In those studies a $K_D$ value of 5 nM was reported for human embryonic kidney 293 cells stably expressing CCR2. Our experiments with U2OS-CCR2 cells resulted in a 5-fold lower $K_D$ value of 0.9 nM. This difference could be the result of the different cell type, different assay buffer, or the longer incubation time used in our assay.

In this study, [$^3$H]-CCR2-RA is reported as the first allosteric radioligand for CCR2. It was characterized as a high-affinity radioligand ($K_D$ = 5.8 nM) that reversibly binds to the receptor. The biphasic dissociation of [$^3$H]-CCR2-RA from CCR2 could be a result of the racemic nature of the radioligand. The $B_{max}$ values for [$^3$H]-CCR2-RA and [$^3$H]-INCB3344 were 31- and 23-fold higher than for $^{125}$I-CCL2. A possible explanation might be that some of the receptors present in vesicular structures in the membrane preparations are accessible to membrane-permeable molecules, such as CCR2-RA and INCB3344, but not to CCL2. In addition, allosteric interactions described within chemokine receptor oligomers might modify the apparent number of binding sites for some radioligands [31, 32]. Finally, antagonists like CCR2-RA and INCB3344 supposedly bind to the G protein–coupled state as well as the uncoupled state of the receptor, whereas the agonist CCL2 presumably binds only to the G protein–coupled state (i.e., labeling a smaller population of receptors). This was confirmed by experiments in the presence of GTP, which uncouples the receptor from its G protein, since these resulted in a complete loss of binding of $^{125}$I-CCL2, whereas binding of [$^3$H]-INCB3344 and [$^3$H]-CCR2-RA was not affected (data not shown). Similar extensive differences in $B_{max}$ values between radiolabeled agonist and antagonist have previously been reported for the CXCR2 chemokine receptor [33]. In any case, the three radioligands do not label the same receptor populations, which may therefore contribute to the different $IC_{50}$ values derived from competition experiments performed with either CCL2 or a small molecule as a radioligand.

INCB3344 and CCR2-RA-[R] were able to displace fully $^{125}$I-CCL2 receptor binding, whereas CCL2 was capable only of displacing 21% of [$^3$H]-INCB3344 binding and 19% of [$^3$H]-CCR2-RA binding. This finding could be explained by the heterogeneity of binding sites and the G protein–uncoupling of a fraction of CCR2. In addition, the incomplete displacement could suggest that CCL2, INCB3344, and CCR2-RA bind to different sites at CCR2. Given the size of INCB3344 (578 Da) and CCR2-RA (352 Da), these ligands can at best only partly overlap with the binding site of the large peptide CCL2 (8600 Da).

The three different radioligands were used to study and compare six structurally different CCR2 antagonists. All antagonists displaced $^{125}$I-CCL2 from the receptor (Fig. 3A; Table 2) with

affinities similar to previously reported data [11, 16-18, 20, 21]. BMS22, RS504393, and Teijin were also able to displace [$^3$H]-INCB3344 binding, which indicated that these four ligands share a common binding site. On the contrary, JNJ-27141491 and CCR2-RA-[R] did not displace [$^3$H]-INCB3344 from CCR2 (Fig. 3B). Analogous results were found in the [$^3$H]-CCR2-RA displacement assay, where INCB3344, BMS22, RS504393, and Teijin did not displace [$^3$H]-CCR2-RA from CCR2 (Fig. 3C). Therefore, we conclude that there are at least two different binding sites for small-molecule antagonists at CCR2. Notably, at high concentrations, JNJ-27141491 and CCR2-RA-[R] significantly increased [$^3$H]-INCB3344 binding to CCR2, whereas INCB3344, BMS22, RS504393, and Teijin significantly increased [$^3$H]-CCR2-RA binding to CCR2 (Table 2). This behavior is indicative for allosteric enhancement, best explained by the two compounds stabilizing the same conformation of the receptor by binding at two topographically different sites [34].



For RS504393, Teijin and BMS22 mutagenesis studies have shown that these molecules bind to the major and/or minor binding pocket of CCR2. RS504393 and Teijin interact with the highly conserved glutamic acid residue E291 most likely via their basic nitrogen atom [11, 13]. For BMS22, the adjacent T292 was found to be important for binding [16], indicating that it shares the same binding pocket as RS504393 and Teijin. Notably, for INCB3344 no such data has been reported yet and here we established that it binds to the same site as RS504393, Teijin and BMS22. The presence of a basic nitrogen in the pyrrolidine ring of INCB3344 suggests a similar interaction with E291.

The structures of JNJ-27141491 and CCR2-RA-[R] contain different chemical features compared with the other antagonists. JNJ-27141491 and CCR2-RA-[R] lack a basic nitrogen, have a lower molecular weight, and are acidic. Their exact binding site or sites at CCR2 remain to be determined. For several other chemokine receptors, the presence of an allosteric binding site has been reported [35]. Whereas some antagonists interact with both the major and minor binding pocket in the transmembrane region, others bind exclusively to either one of these sites. Given the large size of this binding pocket, the two different binding sites that we have identified for CCR2 could both be located in this transmembrane region. In addition, an allosteric binding site on the intracellular side of the receptor in the C-terminal domain has been identified for the chemokine receptors CXCR2, CCR4 and CCR5 [36-38]. This binding site resides close to the site of G protein coupling to the receptor and therefore it is assumed that activation of the G protein is prevented in the presence of an antagonist at this site. The intracellular antagonists of CXCR2 contain an acidic centre [37], which is also present in JNJ-27141491 and CCR2-RA-[R]. In addition, CCR2 and CCR5 are closely related based on sequence similarity. Hence, the presence of such an intracellular binding site for CCR2 is not unlikely.

By means of functional assays, we confirmed that the six compounds described in this article are indeed CCR2 antagonists, at the G protein level, in β-arrestin recruitment and in a novel label-free impedance-based functional assay (Table 3). Analysis of these differential functional responses allowed us to explore whether these ligands show biased antagonism, which has been described for allosteric ligands of other G protein–coupled receptors [39, 40]. Notably, it has been reported that some CCR2 antagonists are capable of discriminating between different functional states of the receptor [41]. In our hands, RS504393 and JNJ-27141491 were slightly more potent inhibitors of G protein activation, whereas Teijin was most potent in the β-arrestin recruitment assay. Except for these small but significant differences, all antagonists were equally potent among the different functional assays, and as such there is little indication of biased antagonism in our assays. As the effect in functional assays is dependent on the off-rate of the antagonists, which are at present unknown, we realize that it is difficult to compare the three functional assays as their incubation times varies from minutes to hours.

We next determined the mechanism of inhibition in a [$^{35}$S]GTPγS assay for INCB3344 and CCR2-RA-[R] as representative compounds binding to different binding sites. INCB3344 behaved as a competitive antagonist, whereas CCR2-RA-[R] showed noncompetitive antagonism for CCR2 with respect to CCL2 (Fig. 7). Agonist stimulation after pre-incubation with an antagonist can result in submaximal receptor stimulation if the antagonist is not sufficiently dissociated to liberate the entire population at the time at which the maximal response is measured [42]. Therefore, we coincubated increasing concentrations of CCL2 in the presence of fixed amounts of antagonist to rule out insurmountable antagonism resulting from slow dissociation kinetics. The mechanism of INCB3344 inhibition was previously addressed in a calcium flux assay in human monocytes and a competition binding assay using $^{125}$I-CCL2 [30]. Both experiments showed a competitive mode of inhibition with respect to CCL2. These results are in good agreement with our competitive profile of INCB3344 in the [$^{35}$S]GTPγS assay.

For CCR2-RA-[R], no detailed pharmacological data were previously published except for its inhibition of pain behavior in an in vivo model with nerve-injured rats [19]. We now provide evidence for a noncompetitive mode of inhibition of CCR2. Based on the results of our binding studies, we assume that CCR2-RA-[R] and JNJ-27141491 bind to a similar site at CCR2 or at least bind to a site that is distinct from the INCB3344's binding pocket. Since JNJ-27141491 was previously described as a noncompetitive antagonist of CCR2, it is likely that CCR2-RA-[R] and JNJ-27141491 bind and inhibit CCR2 via a similar mechanism [20].

In summary, we have demonstrated that the CCR2 antagonists examined in this study can be classified into at least two groups with a different binding site and thereby a different mode of inhibition. Hence, we have provided further insights into CCR2 antagonism, which may be relevant for the development of novel CCR2 inhibitors.

## References


1. Jimenez, F., et al., *CCR2 plays a critical role in dendritic cell maturation: possible role of CCL2 and NF-kappa B.* J Immunol. 184(10): p. 5571-81.
2. Luster, A.D., *Chemokines--chemotactic cytokines that mediate inflammation.* N Engl J Med, 1998. 338(7): p. 436-45.
3. Fantuzzi, L., et al., *Loss of CCR2 expression and functional response to monocyte chemotactic protein (MCP-1) during the differentiation of human monocytes: role of secreted MCP-1 in the regulation of the chemotactic response.* Blood, 1999. 94(3): p. 875-83.
4. Mahad, D.J. and R.M. Ransohoff, *The role of MCP-1 (CCL2) and CCR2 in multiple sclerosis and experimental autoimmune encephalomyelitis (EAE).* Semin Immunol, 2003. 15(1): p. 23-32.
5. Boring, L., et al., *Decreased lesion formation in CCR2-/- mice reveals a role for chemokines in the initiation of atherosclerosis.* Nature, 1998. 394(6696): p. 894-7.
6. Quinones, M.P., et al., *The complex role of the chemokine receptor CCR2 in collagen-induced arthritis: implications for therapeutic targeting of CCR2 in rheumatoid arthritis.* J Mol Med (Berl), 2005. 83(9): p. 672-81.
7. White, F.A., S.K. Bhangoo, and R.J. Miller, *Chemokines: integrators of pain and inflammation.* Nat Rev Drug Discov, 2005. 4(10): p. 834-44.
8. Pease, J.E., et al., *The N-terminal extracellular segments of the chemokine receptors CCR1 and CCR3 are determinants for MIP-1alpha and eotaxin binding, respectively, but a second domain is essential for efficient receptor activation.* J Biol Chem, 1998. 273(32): p. 19972-6.
9. Monteclaro, F.S. and I.F. Charo, *The amino-terminal domain of CCR2 is both necessary and sufficient for high affinity binding of monocyte chemoattractant protein 1. Receptor activation by a pseudo-tethered ligand.* J Biol Chem, 1997. 272(37): p. 23186-90.
10. Surgand, J.S., et al., *A chemogenomic analysis of the transmembrane binding cavity of human G-protein-coupled receptors.* Proteins, 2006. 62(2): p. 509-38.
11. Mirzadegan, T., et al., *Identification of the binding site for a novel class of CCR2b chemokine receptor antagonists: binding to a common chemokine receptor motif within the helical bundle.* J Biol Chem, 2000. 275(33): p. 25562-71.
12. Berkhout, T.A., et al., *CCR2: characterization of the antagonist binding site from a combined receptor modeling/mutagenesis approach.* J Med Chem, 2003. 46(19): p. 4070-86.
13. Hall, S.E., et al., *Elucidation of binding sites of dual antagonists in the human chemokine receptors CCR2 and CCR5.* Mol Pharmacol, 2009. 75(6): p. 1325-36.
14. Rosenkilde, M.M. and T.W. Schwartz, *GluVII:06--a highly conserved and selective anchor point for non-peptide ligands in chemokine receptors.* Curr Top Med Chem, 2006. 6(13): p. 1319-33.
15. Struthers, M. and A. Pasternak, *CCR2 antagonists.* Curr Top Med Chem, 2010. 10(13): p. 1278-98.
16. Cherney, R.J., et al., *Discovery of disubstituted cyclohexanes as a new class of CC chemokine receptor 2 antagonists.* J Med Chem, 2008. 51(4): p. 721-4.
17. Moree, W.J., et al., *Potent antagonists of the CCR2b receptor. Part 3: SAR of the (R)-3-aminopyrrolidine series.* Bioorg Med Chem Lett, 2008. 18(6): p. 1869-73.
18. Brodmerkel, C.M., et al., *Discovery and pharmacological characterization of a novel rodent-active CCR2 antagonist, INCB3344.* J Immunol, 2005. 175(8): p. 5370-8.
19. Bhangoo, S., et al., *Delayed functional expression of neuronal chemokine receptors following focal nerve demyelination in the rat: a mechanism for the development of chronic sensitization of peripheral nociceptors.* Mol Pain, 2007. 3(38).

20. Buntinx, M., et al., *Pharmacological profile of JNJ-27141491 [(S)-3-[3,4-difluorophenyl)-propyl]-5-isoxazol-5-yl-2-thioxo-2,3-dihydro-1H-imida zole-4-carboxyl acid methyl ester], as a noncompetitive and orally active antagonist of the human chemokine receptor CCR2.* J Pharmacol Exp Ther, 2008. 327(1): p. 1-9.

21. Zou, D., et al., *Novel, acidic CCR2 receptor antagonists: from hit to lead.* Letters in Drug Design & Discovery, 2007. 4: p. 185-191.

22. Doyon, J., et al., *Discovery of potent, orally bioavailable small-molecule inhibitors of the human CCR2 receptor.* ChemMedChem, 2008. 3(4): p. 660-9.

23. Xue C, M.B., Feng H, Cao G, Huang T, Zheng C, Robinson DJ, Han A *3-Aminopyrrolidine derivatives as modulators of chemokine receptors*, 2004. Inventors, Incyte Corporation. PCT/US2003/037946.

24. Smith, P.K., et al., *Measurement of protein using bicinchoninic acid.* Anal Biochem, 1985. 150(1): p. 76-85.

25. Xi, B., et al., *The application of cell-based label-free technology in drug discovery.* Biotechnol J, 2008. 3(4): p. 484-95.

26. Yu, N., et al., *Real-time monitoring of morphological changes in living cells by electronic cell sensor arrays: an approach to study G protein-coupled receptors.* Anal Chem, 2006. 78(1): p. 35-43.

27. Cheng, Y. and W.H. Prusoff, *Relationship between the inhibition constant (K1) and the concentration of inhibitor which causes 50 per cent inhibition (I50) of an enzymatic reaction.* Biochem Pharmacol, 1973. 22(23): p. 3099-108.

28. Springael, J.Y., et al., *Allosteric modulation of binding properties between units of chemokine receptor homo- and hetero-oligomers.* Mol Pharmacol, 2006. 69(5): p. 1652-61.

29. Samson, M., et al., *The second extracellular loop of CCR5 is the major determinant of ligand specificity.* J Biol Chem, 1997. 272(40): p. 24934-41.

30. Shin, N., et al., *Pharmacological characterization of INCB3344, a small molecule antagonist of human CCR2.* Biochem Biophys Res Commun, 2009. 387(2): p. 251-5.

31. Sohy, D., M. Parmentier, and J.Y. Springael, *Allosteric transinhibition by specific antagonists in CCR2/CXCR4 heterodimers.* The Journal of biological chemistry, 2007. 282(41): p. 30062-9.

32. El-Asmar, L., et al., *Evidence for negative binding cooperativity within CCR5-CCR2b heterodimers.* Molecular pharmacology, 2005. 67(2): p. 460-9.

33. de Kruijf, P., et al., *Nonpeptidergic allosteric antagonists differentially bind to the CXCR2 chemokine receptor.* J Pharmacol Exp Ther, 2009. 329(2): p. 783-90.

34. Lazareno, S. and N.J. Birdsall, *Detection, quantitation, and verification of allosteric interactions of agents with labeled and unlabeled ligands at G protein-coupled receptors: interactions of strychnine and acetylcholine at muscarinic receptors.* Mol Pharmacol, 1995. 48(2): p. 362-78.

35. Scholten, D.J., et al., *Pharmacological modulation of chemokine receptor function.* Br J Pharmacol, 2011. 165(6): p. 1617-43.

36. Nicholls, D.J., et al., *Identification of a putative intracellular allosteric antagonist binding-site in the CXC chemokine receptors 1 and 2.* Mol Pharmacol, 2008. 74(5): p. 1193-202.

37. Salchow, K., et al., *A common intracellular allosteric binding site for antagonists of the CXCR2 receptor.* Br J Pharmacol, 2010. 159(7): p. 1429-39.

38. Andrews, G., C. Jones, and K.A. Wreggett, *An intracellular allosteric site for a specific class of antagonists of the CC chemokine G protein-coupled receptors CCR4 and CCR5.* Mol Pharmacol, 2008. 73(3): p. 855-67.

39. Kenakin, T. and L.J. Miller, *Seven transmembrane receptors as shapeshifting proteins: the impact of allosteric modulation and functional selectivity on new drug discovery.* Pharmacol Rev, 2010. 62(2): p. 265-304.

40. Magnan, R., et al., *Distinct CCK-2 receptor conformations associated with beta-arrestin-2 recruitment or phospholipase-C activation revealed by a biased antagonist.* Journal of the American Chemical Society, 2013. 135(7): p. 2560-73.

41. Kredel, S., et al., *High-content analysis of CCR2 antagonists on human primary monocytes.* J Biomol Screen, 2011. 16(7): p. 683-93.

42. Vauquelin, G., et al., *New insights in insurmountable antagonism.* Fundam Clin Pharmacol, 2002. 16(4): p. 263-72.

# Chapter 4

## Discovery and mapping of an intracellular antagonist binding site at the chemokine receptor CCR2

Annelien J.M. Zweemer
Julia Bunnik
Margo Veenhuizen
Fabiana Miraglia
Eelke B. Lenselink
Maris Vilums
Henk de Vries
Arthur Gibert
Stefanie Thiele
Mette M. Rosenkilde
Adriaan P. IJzerman
Laura H. Heitman

*Molecular Pharmacology* ***2014*** *86(4):358-368*

## Abstract

The chemokine receptor CCR2 is a G protein-coupled receptor that is involved in many diseases characterized by chronic inflammation, and therefore a large variety of CCR2 small molecule antagonists has been developed. On the basis of their chemical structures these antagonists can be roughly divided into two groups with most likely two topographically distinct binding sites. The aim of the current study was to identify the binding site of one such group of ligands, exemplified by three allosteric antagonists, CCR2-RA-[R], JNJ-27141491 and SD-24.

We first used a chimeric CCR2/CCR5 receptor approach to obtain insight into the binding site of the allosteric antagonists, and additionally introduced eight single point mutations in CCR2 to further characterize the putative binding pocket. All constructs were studied in radioligand binding as well as functional IP turnover assays, providing evidence for an intracellular binding site for CCR2-RA-[R], JNJ-27141491 and SD-24. The most important residues for binding were found to be the highly conserved tyrosine $Y^{7.53}$ and phenylalanine $F^{8.50}$ of the $NPxxYX_{(5,6)}F$ motif, as well as $V^{6.36}$ at the bottom of TM-VI and $K^{8.49}$ in helix-VIII. In addition, we found two other residues at locations surrounding this binding pocket, which differently affected the three allosteric ligands.

These findings demonstrate for the first time the presence of an allosteric intracellular binding site for CCR2 antagonists. This contributes to an increased understanding of the interactions of diverse ligands at CCR2 and may allow a more rational design of future allosteric antagonists.

## Introduction

The chemokine receptor CCR2 is a G protein-coupled receptor (GPCR) that is expressed on monocytes, dendritic cells, activated T lymphocytes and basophils, and therefore it plays an important role in the immune system [1-3]. These immune cells migrate towards increasing concentrations of chemokines at sites of inflammation as part of the immune response, also known as chemotaxis. CCR2 is activated by multiple chemokines, including CCL2, CCL7, CCL8, CCL11, CCL13 and CCL16. Besides its important role in physiology, increased levels of CCR2 and its ligands can induce severe tissue damage. This results in a large variety of diseases that are characterized by chronic inflammation [4-7], which makes CCR2 an attractive drug target for the pharmaceutical industry. As a consequence many CCR2 small molecule antagonists have been developed over the years, but unfortunately all clinical candidates tested so far appeared to lack efficacy in man.



Most small molecule chemokine receptor antagonists bind at the main binding pocket in the upper half (exterior part) of the transmembrane (TM) helices, usually with one part in the so-called major binding pocket (surrounded by TM helices III, IV, V, VI and VII) and the other part in the minor binding pocket (surrounded by TM helices I, II, III and VII) [8]. Many small molecule antagonists contain a positively charged basic nitrogen that interacts with the conserved negatively charged glutamic acid residue (E291$^{7.39}$) in TM-VII, which is directly located in between the major and minor binding pocket [9]. An example of such a CCR2 antagonist is INCB3344 (Fig. 1), to which we refer as an orthosteric antagonist, since it was previously reported to inhibit CCR2 in a competitive manner with respect to the chemokine ligand CCL2 [10, 11]. Interestingly, other classes of antagonists were discovered to bind at a different binding site than INCB3344 [10]. It was shown that these antagonists, CCR2-RA-[R] and JNJ-27141491 (Fig. 1), possess structural features different from the orthosteric antagonists and inhibit CCR2 in a noncompetitive manner with respect to CCL2. The current study took these findings as the starting point to resolve the location of the binding site for these allosteric CCR2 antagonists. For several other chemokine receptors the presence of an allosteric binding site has been reported [12, 13]. Some of these antagonists bind exclusively to the major or minor binding pocket [14] and their binding site can even be directed towards the extracellular loops, as illustrated in the CXCR4 crystal structure for the small molecule antagonist IT1t [15]. In addition, an allosteric binding site on the intracellular side of the receptor in the C-terminal domain has been suggested for the chemokine receptors CXCR2, CCR4 and CCR5 [16-18].

In the present study we first showed that a previously described antagonist with a sulfonamide scaffold (SD-24) is also an allosteric antagonist (Fig. 1) [19]. Subsequently, we used a CCR2/CCR5 chimeric approach to get insight into the binding site of allosteric antagonists for CCR2 and made single point mutations in CCR2 to further map this binding pocket. We discovered the existence of an intracellular binding site in CCR2 that is recognized by (at least) three chemically different classes of antagonists. Finally, we discuss the compounds' mechanism of action and the implications for targeting CCR2 in disease states.

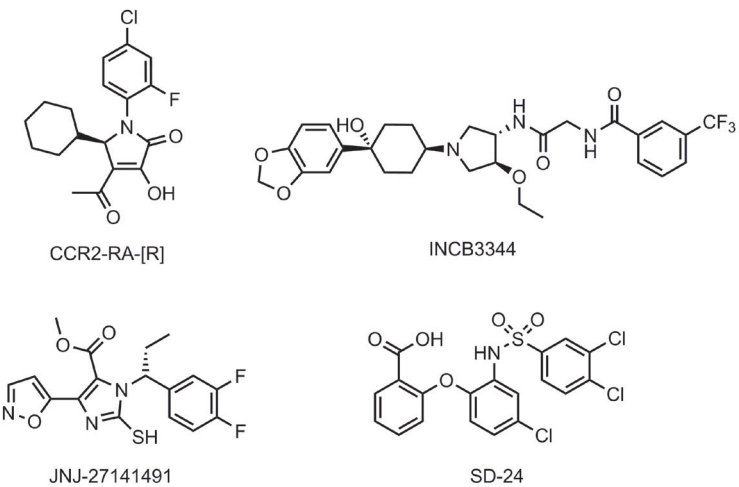



**Fig. 1.** Chemical structures of the orthosteric CCR2 antagonist INCB3344 and the allosteric CCR2 antagonists CCR2-RA-[R], JNJ-27141491 and SD-24.

## Materials and Methods

**Chemicals and reagents.** CCL2 was purchased from PeproTech (Rocky Hill, NJ). INCB3344, JNJ-27141491 and CCR2-RA-[R] were synthesized according to published methods [47-50]. SD-24 (sulfonamide derivative #24 from the Peace et al. paper) was synthesized in-house, according to procedures described previously [19]. [$^{3}$H]-INCB3344 (specific activity 32 Ci mmol$^{-1}$) and [$^{3}$H]-CCR2-RA (specific activity 63 Ci mmol$^{-1}$) were custom-labeled by Vitrax (Placentia, CA). $^{125}$I-CCL2 (2200 Ci/mmol), $^{125}$I-CCL3 (2200 Ci/mmol), [$^{35}$S]GTP$\gamma$S (1250 Ci/mmol) and *myo*-[$^{3}$H] inositol (PT6-271) (94.5 Ci/mmol) were purchased from Perkin-Elmer (Waltham, MA, USA). Bovine serum albumin (BSA, fraction V) was purchased from Sigma (St. Louis, MO, USA). Bicinchoninic acid (BCA) and BCA protein assay reagent were obtained from Pierce Chemical Company (Rockford, IL, USA). Polyethyleneimine (PEI) was obtained from Polysciences Inc.

(Warrington, PA, USA). Wild-type (WT) FLAG-tagged CCR5 was cloned in-house from a leukocyte cDNA library, while WT FLAG-tagged CCR2 cDNA was kindly provided by Dr Tim Wells (GlaxoSmithKline, UK). The chimeric receptor CCR5-CCR2$_{all}$, was previously described [20], whereas CCR2-CCR5$_{C\text{-}term}$ and CCR5-CCR2$_{C\text{-}term}$ were designed in-house and cloned using PCR overlap extension technique (Piscataway, NJ). pcDNA3.1+ plasmid containing the WT CCR2 with a 3x hemagglutinin (HA) epitope tag at the N-terminus was kindly provided by James Pease (Imperial College London, UK). The promiscuous G protein G$\alpha_{\Delta 6qi4myr}$ (G$_{qi4myr}$) was kindly provided by Evi Kostenis (University of Bonn, Germany). Tango CCR2-bla U2OS cells stably expressing human CCR2 (U2OS-CCR2) were obtained from Invitrogen (Carlsbad, CA). CHO (Chinese hamster ovary) cells were obtained from Hans den Dulk (Leiden University, the Netherlands) and COS-7 cells were obtained from ATCC (Rockville, MD). The monoclonal rabbit anti-HA-tag antibody and the HRP-conjugated goat anti-rabbit antibody were obtained from Novus Biologicals (Cambridge UK). The monoclonal mouse anti-FLAG M1 antibody was obtained from Sigma (St. Louis, MO) and the HRP-conjugated goat anti-mouse antibody was obtained from Pierce (Rockford, IL). AG 1-X8 anion exchange resin was obtained from Bio-Rad (Hercules, CA). All other chemicals were obtained from standard commercial sources.



**Site-directed mutagenesis.** pcDNA3.1+ plasmids containing the human CCR2 mutants I208A$^{5.45}$ and E291A$^{7.39}$ (superscript indicates the Ballesteros Weinstein numbering system [21], in which transmembrane residues are assigned two numbers that belong to the helix number and the residue number relative to the most conserved residue in this helix, which is assigned 50) with a 3x hemagglutinin (HA) epitope tag at the N-terminus were kindly provided by James Pease (Hall et al., 2009). All other point mutations were generated by site-directed mutagenesis, using WT HA-tagged CCR2 plasmid DNA as a template for the generation of mutant plasmids by polymerase chain reaction (PCR) using the QuickChange® II Site-directed mutagenesis kit (Stratagene, the Netherlands) and the appropriate oligonucleotide primers (Eurogentec, the Netherlands), under conditions recommended by the manufacturer. All mutants were verified by DNA sequencing before use (LGTC, Leiden University, the Netherlands).

**Cell culture.** COS-7 cells and U2OS-CCR2 cells were cultured as described before [10, 20]. Chinese hamster ovary (CHO) cells were cultured in Ham's F12 culture medium supplemented with 10% (v/v) newborn calf serum, penicillin (50 IU/mL) and streptomycin (50µg/mL) at 37°C and 5% $CO_2$. Cells were subcultured twice weekly at a ratio of 1:20 by trypsinization on 10-cm ø plates.

**Transfections.** Transfections of COS-7 cells with FLAG-tagged CCR2, CCR5 or chimeric receptor were performed by the calcium phosphate precipitation method as described before [22]. Transfections of CHO cells with FLAG-tagged CCR2, CCR5 or chimeric receptor, as well as HA-tagged WT or mutant CCR2, were performed with polyethyleneimine (PEI). For this purpose, CHO cells were grown to 50-60% confluence on 15-cm ø plates and transfected with 10 µg of plasmid DNA per 15-cm ø plate. Briefly, 10 µg of plasmid DNA was diluted in a sterile 150 mM NaCl solution and subsequently mixed with PEI solution (1mg/mL) to obtain a DNA:PEI mass ratio of 1:6. The mixture was incubated for 20 min at room temperature before transfection. The culture medium of the cells was refreshed and 1 mL of DNA/PEI mixture was added to cells and incubated for 48 hrs at 37°C and 5% $CO_2$.

**Cell membrane preparation.** Membranes were prepared as described before [10]. Briefly, cells were scraped from 15-cm ø plates upon which the membranes and cytosolic fractions were separated during several centrifugation steps. Finally, the membrane pellet was resuspended in ice-cold 50 mM Tris-HCl buffer containing 5 mM $MgCl_2$, pH 7.4, and aliquots were stored at −80 °C. Membrane protein concentrations were measured using a BCA protein determination with BSA as a standard [23].

**Cell surface expression by Enzyme-Linked Immunosorbent Assay (ELISA).** For transfections with WT and mutant CCR2 receptors containing a HA-tag, CHO cells were plated 24 hrs after transfection at a density of $1x10^6$ cells per well in a 96-well plate and incubated at 37 ºC and 5% $CO_2$ for 24 hrs. Cells were washed with PBS and incubated with rabbit anti-HA primary antibody (dilution 1:5000 in DMEM) for 30 min at RT. After a subsequent wash with DMEM/HEPES (25 mM), cells were incubated with HRP-conjugated goat anti-rabbit secondary antibody (dilution 1:5000 in DMEM) for 30 min at RT. The cells were washed twice with pre-warmed PBS, after which tetramethyl benzene (TMB) was added for 5 min in the dark at RT. The reaction was stopped by addition of 1 M $H_3PO_4$ and after 5 min absorbance was measured at 450 nm with a Victor$^2$V plate reader (Perkin Elmer, Waltham, MA, USA).

**$^{125}$I-CCL2 binding assays.** $^{125}$I-CCL2 and $^{125}$I-CCL3 whole cell binding assays on COS-7 cells transfected with WT FLAG-tagged CCR2, CCR5 or chimeric receptor were performed as described before [20]. In these assays $^{125}$I-CCL2 was used for CCR2 and the two chimers CCR5-CCR2(all) and CCR2-CCR5(C-term), whereas $^{125}$I-CCL3 was used for CCR5 and the chimer CCR5-CCR2(C-term). $^{125}$I-CCL2 binding assays on U2OS-CCR2 cell membranes were performed as described before [10]. Briefly, the assay was performed in a 100 µL reaction

volume containing 50 mM Tris-HCl buffer (pH 7.4), 5 mM $MgCl_2$, 0.1% 3-((3-cholamidopropyl)-dimethylammonio)-1-propanesulfonate (CHAPS) and 15 µg of U2OS-CCR2 cell membrane protein at 37 °C. Displacement assays were performed with 0.1 nM $^{125}$I-CCL2 using six concentrations of competing ligand for 150 min of incubation. At this concentration, total radioligand binding did not exceed 10% of the amount added to prevent ligand depletion. Non-specific binding was determined with 10 µM INCB3344. Reactions were terminated as described before.

**[$^3$H]-INCB3344 binding assays.** [$^3$H]-INCB3344 membrane binding assays were performed as described before [10]. For the FLAG-tagged CCR2, CCR5 and the chimera's expressed in CHO cells, homologous displacement studies were carried out with 2.1 nM and 5.0 nM [$^3$H]-INCB3344 to be able to determine the equilibrium dissociation constant $K_D$. Studies with HA-tagged WT and mutant receptors of CCR2 were carried out with a single concentration of 5.7 nM [$^3$H]-INCB3344. In all cases, eight concentrations of competing ligand were incubated for 120 min at 25 °C. Non-specific binding for mutant and WT CCR2 receptors was determined in the presence of 10 µM INCB3344. For the WT receptor the measured non-specific binding was equal to the experiments in which 10 µM BMS22 was used, as described in our previous study [10]. In all experiments, total radioligand binding did not exceed 10% of the amount added to prevent ligand depletion.

**[$^3$H]-CCR2-RA binding assays.** [$^3$H]-CCR2-RA membrane binding assay conditions were similar as those for [$^3$H]-INCB3344 binding assays as described before [10]. For the FLAG-tagged CCR2, CCR5 and the chimera's expressed in CHO cells, homologous displacement studies were carried out with 4.5 nM and 7.9 nM [$^3$H]-CCR2-RA to be able to determine the equilibrium dissociation constant $K_D$. Displacement assays with HA-tagged WT and mutant receptors of CCR2 were carried out with a single concentration of 7.9 nM [$^3$H]-CCR2-RA. In all cases, eight concentrations of competing ligand were incubated for 120 min at 25ºC. Non-specific binding was determined in the presence of 10 µM CCR2-RA-[R]. For the WT receptor the measured non-specific binding was equal to the experiments in which 10 µM JNJ-27141491 was used, as described in our previous study [10]. In all experiments, total radioligand binding did not exceed 10% of the amount added to prevent ligand depletion.

**Inositol Phosphate turnover (IP Turnover) assay.** IP turnover was measured in COS-7 cells co-transfected with WT FLAG-tagged CCR2, CCR5 or chimeric receptor and the promiscuous G protein $G_{qi4myr}$, as described before [20].

**[$^{35}$S]GTP$\gamma$S binding assay.** The [$^{35}$S]GTP$\gamma$S assay was performed as described before [10]. To determine G protein activation of the wild-type and mutant CCR2 receptors, 10 µg of CHO cell membranes were pre-incubated with 100 nM CCL2 (single point) or six increasing concentrations of CCL2 for 30 min at 25 °C. Then [$^{35}$S]GTP$\gamma$S (0.3 nM) was added, after which the mixture was incubated for 90 min and samples were harvested as described before.

**Data analysis.** All experiments were analyzed using the non-linear regression curve fitting program Prism 5 (GraphPad, San Diego, CA, U.S.A.). $pK_D$ values for the FLAG-tagged CCR2, CCR5 and chimeric receptors were calculated using the homologous competitive binding curve fit. The $pIC_{50}$ values for WT and mutant CCR2 of INCB3344, CCR2-RA-[R], JNJ-27141491 and SD-24 were obtained by non-linear regression analysis of the displacement curves. Statistical analysis was performed with a two-tailed unpaired Student's *t*-test. All values obtained are means of at least three independent experiments performed in duplicate, unless stated otherwise.

**Antagonist superposition, homology modeling and ligand docking.** To best superimpose the three different antagonists, multiple ligand conformations of each individual compound were generated using MacroModel version 10.1 [24], with mixed torsional/low-mode sampling and default settings. Subsequently the different ligand conformations were aligned using the flexible ligand alignment method within Maestro [25] and selected based on their pose and shape similarity. A homology model of the chemokine CCR2 receptor was constructed using the homology modeling tool within Maestro [25-27]. This model was based on the structure of the chemokine CCR5 receptor co-crystalized with maraviroc (Protein Data Bank: 4MBS). The best model was selected based on the energy-based scoring function, while the sequence alignment between CCR2 and CCR5 was performed using ClustalW as implemented within Maestro. CCR2-RA-[R] was docked into the receptor homology model using the induced fit docking protocol [28, 29]. The grid center was placed based on residues D78$^{2.40}$, Y305$^{7.53}$, K311$^{8.49}$ and F312$^{8.50}$ with an automatic box size. Visualizations were created using PyMOL version 1.5.0.4. [30].

## Results

**Effect of sulfonamide SD-24 on CCR2 radioligand binding.** The sulfonamide derivative SD-24 partially inhibited binding of $^{125}$I-CCL2 to CCR2-expressing U2OS cell membranes to 27 ± 6 % at 10 µM, with a $pIC_{50}$ of 7.2 ± 0.2 (Fig. 2). [$^3$H]-CCR2-RA was fully displaced with a $pK_i$ value of 9.0 ± 0.1. On the contrary, SD-24 slightly increased [$^3$H]-INCB3344 binding to a maximum of 120 % at 1 µM SD-24, indicating it binds at a site different from the previously described [10, 11] orthosteric binding pocket of INCB3344 (Fig. 2).

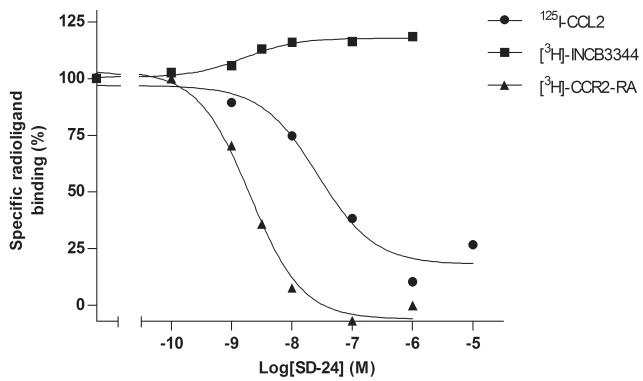



**Fig. 2**. Modulation of $^{125}$I-CCL2, [$^3$H]-INCB3344 and [$^3$H]-CCR2-RA binding to U2OS cell membranes stably expressing CCR2 by increasing concentrations of the CCR2 antagonist SD-24. Results are presented as percentage of bound radioligand for one representative experiment performed in duplicate. SD-24 inhibited binding of $^{125}$I-CCL2 with a $pIC_{50}$ of 7.2 ± 0.2 and [$^3$H]-CCR2-RA with a $pK_i$ of 9.0 ± 0.1. For $^{125}$I-CCL2, 27 ± 6 % radioligand remained bound in the presence of 10 µM SD-24.

**Comparison of CCR2 and CCR5.** In order to identify regions that are responsible for binding of SD-24 and the other allosteric antagonists we compared the affinity of CCR2-RA-[R], JNJ-27141491 and SD-24 for CCR2 and its close homolog CCR5 (Fig. 3A) in whole cell radioligand binding assays using $^{125}$I-CCL2 and $^{125}$I-CCL3, respectively. CCR2-RA-[R] and JNJ-27141491 displaced $^{125}$I-CCL2 from CCR2 with $pIC_{50}$ values of 6.1 ± 0.1 and 6.6 ± 0.1, respectively (Table 1). In addition, JNJ-27141491 inhibited $^{125}$I-CCL3 from binding to CCR5 with a $pIC_{50}$ value of 5.4 ± 0.1, whereas CCR2-RA-[R] did not sufficiently displace $^{125}$I-CCL3 from CCR5 to be able to determine its affinity for CCR5. The affinity of SD-24 for CCR2 could not be measured in this whole cell binding assay, and neither was any displacement of $^{125}$I-CCL3 from CCR5 observed in the presence of SD-24 (Table 1). Differently, in the functional IP turnover assay the $pIC_{50}$ values for CCR2 and CCR5 inhibition could be determined for all antagonists (Table 2). In this assay CCR2-RA-[R], JNJ-27141491 and SD-24 showed a 7-fold, 14-fold and 22-fold reduced potency to inhibit CCR5 compared to CCR2, respectively.

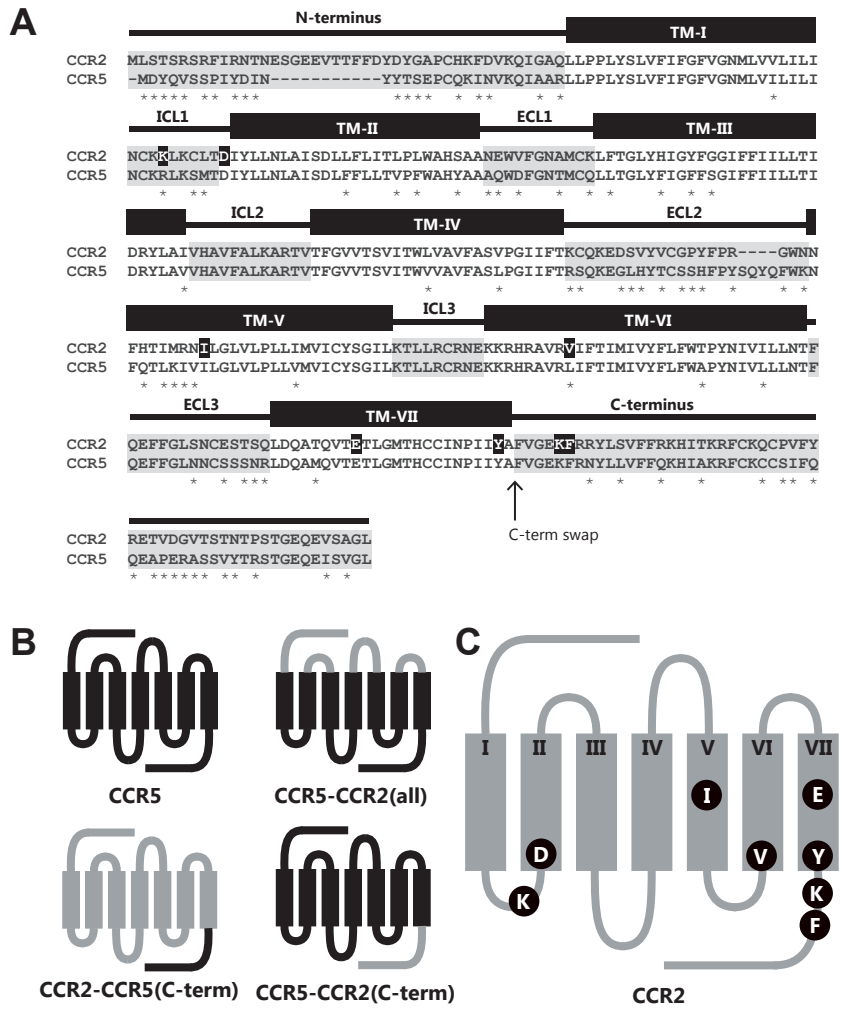



**Fig. 3.** (A) Sequence alignment with ClustalW2 of CCR2 and CCR5, for which the transmembrane regions as well as the intracellular and extracellular loops are indicated (bottom). Differing residues are indicated with an asterisk, and CCR2 residues mutated in this study are indicated in black. The arrow presents the location where the C-termini were swapped. The locations where the extracellular loops of CCR2 were inserted into CCR5 can be found in Thiele *et al.* 2011. (B) Schematic representation of CCR5 and the chimeric receptors CCR5-CCR2(all), CCR2-CCR5(C-term) and CCR5-CCR2(C-term). (C) Schematic representation of CCR2. The approximate location of the residues $K^{2.34}$, $D^{2.40}$, $I^{5.45}$, $V^{6.36}$, $E^{7.39}$, $Y^{7.53}$, $K^{8.49}$ and $F^{8.50}$ is indicated.

**Table 1.** Inhibition of chemokine whole cell binding by the endogenous chemokines or small molecule antagonists, for CCR2, CCR5 and the chimeric receptors expressed in COS-7 cells. The chemokine radioligand that was used for each construct is indicated in the first column.

| | endogenous ligands (CCL2 or CCL3) | | orthosteric INCB3344 | | allosteric CCR2-RA-[R] | | allosteric JNJ-27141491 | | allosteric SD-24 |
|---|---|---|---|---|---|---|---|---|---|
| **Radioligand - Construct** | **$pIC_{50}$ ± S.E.M. and ($IC_{50}$ (nM))** | | | | | | | | |
| $^{125}$I-CCL2 - CCR2 | 9.7 ± 0.2[a] | (0.21) | 7.8 ± 0.2 | (16) | 6.1 ± 0.1 | (746) | 6.6 ± 0.1 | (241) | < 5 |
| $^{125}$I-CCL3 - CCR5 | 8.7 ± 0.4[b] | (1.9) | 5.3 ± 0.2 | (4508) | < 5 | | 5.4 ± 0.1 | (4254) | no displacement |
| $^{125}$I-CCL2 - CCR5-CCR2(all) | 8.9 ± 0.3[a] | (1.3) | 6.3 ± 0.1** | (516) | < 5 | | 5.0 ± 0.1* | (10650) | no displacement |
| $^{125}$I-CCL3 - CCR5-CCR2(C-term) | 8.9 ± 0.2[b] | (1.4) | no displacement | | 5.1 ± 0.1 | (7638) | < 5 | | no displacement |
| $^{125}$I-CCL2 - CCR2-CCR5(C-term) | 8.9 ± 0.2[a] | (1.4) | 7.3 ± 0.1 | (48) | 5.7 ± 0.2 | (1908) | 6.4 ± 0.1 | (364) | < 5 |

Data are presented as mean $pIC_{50}$ ± S.E.M. and mean $IC_{50}$ (nM) of at least three experiments performed in duplicate.
[a] $pIC_{50}$ of CCL2.
[b] $pIC_{50}$ of CCL3.
* p< 0.05 vs. CCR5, Student's *t*-test.
** p< 0.005 vs. CCR5, Student's *t*-test.

**Table 2.** IP turnover activation by chemokines and inhibition by small molecule antagonists for CCR2, CCR5 and the chimeric receptors expressed in COS-7 cells. In case of the assays with the antagonists, a chemokine concentration that evoked 80% of the maximum response ($EC_{80}$) was used. The chemokine that was used for each construct is indicated in the first column.

| | endogenous ligands (CCL2 or CCL3) | | orthosteric INCB3344 | | allosteric CCR2-RA-[R] | | allosteric JNJ-27141491 | | allosteric SD-24 | |
|---|---|---|---|---|---|---|---|---|---|---|
| **Chemokine - Construct** | **$pEC_{50}$ ± S.E.M. and ($EC_{50}$ (nM))** | | **$pIC_{50}$ ± S.E.M. and ($IC_{50}$ (nM))** | | | | | | | |
| CCL2 - CCR2 | 9.2 ± 0.3 | (0.63) | 8.0 ± 0.01 | (10) | 7.0 ± 0.1 | (93) | 7.1 ± 0.1 | (85) | 6.6 ± 0.3 | (236) |
| CCL3 - CCR5 | 8.1 ± 0.2 | (8.0) | 5.3 ± 0.01 | (4645) | 6.2 ± 0.1 | (680) | 5.9 ± 0.1 | (1201) | 5.3 ± 0.1 | (5206) |
| CCL2 - CCR5-CCR2(all) | 9.4 ± 0.3 | (0.41) | 7.0 ± 0.4* | (104) | 5.2 ± 0.2** | (6227) | 5.4 ± 0.2 | (3837) | 5.2 ± 0.1 | (6133) |
| CCL3 - CCR5-CCR2(C-term) | 8.1 ± 0.3 | (7.4) | 5.4 ± 0.1 | (4399) | 6.4 ± 0.1 | (428) | 5.6 ± 0.2 | (2605) | 5.6 ± 0.1* | (2301) |
| CCL2 - CCR2-CCR5(C-term) | 9.3 ± 0.2 | (0.48) | 7.8 ± 0.2 | (18) | 6.9 ± 0.2 | (126) | 6.9 ± 0.1 | (121) | 6.4 ± 0.2 | (388) |

Data are presented as mean $pEC_{50}$ ± S.E.M. and $pIC_{50}$ ± S.E.M. as well as mean $EC_{50}$ (nM) and mean $IC_{50}$ (nM) of at least three experiments performed in duplicate.
* p < 0.05 vs. CCR5, Student's *t*-test.
** p < 0.005 vs. CCR5, Student's *t*-test.

The orthosteric antagonist INCB3344 displaced the radioligands $^{125}$I-CCL2 and $^{125}$I-CCL3 from CCR2 and CCR5, respectively, with a $pIC_{50}$ of 7.8 ± 0.2 and 5.3 ± 0.2 (Table 1). Its $pIC_{50}$ to inhibit IP turnover was 8.0 ± 0.01 for CCR2 and 5.3 ± 0.01 for CCR5 (Table 2). In comparison to the allosteric antagonists, INCB3344 showed a much lower affinity (280-fold) and potency (460-fold) for CCR5 compared to CCR2.

To better determine the affinity of INCB3344 and CCR2-RA-[R] for CCR2 and CCR5 we performed homologous displacement assays on membrane preparations of CHO cells transfected with CCR2 and CCR5. The $pK_D$ of INCB3344 for CCR2 was 8.1 ± 0.1, whereas binding to CCR5 could not be detected at nanomolar concentrations of [$^3$H]-INCB3344. The $pK_D$ of CCR2-RA-[R] for CCR2 and CCR5 was 8.8 ± 0.1 and 7.0 ± 0.1, respectively (Table 3). All these data together suggest that the orthosteric binding site is more divergent between CCR2 and CCR5 than the allosteric binding pocket.

**Table 3.** Displacement of [$^3$H]-INCB3344 binding and [$^3$H]-CCR2-RA binding from CHO membranes expressing FLAG-tagged CCR2, CCR5 and CCR2-CCR5(C-term) receptors.

| | **[$^3$H]-INCB3344** | **[$^3$H]-CCR2-RA** |
|---|---|---|
| **Construct** | **$pK_D$ ± S.E.M. and ($K_D$ (nM))** | |
| CCR2 | 8.1 ± 0.1 (8.3) | 8.8 ± 0.1 (1.7) |
| CCR5 | no binding | 7.0 ± 0.1 (100) |
| CCR2-CCR5(C-term) | 8.6 ± 0.1 (2.3) | 8.7 ± 0.1 (2.0) |

Data are presented as mean $pK_D$ ± S.E.M. or mean $K_D$ (nM) of at least three experiments performed in duplicate.

**CCR2-CCR5 chimeric approach.** Given the high structural similarity between CCR2 and CCR5, we took CCR5 as a template structure to further elucidate the allosteric binding site in CCR2. Therefore we decided to use a chimeric approach to investigate the role of the extracellular loops and intracellular region of the receptor in binding of the antagonists (Fig. 3B). The chimera CCR5-CCR2(all), which consisted of CCR2's extracellular receptor regions, and CCR5 for the remainder of the construct, was used to study the role of the extracellular loops for small molecule binding. In order to study the role of the C-terminus in binding of the antagonists, two novel chimera's were constructed; CCR5-CCR2(C-term) and CCR2-CCR5(C-term), consisting of CCR5 with CCR2 C-terminus, and CCR2 with CCR5 C-terminus, respectively. We confined ourselves to the C-terminus, as the intracellular loops are highly similar in sequence between CCR2 and CCR5 (Fig. 3A).

For the two allosteric antagonists CCR2-RA-[R] and JNJ-27141491, the ability to inhibit binding of $^{125}$I-CCL2 to CCR2 as well as the potency to inhibit IP3 formation by CCL2 was not affected when the C-terminal part of CCR5 was introduced in CCR2 (CCR2-CCR5(C-term)) (Tables 1 and 2). In addition, for CCR2-RA-[R] and JNJ-27141491 no difference was observed in their potency to inhibit IP3 formation by CCL3 between CCR5 and CCR5-CCR2(C-term) (Table 2). The displacement of $^{125}$I-CCL3 from CCR5-CCR2(C-term) by CCR2-RA-[R], JNJ-27141491 and SD-24 could not be compared to CCR5, since their affinities were too low in a number of cases (Table 1). Similarly, SD-24 did not displace $^{125}$I-CCL2 binding from CCR2 and CCR2-CCR5(C-term) (Table 1). However, the $pIC_{50}$ value of SD-24 to inhibit IP3 formation via CCR5-CCR2(C-term) was with 5.6 ± 0.1 slightly higher than the $pIC_{50}$ of 5.3 ± 0.1 for CCR5. All together, the data of the IP turnover assay suggest that non-conserved residues in the C-terminus of CCR2 compared to CCR5 are not involved in binding of the allosteric antagonists CCR2-RA-[R] and JNJ-27141491. For SD-24, a 2-fold increase in potency was observed upon introduction of the CCR2 C-terminus in CCR5, whereas introduction of the CCR5 C-terminus in CCR2 did not result in any changes.

Upon introduction of the extracellular loops of CCR2 in CCR5 (chimer CCR5-CCR2(all)), a significant decrease in potency to inhibit IP turnover was observed for CCR2-RA-[R] as its $pIC_{50}$ value was 5.2 ± 0.2 for CCR5-CCR2(all) compared to 6.2 ± 0.1 in case of CCR5 (Table 2). In the binding assays the affinities of CCR2-RA-[R] and SD-24 for CCR5-CCR2(all) were negligible (Table 1). Differently, a slight decrease in affinity of JNJ-27141491 was observed, since its $pIC_{50}$ value was 5.0 ± 0.1 for CCR5-CCR2(all) compared to 5.4 ± 0.1 for CCR5 (Table 1). It should be noted that we compared binding and activation of CCR5 by $^{125}$I-CCL3/CCL3 with binding and activation of CCR5-CCR2(all) by $^{125}$I-CCL2/CCL2. It can thus not be excluded that activation of these receptors in a molecularly different way could be responsible for the observations.

In contrast to the allosteric antagonists, the inhibitory potency and affinity of the orthosteric antagonist INCB3344 was increased for CCR5 when the extracellular loops of CCR2 were introduced. INCB3344 inhibited $^{125}$I-CCL3 binding to CCR5 and $^{125}$I-CCL2 binding to CCR5-CCR2(all) with a $pIC_{50}$ of 5.3 ± 0.2 and 6.3 ± 0.1, respectively (Table 1). In addition, the potency of INCB3344 to inhibit CCL2-induced CCR5-CCR2(all) activity in the functional assay was increased 45-fold compared to its potency to inhibit CCL3-induced CCR5 activity (Table 2). Next we measured the effect of the C-terminus swap on the affinity and potency of INCB3344. For CCR2-CCR5(C-term) the affinity of INCB3344 and its potency to inhibit IP turnover were not significantly altered compared to CCR2. Exchange of the CCR5 C-terminus with that of CCR2 made INCB3344 unable to displace $^{125}$I-CCL3 from CCR5-CCR2(C-term),

whereas the potency to inhibit IP turnover was similar for CCR5-CCR2(C-term) compared to CCR5.

The small molecule radioligands [$^3$H]-INCB3344 and [$^3$H]-CCR2-RA were only able to bind to CCR2-CCR5(C-term) of all three chimers, with a $pK_D$ of 8.6 ± 0.1 and 8.7 ± 0.1, respectively (Table 3). Thus no significant change compared to the WT CCR2 $pK_D$ of 8.8 ± 0.1 was observed for [$^3$H]-CCR2-RA, in agreement with the chemokine-displacement assays (Table 1 and 3). [$^3$H]-INCB3344 was found to bind slightly better to CCR2-CCR5(C-term) compared to CCR2 ($pK_D$ = 8.1 ± 0.1), somewhat different than observed in the chemokine-displacement assays (Table 1 and 3).

**Identification of intracellular residues involved in CCR2-RA-[R] binding.** To further investigate the possibility of an intracellular binding pocket, we applied a site-directed mutagenesis approach. We initially constructed four mutations in CCR2, K72A$^{2.34}$, D78N$^{2.40}$, Y305A$^{7.53}$ and K311A$^{8.49}$ (Fig 3A+C). K72$^{2.34}$ in ICL1 is one of the few differential residues in the intracellular loops of CCR2 compared to CCR5 (Fig. 3A). Y305$^{7.53}$ is very conserved among G protein-coupled receptors, whereas D78$^{2.40}$ and K311$^{8.49}$ are typical residues among chemokine receptors (see also Discussion). As a control we included I208A$^{5.45}$, which was previously not predicted in any binding site, and E291A$^{7.39}$, which is the highly conserved acidic residue in the orthosteric binding pocket of chemokine receptors. All six mutant receptors were expressed at the cell surface, as determined by whole cell ELISA (Fig 4).

Mutation of Y305$^{7.53}$ into an alanine residue (Y305A) completely abolished [$^3$H]-CCR2-RA binding, whereas the affinity of [$^3$H]-INCB3344 was not affected (Table 4). The affinity of CCR2-RA-[R] for the K311A$^{8.49}$ mutant receptor was 10-fold decreased compared to WT CCR2, whereas the K72A$^{2.34}$ and D78N$^{2.40}$ mutations did not affect binding. The affinity of INCB3344 was not affected by any of these mutations at the intracellular region (Table 4). In contrast, the affinity of INCB3344 was 8-fold decreased for the E291A$^{7.39}$ mutant receptor compared to WT CCR2, whereas the affinity of CCR2-RA-[R] was not affected by this mutation located in the upper half of the receptor. These results reveal that the two residues Y305$^{7.53}$ and K311$^{8.49}$, both located at the transmembrane/intracellular side of the receptor, are involved in binding of the allosteric antagonist CCR2-RA-[R], whereas E291$^{7.39}$ in the orthosteric binding pocket is only important for binding of INCB3344 to CCR2.

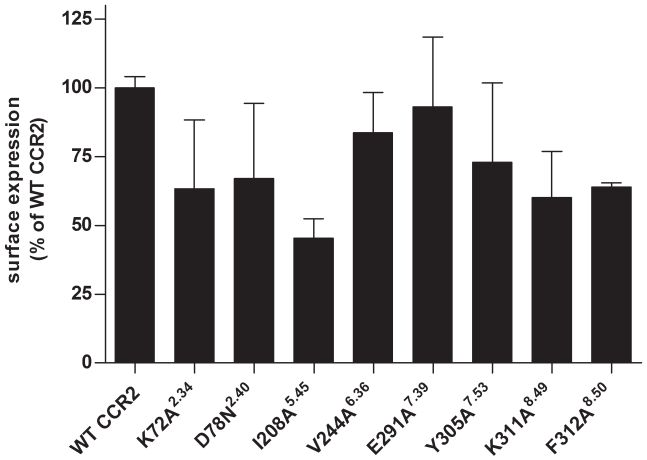



**Fig. 4.** Surface expression of the HA-tagged WT and mutant CCR2 receptors in CHO cells as measured by ELISA. Data was normalized for WT CCR2 expression (100%) and is presented as mean ± SD of at least two experiments performed in quadruplicate.

**Table 4.** Displacement of [$^3$H]-INCB3344 binding and [$^3$H]-CCR2-RA binding from CHO membranes expressing HA-tagged WT and mutant CCR2 receptors.

| | [$^3$H]-INCB3344 | | [$^3$H]-CCR2-RA | |
|---|---|---|---|---|
| | displacement by INCB3344 | displacement by CCR2-RA-[R] | displacement by JNJ-27141491 | displacement by SD-24 |
| **Construct** | pIC$_{50}$ ± S.E.M. and IC$_{50}$ (nM) | | | |
| **WT CCR2** | 7.8 ± 0.03 (16) | 7.8 ± 0.05 (16) | 7.6 ± 0.1 (24) | 7.8 ± 0.1 (16) |
| **K72A$^{2.34}$** | 7.8 ± 0.01 (15) | 7.7 ± 0.1 (21) | 7.3 ± 0.1* (45) | 7.6 ± 0.1 (24) |
| **D78N$^{2.40}$** | 7.8 ± 0.1 (16) | 7.7 ± 0.1 (21) | 7.4 ± 0.1* (43) | 7.5 ± 0.1* (33) |
| **I208A$^{5.45}$** | 7.8 ± 0.1 (17) | 7.7 ± 0.1 (19) | 7.8 ± 0.1 (17) | 7.9 ± 0.02 (12) |
| **V244A$^{6.36}$** | 8.1 ± 0.03** (7.5) | no binding | ND | ND |
| **E291A$^{7.39}$** | 6.9 ± 0.1** (126) | 7.7 ± 0.1 (21) | 7.7 ± 0.1 (22) | 7.7 ± 0.05 (20) |
| **Y305A$^{7.53}$** | 7.7 ± 0.03 (19) | no binding | ND | ND |
| **K311A$^{8.49}$** | 7.7 ± 0.03 (18) | 6.8 ± 0.1** (169) | 7.5 ± 0.1 (30) | 7.1 ± 0.1** (74) |
| **F312A$^{8.50}$** | 8.0 ± 0.1** (9.2) | no binding | ND | ND |

Data are presented as mean pIC$_{50}$ ± S.E.M. and mean IC$_{50}$ (nM) of at least three experiments performed in duplicate.
ND, not determined
* p< 0.05 vs. WT CCR2, Student's *t*-test.
** p< 0.005 vs. WT CCR2, Student's *t*-test.

**Docking of CCR2-RA-[R] in a CCR2 homology model.** To obtain further insight in the binding pose of CCR2-RA-[R], we constructed a CCR2 homology model using the crystal structure of CCR5 (PDB: 4MBS) and docked the antagonist CCR2-RA-[R] in the model. When standard docking was used, only low scoring poses were found. Therefore we employed induced-fit docking to account for the flexibility of the intracellular pocket. Final poses were selected based on both the score and consistency with experimental results. In Figure 5 the interactions of CCR2-RA-[R] with V244$^{6.36}$, K311$^{8.49}$, Y305$^{7.53}$ and F312$^{8.50}$ are visualized. The pocket is shielded by Y305$^{7.53}$ at the top and F312$^{8.50}$ at the side, both enabling hydrophobic interactions with CCR2-RA-[R]. K311$^{8.49}$ is turned towards the bottom of the binding pocket and interacts with one of the carbonyl oxygens in CCR2-RA-[R]. At the side of the binding pocket, V244$^{6.36}$ was found to interact with the hexyl-ring of CCR2-RA-[R]. The residues K72A$^{2.34}$ and D78$^{2.40}$ were not in close proximity to CCR2-RA-[R] (Fig. 5A), which was in agreement with their lack of effect on binding observed in the radioligand binding experiments (Table 4).

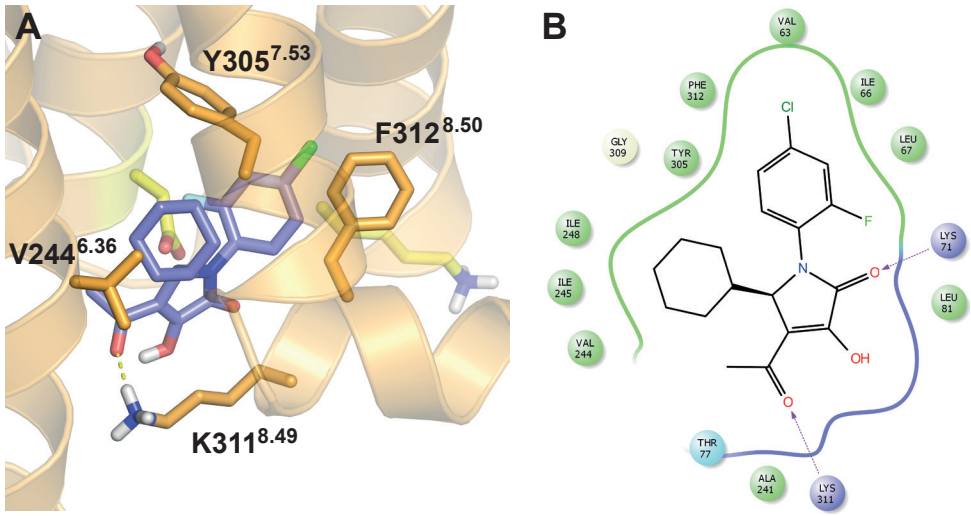



**Fig. 5.** (A) Induced fit docking of CCR2-RA-[R] in a homology model of CCR2 based on the crystal structure of CCR5. The pocket is shielded by Y305$^{7.53}$ at the top and F312$^{8.50}$ at the side, K311$^{8.49}$ is turned towards the bottom of the binding pocket and V244$^{6.36}$ interacts at the side with the hexyl-ring. D78$^{2.40}$ and K72$^{2.34}$ are represented in yellow, as these residues are not predicted to interact with CCR2-RA-[R]. (B) Interaction map of CCR2-RA-[R] with surrounding residues upon induced fit docking.

**Experimental evidence for the docking pose of CCR2-RA-[R].** We determined the effect of mutagenesis of V244$^{6.36}$ in TM-VI and F312$^{8.50}$ in helix-VIII on binding of [$^3$H]-CCR2-RA, since these residues were predicted to be important for binding of CCR2-RA-[R] in the homology model. Both mutant receptors V244A$^{6.36}$ and F312A$^{8.50}$ were expressed at the cell surface, as

determined by whole cell ELISA (Fig. 4). Similar to Y305A$^{7.53}$, the binding of [$^3$H]-CCR2-RA was completely abolished for V244A$^{6.36}$ and F312A$^{8.50}$, while [$^3$H]-INCB3344 was able to bind with a slightly increased affinity to both mutant receptors in comparison to WT CCR2 (Table 4).

**Binding site of JNJ-27141491 and SD-24.** On the assumption that the small molecule antagonists JNJ-27141491 and SD-24 share the same binding site as CCR2-RA-[R], we subjected these two compounds to displacement studies with radiolabeled [$^3$H]-CCR2-RA on the series of CCR2 single point mutations (Table 4). JNJ-27141491 showed a small but significant affinity decrease in displacing [$^3$H]-CCR2-RA compared to wild-type CCR2 for the K72A$^{2.34}$ and D78N$^{2.40}$ mutant receptors of 1.8-fold in both cases. The affinity of SD-24 was 2-fold and 4.4-fold decreased for the D78N$^{2.40}$ and K311A$^{8.49}$ mutant receptors. Due to a lack of [$^3$H]-CCR2-RA binding to V244A$^{6.36}$, Y305A$^{7.53}$ and F312A$^{8.50}$, we could not use these mutants in the heterologous displacement assays. Neither I208A$^{5.45}$ nor E291A$^{7.39}$ affected the binding of the antagonists. These data confirm that JNJ-27141491 and SD-24 bind in the same region as CCR2-RA-[R], albeit with a different orientation, since K72$^{2.34}$, D78$^{2.40}$ and K311$^{8.49}$ differently affected the binding of the three allosteric antagonists. In agreement with these different binding poses, the best possible alignment of the three antagonists illustrated that these structures cannot be fully superimposed (Fig. 6). The substituted aromatic ring of CCR2-RA-[R] is overlaid with the aromatic ring structures of JNJ-27141491 and SD-24. However, at the position of the middle pyrroline ring structure of CCR2-RA-[R], SD-24 contains an aromatic ring whereas JNJ-27141491 extends further with its isoxazole ring.

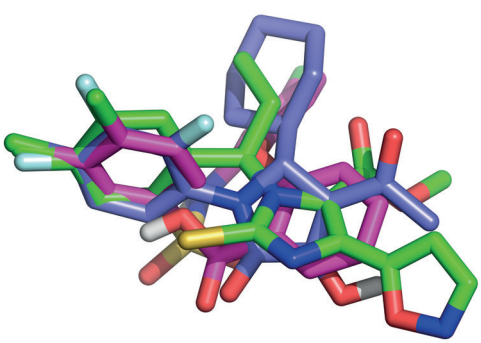


**Fig. 6.** Superimposition of CCR2-RA-[R] (lilac), JNJ-27141491 (green) and SD-24 (magenta). At the bottom right the different properties of the antagonists are illustrated: JNJ-27141491 is extended at this side with an isoxazole ring structure, and the aromatic ring structure of SD-24 is superimposed with the pyrroline ring structure of CCR2-RA-[R].

**Effect of CCR2 mutations on receptor activation.** The effects of the mutations on receptor activation were determined in a [$^{35}$S]GTPγS assay. [$^{35}$S]GTPγS binding was equal for mock transfected CHO cell membranes as for WT CCR2 CHO cell membranes (data not shown), and therefore no basal activity is reported in Figure 7. The mutations K72A$^{2.34}$, V244$^{6.36}$, E291A$^{7.39}$, Y305A$^{7.53}$, K311A$^{8.49}$ and F312A$^{8.50}$ distorted receptor activation as no [$^{35}$S]GTPγS binding window was observed upon addition of 100 nM CCL2 (Fig 5A). CCL2 was found to induce G protein-activation for WT CCR2 with a pEC$_{50}$ value of 7.6 ± 0.2 (Fig. 7B). D78N$^{2.40}$ was the only mutant receptor that allowed significant G protein-activation by CCL2, which yielded a pEC$_{50}$ value of 7.8 ± 0.1 (Fig. 7B).

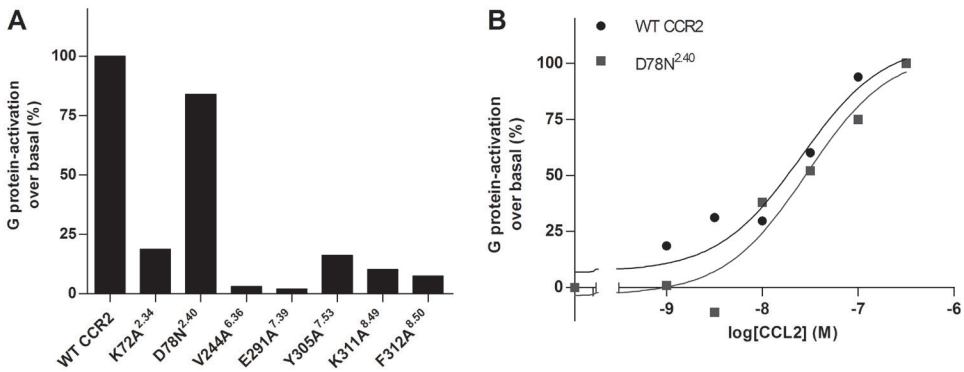



**Fig. 7.** (A) G protein-activation by CCL2 measured in a [$^{35}$S]GTPγS binding assay on CHO cell membranes expressing WT and mutant CCR2 receptors. (B) Concentration-effect curves of CCL2 on WT and D78N$^{2.40}$ CCR2 resulting in a pEC$_{50}$ of 7.6 ± 0.2 and 7.8 ± 0.1, respectively. A representative graph of one experiment performed in duplicate is shown.

## Discussion

Since the early days of GPCR research, our understanding of ligands that activate or inhibit these receptors has increased dramatically [31, 32]. We can now distinguish GPCR ligands with a broad spectrum of activities and mechanisms of action, which implies the presence of multiple binding sites, including so-called allosteric binding sites [33]. In the present study we provided evidence for the presence of an allosteric intracellular binding site for small molecule antagonists of the chemokine receptor CCR2.

Without knowing their location on the receptor we have previously reported on multiple binding sites for small molecule CCR2 ligands, and classified CCR2-RA-[R] and JNJ-27141491 as allosteric antagonists based on radioligand binding studies [10]. Besides these, we now

identified SD-24 to bind at the same allosteric binding pocket at CCR2 (Fig. 2). Structurally related ligands with a pyrazinyl-sulfonamide scaffold have been reported to bind at the intracellular side of CCR4 [16]. Although the precise location of this binding site was not identified, interactions of these antagonists with the C-terminus of CCR4 were reported.

In order to elucidate the location of the CCR2 binding site for CCR2-RA-[R], JNJ-27141491 and SD-24, we constructed several CCR2-CCR5 chimeric receptors to identify regions responsible for binding. CCR2 and CCR5 bear a high sequence similarity of approximately 70%, which makes them perfect candidates for the construction of chimeric receptors [34, 35]. Besides the suggested intracellular binding site for CCR4, other allosteric ligands for chemokine receptors have been reported to interact with the extracellular loops (ECLs). ECL2 contributes to the CXCR4 binding site of the co-crystallized ligand It1 [15], and interactions with ECL2 were reported for the CCR5 antagonists AK530 [36], aplaviroc [20] and small molecule ligands targeting CCR1 and CCR8 [37].



We constructed CCR2-CCR5 chimeras in which either these extracellular regions or the C-terminus were swapped. Binding of the orthosteric CCR2 antagonist INCB3344 was not affected after exchange of the C-terminus in the chemokine-displacement assays, but the binding to CCR5 was increased when extracellular loops of CCR2 were introduced. This fits very well with an orthosteric binding mode, since other small molecule chemokine receptor ligands that bind to the major binding pocket have been found to also interact with ECL2 [20, 36, 37]. However, CCR5 binding of the allosteric antagonists CCR2-RA-[R], JNJ-27141491 and SD-24 was not improved after introduction of the ECLs of CCR2. The affinity and potency of CCR2-RA-[R] and JNJ-27141491 did not change after swapping the C-terminus between CCR2 and CCR5, while for SD-24 a small but significant increase in potency was measured upon introduction of the CCR2 C-terminus in CCR5. It should be noted that intracellular antagonists need to pass the cell membrane before they can exert receptor inhibition in case of the whole cell binding assays and functional assays. In these studies, the allosteric antagonists remarkably displayed up to 10-fold higher potency in the whole cell IP3 assay performed at 37 ºC compared to their $IC_{50}$ in the whole cell binding assay performed at 4 ºC, whereas INCB3344 behaved similarly in both assays. In addition, the binding of the allosteric ligands to CCR2 in the whole cell assays at 4 ºC were much higher than the corresponding values in the membrane assays at 37 ºC (Table 1 and Fig. 2) [10]. Although different cellular systems were used in these distinct assays, the antagonist binding to the intracellular binding pocket could also explain the decreased affinities in whole cell assays at 4ºC due to putative difficulties to enter the cell at such a low temperature.

To explore the possibility of an intracellular binding site, we focused on three conserved residues among chemokine receptors that were previously reported to be involved in small molecule binding at CXCR2, being D78$^{2.40}$, Y305$^{7.53}$ and K311$^{8.49}$ [18]. The binding of [$^{3}$H]-CCR2-RA was completely abolished for Y305A$^{7.53}$, and a 10-fold decreased affinity was observed for K311A$^{8.49}$. Upon considering the important GPCR motifs in this intracellular region and subsequent induced fit docking in a CCR2 homology model we identified F312$^{8.50}$ and V244$^{6.36}$ as part of the intracellular pocket, and mutagenesis of these residues into alanine completely prevented [$^{3}$H]-CCR2-RA from binding. This data is in line with the unaffected affinity of the allosteric antagonists for the chimera's in which the C-terminus was swapped, since K$^{8.49}$ and F$^{8.50}$ are present in both CCR2 and CCR5.

Y305$^{7.53}$ is the highly conserved tyrosine in the NPxxY motif found in 92% of class A GPCRs and this motif has been shown to be important for receptor internalization, receptor signalling and activation [38-40]. For CCR2 we confirmed its critical role in signalling, since a loss of G protein-activation was observed for Y305A$^{7.53}$ (Fig. 7). The increasing number of GPCR crystal structures show that Y305$^{7.53}$ can interchange between multiple different states [41], which emphasizes the flexibility of this residue and therefore also its potential to contribute to the creation of an intracellular small molecule binding pocket.

Together with F312$^{8.50}$ which is conserved in 68% of class A GPCRs, Y305$^{7.53}$ forms the NPxxYx$_{5,6}$F motif [38]. The π-stacking interaction between F312$^{8.50}$ and Y305$^{7.53}$ directly links TM-VII and helix-VIII and keeps the receptor in an inactive state [40], as observed in multiple crystal structures including the recent CCR5 structure [42]. Upon activation, the aromatic stacking interaction is disrupted which allows Y305$^{7.53}$ to rotate into the helical TM core to permit receptor signalling [41]. In induced-fit docking with CCR2-RA-[R] we observed that Y305$^{7.53}$ likely shields the top of the binding pocket, whereas F312$^{8.50}$ is positioned between TM-VII and TM-I and may therefore contribute to hydrophobic interactions with the space-filling chlorine substituent on the phenyl ring of CCR2-RA-[R] (Fig. 5).

Besides Y305$^{7.53}$ and F312$^{8.50}$, the residues V244$^{6.36}$ and K311$^{8.49}$ were found important for binding of CCR2-RA-[R]. K311$^{8.49}$ is a basic, positively charged residue and therefore a likely partner to interact with the partially negative charge on the oxygen present in CCR2-RA-[R] (Fig. 1 and 5). This interaction was visualized in the docking pose, in which K311$^{8.49}$ was found to shield the bottom of the binding pocket. K$^{8.49}$ is highly conserved among chemokine receptors (68.4%), but otherwise not prevalent among class A GPCRs (5.7%). Besides in CCR2, this residue was also found to be important in CXCR2 for interaction with the acidic Pteridone-1, Sch527123 and SB265610 antagonists [17, 18]. It would be interesting to study whether such a basic residue at this position is facilitating the presence of a small molecule

binding pocket, in view of the prevalence of intracellular antagonists among the chemokine receptor family so far.

The loss of [$^{3}$H]-CCR2-RA binding upon the mutation of V244$^{6.36}$ into alanine confirms that TM-VI is involved in the creation of the intracellular small molecule binding pocket. Notably, it is TM-VI that moves outward on activation of GPCRs as has become evident from a comparison between active and inactive state crystal structures [43]. Besides steric hindrance by the antagonist for G protein binding, the fixation of TM-VI in an inactive state might be another mechanism by which these antagonists exert their inhibitory effect. Interestingly this valine residue is among the few differential intracellular residues between CCR2 and CCR5, since a leucine is present on this position in CCR5 (Fig. 3A). Clearly the presence of a valine is very important for high affinity binding of CCR2-RA-[R], and the extended alkyl chain of the leucine in CCR5 may cause steric hindrance preventing high affinity binding of CCR2-RA-[R].



JNJ-27141491 and SD-24 share the intracellular binding pocket of CCR2-RA-[R], but were found to interact differently with surrounding residues. K311A$^{8.49}$ showed a significant reduction in affinity for SD-24 (4-fold), whereas no change was observed for JNJ-27141491. A 2-fold change in affinity was observed for D78N$^{2.40}$ for both JNJ-27141491 and SD-24, and K72A$^{2.34}$ only affected JNJ-27141491. These two residues were not important for binding of CCR2-RA-[R], but do surround its binding pocket and therefore serve as likely interaction partners for structurally different antagonists like JNJ-27141491 and SD-24 (Fig. 5 and 6).

Importantly, the affinity of the orthosteric antagonist INCB3344 was not affected for any of the mutations at the intracellular interface. Instead a significantly reduced affinity of INCB3344 was observed for the E291A$^{7.39}$ mutation (8-fold), as was published before for other orthosteric antagonists [44, 45]. Of note, this is the first study with experimental data that confirms the interaction of INCB3344 with E291$^{7.39}$ of CCR2 – a residue that is known to function as an anchor point for many positively charged CC-chemokine receptor small molecules [9, 45]. Interestingly a slight increase in INCB3344 affinity was observed for the F312A$^{8.50}$ and V244A$^{6.36}$ mutant receptors. This could imply that these mutants induce an inactive conformation of the receptor, in agreement with their lack of G protein-activation in the [$^{35}$S]GTPγS assay, and thereby enhance binding of INCB3344.

Intracellular binding sites have become subject of study over the past few years. The cytoplasmic tails of CCR4, CCR5 and CXCR1 have been implicated in the binding of antagonists, as were several specific intracellular residues for antagonists of CXCR2, including equivalent residues we studied [16-18]. In addition, an allosteric modulator of the PAR1 receptor was found to act through helix-VIII [46]. In the current study we largely identified the location of this intracellular binding pocket for CCR2. Notably, we were for the first time able to visualize

such an intracellular binding pocket upon induced-fit docking of CCR2-RA-[R] in a CCR2 homology model that was constructed based on the recent crystal structure of CCR5 [42]. Previous attempts to predict the location of intracellular binding pockets in homology models most likely failed due to the lack of a closely related crystal structure [18].

In summary, the evidence for intracellular binding pockets at (chemokine) GPCRs is accumulating. The results of our mutagenesis and docking studies provide evidence for such an allosteric binding site on CCR2 at a defined location and may facilitate the design of novel intracellular antagonists for this and other chemokine receptors, and, hopefully, for GPCRs in general.

## References


1. Jimenez, F., et al., *CCR2 plays a critical role in dendritic cell maturation: possible role of CCL2 and NF-kappa B.* J Immunol, 2010. 184(10): p. 5571-81.
2. Luster, A.D., *Chemokines--chemotactic cytokines that mediate inflammation.* N Engl J Med, 1998. 338(7): p. 436-45.
3. Fantuzzi, L., et al., *Loss of CCR2 expression and functional response to monocyte chemotactic protein (MCP-1) during the differentiation of human monocytes: role of secreted MCP-1 in the regulation of the chemotactic response.* Blood, 1999. 94(3): p. 875-83.
4. Mahad, D.J. and R.M. Ransohoff, *The role of MCP-1 (CCL2) and CCR2 in multiple sclerosis and experimental autoimmune encephalomyelitis (EAE).* Semin Immunol, 2003. 15(1): p. 23-32.
5. Quinones, M.P., et al., *The complex role of the chemokine receptor CCR2 in collagen-induced arthritis: implications for therapeutic targeting of CCR2 in rheumatoid arthritis.* J Mol Med (Berl), 2005. 83(9): p. 672-81.
6. Boring, L., et al., *Decreased lesion formation in CCR2-/- mice reveals a role for chemokines in the initiation of atherosclerosis.* Nature, 1998. 394(6696): p. 894-7.
7. White, F.A., S.K. Bhangoo, and R.J. Miller, *Chemokines: integrators of pain and inflammation.* Nat Rev Drug Discov, 2005. 4(10): p. 834-44.
8. Surgand, J.S., et al., *A chemogenomic analysis of the transmembrane binding cavity of human G-protein-coupled receptors.* Proteins, 2006. 62(2): p. 509-38.
9. Rosenkilde, M.M. and T.W. Schwartz, *GluVII:06--a highly conserved and selective anchor point for non-peptide ligands in chemokine receptors.* Curr Top Med Chem, 2006. 6(13): p. 1319-33.
10. Zweemer, A.J., et al., *Multiple Binding Sites for Small-Molecule Antagonists at the CC Chemokine Receptor 2.* Mol Pharmacol, 2013. 84(4): p. 551-61.
11. Shin, N., et al., *Pharmacological characterization of INCB3344, a small molecule antagonist of human CCR2.* Biochem Biophys Res Commun, 2009. 387(2): p. 251-5.
12. Scholten, D.J., et al., *Pharmacological modulation of chemokine receptor function.* Br J Pharmacol, 2011. 165(6): p. 1617-43.
13. Maeda, K., et al., *Structural and molecular interactions of CCR5 inhibitors with CCR5.* J Biol Chem, 2006. 281(18): p. 12688-98.
14. Rosenkilde, M.M., et al., *The minor binding pocket: a major player in 7TM receptor activation.* Trends Pharmacol Sci, 2010. 31(12): p. 567-74.
15. Wu, B., et al., *Structures of the CXCR4 chemokine GPCR with small-molecule and cyclic peptide antagonists.* Science, 2010. 330(6007): p. 1066-71.
16. Andrews, G., C. Jones, and K.A. Wreggett, *An intracellular allosteric site for a specific class of antagonists of the CC chemokine G protein-coupled receptors CCR4 and CCR5.* Mol Pharmacol, 2008. 73(3): p. 855-67.
17. Nicholls, D.J., et al., *Identification of a putative intracellular allosteric antagonist binding-site in the CXC chemokine receptors 1 and 2.* Mol Pharmacol, 2008. 74(5): p. 1193-202.
18. Salchow, K., et al., *A common intracellular allosteric binding site for antagonists of the CXCR2 receptor.* Br J Pharmacol, 2010. 159(7): p. 1429-39.
19. Peace, S., et al., *Identification of a sulfonamide series of CCR2 antagonists.* Bioorg Med Chem Lett, 2010. 20(13): p. 3961-4.
20. Thiele, S., et al., *Allosteric and orthosteric sites in CC chemokine receptor (CCR5), a chimeric receptor approach.* J Biol Chem, 2011. 286(43): p. 37543-54.
21. Ballesteros, J.A., Weinstein, H, *Integrated methods for the construction of three dimensional models and computational probing of structure-function relations in G-protein coupled receptors.* Methods Neurosci, 1995. 25: p. 366-428.

22. Kissow, H., et al., *Glucagon-like peptide-1 (GLP-1) receptor agonism or DPP-4 inhibition does not accelerate neoplasia in carcinogen treated mice.* Regul Pept, 2012. 179(1-3): p. 91-100.
23. Smith, P.K., et al., *Measurement of protein using bicinchoninic acid.* Anal Biochem, 1985. 150(1): p. 76-85.
24. Schrodinger, MacroModel, version 10.1, LLC, New York, NY, 2013.
25. Schrodinger, Prime, version 3.2, LLC, New York, NY, 2013.
26. Jacobson, M.P., et al., *A hierarchical approach to all-atom protein loop prediction.* Proteins, 2004. 55(2): p. 351-67.
27. Jacobson, M.P., et al., *On the role of the crystal environment in determining protein side-chain conformations.* J Mol Biol, 2002. 320(3): p. 597-608.
28. Sherman, W., H.S. Beard, and R. Farid, *Use of an induced fit receptor structure in virtual screening.* Chem Biol Drug Des, 2006. 67(1): p. 83-4.
29. Schrodinger, Schrodinger Suite 2013-2 Induced Fit docking protocol; Glide version 6.0, Schrodinger, LLC, New York, NY, 2013; Prime version 3.3, Schrodinger, LLC, New York, NY, 2013.
30. Schrodinger, The PyMOL Molecular Graphics System, Version 1.5.0.4 Schrodinger, LLC.
31. Furchgott, R.F., *Receptor mechanisms.* Annu Rev Pharmacol, 1964. 4: p. 21-50.
32. De Lean, A., J.M. Stadel, and R.J. Lefkowitz, *A ternary complex model explains the agonist-specific binding properties of the adenylate cyclase-coupled beta-adrenergic receptor.* J Biol Chem, 1980. 255(15): p. 7108-17.
33. Wootten, D., A. Christopoulos, and P.M. Sexton, *Emerging paradigms in GPCR allostery: implications for drug discovery.* Nat Rev Drug Discov, 2013. 12(8): p. 630-44.
34. Shields, D.C., *Gene conversion among chemokine receptors.* Gene, 2000. 246(1-2): p. 239-45.
35. Toda, E., et al., *FROUNT is a common regulator of CCR2 and CCR5 signaling to control directional migration.* J Immunol, 2009. 183(10): p. 6387-94.
36. Maeda, K., et al., *Involvement of the second extracellular loop and transmembrane residues of CCR5 in inhibitor binding and HIV-1 fusion: insights into the mechanism of allosteric inhibition.* J Mol Biol, 2008. 381(4): p. 956-74.
37. Jensen, P.C., et al., *Reversed binding of a small molecule ligand in homologous chemokine receptors - differential role of extracellular loop 2.* Br J Pharmacol, 2012. 166(1): p. 258-75.
38. Fritze, O., et al., *Role of the conserved NPxxY(x)5,6F motif in the rhodopsin ground state and during activation.* Proc Natl Acad Sci U S A, 2003. 100(5): p. 2290-5.
39. Kalatskaya, I., et al., *Mutation of tyrosine in the conserved NPXXY sequence leads to constitutive phosphorylation and internalization, but not signaling, of the human B2 bradykinin receptor.* J Biol Chem, 2004. 279(30): p. 31268-76.
40. Nygaard, R., et al., *Ligand binding and micro-switches in 7TM receptor structures.* Trends Pharmacol Sci, 2009. 30(5): p. 249-59.
41. Hulme, E.C., *GPCR activation: a mutagenic spotlight on crystal structures.* Trends Pharmacol Sci, 2013. 34(1): p. 67-84.
42. Tan, Q., et al., *Structure of the CCR5 chemokine receptor-HIV entry inhibitor maraviroc complex.* Science, 2013. 341(6152): p. 1387-90.
43. Kruse, A.C., et al., *Activation and allosteric modulation of a muscarinic acetylcholine receptor.* Nature, 2013. 504(7478): p. 101-6.
44. Hall, S.E., et al., *Elucidation of binding sites of dual antagonists in the human chemokine receptors CCR2 and CCR5.* Mol Pharmacol, 2009. 75(6): p. 1325-36.
45. Mirzadegan, T., et al., *Identification of the binding site for a novel class of CCR2b chemokine receptor antagonists: binding to a common chemokine receptor motif within the helical bundle.* J Biol Chem, 2000. 275(33): p. 25562-71.

46. Dowal, L., et al., *Identification of an antithrombotic allosteric modulator that acts through helix 8 of PAR1*. Proc Natl Acad Sci U S A, 2011. 108(7): p. 2951-6.

47. Brodmerkel, C.M., et al., *Discovery and pharmacological characterization of a novel rodent-active CCR2 antagonist*, INCB3344. J Immunol, 2005. 175(8): p. 5370-8.

48. Xue, C.B., et al., *3-Aminopyrrolidine derivatives as modulators of chemokine receptors*, 2004. Inventors, Incyte Corporation. PCT/US2003/037946.

49. Zou, D., et al., *Novel, acidic CCR2 receptor antagonists: from hit to lead*. Lett Drug Des Discov, 2007. 4: p. 185-191.

50. Doyon, J., et al., *Discovery of potent, orally bioavailable small-molecule inhibitors of the human CCR2 receptor*. Chem Med Chem, 2008. 3 (4): p. 660-9.

# Chapter 5

## Allosteric modulation of the chemokine receptor CCR2 by amiloride analogues and sodium ions

Annelien J.M. Zweemer
Dora M. Hammerl
Arnault Massink
Margo Veenhuizen
Eelke B. Lenselink
Henk de Vries
Laura H. Heitman
Adriaan P. IJzerman

*Manuscript in preparation*

## Abstract

The chemokine receptor CCR2 is a G protein-coupled receptor (GPCR) that is expressed on immune cells and involved in many diseases characterized by inflammation. Previously two distinct binding pockets were reported for small molecules targeting this receptor. In the present study, we revealed yet another binding pocket via which amiloride analogues and sodium ions were discovered to modulate CCR2.

In radioligand binding studies the amiloride analogue HMA allosterically inhibited binding of the agonist $^{125}$I-CCL2, the orthosteric antagonist [$^{3}$H]-INCB3344 and the intracellular antagonist [$^{3}$H]-CCR2-RA-[R]. Differently, sodium ions only allosterically inhibited $^{125}$I-CCL2 binding, while they enhanced binding of [$^{3}$H]-CCR2-RA-[R]. Three residues located in the core of the transmembrane domain, D88$^{2.50}$, W256$^{6.48}$ and H297$^{7.45}$, turned out to be important for modulation of the antagonist radioligands, since mutation of these residues abolished or diminished the allosteric effects induced by HMA and sodium ions. Upon induced-fit docking of HMA in a homology model of CCR2, we visualized its interaction with D88$^{2.50}$, W256$^{6.48}$ and H297$^{7.45}$ and predicted additional surrounding residues of this binding pocket.

With this work we identified a third binding pocket for small molecules at CCR2, which is located in the core domain of the receptor. By means of the intracellular radioligand [$^{3}$H]-CCR2-RA-[R] we were able to demonstrate allosteric modulation of the intracellular CCR2 domain by HMA and sodium ions, which has not yet been reported for other GPCRs. This work contributes to our knowledge of allosteric modulation of GPCRs, and offers novel opportunities for targeting CCR2.

## Introduction

G protein-coupled receptors (GPCRs) comprise the largest family of cell-surface signal-transduction proteins in mammalian cells [1]. They transfer signals into the cell upon binding of their endogenous ligand at the extracellular face of the receptor. However, during the last decades many small molecule ligands and endogenous chemical entities have been discovered to bind at sites different from where the endogenous ligand binds, so-called allosteric sites [2]. Via these sites they can activate, inhibit or modulate the response of the GPCR. In this study we reveal a novel allosteric binding site in the chemokine receptor CCR2 that allows amiloride analogues and sodium ions to modulate the receptor.

CCR2 is a member of the CC-chemokine receptors which belong to the family of class A GPCRs. It is mainly expressed on monocytes, dendritic cells and lymphocytes, and therefore this receptor is important for correct functioning of the immune system [3, 4]. However, CCR2 is also involved in a variety of diseases including atherosclerosis, rheumatoid arthritis and chronic pain, which makes it an attractive target for the pharmaceutical industry [5]. Many CCR2 small molecule antagonists have been developed, but unfortunately without any clinical success so far. Development of allosteric drugs might offer therapeutic benefits for targeting this receptor [6].

CCR2 is mainly activated by its endogenous chemokine ligand CCL2, which is a peptide of 76 amino acids that binds to the extracellular loops (ECLs) and the TM domain of CCR2 [7]. The numerous small molecule antagonists that have been synthesized so far are chemically divergent, and were recently discovered to bind to two distinct binding sites at CCR2 [8]. One class of antagonists binds in the main binding pocket, located at the upper half of the TM domain of the receptor (orthosteric site), while the other class binds at the intracellular side of the receptor (allosteric site) (Chapter 4). The presence of these multiple binding sites alerted us to investigate whether CCR2 is also prone to modulation by typical GPCR modulators such as amiloride analogues and sodium ions, and if so, via which binding site this is manifested. Amiloride analogues and sodium ions have been found to modulate several class A GPCRs, including adenosine, dopamine and opioid receptors [9-11]. The binding pocket for these ligands is located in the core of the TM-domain, surrounded by the highly conserved residues $D^{2.50}$ and $W^{6.48}$. The position of the sodium ion within this pocket has been revealed in high resolution crystal structures of the inactive $A_{2A}$ adenosine receptor ($A_{2A}$AR) [12], the inactive protease-activated receptor 1 (PAR1) [13], and the inactive δ-opioid receptor (δ-OR) [11]. In addition, several biochemical studies provided proof that amiloride analogues bind to this same binding pocket in e.g., the α2-adrenergic receptor [36] and the $A_{2A}$AR [10, 14].

Up to date there is no evidence of the presence of such a sodium binding pocket for chemokine receptors, and neither has modulation of this receptor family by amiloride analogues been researched. In the present study, we took advantage of the availability of two different tool compounds, the orthosteric antagonist radioligand [$^3$H]-INCB3344 and the intracellular antagonist radioligand [$^3$H]-CCR2-RA-[R], to study CCR2 modulation by the sodium ions and amiloride analogues. We unmasked a third binding pocket for small molecules at CCR2, and thereby revealed that this receptor bears small molecule binding pockets throughout the entire transmembrane region. Therefore, this study offers novel opportunities for targeting CCR2.

## Materials and methods

**Chemicals and reagents.** INCB3344 and CCR2-RA-[R] were synthesized according to published methods [15-17]. [$^3$H]-INCB3344 (specific activity 32 Ci mmol$^{-1}$) and [$^3$H]-CCR2-RA-[R] (specific activity 60 Ci mmol$^{-1}$) were custom-labeled by Vitrax (Placentia, CA). Bovine serum albumin (BSA, fraction V) was purchased from Sigma (St. Louis, MO, USA). Bicinchoninic acid (BCA) and BCA protein assay reagent were obtained from Pierce Chemical Company (Rockford, IL, USA). Tango CCR2-bla U2OS cells stably expressing human CCR2 (U2OS-CCR2) were obtained from Invitrogen (Carlsbad, CA). Chinese hamster ovary (CHO) cells were obtained from Hans den Dulk (Leiden University, the Netherlands). pcDNA3.1+ plasmid containing wild-type (WT) CCR2 with a 3x hemagglutinin (HA) epitope tag at the N-terminus was kindly provided by James Pease (Imperial College London, UK) [18]. The monoclonal rabbit anti-HA-tag antibody and the HRP-conjugated goat anti-rabbit antibody were obtained from Novus Biologicals (Cambridge UK). LiCl was obtained from Merck KGaA (Darmstadt, Germany). KCl, NaCl, amiloride (3,5-diamino-6-chloro-*N*-[diaminomethylene]pyrazine-2-carboxamide) and HMA (5-[N,N-hexamethylene]amiloride) were purchased from Sigma Aldrich (Zwijndrecht, the Netherlands). MGCMA (5-[N-methyl-N-guanodinocarbonyl-methyl]amiloride), benzamil (3,5-diamino-N-[(1E)-amino-(benzylamino)methylidene]-6-chloropyrazine-2-carboxamide), MIBA (5-[N-methyl-N-isobutyl]amiloride) and phenamil (3,5-diamino-N-[imino(phenylamino) methyl]pyrazinecarboxamide) were obtained from Dr E. J. Cragoe (Lansdale, USA) and were synthesized as described before [19]. Sodium butyrate was obtained from Fisher Scientific (Landsmeer, NL). Polyethylenimine (PEI) was obtained from Polysciences Inc (Eppelheim, Germany). All other chemicals were obtained from standard commercial sources.

**Cell culture.** U2OS-CCR2 cells were cultured as described before [8]. CHO cells were cultured in DMEM/Ham's F12 medium supplemented with 10% fetal calf serum, 50 IU/ml penicillin, and 50 µg/ml streptomycin, in a humidified atmosphere at 37 °C and 5% $CO_2$. Cells were subcultured twice a week at a ratio of 1:20 on 10 cm ø or 15 cm ø plates by trypsinization.

**Site-directed mutagenesis.** D88A$^{2.50}$, W256A$^{6.48}$ and H297A$^{7.45}$ mutations (superscript indicates the Ballesteros Weinstein numbering system [20], in which transmembrane residues are assigned two numbers that belong to the helix number and the residue number relative to the most conserved residue in this helix, which is assigned 50) were generated by site-directed mutagenesis using WT HA-tagged CCR2 plasmid DNA as a template for the generation of mutant plasmids by polymerase chain reaction (PCR) using the QuickChange®II site-directed mutagenesis kit (Stratagene, the Netherlands) and the appropriate oligonucleotide primers (Eurogentec, the Netherlands), under conditions recommended by the manufacturer. All mutants were verified by DNA sequencing before use (LGTC, The Netherlands).



**PEI transfections.** WT and mutant CCR2 receptors were transiently transfected into CHO cells using PEI. One day prior to transfection CHO cells were split in a ratio of 1:9 on 15 cm ø plates, to reach 50-60% confluence. 10 µg of plasmid DNA was diluted in a sterile 150 mM NaCl solution and subsequently mixed with PEI solution (1 mg/mL) to obtain a DNA:PEI mass ratio of 1:6. The mixture was incubated for 20 min at room temperature before transfection. The culture medium of the cells was refreshed and 1 mL of DNA/PEI mixture was added to cells and incubated for 48 hrs at 37 °C and 5% $CO_2$. In case of transfections with mutant CCR2 receptors, 500 µl sodium butyrate (final concentration of 5 mM) was added to each plate after 24 hrs in order to increase the receptor expression [21].

**Cell surface expression by Enzyme-Linked Immunosorbent Assay (ELISA).** Cell surface expression of WT and mutant CCR2 constructs, all containing a HA-tag, was measured by enzyme linked immunosorbent assay (ELISA). In a 96-well plate, $1x10^6$ cells per well were plated 24 hrs after transfection and incubated at 37 °C, 5% $CO_2$. 48 hrs after transfection cells were fixed with 3.7% formaldehyde. The cells were washed with DMEM and the primary antibody (monoclonal rabbit anti-HA-tag 1:5000 in DMEM) was incubated for 30 min at RT. After removal of the primary antibody, the cells were washed with DMEM/25 mM HEPES and dried for 10 min. Subsequently, a mixture of the secondary antibody (HRP-conjugated goat anti-rabbit 1:5000 in DMEM) was incubated for 30 min. The cells were washed twice with PBS (37 °C) and left to dry for 10 min at RT. 100 µl tetramethylbenzene (TMB) was added in the

dark and incubated for 5 min. The reaction was stopped after addition of 100 µl 1 M $H_3PO4$. After 5 min, absorbance was measured at 450 nm with a Victor2V plate reader (Perkin Elmer, Waltham, MA, USA).

**Cell membrane preparation**. Preparation of membranes was performed as described before [8]. Briefly, cells were scraped from 15 cm ø plates upon which the membranes and cytosolic fractions were separated during several centrifugation steps. Finally, the membrane pellet was resuspended in ice-cold 50 mM Tris-HCl buffer containing 5 mM $MgCl_2$, pH 7.4, and aliquots were stored at −80 °C. Membrane protein concentrations were measured using a BCA protein determination with BSA as a standard [22].

**[$^3$H]-INCB3344 binding assays.** Binding assays were performed in a 100 µL reaction volume containing 50 mM Tris-HCl buffer (pH 7.4), 5 mM $MgCl_2$, 0.1% CHAPS and 7.5 µg of membrane protein for WT CCR2 membranes and 20-40 µg for mutant receptors, at 25 °C. Saturation experiments were performed using 12 different concentrations of radioligand from 0.5 to 20 nM for 120 min of incubation. Non-specific binding was determined at three concentrations of radioligand with 10 µM BMS22. Displacement assays were carried out with 3.5 nM [$^3$H]-INCB3344 using 10 concentrations of competing ligand for 120 min of incubation. In dissociation experiments the membranes were first incubated with 3.5 nM [$^3$H]-INCB3344 for 90 min. Dissociation was initiated by addition of 10 µM BMS22 in the absence or presence of modulator at different time points during 180 min. Homologous competition experiments with mutant receptors were performed with 3.5 nM [$^3$H]-INCB3344 and increasing concentrations of unlabeled INCB3344 for an incubation time of 120 min. For assays with the mutant receptors and NaCl or HMA, a radioligand concentration of 6.0 nM was used. The assays were terminated as described before [8]. In all experiments, total radioligand binding did not exceed 10% of the amount added to prevent ligand depletion.

**[$^3$H]-CCR2-RA-[R] binding assays.** Assay conditions were similar as described for [$^3$H]-INCB3344 binding assays, unless otherwise stated. Saturation experiments were carried out using 12 different concentrations of radioligand from 0.1 to 75 nM for 120 min of incubation. Non-specific binding was determined at three concentrations of radioligand with 10 µM JNJ-27141491. Displacement assays were carried out with 7.0 nM [$^3$H]-CCR2-RA-[R] using 10 concentrations of competing ligand for 120 min of incubation. Kinetic experiments were performed at 15 °C. For dissociation experiments the membranes were first incubated with 7.0 nM [$^3$H]-CCR2-RA-[R] for 90 min. Dissociation was initiated upon addition of 10 µM of JNJ-

27141491 in the absence or presence of modulator at different time points during 180 min. For displacement and dissociation assays non-specific binding was determined with 10 µM JNJ-27141491. Homologous competition experiments with mutant receptors were performed with 20 nM [$^3$H]-CCR2-RA-[R] and increasing concentrations of unlabeled CCR2-RA-[R] for an incubation time of 120 min. Non-specific binding was determined with 10 µM CCR2-RA-[R]. For assays with the mutant receptors and NaCl or HMA, a radioligand concentration of 20 nM was used. For measurements with HMA, nonspecific binding was determined for every data point with a combination of 10 µM CCR2-RA-[R] and 0.1 mM HMA. The assays were terminated as described before [8]. In all experiments, total radioligand binding did not exceed 10% of the amount added to prevent ligand depletion.

**$^{125}$I-CCL2 dissociation assay.** The assay was performed in a 100 µL reaction volume containing 50 mM Tris-HCl buffer (pH 7.4), 5 mM $MgCl_2$ and 0.1% 3-((3-cholamidopropyl)-dimethylammonio)-1-propanesulfonate (CHAPS). 15 µg of U2OS-CCR2 membrane protein was incubated with 0.1 nM $^{125}$I-CCL2 for 2 hrs at 37ºC. Subsequently, dissociation was initiated upon addition of 50 nM CCL2 in the absence or presence of modulator at different time points. Non-specific binding was determined with 10 µM INCB3344. The assay was terminated as described before [8]. Total radioligand binding did not exceed 10% of the amount added to prevent ligand depletion.

**Homology modeling and docking.** A homology model of the chemokine CCR2 receptor was constructed using the homology modeling tool within Maestro [23-25]. This model was based on the structure of the chemokine CCR5 receptor co-crystalized with maraviroc (Protein Data Bank: 4MBS). The best model was selected based on the energy-based scoring function, the alignment between CCR2 and CCR5 was performed using ClustalW as implemented within Maestro. HMA was docked using the induced fit docking protocol [26, 27]. The grid center was placed based on residues D88$^{2.50}$, W256$^{6.48}$ and H297$^{7.45}$ with an automatic box size. Visualizations were created using PyMOL version 1.6.0.0. [28].

**Data analysis.** All experiments were analyzed using the non-linear regression curve fitting program Prism 5 (GraphPad, San Diego, CA, U.S.A.). The $pIC_{50}$ values of HMA and MIBA were obtained by non-linear regression analysis of the displacement curves. The $pK_{D,}$ defined as – $\log_{10}K_D$, and $B_{max}$ values of [$^3$H]-INCB3344 and [$^3$H]-CCR2-RA-[R] for WT CCR2 were obtained by computer analysis of saturation curves according to the equation bound = $(B_{max}*[L])/([L]+K_d)$ where $B_{max}$ is the maximal number of binding sites (pmol/mg) and $K_D$ is the concentration

of radioligand required to reach half-maximal binding. The $pK_D$ values of [$^3$H]-INCB3344 and [$^3$H]-CCR2-RA-[R] for mutant CCR2 receptors were calculated from homologous competition experiments using the Cheng-Prusoff equation, assuming that unlabeled and labeled INCB3344 had identical affinities, and the same for unlabeled and labeled CCR2-RA-[R] [29]. The dissociation rate constant ($k_{off}$) was obtained by computer analysis of the exponential decay of radioligand binding to the receptor. [$^3$H]-INCB3344 experiments were fitted according to monophasic equations. Dissociation of [$^3$H]-CCR2-RA-[R] occurred in a biphasic manner. Binding data from $^{125}$I-CCL2 dissociation kinetic experiments were fitted assuming monophasic or biphasic dissociation curves. By the F-test, a significant better fit for biphasic dissociation was found for curves with addition of HMA and NaCl. Data shown are the mean ± S.E.M. of at least 3 separate experiments performed in duplicate. Statistical analysis was performed with a two-tailed unpaired Student's *t*-test.

## Results

**Antagonist equilibrium binding assays.** To determine if CCR2 was susceptible to modulation by amiloride analogues (Fig. 1) and sodium ions, we performed equilibrium binding studies with the radiolabeled orthosteric antagonist [$^3$H]-INCB3344 and allosteric antagonist [$^3$H]-CCR2-RA-[R].

Addition of 0.1 mM amiloride, benzamil, phenamil or MGCMA did not result in any radioligand displacement (data not shown). Differently, [$^3$H]-INCB3344 was displaced by HMA and MIBA with a $pIC_{50}$ of 4.1 ± 0.1 and 3.8 ± 0.0, respectively (Fig. 2A+B). The allosteric radioligand [$^3$H]-CCR2-RA-[R] was also displaced by both HMA and MIBA with a $pIC_{50}$ of 4.1 ± 0.1 and 3.9 ± 0.0 (Fig. 2A+B). These data indicate that CCR2 possesses a binding pocket for amiloride analogues, among which HMA binds with the highest affinity. In addition, the hill slopes of the curves deviated from unity, being -1.9 ± 0.1 (HMA) and -1.9 ± 0.5 (MIBA) for displacement of [$^3$H]-INCB3344, and -2.1 ± 0.1 (HMA) and -2.0 ± 0.3 (MIBA) for displacement of [$^3$H]-CCR2-RA-[R] (Table 1). This suggests that HMA and MIBA bind to CCR2 in an allosteric manner with respect to both antagonist radioligands.

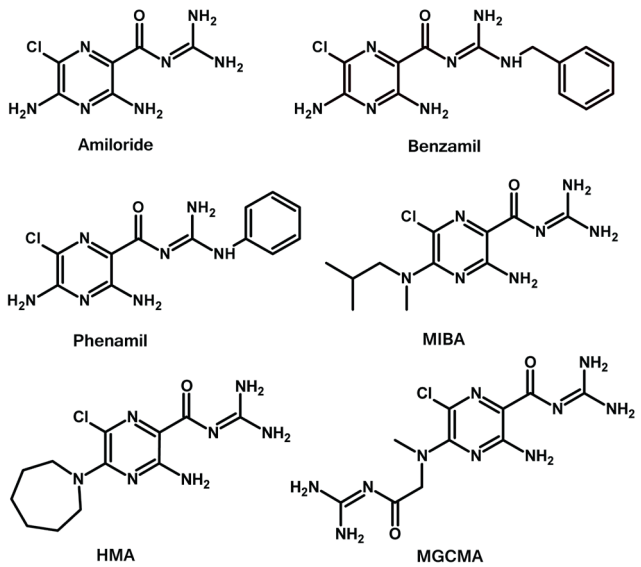



**Fig. 1.** Chemical structures of amiloride and the amiloride analogues HMA, MIBA, benzamil, phenamil and MGCMA.

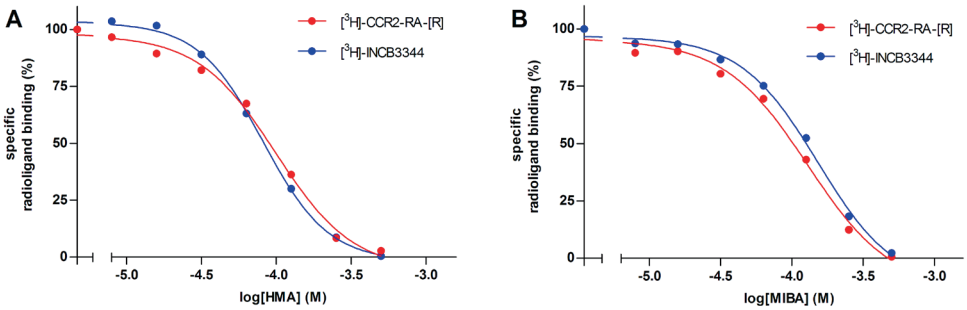



**Fig. 2.** Displacement of the orthosteric antagonist [$^3$H]-INCB3344 and the allosteric antagonist [$^3$H]-CCR2-RA-[R] from CHO cell membranes transiently expressing CCR2, upon addition of increasing concentrations of the amiloride analogues HMA (A) or MIBA (B). Results are presented as percentage of bound radioligand for one representative experiment performed in duplicate.

**Table 1.** Displacement of [$^3$H]-INCB3344 and [$^3$H]-CCR2-RA-[R] by HMA and MIBA from CHO cell membranes transiently expressing CCR2.

| | orthosteric [$^3$H]-INCB3344 | | allosteric [$^3$H]-CCR2-RA-[R] | |
|---|---|---|---|---|
| **amiloride analogue** | **HMA** | **MIBA** | **HMA** | **MIBA** |
| **pIC$_{50}$ ± S.E.M.** | 4.1 ± 0.1 | 3.8 ± 0.0 | 4.1 ± 0.1 | 3.9 ± 0.0 |
| **hill slope** | -1.9 ± 0.1 | -1.9 ± 0.5 | -2.1 ± 0.1 | -2.0 ± 0.3 |

Data presented as pIC$_{50}$ (mean ± S.E.M.) of three independent experiments performed in duplicate.

Besides the amiloride analogues, we also included sodium ions in the antagonist radioligand binding studies. Interestingly, high concentrations of NaCl significantly enhanced binding of the allosteric antagonist [$^3$H]-CCR2-RA-[R] up to 131 ± 7 % at 1 M, whereas binding of the orthosteric antagonist [$^3$H]-INCB3344 was not affected (Fig. 3A). To further investigate if the enhanced binding of [$^3$H]-CCR2-RA-[R] was the result of CCR2 modulation by the sodium cation or rather the chloride anion, we performed similar binding experiments in the presence of 1 M LiCl or KCl. LiCl significantly enhanced binding of [$^3$H]-CCR2-RA-[R] up to 169 ± 16 %, whereas [$^3$H]-CCR2-RA-[R] binding in the presence of 1 M KCl was not affected (Fig. 3B).

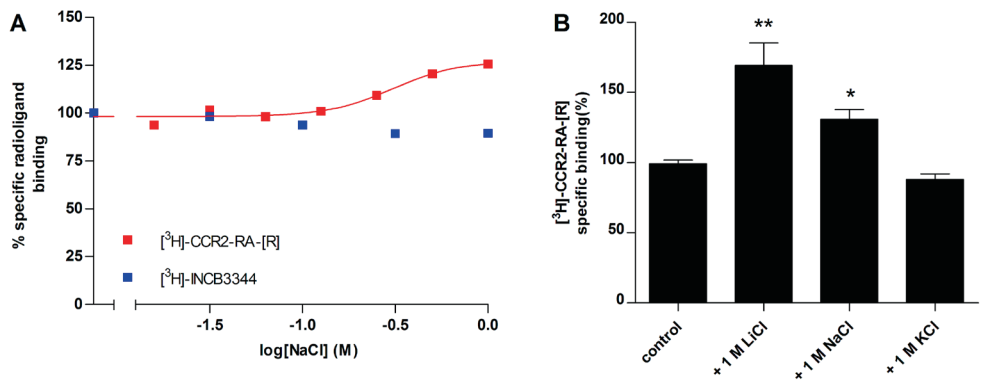



**Fig. 3.** (A) Modulation of binding of the orthosteric antagonist [$^3$H]-INCB3344 and the allosteric antagonist [$^3$H]-CCR2-RA-[R] to CHO cell membranes transiently expressing CCR2 by increasing concentrations of NaCl. Results are presented as percentage of bound radioligand for one representative experiment performed in duplicate. (B) Modulation of binding of the allosteric antagonist [$^3$H]-CCR2-RA-[R] by 1 M LiCl, NaCl or KCl. Results are presented as mean ± S.E.M. for at least three independent experiments performed in triplicate. * $p < 0.05$ vs. control, ** $p < 0.005$ vs. control, Student's *t*-test.

**Antagonist radioligand dissociation assays.** Since the equilibrium binding studies indicated allosteric interactions of the amiloride analogues and sodium ions with respect to one or both of the antagonist radioligands, we continued with kinetic binding studies to further explore their mode of action. For both radioligands [$^3$H]-INCB3344 and [$^3$H]-CCR2-RA-[R], dissociation was initiated by the addition of excess competing unlabeled ligand in the presence and absence of the most potent amiloride analogue HMA and a physiological concentration (150 mM) of sodium ions. In the presence of 0.1 mM HMA the dissociation rate of the orthosteric antagonist [$^3$H]-INCB3344 was 0.030 ± 0.001 min$^{-1}$, which was significantly faster than 0.024 ± 0.002 min$^{-1}$ in the control situation (Fig. 4A, Table 2). [$^3$H]-CCR2-RA-[R] dissociated in a biphasic manner from the receptor, with the fast phase accounting for 48% of the dissociation

(Table 2). In the presence of 0.1 mM HMA we observed an increased, albeit not significant (p = 0.13), fast phase dissociation rate of 0.27 ± 0.09 $min^{-1}$ compared to 0.10 ± 0.03 $min^{-1}$ in the control situation (Fig. 4B, Table 2). The percentage of fast phase dissociation was not affected in the presence of HMA, nor was $k_{slow}$. These data suggest noncompetitive interactions of HMA with respect to both radioligands. On the other hand, addition of 150 mM NaCl did not significantly affect the dissociation rate of either one of the antagonist radioligands (Fig. 4, Table 2).

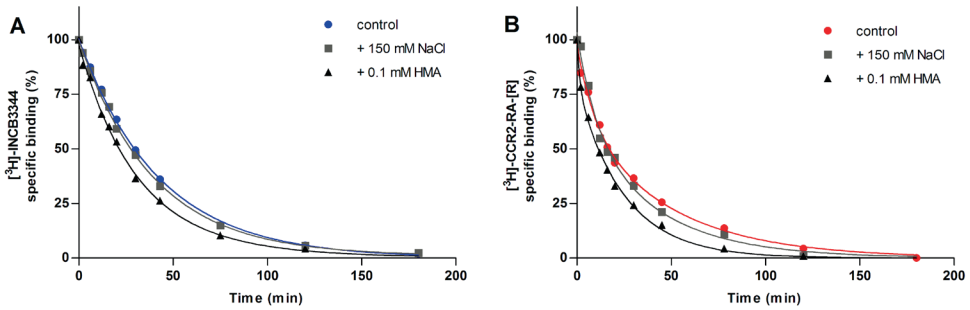



**Fig. 4.** Dissociation of the antagonist radioligands from CHO cell membranes transiently expressing CCR2. (A) Dissociation of [$^3$H]-INCB3344 was initiated upon addition of 10 µM competing ligand BMS22 in the presence and absence of 0.1 mM HMA or 150 mM NaCl at various time points. (B) Dissociation of [$^3$H]-CCR2-RA-[R] was initiated upon addition of 10 µM competing ligand JNJ-27141491 in the presence and absence of 0.1 mM HMA or 150 mM NaCl at various time points. Results are presented as percentage of bound radioligand for one representative experiment performed in duplicate.

**Table 2.** Dissociation rate of [$^3$H]-INCB3344 and [$^3$H]-CCR2-RA-[R] from CHO cell membranes transiently expressing CCR2 in the presence and absence of NaCl and HMA.

| | orthosteric [$^3$H]-INCB3344 | | | allosteric [$^3$H]-CCR2-RA-[R] | | |
|---|---|---|---|---|---|---|
| | control | + 150 mM NaCl | + 0.1 mM HMA | control | + 150 mM NaCl | + 0.1 mM HMA |
| $k_{fast}$ ($min^{-1}$) | 0.024 ± 0.002 | 0.025 ± 0.001 | 0.030 ± 0.001* | 0.10 ± 0.03 | 0.16 ± 0.07 | 0.27 ± 0.09 |
| $k_{slow}$ ($min^{-1}$) | n.a. | n.a. | n.a. | 0.022 ± 0.005 | 0.030 ± 0.005 | 0.030 ± 0.009 |
| % fast | 100 | 100 | 100 | 48 ± 6 | 43 ± 9 | 50 ± 12 |

Data presented as mean ± S.E.M. of three independent experiments performed in duplicate.
n.a., not applicable
* p< 0.05 vs. control, Student's *t*-test.

**Antagonist saturation binding assays.** To confirm the observed noncompetitive effects of HMA in the dissociation studies, we performed saturation binding experiments of [$^3$H]-INCB3344 and [$^3$H]-CCR2-RA-[R] in the presence and absence of 80 µM HMA. As a control we added unlabeled INCB3344 or CCR2-RA-[R]. Addition of HMA significantly decreased

the $B_{max}$ of the orthosteric antagonist [$^3$H]-INCB3344, from 11 ± 1 pmol/mg in the control situation to 7.9 ± 0.6 pmol/mg in the presence of HMA (Fig. 5A and Table 3). The $pK_D$ of 8.7 ± 0.0 was decreased to 8.5 ± 0.1 in the presence of HMA. The decrease in $B_{max}$ suggests a noncompetitive interaction of HMA and INCB3344, whereas the small but significant decrease in the affinity of [$^3$H]-INCB3344 would reflect a competitive interaction. Differently, the $B_{max}$ of [$^3$H]-INCB3344 was not affected in the presence of INCB3344, whereas its $pK_D$ was decreased to 8.3 ± 0.0 (Fig. 5A and Table 3), both in agreement with a competitive mode of interaction. The $B_{max}$ for [$^3$H]-CCR2-RA-[R] of 10 ± 0.4 pmol/mg was decreased to 7.8 ± 0.9 pmol/mg in the presence of HMA (Fig. 5B, Table 3). In addition, the $pK_D$ of 8.1 ± 0.1 of [$^3$H]-CCR2-RA-[R] was not significantly changed by HMA, which suggests a purely noncompetitive mode of interaction. In the presence of CCR2-RA-[R] the $B_{max}$ of [$^3$H]-CCR2-RA-[R] was not affected, whereas its $pK_D$ was decreased to 7.6 ± 0.1 (Fig. 5B and Table 3). These data are in agreement with a competitive mode of interaction.

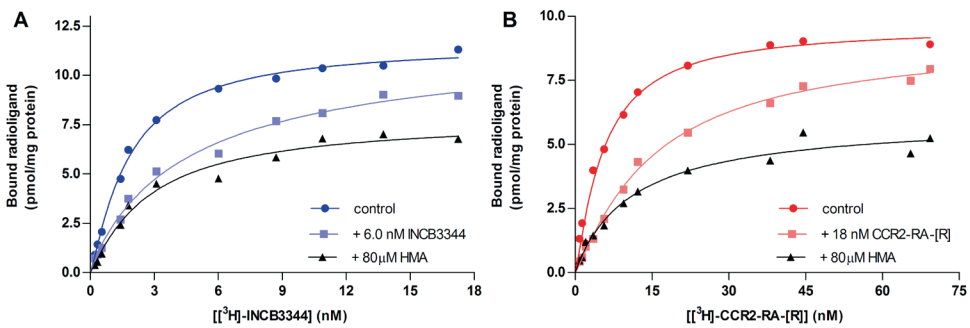



**Fig. 5.** Saturation binding of the antagonist radioligands to CHO cell membranes transiently expressing CCR2. (A) Binding of the orthosteric antagonist [$^3$H]-INCB3344 in the presence and absence of 6.0 nM INCB3344 or 80 µM HMA. (B) Binding of allosteric antagonist [$^3$H]-CCR2-RA-[R] from CHO membranes transiently expressing CCR2 in the presence and absence of 6.0 nM CCR2-RA-[R] or 80 µM HMA. Results are presented as amount of bound radioligand in pmol/mg protein of one representative experiment performed in duplicate.

**Table 3.** Saturation binding of [$^3$H]-INCB3344 and [$^3$H]-CCR2-RA-[R] to CHO cell membranes transiently expressing CCR2 in the presence and absence of HMA or competing unlabeled ligand.

| | orthosteric [$^3$H]-INCB3344 | | | allosteric [$^3$H]-CCR2-RA-[R] | | |
|---|---|---|---|---|---|---|
| | control | + 6.0 nM INCB3344 | + 80 µM HMA | control | + 18 nM CCR2-RA-[R] | + 80 µM HMA |
| $B_{max}$ (pmol/mg) | 11 ± 0.7 | 11 ± 0.8 | 7.9 ± 0.6* | 10 ± 0.4 | 11 ± 0.7 | 7.8 ± 0.9* |
| $pK_D$ | 8.7 ± 0.0 | 8.3 ± 0.0** | 8.5 ± 0.1* | 8.1 ± 0.1 | 7.6 ± 0.1* | 7.8 ± 0.2 |

Data presented as mean ± S.E.M. of three independent experiments performed in duplicate.
* p< 0.05 vs. control, Student's *t*-test.
** p< 0.005 vs. control, Student's *t*-test.

**Agonist modulation by HMA and NaCl.** Besides the modulation of antagonist binding, we also determined the effect of HMA and NaCl on the dissociation of the agonist radioligand $^{125}$I-CCL2. These assays were performed with membrane preparations of U2OS cells stably expressing CCR2, since the non-specific binding of $^{125}$I-CCL2 to these membranes was substantially lower compared to that for membranes of CHO cells transfected with CCR2. Dissociation of $^{125}$I-CCL2 was initiated by an excess of CCL2 in the presence and absence of 0.1 mM HMA or 150 mM NaCl. The dissociation in the control situation was monophasic with a rate of 0.030 ± 0.002 min$^{-1}$, whereas in the presence of HMA or NaCl a biphasic dissociation pattern was observed (Fig. 6 and Table 4). Although the dissociation rates could therefore not be directly compared, enhanced $^{125}$I-CCL2 dissociation was observed in both cases compared to the control situation (Fig. 6 and Table 4). These data show that the endogenous chemokine ligand is allosterically modulated by HMA and NaCl. Notably, physiological NaCl concentrations apparently increased the dissociation rate of $^{125}$I-CCL2, whereas the dissociation rate of the antagonist radioligands at this concentration of NaCl was not affected.



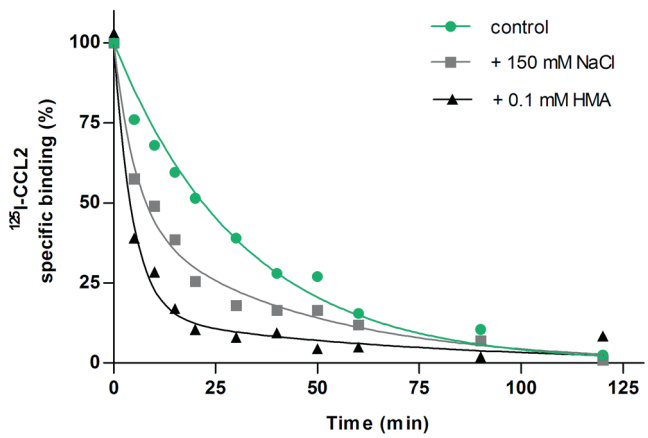



**Fig. 6.** Dissociation of agonist radioligand $^{125}$I-CCL2 from U2OS membranes stably expressing CCR2. Dissociation was initiated upon addition of 50 nM CCL2 in the presence or absence of 0.1 mM HMA or 150 mM NaCl at different time points. Results are presented as percentage of bound radioligand for one representative experiment performed in duplicate.

**Table 4.** Dissociation rates of $^{125}$I-CCL2 from U2OS cell membranes stably expressing CCR2 in the presence and absence of NaCl and HMA.

| | control | + 150 mM NaCl | + 0.1 mM HMA |
|---|---|---|---|
| $k_{fast}$ (min$^{-1}$) | 0.030 ± 0.002 | 0.21 ± 0.01 | 0.29 ± 0.03 |
| $k_{slow}$ (min$^{-1}$) | n.a. | 0.025 ± 0.001 | 0.010 ± 0.003 |
| % fast | 100 | 46 ± 7 | 86 ± 2 |

Data presented as mean ± S.E.M. of three independent experiments performed in duplicate.
n.a., not applicable

**The effect of mutations in the core TM domain on antagonist binding.** In the radioligand binding studies presented above we observed allosteric modulation of $^{125}$I-CCL2, [$^3$H]-INCB3344 and [$^3$H]-CCR2-RA-[R] by HMA, and allosteric modulation of $^{125}$I-CCL2 and [$^3$H]-CCR2-RA-[R] by sodium ions. This suggests that HMA and sodium ions bind to a site other than the orthosteric binding site in the TM domain and distinct from the allosteric binding site at the intracellular side of the receptor. To elucidate the location of this additional binding site, we mutated three residues in the core region of the TM domain, D88$^{2.50}$, W256$^{6.48}$ and H297$^{7.45}$.

By means of whole cell ELISA we measured the expression of the mutant receptors. Cell surface expression of D88A$^{2.50}$, W256A$^{6.48}$ and H297A$^{7.45}$ was 46 %, 19 % and 14 % compared to wild type CCR2 (Fig. 7), suggesting that mutations in the core domain affected the stability of the receptor and/or its transport to the cell membrane. Nevertheless, with sufficient amounts of membrane protein and radioligand we were able to measure the affinity of [$^3$H]-INCB3344 and [$^3$H]-CCR2-RA-[R] in homologous displacement assays. Binding of [$^3$H]-INCB3344 to W256A$^{6.48}$ could not be detected, whereas the p$K_D$ for D88A$^{2.50}$ and H297A$^{7.45}$ was 8.5 ± 0.3 and 8.6 ± 0.1 with a $B_{max}$ of 1.8 ± 0.7 pmol/mg and 0.49 ± 0.17 pmol/mg, respectively (Table 5). The affinity of [$^3$H]-INCB3344 for these two mutant receptors was therefore similar to the p$K_D$ of 8.7 ± 0.0 for WT CCR2. The intracellular antagonist [$^3$H]-CCR2-RA-[R] was able to bind to all mutant receptors, with a p$K_D$ of 7.3 ± 0.2, 6.7 ± 0.1 and 6.8 ± 0.1 for D88A$^{2.50}$, W256A$^{6.48}$ and H297A$^{7.45}$ (Table 5). Compared to the p$K_D$ of 8.1 ± 0.1 for WT CCR2, the affinity of [$^3$H]-CCR2-RA-[R] for all three mutant receptors was substantially decreased. The $B_{max}$ of [$^3$H]-CCR2-RA-[R] for the D88A$^{2.50}$, W256A$^{6.48}$ and H297A$^{7.45}$ mutant receptors was 2.0 ± 0.6 pmol/mg, 2.8 ± 0.5 pmol/mg and 3.1 ± 0.5 pmol/mg, respectively (Table 5).

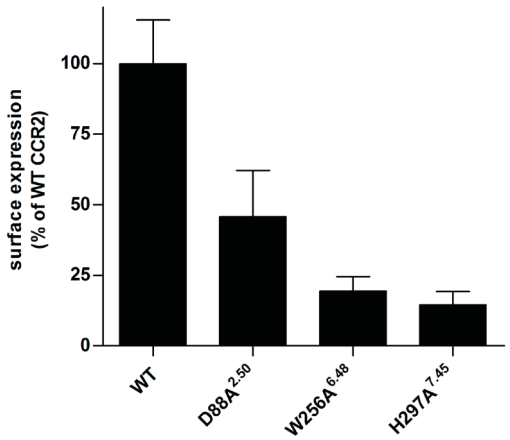



**Fig. 7.** Surface expression of the HA-tagged WT and mutant CCR2 receptors in CHO cells as measured by ELISA. Data was normalized for WT CCR2 expression (100%) and is presented as mean ± SD of at least two experiments performed in quadruplicate.



**Table 5.** The affinity ($pK_D$) and maximum number of binding sites ($B_{max}$) of [$^3$H]-INCB3344 and [$^3$H]-CCR2-RA-[R] for three mutant CCR2 receptors that were transiently expressed on CHO cell membranes. Values were determined from homologous competition experiments with the unlabeled ligands INCB3344 and CCR2-RA-[R], respectively.

| | orthosteric [$^3$H]-INCB3344 | | allosteric [$^3$H]-CCR2-RA-[R] | |
|---|---|---|---|---|
| **construct** | **$pK_D$** | **$B_{max}$ (pmol/mg)** | **$pK_D$** | **$B_{max}$ (pmol/mg)** |
| **D88A$^{2.50}$** | 8.5 ± 0.3 | 1.8 ± 0.7 | 7.3 ± 0.2 | 2.0 ± 0.6 |
| **W256A$^{6.48}$** | no binding | | 6.7 ± 0.1 | 2.8 ± 0.5 |
| **H297A$^{7.45}$** | 8.6 ± 0.1 | 0.49 ± 0.17 | 6.8 ± 0.1 | 3.1 ± 0.5 |

Data presented as mean ± S.E.M. of three independent experiments performed in duplicate.

**The effect of mutations in the core TM domain on modulation by HMA and sodium ions.** Antagonist radioligand binding was measured for WT CCR2 as well as for the mutant receptors D88A$^{2.50}$, W256A$^{6.48}$ and H297A$^{7.45}$ upon addition of 1 M NaCl or 0.1 mM HMA. The results of these experiments will be discussed per mutant in this section.

For D88A$^{2.50}$, the percentage of [$^3$H]-INCB3344 binding in the presence of 0.1 mM HMA increased to 34 ± 6 % compared to 20 ± 2 % for WT CCR2 (Fig. 8A). Similarly, the percentage of [$^3$H]-CCR2-RA-[R] binding to D88A$^{2.50}$ in presence of 0.1 mM HMA increased to 62 ± 5 % compared to 18 ± 2 % for WT CCR2 (Fig. 8B), indicating that the ability of HMA to displace both antagonists decreased upon mutation of D88$^{2.50}$. Addition of 1 M NaCl did not affect [$^3$H]-INCB3344 binding to WT CCR2, neither was a significant change observed for D88A$^{2.50}$ (Fig. 8A). However, enhanced binding of [$^3$H]-CCR2-RA-[R] was observed for WT CCR2 in the

presence of 1 M NaCl, to a percentage of 133 ± 5, which was reduced to 96 ± 4 % upon introduction of D88A$^{2.50}$ (Fig. 8B). These results indicate that D88$^{2.50}$ is involved in sodium ion binding in CCR2.

For W256A$^{6.48}$ we did not measure any binding of [$^3$H]-INCB3344, and therefore we solely used [$^3$H]-CCR2-RA-[R] to study the effects of NaCl and HMA. No displacement of [$^3$H]-CCR2-RA-[R] was observed upon addition of 0.1 mM HMA (Fig. 8B), revealing a crucial role for W256$^{6.48}$ in CCR2 modulation by HMA. In the presence of 1 M NaCl, binding of [$^3$H]-CCR2-RA-[R] was increased to 117 ± 8 %, although not significant with respect to the control situation ($p = 0.1$) (Fig. 8B). This indicates that W256A$^{6.48}$ is important for the allosteric enhancement by sodium ions that was observed for the WT receptor.

For H297A$^{7.45}$, the percentage of [$^3$H]-INCB3344 and [$^3$H]-CCR2-RA-[R] binding compared to WT in the presence of 0.1 mM HMA significantly increased to 30 ± 5 % and 82 ± 7 %, respectively (Fig. 8A+B). In addition, the ability of sodium ions to enhance [$^3$H]-CCR2-RA-[R] binding was completely abolished since only 82 ± 6 % of radioligand binding was measured compared to 133 ± 5 % for the WT receptor (Fig. 8B). These data indicate that the ability of both HMA and sodium ions to modulate CCR2 decreased upon mutation of H297$^{7.45}$.

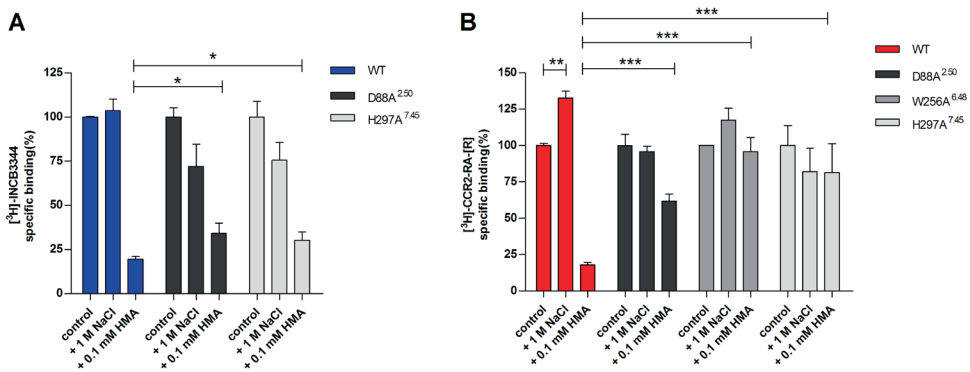



**Fig. 8.** Equilibrium binding of the orthosteric antagonist [$^3$H]-INCB3344 (A) and the allosteric antagonist [$^3$H]-CCR2-RA-[R] (B) in the presence and absence of 1 M NaCl or 0.1 mM HMA. For these experiments CHO cell membranes transiently expressing WT or mutant CCR2 were used. Data are presented as mean ± S.E.M of the percentage of bound radioligand of at least three independent experiments performed in triplicate. * $p < 0.05$ vs. WT, ** $p < 0.01$ vs. control, *** $p < 0.01$ vs. WT, Student's *t*-test.

**Docking of HMA in a CCR2 homology model.** We constructed a CCR2 homology model using the crystal structure of CCR5 (PDB: 4MBS), and performed docking of HMA therein. The positively charged guanidinium group of HMA was docked towards the bottom of the binding pocket where it formed ionic interactions with the negatively charged D88$^{2.50}$ (Fig.

9A+B). For W256$^{6.48}$, a hydrogen bonding interaction with the oxygen of HMA (Fig. 9A) as well as π-stacking interactions with the pyrimidine core (Fig. 9B) was predicted. Yet another interaction, between H297$^{7.45}$ and the oxygen of HMA, is visualized in the docking pose as well as the interaction map (Fig. 9A+B).

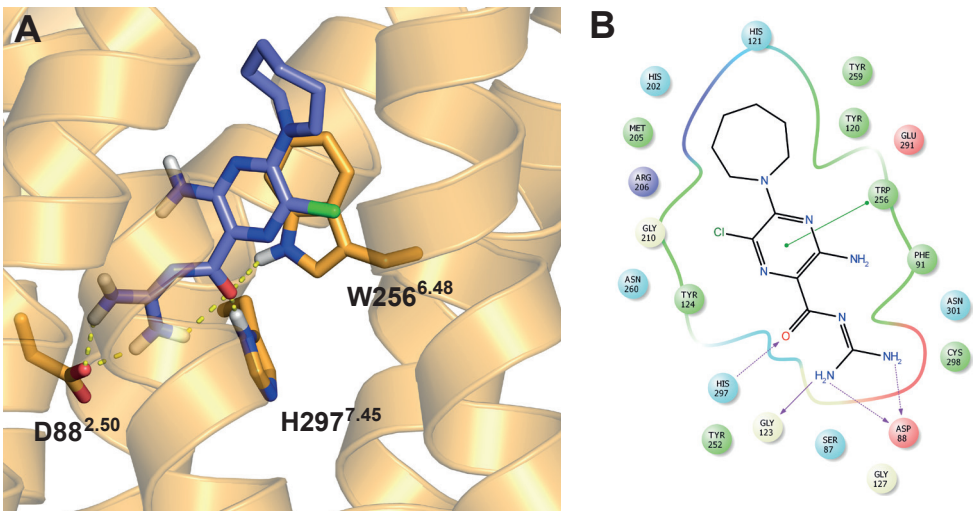



**Fig. 9.** (A) Induced fit docking of HMA in a homology model of CCR2 based on the crystal structure of CCR5. An ionic interaction between D88$^{2.50}$ and the guanidinium group of HMA and between H297$^{7.45}$ and the oxygen of HMA is illustrated, as well as a hydrogen bonding interaction of W256$^{6.48}$ and the oxygen of HMA. (B) The 2D interaction map that illustrates an additional π-stacking interaction between W256$^{6.48}$ and the pyrimidine core of HMA, as well as all surrounding residues.

## Discussion

Modulation of GPCRs by sodium ions and amiloride analogues has been described for a number of class A GPCRs, including adrenergic receptors [30], adenosine receptors [10, 12], dopamine receptors [9] and opioid receptors [11]. This ubiquitous amount of data among various GPCRs suggests interactions with a very conserved site, providing evidence for a common allosteric mechanism [31]. With the present study we add the first chemokine receptor, CCR2, to the list of GPCRs that are modulated by amiloride analogues and sodium ions. For CCR2 two distinct small molecule binding pockets have previously been identified [8], of which one is located at the upper half of the TM domain, whereas as the other pocket resides at the intracellular side of the receptor (Chapter 4). Here we provide evidence for modulation of CCR2 by the amiloride analogue HMA and sodium ions via yet another site,

suggesting that CCR2 comprises three distinct small molecule binding pockets. Moreover, by means of the intracellular radioligand [$^{3}$H]-CCR2-RA-[R] as a unique tool compound, we were able to study the influence at the intracellular side of the receptor induced by HMA and sodium ions.

In radioligand binding assays we observed allosteric modulation of $^{125}$I-CCL2 and [$^{3}$H]-CCR2-RA-[R] by sodium ions. We measured increased binding of the intracellular antagonist [$^{3}$H]-CCR2-RA-[R] at a high concentration of 1 M NaCl. To address the question whether sodium or chloride ions are responsible for this effect, we also examined the effects of equal concentrations of LiCl and KCl. Their differential effects strongly pointed to the involvement of monovalent cations rather than (chloride) anions. Lithium ions, which have a smaller diameter than sodium ions, even further enhanced [$^{3}$H]-CCR2-RA-[R] binding, while the larger potassium ions did not modulate antagonist binding at all. These data suggest that the size of the cations that are able to modulate CCR2 antagonist binding is restricted to the 116 pm diameter of sodium. A physiologically relevant NaCl concentration of 150 mM did not affect binding of [$^{3}$H]-CCR2-RA-[R], but increased the dissociation rate of $^{125}$I-CCL2. This latter finding is in line with data for other GPCRs indicating that sodium ions stabilize the inactive state of the receptor and decreases the affinity of agonists [12, 32-34]. While this is the first study to report the effect of sodium ions on an intracellular GPCR antagonist, allosteric enhancement of orthosteric antagonists by NaCl has previously been described for among others dopamine, adenosine and α2-adrenergic receptors [9, 10, 33, 34]. Interestingly, in our study the binding of the orthosteric antagonist INCB3344 was not modulated by NaCl. It should be noted that all orthosteric GPCR antagonists for which binding was previously found to be enhanced by NaCl, behaved as inverse agonists. Therefore enhancement by NaCl, which stabilizes the inactive state of the receptor, is compliant with their mechanism of action. For INCB3344 no such inverse agonism has been detected [8, 35], which could explain the lack of effect of NaCl.

Previous studies have shown that amiloride and its analogues bind to the same binding pocket as sodium ions [12, 36]. They are known to decrease agonist binding, and in contrast to sodium ions, they also decrease antagonist binding [10, 34, 36]. For CCR2 we discovered that the amiloride analogues HMA and MIBA displaced the orthosteric antagonist [$^{3}$H]-INCB3344 as well as the intracellular antagonist [$^{3}$H]-CCR2-RA-[R] with similar potencies. In kinetic experiments in the presence of HMA we observed increased dissociation rates for both antagonist radioligands as well as for the radiolabeled agonist $^{125}$I-CCL2. Saturation binding experiments in the presence of HMA revealed characteristics of a noncompetitive ligand with respect to the allosteric antagonist [$^{3}$H]-CCR2-RA-[R] and mixed effects with respect to the

orthosteric antagonist [$^3$H]-INCB3344. All these results together strongly indicate allosteric modulation of CCR2 by HMA, acting via yet another allosteric binding pocket for small molecules on CCR2. The mixed effect in the saturation binding assay with [$^3$H]-INCB3344 could indicate that the binding site of HMA and INCB3344 are partially overlapping. Nevertheless, whereas INCB3344 enhanced binding of [$^3$H]-CCR2-RA-[R] [8], HMA completely displaced this radioligand from CCR2. Although HMA and INCB3344 most likely bind in close proximity, these two ligands clearly induce distinct conformational changes of CCR2.

Several highly conserved amino acid residues in class A non-olfactory GPCRs have been reported to be involved in sodium ion and/or HMA binding, including D$^{2.50}$ (92% conserved), W$^{6.48}$ (78% conserved) and N$^{7.45}$ (63% conserved) [11-14]. CCR2 contains the residues D88$^{2.50}$ and W256$^{6.48}$, but at position 7.45 a histidine is present instead of an asparagine. H$^{7.45}$ is highly conserved among chemokine receptors (87%), but otherwise not prevalent in class A GPCRs (10%) (GMOS web interface. http://lmc.uab.cat/gmos/, accessed on 25-02-2014). In our studies, mutation of W256A$^{6.48}$ completely prevented [$^3$H]-INCB3344 from binding, whereas its affinity for D88A$^{2.50}$ and H297A$^{7.45}$ was only slightly decreased. Since W$^{6.48}$ is located at the top of the sodium binding pocket [11, 12] (Fig. 9A) and was previously found to interact with the CCR5 antagonist maraviroc [37], this residue in CCR2 could be an interaction partner for INCB3344. Binding studies with the intracellular radioligand [$^3$H]-CCR2-RA-[R] revealed dramatic conformational changes of the intracellular region of the receptor by mutations in the sodium binding pocket, since the affinity of CCR2-RA-[R] for all mutant receptors was drastically decreased compared to WT CCR2. D$^{2.50}$ and W$^{6.48}$ are known to be critical residues for the conformational changes at the intracellular side between inactive and active states of a GPCR. Both residues were predicted to participate in a water-mediated hydrogen-bonding network with other residues that include N$^{7.49}$ and Y$^{7.53}$ of the NPxxY motif at the bottom of TM-VII [38, 39].

Since we were able to measure binding of at least one of the antagonist radioligands for all three mutant receptors, we examined the effect of these residues on modulation of CCR2 by sodium ions and HMA. D88$^{2.50}$ revealed a critical role for modulation by sodium ions, as enhancement of the intracellular radioligand [$^3$H]-CCR2-RA-[R] was completely abolished for the D88A$^{2.50}$ mutant receptor. Recent high-resolution crystal structures of the δ-OR, $A_{2A}$AR and PAR1 confirm the central role of D$^{2.50}$ in the coordination of the sodium ion [11-13]. Our findings suggest that such a sodium ion binding site is present in CCR2 as well. Mutation of W256$^{6.48}$ into alanine also partially reduced the enhanced [$^3$H]-CCR2-RA-[R] binding upon addition of NaCl, indicating that W$^{6.48}$ is involved in the formation of the sodium binding pocket of CCR2. In the crystal structures of the $A_{2A}$AR and the δ-OR, hydrogen bonding interactions

between $W^{6.48}$ and water molecules surrounding the sodium pocket were identified [11, 12], but the exact role of $W^{6.48}$ in antagonist modulation by sodium ions in these receptors remains to be deciphered. Additionally we found that $H297^{7.45}$ was necessary for the sodium ion to enhance binding of [$^3$H]-CCR2-RA-[R]. This residue is therefore likely to play a similar role as the conserved $N^{7.45}$ in the majority of other GPCRs in the creation of the binding pocket for the sodium ion [11, 12].

Mutation of $W256^{6.48}$ completely prevented CCR2 modulation by 0.1 mM HMA, whereas $D88A^{2.50}$ and $H297A^{7.45}$ still allowed HMA to displace both antagonist radioligands, although to a lesser extent as for WT CCR2. The important role of $W^{6.48}$ is in agreement with a study of the $A_{2A}$AR in which extensive steric interactions between $W^{6.48}$ and HMA were predicted upon induced fit docking [14]. However, the observed decrease in the potency of HMA to displace the CCR2 antagonists is opposite to a 4-fold increase in affinity that was previously found for the $A_3$ adenosine receptor ($A_3$AR) upon mutation of $W^{6.48}$ into alanine [34]. Although this binding pocket is highly conserved among class A GPCRs, small modifications due to a few differential residues might lead to distinct positioning of HMA in this pocket. From the 15 conserved GPCR residues that are lining the sodium ion binding pocket in inactive GPCR crystal structures [14], 6 are different for CCR2, including $S87^{2.49}$, $G127^{3.39}$, $I131^{3.43}$, $Y252^{6.44}$, $H297^{7.45}$, $C298^{7.46}$. Except for $I131^{3.43}$, all these residues were predicted to be in close proximity of HMA in CCR2 (Fig. 9B), which could therefore be a reason for the observed differences in HMA and sodium ion modulation of CCR2 compared to other GPCRs.

In agreement with radioligand binding studies, molecular docking of HMA in the homology model of CCR2 revealed direct ionic and hydrogen bonding interactions with $D88^{2.50}$ and $H297^{7.45}$. In addition, hydrogen bonding as well as π-stacking interactions between HMA and $W256^{6.48}$ were predicted. The lack of affinity that was observed in the radioligand binding assays for amiloride and its analogues phenamil, benzamil and MGCMA further supports this docking pose of HMA in our model. The phenyl ring of benzamil and phenamil that is attached to the guanidinium group would cause steric hindrance, and interference with the ionic interactions between HMA and $D^{2.50}$. In addition, at the top of the binding pocket the hydrophobic hexamethylene group of HMA and the N-methyl-N-isobutyl group of MIBA seem to be involved in crucial hydrophobic interaction, since the lack of such a group in amiloride and the presence of a positively charged substituent in MGCMA prevented these ligands from binding.

In summary we have revealed that CCR2 is modulated by amiloride analogues as well as sodium ions, which is mediated via a third small molecule binding pocket in the core of the TM domain. Due to its close proximity to the orthosteric binding pocket, this finding

could potentially lead to the development of bitopic ligands binding to both sites. These ligands might have distinct pharmacological properties since they target a domain that is so important for conformational rearrangements of the entire receptor. Our findings provide further understanding of sodium ion and HMA modulation, via a highly conserved site, and offer novel opportunities for targeting CCR2 and GPCRs in general.

## References


1. Lagerstrom, M.C. and H.B. Schioth, *Structural diversity of G protein-coupled receptors and significance for drug discovery.* Nat Rev Drug Discov, 2008. 7(4): p. 339-57.
2. Christopoulos, A., *Allosteric binding sites on cell-surface receptors: novel targets for drug discovery.* Nat Rev Drug Discov, 2002. 1(3): p. 198-210.
3. Hodge, D.L., et al., *MCP-1/CCR2 interactions direct migration of peripheral B and T lymphocytes to the thymus during acute infectious/inflammatory processes.* Eur J Immunol, 2012. 42(10): p. 2644-54.
4. Provoost, S., et al., *Monocyte-derived dendritic cell recruitment and allergic T(H)2 responses after exposure to diesel particles are CCR2 dependent.* J Allergy Clin Immunol, 2012. 129(2): p. 483-91.
5. Struthers, M. and A. Pasternak, *CCR2 antagonists.* Curr Top Med Chem, 2010. 10(13): p. 1278-98.
6. Wang, L., et al., *Allosteric modulators of g protein-coupled receptors: future therapeutics for complex physiological disorders.* J Pharmacol Exp Ther, 2009. 331(2): p. 340-8.
7. Allen, S.J., S.E. Crown, and T.M. Handel, *Chemokine: receptor structure, interactions, and antagonism.* Annu Rev Immunolog, 2007. 25: p. 787-820.
8. Zweemer, A.J., et al., *Multiple Binding Sites for Small-Molecule Antagonists at the CC Chemokine Receptor 2.* Mol Pharmacol, 2013. 84(4): p. 551-61.
9. Ericksen, S.S., et al., *Ligand selectivity of D2 dopamine receptors is modulated by changes in local dynamics produced by sodium binding.* J Pharmacol Exp Ther, 2009. 328(1): p. 40-54.
10. Gao, Z.G. and A.P. IJzerman, *Allosteric modulation of A(2A) adenosine receptors by amiloride analogues and sodium ions.* Biochem Pharmacol, 2000. 60(5): p. 669-76.
11. Fenalti, G., et al., *Molecular control of delta-opioid receptor signalling.* Nature, 2014. 506(7489): p. 191-6.
12. Liu, W., et al., *Structural basis for allosteric regulation of GPCRs by sodium ions.* Science, 2012. 337(6091): p. 232-6.
13. Zhang, C., et al., *High-resolution crystal structure of human protease-activated receptor 1.* Nature, 2012. 492(7429): p. 387-92.
14. Gutierrez-de-Teran, H., et al., *The role of a sodium ion binding site in the allosteric modulation of the A(2A) adenosine G protein-coupled receptor.* Structure, 2013. 21(12): p. 2175-85.
15. Brodmerkel, C.M., et al., *Discovery and pharmacological characterization of a novel rodent-active CCR2 antagonist, INCB3344.* J Immunol, 2005. 175(8): p. 5370-8.
16. Xue, C.B., et al., *3-Aminopyrrolidine derivatives as modulators of chemokine receptors,* 2004. Inventors, Incyte Corporation. PCT/US2003/037946.
17. Zou, D., et al., *Novel, acidic CCR2 receptor antagonists: from hit to lead.* Lett Drug Des Discov, 2007. 4: p. 185-191.
18. Hall, S.E., et al., *Elucidation of binding sites of dual antagonists in the human chemokine receptors CCR2 and CCR5.* Mol Pharmacol, 2009. 75(6): p. 1325-36.
19. Cragoe, E.J., Jr., et al., *Pyrazine diuretics. II. N-amidino-3-amino-5-substituted 6-halopyrazinecarboxamides.* J Med Chem, 1967. 10(1): p. 66-75.
20. Ballesteros, J.A., Weinstein, H, *Integrated methods for the construction of three dimensional models and computational probing of structure-function relations in G-protein coupled receptors.* Methods Neurosci, 1995. 25: p. 366-428.
21. Cuisset, L., et al., *The effects of sodium butyrate on transcription are mediated through activation of a protein phosphatase.* J Biol Chem, 1997. 272(39): p. 24148-53.

22. Smith, P.K., et al., *Measurement of protein using bicinchoninic acid.* Anal Biochem, 1985. 150(1): p. 76-85.
23. Schrodinger, *Prime, version 3.2,* LLC, New York, NY, 2013.
24. Jacobson, M.P., et al., *A hierarchical approach to all-atom protein loop prediction.* Proteins, 2004. 55(2): p. 351-67.
25. Jacobson, M.P., et al., *On the role of the crystal environment in determining protein side-chain conformations.* J Mol Biol, 2002. 320(3): p. 597-608.
26. Sherman, W., H.S. Beard, and R. Farid, *Use of an induced fit receptor structure in virtual screening.* Chem Biol Drug Des, 2006. 67(1): p. 83-4.
27. Schrodinger, Schrodinger Suite 2013-2 Induced Fit docking protocol; Glide version 6.0, Schrodinger, LLC, New York, NY, 2013; Prime version 3.3, Schrodinger, LLC, New York, NY, 2013.
28. Schrodinger, The PyMOL Molecular Graphics System, Version 1.6.0.0 Schrodinger, LLC.
29. Cheng, Y. and W.H. Prusoff, *Relationship between the inhibition constant (K1) and the concentration of inhibitor which causes 50 per cent inhibition (I50) of an enzymatic reaction.* Biochem Pharmacol, 1973. 22(23): p. 3099-108.
30. Leppik, R.A. and N.J. Birdsall, *Agonist binding and function at the human alpha(2A)-adrenoceptor: allosteric modulation by amilorides.* Mol Pharmacol, 2000. 58(5): p. 1091-9.
31. Katritch, V., V. Cherezov, and R.C. Stevens, *Structure-function of the G protein-coupled receptor superfamily.* Annu Rev Pharmacol Toxicol, 2013. 53: p. 531-56.
32. Neve, K.A., *Regulation of dopamine D2 receptors by sodium and pH.* Mol Pharmacol, 1991. 39(4): p. 570-8.
33. Horstman, D.A., et al., *An aspartate conserved among G-protein receptors confers allosteric regulation of alpha 2-adrenergic receptors by sodium.* J Biol Chem, 1990. 265(35): p. 21590-5.
34. Gao, Z.G., et al., *Identification of essential residues involved in the allosteric modulation of the human A(3) adenosine receptor.* Mol Pharmacol, 2003. 63(5): p. 1021-31.
35. Shin, N., et al., *Pharmacological characterization of INCB3344, a small molecule antagonist of human CCR2.* Biochem Biophys Res Commun, 2009. 387(2): p. 251-5.
36. Howard, M.J., et al., *Interactions of amiloride with alpha- and beta-adrenergic receptors: amiloride reveals an allosteric site on alpha 2-adrenergic receptors.* Mol Pharmacol, 1987. 32(1): p. 53-8.
37. Tan, Q., et al., *Structure of the CCR5 chemokine receptor-HIV entry inhibitor maraviroc complex.* Science, 2013. 341(6152): p. 1387-90.
38. Hulme, E.C., *GPCR activation: a mutagenic spotlight on crystal structures.* Trends Pharmacol Sci, 2013. 34(1): p. 67-84.
39. Standfuss, J., et al., *The structural basis of agonist-induced activation in constitutively active rhodopsin.* Nature, 2011. 471(7340): p. 656-60.

# Chapter 6

## Structure-Kinetics Relationships – an overlooked parameter in hit-to-lead optimization: a case of cyclopentylamines as CCR2 antagonists

Maris Vilums*
Annelien J.M. Zweemer*
Zhiyi Yu
Henk de Vries
Julia M. Hillger
Hannah Wapenaar
Ilse A.E. Bollen
Farhana Barmare
Raymond Gross
Jeremy Clemens
Paul Krenitsky
Johannes Brussee
Dean Stamos
John Saunders
Laura H. Heitman
Adriaan P. IJzerman

**These authors contributed equally*

*Journal of Medicinal Chemistry* **2013** 56(19):7706-7714

## Abstract

Preclinical models of inflammatory diseases (e.g., neuropathic pain, rheumatoid arthritis, and multiple sclerosis) have pointed to a critical role of the chemokine receptor 2 (CCR2) and chemokine ligand 2 (CCL2). However, one of the biggest problems of high-affinity inhibitors of CCR2 is their lack of efficacy in clinical trials. We report a new approach for the design of high-affinity and long-residence-time CCR2 antagonists. We developed a new competition association assay for CCR2, which allows us to investigate the relation of the structure of the ligand and its receptor residence time (i.e., structure–kinetic relationship (SKR)) next to a traditional structure–affinity relationship (SAR). By applying combined knowledge of SAR and SKR, we were able to re-evaluate the hit-to-lead process of cyclopentylamines as CCR2 antagonists. Affinity-based optimization yielded compound **1** with good binding ($K_i$ = 6.8 nM) but very short residence time (2.4 min). However, when the optimization was also based on residence time, the hit-to-lead process yielded compound **22a**, a new high-affinity CCR2 antagonist (3.6 nM), with a residence time of 135 min.

## Introduction

Chemokines are a class of chemoattractant cytokines, and their main action is to control the trafficking and activation of leukocytes and other cell types for a range of inflammatory and non-inflammatory conditions. One of these, monocyte chemotactic protein-1 (MCP-1/chemokine ligand 2 (CCL2)), acts on monocytes, memory T cells, and basophils [1]. It creates a chemotactic gradient and activates the movement of immune cells to the site of inflammation by binding to its cell-surface receptor, chemokine receptor 2 (CCR2) [2]. This CCL2/CCR2 pair is overexpressed in several inflammatory conditions, in which excessive monocyte recruitment is observed. CCR2 and CCL2 knockout mice and CCR2 or CCL2 antibody-treated rodents show decreased recruitment of monocytes and produce considerably decreased inflammatory responses [3]. This indicates CCR2 as a potential target for the treatment of several immune-based inflammatory diseases and conditions, such as multiple sclerosis [4], atherosclerosis [5], rheumatoid arthritis [6], diabetes [7], asthma [8], and neuropathic pain [9].

In the past decade, there has been an increasing interest in the development of small-molecule antagonists of the CCR2 receptor, resulting in the disclosure of many different chemical classes. However, there are still no selective CCR2 antagonists on the market for the treatment of inflammatory diseases. Clinical trials, thus far, have failed mostly because of the lack of efficacy, including the one for the CCR2 antagonist MK-0812 (Fig. 1) [10].



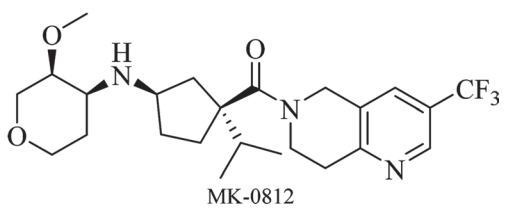



**Fig. 1.** CCR2 antagonist MK-0812

It has been suggested that binding kinetics, especially the lifetime of the ligand–receptor complex, can be used as a predictor for drug efficacy and safety [11, 12]. The concept of binding kinetics is often overlooked in the early phase of drug discovery; however, incorporation of this parameter could help to decrease the attrition rate in later stages of drug development [13]. In this concept of kinetics, an additional pharmacological parameter, the ligand–receptor residence time (RT; the reciprocal of the dissociation rate constant $k_{off}$), is defined [14], which is a measure for the duration that a ligand is bound to its target.

In this study, we first evaluated several reference CCR2 antagonists using a recently developed competition association assay for CCR2 that yielded the respective association and dissociation rate constants. As our starting point, we chose compound **1**, which was also the lead compound in the process that led to the development of MK-0812 by the Merck group [10]. The determination of the binding kinetics of several known structures with this particular scaffold subsequently allowed us to generate a new series of high-affinity and long-residence-time CCR2 antagonists based on structure **2**, which was previously abandoned by other groups in optimization steps because of its modest binding affinity (Fig. 2) [15].

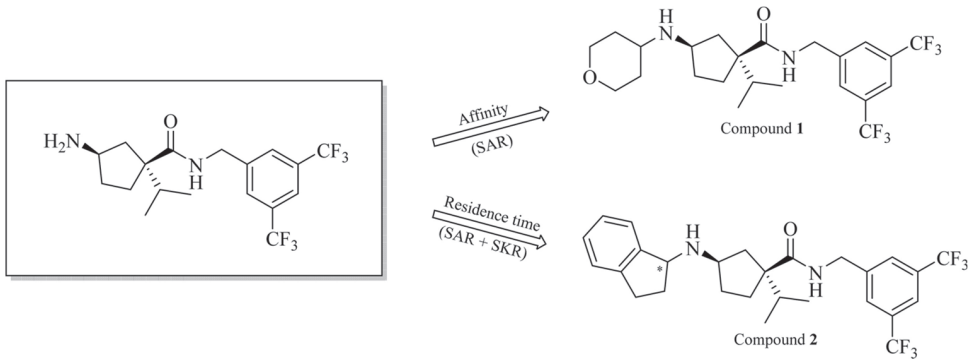



**Fig. 2.** RT and affinity values are both pharmacological parameters that may, however, suggest different lead structures.

## Materials and Methods

### Chemistry

**Chemicals and reagents.** All solvents and reagents were purchased from commercial sources and were of analytical grade. Demineralized water is simply referred to as $H_2O$, because it was used in all cases, unless stated otherwise (i.e., brine). $^{1}H$ and $^{13}C$ nuclear magnetic resonance (NMR) spectra were recorded on a Bruker AV 400 liquid spectrometer ($^{1}H$ NMR, 400 MHz; $^{13}C$ NMR, 100 MHz) or using a Bruker 500 MHz Avance III NMR spectrometer (compounds **22a** and **22b**) at ambient temperature. Chemical shifts are reported in parts per million (ppm), are designated by δ, and are downfield to the internal standard tetramethylsilane (TMS). Coupling constants are reported in hertz and are designated as *J*. Analytical purity of the final compounds was determined by high-performance liquid chromatography (HPLC) with a Phenomenex Gemini 3 µm C18 110A column (50 × 4.6 mm,

3 µm), measuring UV absorbance at 254 nm. The sample preparation and HPLC method for compounds **1**, **2**, **7**–**9**, and **11**, **12** were as follows: 0.3–0.8 mg of compound was dissolved in 1 mL of a 1:1:1 mixture of $CH_3CN/H_2O$/*t*-BuOH and eluted from the column within 15 min at a flow rate of 1.0 mL. The elution method was set up as follows: 1–4 min isocratic system of $H_2O/CH_3CN$/1% TFA in $H_2O$, 80:10:10; from the 4th min, a gradient was applied from 80:10:10 to 0:90:10 within 9 min, followed by 1 min of equilibration at 0:90:10 and 1 min at 80:10:10. All compounds showed a single peak at the designated retention time and are at least 95% pure. High-resolution mass spectral analyses (HRMS) were performed on LTQ-Orbitrap FTMS operated in a positive ionization mode with an electrospray ionization (ESI) source, with the following conditions: mobile phase A, 0.1% formic acid in water; mobile phase B, 0.08% formic acid in $CH_3CN$; gradient, 10–80% B in 26 min; and flow rate, 0.4 mL/min. Preparative HPLCs (for compounds **10** and **13**–**32**) were performed on a Waters AutoPurification HPLC–ultraviolet (UV) system with a diode array detector using a Luna C18 Phenomenex column (75 × 30 mm, 5 µm), and a linear gradient from 1 to 99% of mobile phase B was applied. Mobile phase A consisted of 5 mM HCl solution, and mobile phase B consisted of acetonitrile. The flow rate was 50 mL/min. Liquid chromatography–mass spectrometry (LC–MS) analyses were performed using an Onyx C18 monolithic column (50 × 4.6 mm, 5 µm), and a linear gradient from 1 to 99% mobile phase B was applied. Mobile phase A consisted of 0.05% TFA in water, and mobile phase B consisted of 0.035% TFA in acetonitrile. The flow rate was 12 mL/min. Separations of enantiomers were accomplished using chiral SFC. The column was Phenomenex Lux-4 (250 × 10 mm, 5 µm). The mobile phase condition of 10% MeOH with 20 mM $NH_3$ and 90% $CO_2$ was applied at a flow rate of 10.0 mL/min. Optical rotations were measured on a Perkin-Elmer polarimeter in $CHCl_3$ at 20 °C. Thin-layer chromatography (TLC) was routinely consulted to monitor the progress of reactions, using aluminum-coated Merck silica gel $F^{254}$ plates. Purification by column chromatography was achieved by use of Grace Davison Davisil silica column material (LC60A, 30–200 µm). The procedure for a series of similar compounds is given as a general procedure for all within that series, annotated by the numbers of the compounds.



**(1*S*,3*R*)-methyl-3-((tert-butoxycarbonyl)amino)-1-isopropylcyclopentanecarboxylate (3).** Synthesis of (1*S*,3*R*)-methyl-3-((tert-butoxycarbonyl)amino)-1-isopropylcyclopentanecarboxylate (**3**) was achieved following the synthetic approach reported by Kothandaraman et al [15].

**(1*S*,3*R*)-3-(*tert*-Butoxycarbonylamino)-1-isopropylcyclopentanecarboxylic Acid (4).** A solution of ester **3** (4.20 g, 14.72 mmol) in EtOH (30 mL) and 4 M aqueous lithium hydroxide (LiOH aqueous, 40 mL) was refluxed for 4 h. After concentration in vacuum, the solution was acidified with aqueous hydrochloric acid and extracted with DCM/$H_2O$. The organic layer was dried over $MgSO_4$ and, after concentration in vacuum, yielded the desired product as a yellow powder (3.62 g, 91%). $^1$H NMR (400 MHz, $CDCl_3$) δ: 10.75 (s, 1H), 6.53$^a$ (s, 0.5H), 5.05$^b$ (s, 0.5H), 3.98 – 3.78 (m, 1H), 2.25 – 1.50 (m, 7H), 1.40 (d, J = 16.8 Hz, 9H), 0.86 (d, J = 6.8 Hz, 6H); $^{13}$C NMR (100 MHz, $CDCl_3$): δ 182.9$^a$, 181.7$^b$, 157.6$^b$, 155.6$^a$, 80.4$^b$, 79.1$^a$, 56.9, 52.8$^b$, 51.7$^a$, 38.6$^b$, 38.2$^a$, 35.0$^b$, 34.5$^a$, 33.2$^a$, 32.9$^b$, 32.1$^a$, 31.8$^b$, 28.3, 18.7, 18.2$^b$, 18.0$^a$. *a* and *b* are indicated for different rotamers.

***tert*-Butyl(3-((3,5-bis(trifluoromethyl)benzyl)carbamoyl)-3-isopropylcyclopentyl) Carbamate (5).** Compound **4** (1.53 g, 5.65 mmol) was dissolved in 50 mL of DCM. To this mixture 3,5 bis(trifluoromethyl) benzylamine (1.89 g, 5.65 mmol) was added with DiPEA (2.95 mL, 16.9 mmol), PyBrOP (2.64 g, 5.65 mmol), and DMAP (0.55 g, 4.5 mmol). The reaction mixture was stirred for 24 h at room temperature. The product was extracted with DCM/ citric acid solution in water and then with DCM/1 M NaOH. The organic layer was dried with $MgSO_4$ and evaporated. The product was purified by column chromatography (0–100% ethyl acetate in DCM) to give the product as a yellow oil (2.33 g, 83%). $^1$H NMR (400 MHz, $CDCl_3$) δ: 7.69 (s, 3H), 7.25 (br s, 1H), 5.17 (br.s, 1H), 4.51–4.49 (m, 2H), 3.81 (br s, 1H), 1.99–1.90 (m, 4H), 1.69–1.72 (m, 2H), 1.50–1.58 (m, 1H), 1.36 (s, 9H), 0.74–0.77 (m, 6 H). $^{13}$C NMR (100 MHz, $CDCl_3$) δ: 178.6, 155.6, 142.1, 132.2, 131.8, 131.5, 131.2, 127.4, 127.3, 124.5, 121.8, 121.0, 119.1, 78.9, 57.6, 51.6, 42.8, 36.3, 34.6, 33.3, 32.6, 28.2, 18.7, 17.5.

**3-Amino-*N*-(3,5-bis(trifluoromethyl)benzyl)-1-isopropylcyclopentanecarboxamide (6).** Trifluoroacetic acid (20 mL) was added to a solution of compound **5** (2.33 g, 4.6 mmol) in 50 mL of DCM. The reaction mixture was stirred for 1 h at room temperature. The reaction mixture was neutralized with 1 M NaOH and extracted with DCM. The organic layer was dried with $MgSO_4$, filtered, and evaporated to give the product as a yellow crystal (1.55 g, 85%). $^1$H NMR (400 MHz, $CDCl_3$) δ: 9.16 (br s, 1H), 7.70–7.67 (m, 3H), 4.50–4.39 (m, 2H), 3.61–3.60 (m, 1H), 2.22–2.15 (m, 1H), 2.02–1.95 (m, 1H), 1.85–1.64 (m, 3H), 1.42–1.37 (m, 2H), 0.82–0.80 (m, 6H). $^{13}$C NMR (100 MHz, $CDCl_3$) δ: 179.4, 142.5, 131.8, 131.5, 131.2, 130.9, 127.3, 127.2, 124.6, 121.9, 120.4, 119.2, 57.3, 52.2, 42.4, 39.7, 35.3, 33.9, 33.6, 18.8, 16.9.

**General procedure for the synthesis of compounds 1, 2, and 11, 12.** Amine **6** was dissolved in 4 mL of dichloroethane in a 5 mL reaction tube, and the corresponding ketone (1 equiv) was added. Sequentially, acetic acid (1 equiv) and sodium triacetoxyborohoydride (1.5 equiv) were added. The reaction mixture was stirred for 18 h at room temperature and then washed with 1 M NaOH and $H_2O$. The organic layer was dried with $MgSO_4$, filtered, and evaporated. The product was purified by column chromatography (0–100% ethyl acetate in DCM) to give the desired product.

**(1*S*,3*R*)-*N*-(3,5-Bis(trifluoromethyl)benzyl)-1-isopropyl-3-((tetrahydro-2*H*-pyran-4-yl) amino)cyclopentanecarboxamide (1).** Yield = 21%. $^1$H NMR (400 MHz, $CDCl_3$) δ: 9.16 (s, 1H), 7.76–7.73 (m, 3H), 4.56–4.53 (m, 2H), 3.98–3.89 (m, 2H), 3.57–3.53 (m, 1H), 3.43–3.28 (m, 2H), 2.66–2.61 (m, 1H), 2.36–2.30 (m, 1H), 2.03–1.80 (m, 2H), 1.78–1.6 (m, 5H), 1.49–1.40 (m, 1H), 1.31–1.20 (m, 3H), 0.93–0.89 (m, 6H). $^{13}$C NMR (400 MHz, $CDCl_3$) δ: 179.1, 142.4, 131.8, 131.54, 131.2, 130.9, 127.7, 127.3, 124.6, 121.8, 121.0, 119.2, 66.9, 66.9, 57.5, 54.8, 51.9, 42.6, 37.1, 35.1, 34.3, 33.7, 33.6, 33.3, 19.5, 17.0. LC–MS: 481$^+$; $t_R$ = 7.01 min.

**(1*S*,3*R*)-*N*-(3,5-Bis(trifluoromethyl)benzyl)-3-((2,3-dihydro-1*H*-inden-1-yl)amino)-1-isopropylcyclopentanecarboxamide (2).** Yield = 25% (mixture of diastereomers). $^1$H NMR (400 MHz, $CDCl_3$) δ: 9.48 (s, 1H), 7.76–7.74 (m, 3H), 7.22–7.05 (m, 4H), 4.60–4.50 (m, 2H), 4.28–4.22 (m, 1H), 3.70–3.60 (m, 1H), 3.00–2.90 (m, 1H), 2.87–2.78 (m, 1H), 2.70–2.34 (m, 3H), 2.1–1.53 (m, 6H), 0.93–0.89 (m, 6H). $^{13}$C NMR (400 MHz, $CDCl_3$) δ: 179.4, 144.5, 144.4, 144.6, 131.8, 131.5, 127.9, 127.6, 126.3, 126.2, 125.0, 123.5, 123.5, 122.0 121.9, 61.3, 58.0, 56.6, 42.6, 37.2, 36.0, 34.5, 33.9, 33.7, 33.4, 19.6, 17.0. LC–MS: 513$^+$; $t_R$ = 8.12 min.

**General procedure for the synthesis of compounds 7–9.** Amine **6** (1 equiv) was disolved in 4 mL of acetonitrile, and coresponding alkylating agent (1.2 equiv) was added. Sequentually, DiPEA (1.2 equiv) was added. The reaction mixture was stirred in a microwave for 2 h at 60 °C and purified with column chromatography (60% ethylacetate, 20% DCM, 20% petroleum ether, and 0–3% triethylamine in ethyl acetate).

**(1*S*,3*R*)-3-(Benzylamino)-*N*-(3,5-bis(trifluoromethyl)benzyl)-1-isopropylcyclopentane-1-carboxamide (7).** Yield = 27% (as HCl salt). $^1$H NMR (400 MHz, $CDCl_3$) δ: 9.40 (br s, 1H), 7.73 (s, 1H), 7.66 (s, 2H), 7.30–7.24 (m, 3H), 7.16–7.13 (m, 2H), 4.44 (d, $J$ = 4.8 Hz, 2H), 3.73 (d, $J$ = 2.4 Hz, 2H), 3.46–3.41 (m, 1H), 2.41–2.33 (m, 1H), 2.02–1.90 (m, 4H), 1.85–1.78 (m, 2H), 1.59–1.52 (m, 1H), 0.91 (dd, $J^1$ = 10.8 Hz, $J^2$ = 6.8 Hz, 6H). $^{13}$C NMR (100 MHz, $CDCl_3$) δ: 179.4,

142.6, 139.0, 132.0, 131.7, 131.3, 131.0, 128.6, 127.8, 127.5, 127.3, 124.6, 121.9, 120.8, 58.8, 58.7, 57.3, 51.9, 42.5, 35.3, 33.5, 33.1, 19.5, 16.9. LC–MS: $487^{+}$; $t_R$: 7.40 min.

**General procedure for the synthesis of compounds 10 and 13–32.** To a series of 1.5 mL glass tubes was added amine **6** in NMP (0.95 M, 0.095 mmol), followed by solutions of different ketones (0.5 M, 0.1 mmol) in NMP, and these mixtures were subsequently treated with acetic acid (0.1 mmol), followed by 5-ethyl-2-methyl-pyridine borane (PEMB) (0.2 mmol). The reaction mixture was heated at 65 °C on a reaction block for 24 h. The reaction mixtures were purified directly using an automated mass-guided reverse-phase HPLC, and product-containing fractions were concentrated to give final products of >90% purity, as judged by LC–MS (average of 220 and 254 nm traces).

**Biology**

**Chemicals and reagents.** $^{125}$I-CCL2 (2200 Ci/mmol) was purchased from Perkin-Elmer (Waltham, MA). INCB3344 was synthesized as described previously [16, 17]. [$^3$H]-INCB3344 (specific activity of 32 Ci $mmol^{-1}$) was custom-labeled by Vitrax (Placentia, CA), for which a dehydrogenated precursor of INCB3344 was provided. Tango CCR2-*bla* U2OS cells stably expressing human CCR2 were obtained from Invitrogen (Carlsbad, CA).

**Cell culture and membrane preparation.** U2OS cells stably expressing the human CCR2 receptor (Invitrogen, Carlsbad, CA) were cultured in McCoys5a medium supplemented with 10% fetal calf serum, 2 mM glutamine, 0.1 mM non-essential amino acids (NEAAs), 25 mM 4-(2-hydroxyethyl)piperazine-1-ethanesulfonic acid (HEPES), 1 mM sodium pyruvate, 100 IU/mL penicillin, 100 µg/mL streptomycin, 100 µg/mL G418, 50 µg/mL hygromycin, and 125 µg/mL zeocin in a humidified atmosphere at 37 °C and 5% $CO_2$. Cell culture and membrane preparation were performed as described previously [18].

**$^{125}$I-CCL2 displacement assay.** Binding assays were performed as described previously [18].

**[$^3$H]-INCB3344 competition association assay.** The kinetic parameters of unlabeled ligands at 25 °C were determined using the competition association assay described by Motulsky and Mahan [19]. At different time points, 10 µg of U2OS–CCR2 membranes was added to 1.8 nM [$^3$H]-INCB3344 in a total volume of 100 µL of assay buffer in the absence or presence of competing ligand. To validate the assay, three concentrations of INCB3344 (1-, 3-, and 10-fold its $K_i$ value of [$^3$H]-INCB3344 displacement) were used. This validation

showed that using a single concentration (that equals the $K_i$) of unlabeled ligand was sufficient to accurately measure $k_{on}$ and $k_{off}$. Incubation was terminated by dilution with ice-cold 50 mM tris(hydroxymethyl)aminomethane (Tris)-HCl buffer supplemented with 0.05% 3-[(3-cholamidopropyl)dimethylammonio]-1-propanesulfonate (CHAPS). Separation of bound from free radioligand was performed by rapid filtration through a 96-well GF/B filter plate pre-coated with 0.25% polyethylenimine (PEI) using a Perkin-Elmer FilterMate harvester (Perkin-Elmer, Groningen, Netherlands). Filters were washed 10 times with ice-cold wash buffer. A total of 25 µL of Microscint scintillation cocktail (Perkin-Elmer, Waltham, MA) was added to each well, and the filter-bound radioactivity was determined by scintillation spectrometry using the P-E 1450 Microbeta Wallac Trilux scintillation counter (Perkin-Elmer). Kinetic parameters of unlabeled ligands were calculated using eq 3, as mentioned below in the Data Analysis section.

**[$^3$H]-INCB3344 dual-point competition association assay.** KRI values of unlabeled ligands were determined using the dual-point competition association assay as described previously, in which radioligand binding was determined at two different time points [20]. Time point $t_1$ represents the time at which radioligand binding reached 99.5% of total binding at equilibrium.

$$t_1 = 8 \cdot t_{1/2,association} \quad (1)$$

The second time point ($t_2$) was arbitrarily set at 4 h, where little but reliably measurable, specific binding remained. A total of 10 µg of U2OS–CCR2 membranes were incubated for 50 min ($t_1$) or 240 min ($t_2$) in a total volume of 100 µL of assay buffer with 1.8 nM [$^3$H]-INCB3344 in the absence or presence of unlabeled ligands at 25 °C. The amount of radioligand bound to the receptor was measured after co-incubation of the unlabeled ligands at 1-fold their respective $K_i$ value in the $^{125}$I-CCL2 displacement assay. Incubations were terminated, and samples were obtained as described under the [$^3$H]-INCB3344 Competition Association Assay section. KRI values of unlabeled ligands were calculated using eq 2, as mentioned below in the Data Analysis section.

**Data analysis**. All experiments were analyzed using the nonlinear regression curve fitting program Prism 5 (GraphPad, San Diego, CA). For radioligand displacement data, $K_i$ values were calculated from $IC_{50}$ values using the Cheng and Prusoff equation [21]. Data of the dual-point competition association assay were analyzed as described previously [20].

KRI values were calculated by dividing the specific radioligand binding measured at $t_1$ ($B_{t1}$) by its binding at $t_2$ ($B_{t2}$) in the presence of unlabeled competing ligand as follows:

$$KRI = B_{t1} / B_{t2} \tag{2}$$

Association and dissociation rates for unlabeled ligands were determined by nonlinear regression analysis of the competition association data as described by Motulsky and Mahan [19]

$$\begin{gathered} K_A = k_1[L] \cdot 10^{-9} + k_2 \\ K_B = k_3[I] \cdot 10^{-9} + k_4 \\ S = \sqrt{(K_A - K_B)^2 + 4 \cdot k_1 \cdot k_3 \cdot L \cdot I \cdot 10^{-18}} \\ K_F = 0.5(K_A + K_B + S) \\ K_S = 0.5(K_A + K_B - S) \\ Q = \frac{B_{\max} \cdot k_1 \cdot L \cdot 10^{-9}}{K_F - K_S} \\ Y = Q \cdot \left(\frac{k_4 \cdot (K_F - K_S)}{K_F \cdot K_S} + \frac{k_4 - K_F}{K_F} e^{(-K_F \cdot X)} - \frac{k_4 - K_S}{K_S} e^{(-K_S \cdot X)}\right) \end{gathered} \tag{3}$$

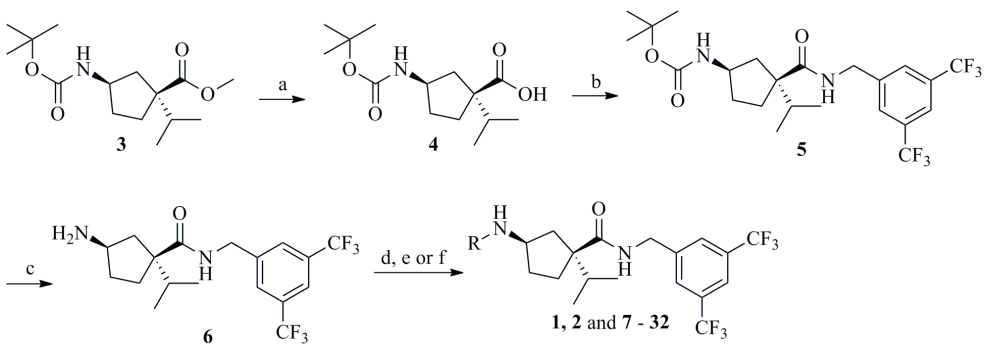
where $X$ is the time (min), $Y$ is the specific binding (disintegrations per minute (DPM)), $k_1$ is $k_{on}$ ($M^{-1}$ $min^{-1}$) of [$^3$H]-INCB3344 predetermined in association experiments, $k_2$ is $k_{off}$ ($min^{-1}$) of [$^3$H]-INCB3344 predetermined in dissociation experiments, $L$ is the concentration of [$^3$H]-INCB3344 used (nM), $B_{max}$ is the total binding (DPM), and $I$ is the concentration of unlabeled ligand (nM). Fixing these parameters into eq 3 allows for the following parameters to be calculated: $k_3$ is $k_{on}$ ($M^{-1}$ $min^{-1}$) of the unlabeled ligand, and $k_4$ is $k_{off}$ ($min^{-1}$) of the unlabeled ligand. The association and dissociation rates were used to calculate the "kinetic $K_D$" as follows:

$$K_D = k_{off} / k_{on} \tag{4}$$

The RT was calculated according to the formula RT = $1/k_{off}$.

## Results and discussion

**Chemistry**. Synthesis of (1*S*,3*R*)-methyl-3-((tert-butoxycarbonyl)amino)-1-isopropylcyclopentanecarboxylate (**3**) was achieved following the synthetic approach reported by Kothandaraman et al. [15]. The desired *N-tert*-butyloxycarbonyl (Boc)-protected ester **3** was saponified to yield acid **4**. Subsequently, acid **4** was used in the peptide-coupling reaction with 3,5-bis(trifluoromethyl)benzylamine to yield amide **5** under bromo-tris-pyrrolidino phosphoniumhexafluorophosphate (PyBroP) conditions [22]. Removal of the *N*-Boc group with trifluoroacetic acid (TFA) in dichloromethane (DCM) produced amine **6**. Reductive amination with different ketones under $NaBH(AcO)_3$ conditions afforded the desired products **1**, **2**, and **11**, **12**. Compounds **7**–**9** were synthesized by alkylating amine **6** with different alkylating agents. Compounds **10** and **13**–**32** were generated from amine **6** and an array of different ketones with 5-ethyl-2-methylpyridine borane complex (PEMB) under conditions reported by Burkhardt and Coleridge (Scheme 1) [23].




**Scheme 1**. Synthesis of CCR2 antagonists. Reagents and conditions: (a) 4 M LiOH aqueous, MeOH, reflux, 4 h, 91%; (b) 3,5-bis(trifluoromethyl)benzylamine, PyBrOP, N,N-diisopropylethylamine (DiPEA), N,N-dimethylaminopyridine (DMAP), DCM, room temperature, 24 h, 83%; (c) TFA, DCM, room temperature, 1 h, 85%; (d) corresponding ketone, $(AcO)_3BHNa$, AcOH, DCE, room temperature, 18 h, 21–86% (compounds 1, 2, and 11, 12); (e) corresponding alkylating agent, DiPEA, $CH_3CN$, 60 °C, 2 h, 14–54% (compounds 7–9); (f) for array synthesis, corresponding ketone, 5-ethyl-2-methylpyridine borane (PEMB), AcOH, N-methylpyrrolidone (NMP), 65 °C, 24 h (compounds 10 and 13–32).

**Biology**. To determine the binding affinity, all compounds were tested in a $^{125}$I-CCL2 displacement assay on human bone osteosarcoma (U2OS)–CCR2 membrane preparations as described previously by our group [18]. Several methods can be used to determine ligand binding kinetics (e.g., a kinetic radioligand binding assay [24], surface plasmon resonance (SPR) [25], "two-step" competition binding assay [26], and "Tag-lite" Cisbio [27]). Most of these assays require special modifications of the target protein or the ligand. Therefore, we

chose to use the competition association assay, because this assay allowed us to determine the kinetics of unlabeled ligands to the receptor expressed in membrane preparations. In our hands, this is the most robust and accurate assay to measure kinetics of unlabeled ligands.

**Validation of the [$^3$H]-INCB3344 competition association assay for CCR2**. A competition association assay was set up to determine the kinetic parameters of unlabeled ligands [19]. For this assay, we used the radiolabeled small-molecule CCR2 antagonist [$^3$H]-INCB3344 [28], instead of the endogenous agonist protein radioligand $^{125}$I-CCL2. Because of the large size of CCL2 (8600 Da), there is at best only a partial overlap in the binding site with small-molecule antagonists. Because the theoretical model of the competition association assay is based on the assumption that unlabeled and radiolabeled ligands should compete for the same binding site, we decided to use [$^3$H]-INCB3344 in our assay. This radioligand bears considerable chemical resemblance to the compounds reported in this study. We first validated this method by measuring the competition association of [$^3$H]-INCB3344 in the absence and presence of three different concentrations of INCB3344 (1-, 3-, and 10-fold its $K_i$) (Fig. 3). This resulted in $k_{on}$ and $k_{off}$ values for unlabeled INCB3344 of 0.035 ± 0.010 nM$^{-1}$ min$^{-1}$ and 0.024 ± 0.002 min$^{-1}$, respectively, at 25 °C (Table 1). The corresponding RT was 43 ± 2 min. These results were in good agreement with $k_{on}$ and $k_{off}$ values of [$^3$H]-INCB3344 binding from "traditional" association and dissociation experiments, 0.054 ± 0.002 nM$^{-1}$ min$^{-1}$ and 0.013 ± 0.002 min$^{-1}$, respectively [18] (Table 1).

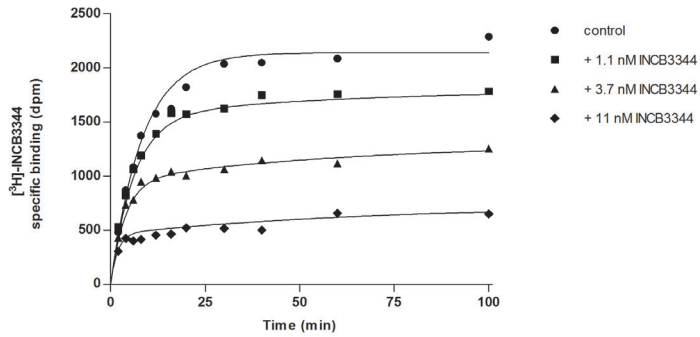



**Fig. 3.** Competition association assay with [$^3$H]-INCB3344 at 25 ºC in the absence or presence of 1.1, 3.7 and 11 nM unlabeled INCB3344.

**Table 1.** Comparison of equilibrium binding and kinetic parameters of INCB3344 determined using different methods

| assay | $K_D/K_i$ (nM) | $k_{on}$ ($nM^{-1}$ $min^{-1}$) | $k_{off}$ ($min^{-1}$) |
|---|---|---|---|
| saturation binding[a] | 0.90 ± 0.03 | NA[b] | NA |
| displacement[c] | 1.2 ± 0.1 | NA | NA |
| association and dissociation[d] | 0.23 ± 0.04 | 0.054 ± 0.002 | 0.013 ± 0.002 |
| competition association[e] | 0.72 ± 0.19 | 0.035 ± 0.010 | 0.024 ± 0.002 |

Data are presented as mean ± S.E.M. of three independent experiments performed in duplicate.
[a]Saturation binding of 1- 45 nM [$^3$H]-INCB3344 to CCR2 at 25 ºC.
[b]NA = not applicable.
[c]Displacement of 3.5 nM [$^3$H]-INCB3344 from CCR2 at 25 ºC.
[d]Association and dissociation of [$^3$H]-INCB3344 measured in standard kinetic assays at 25 ºC.
[e]Association and dissociation of INCB3344 measured in competition association assays at 25 ºC.

**Screening of CCR2 antagonists using the dual-point competition association assay**. The competition association assay described above is laborious and time-consuming, and hence, we developed a so-called dual-point competition association assay for CCR2, according to principles that we recently established for the adenosine $A_1$ receptor [20]. To this end, we co-incubated [$^3$H]-INCB3344 with unlabeled antagonists at a concentration equal to their $K_i$ value that was determined in the $^{125}$I-CCL2 displacement assay. The so-called kinetic rate index (KRI) was calculated by dividing the specific radioligand binding at 50 min ($t_1$) by the binding at 240 min ($t_2$). In this assay, antagonists with a slower dissociation rate and, therefore, a longer RT than [$^3$H]-INCB3344 would result in a KRI > 1 (Fig. 4).



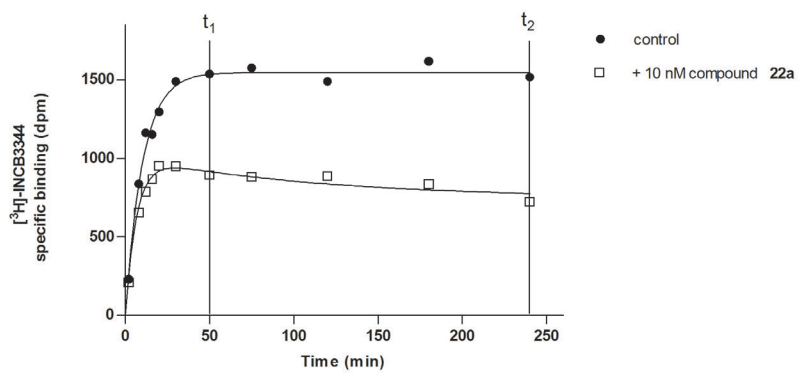
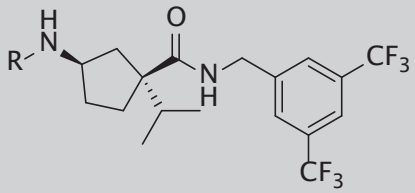



**Fig. 4.** Representative competition association curves of control and long-residence-time compound **22a**. $B_{t1}$, specific radioligand binding at the first time point ($t_1$ = 50 min); $B_{t2}$, specific radioligand binding at the second time point ($t_2$ = 240 min). KRI is defined as $B_{t1}/B_{t2}$, which equaled 1.2 for compound **22a**.

**Structure–affinity relationships (SARs) versus structure–RT relationships**

The 3-amino-1-isopropylcyclopentanecarboxamide scaffold has been extensively evaluated on the basis of binding affinities for CCR2 and selectivity against other chemokine receptors and the human ether-à-go-go-related gene (hERG) channel [15, 29, 30]. Therefore, we decided to resynthesize several reported derivatives of compound **1** [15, 31] and determine their binding affinity in radioligand displacement assays (Table 2). Introduction of the benzyl group yielded compound **7** with an affinity of 437 nM. When the spacer length between the phenyl ring and basic nitrogen was extended to ethyl, binding was almost lost (compound **8**; $K_i$ = 2400 nM). Prolonging the chain to propyl allowed us to regain affinity (compound **9**; $K_i$ = 134 nM). Combining the knowledge of compounds **7** and **9** in one structure yielded the indane derivative compound **2** with even more improved affinity ($K_i$ = 50 nM). Expanding the ring system to tetrahydronaphthalene resulted in an additional increase in affinity (compound **10**; $K_i$ = 33 nM). Removal of aromatics yielded compound **11** with a cyclohexane ring, which showed a decrease in affinity ($K_i$ = 110 nM), but incorporation of heteroatoms in the 4 position regained affinity (compounds **1** and **12**; $K_i$ = 6.8 and 31 nM, respectively) as described by Kothandaraman et al. [15]. On the basis of affinity alone, compound **1** would be the logical choice for lead optimization, which yielded the clinical candidate MK-0812 in the case of the Merck research group [10]. However, the kinetic evaluation of these known structures in a competition association assay allowed us to use an additional parameter, RT. In this assay, the best affinity compound **1** had a RT of 2.4 min, while compound **2** had a 4-fold longer RT of 9.5 min (Table 2). Structurally closely related compound **10** had a RT of 5.6 min, which convinced us to continue with compounds **2** and **10**, because they had a longer RT.

**Table 2.** Binding affinities and residence time (RT) of compounds **1**, **2**, **7** – **12**.



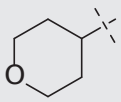
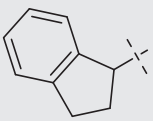
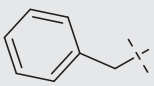
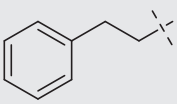
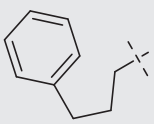
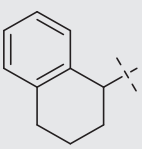
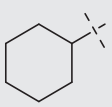
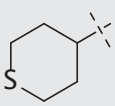
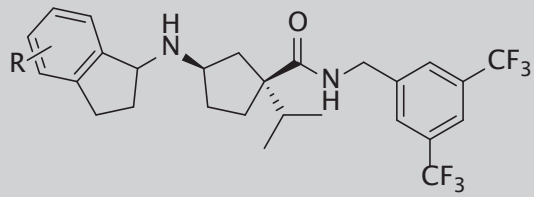
| Nr. | R | $K_i$ (nM) ± S.E.M. (n=3) | RT (min) |
|---|---|---|---|
| **1** |  | 6.8 ± 2.2 | 2.4 ± 0.2 |
| **2** |  | 50 ± 8 | 9.5 ± 1.5 |
| **7** |  | 437 ± 62 | - |
| **8** |  | 2400 ± 900 | - |
| **9** |  | 134 ± 35 | - |
| **10** |  | 33 ± 2 | 5.6 ± 0.5 |
| **11** |  | 110 ± 13 | 1.9 ± 0.4 |
| **12** |  | 31 ± 9 | 4.3 ± 1.4 |

**Table 3.** Binding affinities and KRI of indenyl derivatives **2** and **13 – 28**.




| Nr. | R | $K_i$ (nM) ± SEM (n=3) | KRI (n=2) |
|---|---|---|---|
| **2** | H | 50 ± 8 | 0.7 (0.7/0.7) |
| **13** | 4-$NH_2$ | 43 ± 7 | 0.8 (0.7/0.8) |
| **14** | 4-OH | 86 ± 8 | 0.6 (0.5/0.8) |
| **15** | 4-CN | 70 ± 11 | 0.8 (0.7/0.8) |
| **16** | 4-Me | 26 %[a] | - |
| **17** | 4-OMe | 30 %[a] | - |
| **18** | 5-OMe | 6.1 ± 0.7 | 0.6 (0.6/0.6) |
| **19** | 5-OH | 29 ± 2 | 0.7 (0.7/0.8) |
| **20** | 5-F | 30 %[a] | - |
| **21** | 5-Cl | 18 ± 1 | 1.1 (1.1/1.2) |
| **22** | 5-Br | 7.2 ± 0.5 | 1.1 (1.0/1.1) |
| **23** | 6-Cl | 28 %[a] | - |
| **24** | 6-Me | 55 ± 2 | 0.8 (0.8/0.8) |
| **25** | 6-CN | 54 ± 4 | 0.6 (0.6/0.6) |
| **26** | 4;5-di-OMe | 130 ± 6 | - |
| **27** | 5;6-di-OMe | 3.9 ± 0.3 | 0.7 (0.7/0.7) |
| **28** | 5;6-(-$OCH_2O$-) | 6.3 ± 0.8 | 0.6 (0.6/0.7) |

[a]Percent displacement at 1μM $^{125}$I-CCL2.

Using a number of commercially available indanones, we introduced different substituents on the indane ring (Table 3) to cover chemical space as broadly as possible. The SAR exploration on the 4 position showed that H-bond-accepting and hydrophilic groups are tolerated. The 4-$NH_2$ group led to a minor increase (compound **13**; $K_i$ = 43 nM), but 4-OH and 4-CN groups showed a decrease in affinity (compounds **14** and **15**; $K_i$ = 86 and 70 nM, respectively). 4-Me (compound**16**) and 4-MeO (compound **17**) were not tolerated on this position (26 and 30% displacement at 1 μM, respectively). On the 5 position, methoxy and hydroxyl groups improved the affinity, which had also been suggested for other

CCR2 antagonists [30, 32]. The methoxy group (compound **18**) showed an 8-fold increase in affinity (6.1 nM), while the hydroxyl group (compound **19**) displayed a less than 2-fold increase compared to the unsubstituted indenyl derivative (29 and 50 nM, respectively). On the contrary, the introduction of fluorine, which was previously reported as the best substituent in arylpiperidine analogues by Pasternak et al. [30], resulted in a dramatic decrease in affinity in the case of the indenyl derivative (compound**20**; 30% displacement at 1 μM). 5-Cl substitution yielded better affinity than 5-F (compound **21**; 18 nM), and 5-Br was better than 5-Cl (compound **22**; 7.2 nM). 6-Cl (compound **23**) led to a dramatic decrease in affinity (28% displacement at 1 μM). However, 6-Me and 6-CN groups were tolerated, having similar affinities to the unsubstituted indane ring (compounds **24** and **25**; $K_i$ = 55 and 54 nM, respectively).

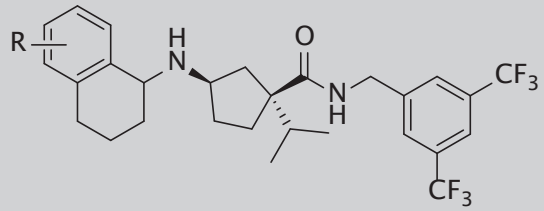
We continued the investigation with the analysis of disubstitution, learning that the combination of 4,5 substitution resulted in more than a 2-fold decrease in affinity (compound**26**; $K_i$ = 130 nM). On the contrary, the 5,6-dimethoxy group yielded compound **27** with a high affinity of 3.9 nM. Connecting the dimethoxy groups into a dioxolane ring yielded a small decrease in affinity (compound **28**; $K_i$ = 6.3 nM).



Using the knowledge of the best position for substitution, we continued the investigation on the 1,2,3,4-tetrahydronaphthalene ring by introducing substituents on the 5 position (Table 4). Electron-donating groups showed very similar results to what we found for the indenyl moiety. Compounds **29** and **30** showed good affinity (27 and 35 nM, respectively), while electron-withdrawing groups showed a decrease or complete lack of affinity (compounds **31** and **32**).

After SAR evaluation, the higher affinity compounds were screened in our kinetic assay to determine their KRI value [20] (see also Figure 2). A KRI value of <1 indicates that the RT of a tested compound is shorter than the RT of the radioligand (less than 43 min in this particular case). A KRI value of >1 reflects a RT of more than 43 min.

**Table 4.** Binding affinities and KRI of tetrahydronaphthalene derivatives **10** and **29 – 32**.

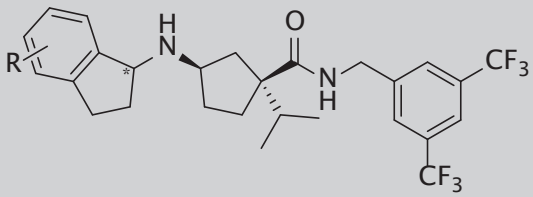



| Nr. | R | $K_i$ (nM) ± SEM (n=3) | KRI |
|---|---|---|---|
| **10** | H | 33 ± 2 | 0.6 (0.6/0.5) |
| **29** | 5-OMe | 27 ± 1 | 0.7 (0.7/0.8) |
| **30** | 5-OH | 35 ± 2 | 0.8 (0.7/0.8) |
| **31** | 5-Br | 48%[a] | - |
| **32** | 5-COOH | 0%[a] | - |

[a]Percent displacement at 1 μM $^{125}$I-CCL2.

Compound **2** in the screen showed a KRI value of 0.7 (RT = 9.5 min). However, compounds **21**and **22** had higher KRI values (1.1 for both compounds). These compounds were tested in a full competition association assay to determine their association and dissociation rate constants (Table 5). Increasing the size of the substituent, change from 5-Cl to 5-Br (compound **21** versus compound **22**), also yielded longer RTs (56 and 94 min, respectively). Compound **22** was separated in two diastereomers by preparative supercritical fluid chromatography (SFC) using a Phenomenex Lux-4 column (Phenomenex, Inc.). The first compound to elute (**22a**) had an affinity of 3.6 nM. However, the second compound (**22b**) to elute had a 100-fold decreased affinity ($K_i$ = 289 nM). These separated diastereomers had very similar $k_{off}$ rates (Table 5), which translated to similar RTs (compound **22a**, RT = 135 min; compound **22b**, RT = 77 min), but a significant difference was observed for their $k_{on}$ rates. Apparently, the stereochemistry of the indane ring system has a major impact on the compound association rate to the receptor, while the dissociation is not affected.

**Table 5.** Kinetic data of compounds **21**, **22**, **22a** and **22b**.




| Nr. | R | $K_i$ (nM) ± SEM (n=3) | $k_{on}$ ($nM^{-1}$ $min^{-1}$) | $k_{off}$ ($min^{-1}$) | RT (min) |
|---|---|---|---|---|---|
| **21** | 5-Cl | 18 ± 1 | 0.0027 ± 0.0006 | 0.020 ± 0.004 | 56 ± 14 |
| **22** | 5-Br | 7.2 ± 0.5 | 0.010 ± 0.002 | 0.011 ± 0.0002 | 94 ± 3 |
| **22a** | 5-Br | 3.6 ± 0.9 | 0.0053 ± 0.0007 | 0.0074 ± 0.0004 | 135 ± 8 |
| **22b** | 5-Br | 289 ± 94 | 0.00030 ± 0.00007 | 0.015 ± 0.004 | 77 ± 18 |

## Conclusion

We have demonstrated that, next to affinity, additional knowledge of the RT is useful for selecting and developing new CCR2 antagonists. (1*S*,3*R*)-*N*-(3,5-Bis(trifluoromethyl)benzyl)-3-((5-bromo-2,3-dihydro-1*H*-inden-1-yl)amino)-1-isopropylcyclopentanecarboxamide (**22a**) had a RT of 135 min. In comparison to the best affinity compound from the first SAR screening, i.e., compound **1** (Table 1), compound **22a** had a 56-fold increased RT while having similar affinity. This indicates that affinity and RT do not correlate; moreover, while SAR driven hit-to-lead optimizations often fail in later stages of drug development because of the lack of efficacy (e.g., MK-0812), it has been shown on other targets that RT is linked to the duration of the *in vivo* antagonist effect [33-35]. Compound **22a** may thus be a useful tool to test whether prolonged blockade of CCR2 has a beneficial effect on CCR2-related disorders, such as neuropathic pain.

## References


1. Charo, I.F. and R.M. Ransohoff, *The many roles of chemokines and chemokine receptors in inflammation.* The New England journal of medicine, 2006. 354(6): p. 610-21.
2. Serbina, N.V. and E.G. Pamer, *Monocyte emigration from bone marrow during bacterial infection requires signals mediated by chemokine receptor CCR2.* Nat Immunol, 2006. 7(3): p. 311-317.
3. Leuschner, F., et al., *Therapeutic siRNA silencing in inflammatory monocytes in mice.* Nat Biotechnol, 2011. 29(11): p. 1005-10.
4. Fife, B.T., et al., *CC chemokine receptor 2 is critical for induction of experimental autoimmune encephalomyelitis* J Exp Med, 2000. 192(6): p. 899-905.
5. Dawson, T.C., et al., *Absence of CC chemokine receptor-2 reduces atherosclerosis in apolipoprotein E-deficient mice.* Atherosclerosis, 1999. 143(1): p. 205-11.
6. Ogata, H., et al., *The role of monocyte chemoattractant protein-1 (MCP-1) in the pathogenesis of collagen-induced arthritis in rats* J Pathol, 1997. 182(1): p. 106-14.
7. Kanda, H., et al., *MCP-1 contributes to macrophage infiltration into adipose tissue, insulin resistance, and hepatic steatosis in obesity.* J Clin Invest, 2006. 116(6): p. 1494-505.
8. Kim, Y.K., et al., *Association between a genetic variation of CC chemokine receptor-2 and atopic asthma.* Allergy, 2007. 62(2): p. 208-9.
9. White, F.A., P. Feldman, and R.J. Miller, *Chemokine Signaling and the Management of Neuropathic Pain.* Mol Interv, 2009. 9(4): p. 188-195.
10. Struthers, M. and A. Pasternak, *CCR2 antagonists.* Curr Top Med Chem, 2010. 10(13): p. 1278-98.
11. Swinney, D.C., *Biochemical mechanisms of drug action: what does it take for success?* Nat Rev Drug Discov, 2004. 3(9): p. 801-808.
12. Copeland, R.A., D.L. Pompliano, and T.D. Meek, *Drug-target residence time and its implications for lead optimization.* Nat Rev Drug Discov, 2006. 5(9): p. 730-9.
13. Zhang, R.M. and F. Monsma, *Binding kinetics and mechanism of action: toward the discovery and development of better and best in class drugs.* Exp Opin Drug Discov, 2010. 5(11): p. 1023-1029.
14. Copeland, R.A., *Evaluation of enzyme inhibitors in drug discovery. A guide for medicinal chemists and pharmacologists.* Methods Biochem Anal, 2005. 46: p. 1-265.
15. Kothandaraman, S., et al., *Design, synthesis, and structure-activity relationship of novel CCR2 antagonists.* Bioorg Med Chem Lett, 2009. 19(6): p. 1830-4.
16. Xue, C.M., B.; Feng, H.; Cao, G.; Huang, T.; Zheng, C.; Robinson, D. J.; Han, A., *3-Aminopyrrolidine derivatives as modulators of chemokine receptors.* Patent WO2004050024, June 17, 2004.
17. Brodmerkel, C.M., et al., *Discovery and pharmacological characterization of a novel rodent-active CCR2 antagonist, INCB3344.* J Immunol, 2005. 175(8): p. 5370-8.
18. Zweemer, A.J.M., et al., *Multiple Binding Sites for Small-Molecule Antagonists at the CC Chemokine Receptor 2.* Mol Pharmacol, 2013. 84(4): p. 551-561.
19. Motulsky, H.J. and L.C. Mahan, *The kinetics of competitive radioligand binding predicted by the law of mass action.* Mol Pharmacol, 1984. 25(1): p. 1-9.
20. Guo, D., et al., *Dual-Point Competition Association Assay: A Fast and High-Throughput Kinetic Screening Method for Assessing Ligand-Receptor Binding Kinetics.* J Biomol Screen, 2013. 18(3): p. 309-320.

21. Cheng, Y. and W.H. Prusoff, *Relationship between Inhibition Constant (K1) and Concentration of Inhibitor Which Causes 50 Per Cent Inhibition (I50) of an Enzymatic-Reaction.* Biochem Pharmacol, 1973. 22(23): p. 3099-3108.
22. Frerot, E., et al., *Pybop and Pybrop - 2 Reagents for the Difficult Coupling of the Alpha,Alpha-Dialkyl Amino-Acid, Aib.* Tetrahedron, 1991. 47(2): p. 259-270.
23. Burkhardt, E.R. and B.M. Coleridge, *Reductive amination with 5-ethyl-2-methylpyridine borane.* Tetrahedron Lett, 2008. 49(35): p. 5152-5155.
24. Casarosa, P., et al., *Functional and biochemical rationales for 24-h long duration of action of olodaterol.* J Pharmacol Exp Ther, 2011. 377: p. 600-609.
25. Rich, R.L., et al., *Kinetic analysis of estrogen receptor/ligand interactions.* Proc Natl Acad Sci U S A, 2002. 99(13): p. 8562-7.
26. Packeu, A., et al., *Estimation of the dissociation rate of unlabelled ligand-receptor complexes by a 'two-step' competition binding approach.* Br J Pharmacol, 2010. 161(6): p. 1311-28.
27. *http://www.htrf.com/tag-lite-technology*.
28. Shin, N., et al., *Pharmacological characterization of INCB3344, a small molecule antagonist of human CCR2.* Biochem Biophys Res Comm, 2009. 387(2): p. 251-5.
29. Yang, L., et al., *Discovery of 3-piperidinyl-1-cyclopentanecarboxamide as a novel scaffold for highly potent CC chemokine receptor 2 antagonists.* J Med Chem, 2007. 50(11): p. 2609-11.
30. Pasternak, A., et al., *Potent heteroarylpiperidine and carboxyphenylpiperidine 1-alkyl-cyclopentane carboxamide CCR2 antagonists.* Bioorg Med Chem Lett, 2008. 18(3): p. 994-8.
31. Goble, S.D., et al., *Alkylamino, arylamino, and sulfonamido cyclopentyl amide modulators of chemokine receptor activity.* U.S. Patent 2007/117797, May 24, 2007.
32. Zhang, X., et al., *Overcoming hERG activity in the discovery of a series of 4-azetidinyl-1-aryl-cyclohexanes as CCR2 antagonists.* Bioorg Med Chem Lett, 2011. 21(18): p. 5577-82.
33. Van Liefde, I. and G. Vauquelin, *Sartan-AT1 receptor interactions: in vitro evidence for insurmountable antagonism and inverse agonism.* Mol Cell Endocrinol, 2009. 302(2): p. 237-43.
34. Casarosa, P., et al., *Preclinical evaluation of long-acting muscarinic antagonists: comparison of tiotropium and investigational drugs.* J Pharmacol Exp Ther, 2009. 330(2): p. 660-8.
35. Anthes, J.C., et al., *Biochemical characterization of desloratadine, a potent antagonist of the human histamine H(1) receptor.* Eur J Pharmacol, 2002. 449(3): p. 229-37.

# Chapter 7

## Conclusions and future perspectives

In this thesis the molecular pharmacology of the chemokine receptor CCR2 has been extensively studied and discussed. Insights in the mechanism of action of novel as well as existing drug-like molecules for CCR2 were presented. This chapter concludes the findings of these studies, to then discuss its impact on drug discovery and to reflect on future directions of this research field.

## Conclusions

**Multiple binding sites for small molecules at CCR2**

CCR2 is a membrane-bound receptor protein that transduces signals into the cell due to direct interactions with a number of signalling molecules. It is activated by its endogenous chemokine ligands at the extracellular side, which each most likely bind in a slightly different manner to the extracellular and TM domains, given their distinct effects (Chapter 2). Receptor activation allows interactions with large proteins such as G proteins and β-arrestins at the intracellular side of the GPCR, which is often preceded or followed by additional GPCR-interacting proteins (GIPs) [1-3]. Therefore, CCR2, as well as all other GPCRs, naturally possesses multiple binding sites for ligands or proteins. In my thesis I conclude that such distinct binding sites also exist for chemically-derived small molecule ligands for the chemokine receptor CCR2 (Chapter 3). Not only do these ligands bind to the well-established binding sites at the extracellular or TM domain regions, but also to the core region of the receptor and at a hitherto unknown intracellular binding pocket (Chapters 4 and 5, Fig. 1).

**Novel routes towards insurmountable inhibition of CCR2**

Throughout this thesis I have presented data on the mechanism of action of orthosteric antagonists and allosteric antagonists. In Chapter 3 it was described that the allosteric antagonists act in a noncompetitive manner with respect to the endogenous chemokine CCL2. This implies that the maximal response of the receptor is suppressed even when high concentrations of the agonist CCL2 are present; a phenomenon that has been described as insurmountable antagonism in *in vitro* functional assays [4, 5]. Due to this property, insurmountable antagonists are proposed to be highly clinically relevant. This situation is particularly relevant for chemokine receptors, since chemokine levels are highly increased (1-10 nM) during inflammatory conditions [6-8]. In addition, as discussed in Chapter 2, chemokines are sequestered on glycosaminoglycans (GAGs) near the chemokine receptors, thereby creating a depot in close proximity to the receptor that further increases the local concentration of these ligands. Leukocytes expressing CCR2 that pass the site of inflammation, will only be inhibited from chemotaxis towards these sites if a drug can bind irrespective of the high local chemokine concentrations; a requirement that is fulfilled by the allosteric insurmountable antagonists described in Chapters 3 and 4. The binding site of these antagonists was discovered to be located at the intracellular side of the receptor. Since the surrounding amino acid residues of these ligands have now been revealed (Chapter 4), this may facilitate the design of novel and improved allosteric insurmountable antagonists.

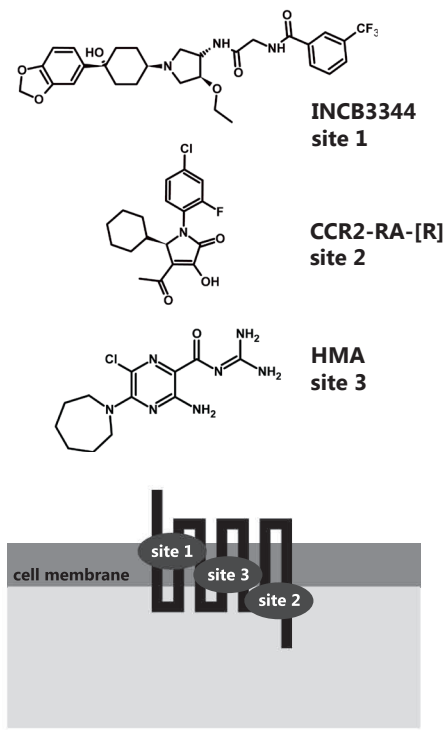



**Fig. 1.** Schematic representation of CCR2 with its multiple ligand binding sites throughout the entire transmembrane domain. A representative ligand for each of these binding sites is depicted at the top.

An allosteric mode of action is not the only possibility to obtain insurmountable antagonism, since orthosteric antagonists with a long residence time on the receptor can manifest a similar inhibition profile [5]. In this latter scenario, the orthosteric antagonists are bound to the receptor for such a long time that they prevent agonists from binding and thereby diminish their maximum effect. The structure-kinetics relationship (SKR) presented in Chapter 6 is among the first examples of a comprehensive medicinal chemistry approach that aims to increase ligand residence times. Small structural changes prolonged the residence time of these antagonists, revealing the first molecular determinants that can lead to insurmountable antagonism via this orthosteric binding pocket. Importantly, SKR-driven ligand optimization resulted in final compounds distinct from a situation in which the affinity would have driven the optimization process. This emphasizes that SKR should be incorporated in early stages of hit-to-lead optimization in order to identify long residence time antagonists.

In summary, it can be concluded that two distinct paths towards insurmountable antagonism for CCR2 have been paved.

## Future perspectives

A variety of pharmacological topics are covered in thesis, ranging from allosteric modulation and insurmountability to ligand binding kinetics and biased signalling. In addition, the functioning and regulation of the intertwined chemokine receptor system was discussed, along with the challenges to target these receptors in the clinic. The following sections will discuss some future perspectives of all these findings for targeting CCR2, and GPCRs in general.

### CCR2 as a single drug target

This thesis is mainly focused on the molecular pharmacology of CCR2, without emphasis on any particular disease state to which this receptor is associated. However, the complexity and functioning of the chemokine receptor system was discussed in Chapter 2, and should also be taken into account while speculating on the future directions of disease management through CCR2 antagonism. For example in rheumatoid arthritis (RA), patients suffer from joint pain, stiffness, and swelling as a result of synovial inflammation. CCR2 is clearly involved in this disease, concluded from many *in vitro* studies as well as *in vivo* animal studies in which knock-out or pharmacological blockade of CCR2 decreased disease symptoms [9]. Nevertheless, no clinical trial targeting CCR2 in this disease has been proven successful so far [10]. There can be multiple reasons for this failure, including inappropriate drug-receptor kinetics or molecular mechanisms of action, i.e. surmountable vs. insurmountable antagonism, as discussed in Chapters 3, 4 and 6. Additionally, in case of these complex inflammatory diseases it must be remembered that multiple chemokines as well as multiple chemokine receptors are involved, which can in turn have both synergistic and counteracting modes of action (Chapter 2). In case of RA, monocytes in peripheral blood of RA patients expressed higher levels of CCR2 than CCR5 [11]. In contrast, substantially higher expression of CCR5 compared to CCR2 was observed on macrophages in synovial fluid [11]. Yet another study revealed that neither CCR2 nor CCR5 antagonists were able to block chemotaxis of monocytes towards synovial fluid of patients, but inhibition of CCR1 was proven to be effective [12]. In this particular case it should be identified which receptor(s) are critical for the migration of monocytes towards the synovial compartment in RA in order to know which receptor(s) to target [13].

There are several other diseases for which multiple chemokine receptors have been found to be involved, which has stimulated the development of dual antagonists, mainly for CCR2 and CCR5 [14, 15]. The dual CCR2 and CCR5 antagonist cenicriviroc has made most progress so far, since it is has entered phase 3 clinical trials for the treatment of HIV-1 infection,

and is currently also in preclinical development for fibrosis, graft-versus-host disease, and other indications in which CCR5 and CCR2 play a role [14, 16]. Future results of these ongoing trials will demonstrate whether dual inhibition is the key to successful treatments for these and other diseases, like RA (see above). For this particular disease, one could think of dual/triple antagonists that additionally target CCR1, which does not seem impossible in view of the high sequence similarity of CCR1, CCR2 and CCR5 [17]. Regarding this polypharmacology as an approach [18], the development of dual intracellular antagonists could be another way to proceed, given the evidence that such a binding pocket is at least conserved among the highly homologous chemokine receptors CCR2 and CCR5 (Chapter 4).

**The INS of ligand binding to GPCRs**

***Intracellular CCR2 antagonists.*** In Chapter 4 the discovery of an intracellular binding pocket for small molecule antagonists of CCR2 was presented. This is the first time that such a binding pocket was extensively mapped on a GPCR by means of mutations, and visualized in a homology model of CCR2 upon induced-fit docking of the antagonist CCR2-RA-[R]. The most recent review on CCR2 small molecule antagonists includes approximately 30 different structural scaffolds, of which only 10% is likely to bind to the intracellular pocket based on structural similarity with the antagonists presented in this thesis [19]. Therefore, the identification of this binding pocket in Chapter 4 will allow chemists to further explore this allosteric site. In addition, the radioligand binding studies in Chapter 3 revealed that the intracellular and orthosteric antagonists enhanced binding of each other to CCR2. Hence, it would be interesting to further study the nature of this enhancement, since a similar level of inhibition might be achieved with lower doses of both antagonists due to a synergistic mode of action.

***Allosteric modulation of CCR2 signalling by intracellular ligands.*** Now that the binding properties of the intracellular CCR2 antagonists have been elucidated, several future research questions arise with respect to the effect of these allosteric ligands on a functional level. As mentioned in Chapter 2, CCR2 has been found to function as both a monomer and a (hetero)dimer. The allosteric intracellular antagonists might differentially inhibit these multimeric complexes compared to the orthosteric antagonists. In addition, a total of eight chemokine ligands can bind to CCR2, all exerting distinct actions as described in Chapter 2. The intracellular antagonists might differentially inhibit these endogenous chemokines compared to the competitive orthosteric antagonists (Fig. 2), and depending on their role in disease states this could have an impact on their efficacy *in vivo*.

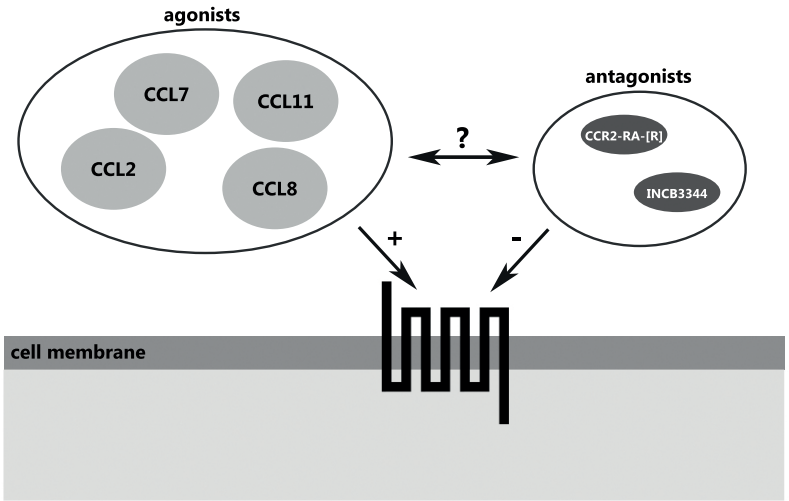



**Fig. 2.** CCR2 can be activated by multiple endogenous chemokines, including CCL2, CCL7, CCL8 and CCL11. In this thesis multiple antagonists with a distinct binding site and mechanism of action were discovered, among which the orthosteric antagonist INCB3344 and the allosteric antagonist CCR2-RA-[R]. It remains a question for further research how these two distinct antagonists affect the receptor activation that is induced by the multiple endogenous chemokines.

Besides a distinct action in the presence of the different chemokine ligands for CCR2, one could also hypothesize that a small molecule ligand might exert biased antagonism itself, in which it inhibits certain signalling pathways better than others [20, 21]. There is one study that reported such behavior for a set of 24 CCR2 antagonists, in which inhibition of CCL2 stimulation was compared in five different functional assays [22]. Although the structures of these antagonists were not reported, and the effect in a functional assay is dependent on the off-rate of the antagonists and the incubation time of the assay, it is at least a first indication of biased antagonism for CCR2. Now that the receptor's distinct antagonist binding sites have been revealed, this phenomenon should be further investigated.

***Intracellular CCR2 antagonists in vivo.*** Speculations on distinct *in vivo* effects of allosteric antagonists compared to orthosteric antagonists can be made based on several clinical studies with CCR2 antagonists. Most of the trials involve orthosteric antagonists, and in many of these studies enhanced CCL2 plasma levels were previously reported upon administration of the antagonists, including for INCB3344 [10, 23, 24]. These enhanced CCL2 levels could in turn diminish the inhibitory action of the administered antagonist due to direct competition. In contrast, no elevation of systemic CCL2 levels was observed in a recent phase II study in type 2 diabetics with the antagonist CCX140-B [25, 26]. Although the chemical identity

of CCX140-B has not been revealed, it is likely to be an allosteric (intracellular) antagonist since the associated patent describes a chemical scaffold that closely resembles SD-24 from Chapter 4 [27]. The allosteric nature of this ligand might be the cause of different modulation of CCL2 plasma levels compared to orthosteric antagonists. As described in Chapter 2, CCL2 is scavenged by CCR2 *in vivo* [28]. This implies that the CCR2-CCL2 complex can be internalized to regulate the level of CCL2 in the extracellular environment. So far, the effect of small molecule antagonists on this internalization pathway has not been studied for CCR2. However, a very recent *in vitro* study that compared orthosteric and intracellular antagonists of CCR4 revealed that orthosteric antagonists were able to induce internalization of CCR4, whereas intracellular antagonists left CCR4 surface expression unaffected [29]. Whether this phenomenon is also applicable to CCR2, linking the unaffected plasma levels of CCL2 to a lack of CCR2 internalization by an allosteric mode of inhibition, remains to be determined. However, these studies indicate that orthosteric and allosteric antagonists may differentially inhibit the CCR2-CCL2 axis *in vivo*.

***Intracellular ligands for GPCRs.*** During the last couple of years the intracellular region of GPCRs has become of increasing interest, either for therapeutic interventions or to study receptor functioning in general [30, 31]. Indications of intracellular GPCR binding pockets have been reported previously for CCR4, CCR5, CXCR1, CXCR2 and PAR1 [32-35]. In addition, the intracellular CCR2 antagonists CCR2-RA-[R], JNJ-27141491 and SD-24 from Chapters 3 and 4 have been reported to also bind to CCR1 [36-38]. Together these data suggest that an intracellular binding pocket for small molecule antagonists could be a shared feature among chemokine receptors, or even GPCRs in general. Such an intracellular antagonist binding pocket could be highly interesting for certain GPCRs, for example for those that have their endogenous ligand tethered at the extracellular side, like the PAR1 receptor [39]. These tethered ligands directly compete with orthosteric antagonists, preventing them to sufficiently block the receptor. Besides receptor blockade with long residence time orthosteric antagonists, inhibition via an intracellular allosteric site would be beneficial for targeting such receptors. For PAR1 this is likely to be possible, since indications of an intracellular binding pocket have been reported for this receptor [34].

Intracellular antagonists act at the interface of the receptor and its signalling molecules, and therefore they most likely act as inverse agonists, inhibiting the basal activity or constitutive signalling of the receptor. This is indeed the case for the intracellular CXCR2 antagonist Sch527123 [32, 40], which has been found efficacious in a Phase II clinical trial for asthma [41]. Although the extent of constitutive activity in disease states remains largely

unknown, many GPCR antagonists are in fact inverse agonists [42]. Some of these drugs have been presented to display higher clinical efficacy than neutral antagonists targeting the same receptor [43, 44].

Last but not least, it is tempting to speculate on possibilities to enhance or activate GPCR signalling via the intracellular side. Small lipidated peptide sequences named pepducins have been proposed to act via the intracellular side of the receptor, and can thereby activate, inhibit or modulate various GPCRs, including the chemokine receptor CXCR4 [31, 45, 46]. In Chapter 4 the intracellular binding pocket for CCR2 small molecule antagonists was identified, which is surrounded by TM-I, II, VI and VII. One of the possible mechanisms of inhibition by these antagonists is the fixation of TM-VI, since relatively large outward movements of TM-VI are necessary for activation of the receptor [47, 48]. It would be interesting to study whether small molecule agonists can be designed that favor this outward movement of TM-VI, thereby creating a binding site for signalling proteins such as the G protein [49].

**The OUTS of ligand binding to CCR2**

Several orthosteric CCR2 antagonists were described in Chapter 3, of which INCB3344 was radiolabeled and further studied. The binding site of other orthosteric antagonists was previously reported to reside in the upper half of the TM domain [50]. A similar location for binding of INCB3344 was confirmed in Chapter 4, where the conserved glutamate residue $E^{7.39}$ was identified to be important for binding. In close proximity to this binding site, an additional binding pocket for small molecule ligands and sodium ions was discovered (Chapter 5). This pocket is located in the core domain of the receptor, and allows amiloride analogues and sodium ions to modulate CCR2. Besides targeting one particular antagonist binding site, inhibition via multiple pockets simultaneously might offer additional opportunities to antagonize CCR2. This could for example be established via so-called bitopic ligands that would be able to bind both the binding pocket in the core domain as well as the orthosteric binding pocket [51].

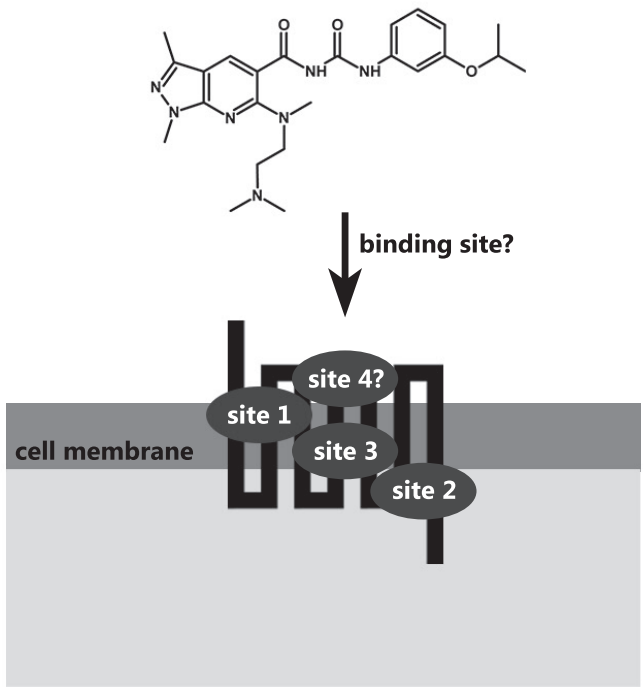



**Fig. 3.** Chemical structure of the most potent heteroaroylphenylurea CCR2 antagonist described by Laborde *et al*. [56]. This antagonist inhibits CCR2 in a different manner than the antagonists that bind to sites 1, 2 and 3, and was previously suggested to interact with extracellular domains of the receptor. This raises the question if a fourth small molecule binding site exists in CCR2.

Binding and activation of CCR2 by its endogenous chemokines is highly dependent on the extracellular loops (ECLs) as well as the N-terminus [52]. The role of the ECLs in antagonist binding to CCR2 has not yet been deciphered, but the results on chimeric CCR2-CCR5 receptors in Chapter 4 suggest that these loops may also be involved in the binding of the orthosteric antagonist INCB3344. A general analysis of the extracellular domains for class A GPCRs has previously revealed that these parts of the receptor can host allosteric binding sites [53]. For CCR2, there is one particular antagonist described in literature that has been suggested to mediate its inhibitory action via extracellular domains of the receptor [54, 55]. This heteroaroylphenylurea CCR2 antagonist is structurally different from all of the antagonists reported in this thesis [56], and is also unique compared to all other CCR2 antagonist chemotypes [19]. Interestingly, this antagonist does not inhibit binding of CCL2 to the receptor, while it inhibits CCL2-induced chemotaxis *in vitro* as well as *in vivo* [56]. A lack of chemokine displacement was previously also reported for the CCR5 antagonist aplaviroc

[57] as well as the CXCR1 antagonist repertaxin [58], and is indicative of an allosteric mode of action. Whether this heteroaroylphenylurea antagonist indeed binds to a pocket within the extracellular domains remains to be determined (Fig. 3), but it does inhibit the receptor in a very distinct manner compared to the antagonists described in this thesis.

**Keeping up with kinetics**

In Chapter 6 the kinetics of antagonist binding to CCR2 were explored. Although this study was solely focused on orthosteric antagonists, a similar approach can be applied to the intracellular antagonists in the future. In fact, it has already been demonstrated that intracellular antagonists have potential to result in prolonged receptor blockade, since a residence time of 29 hours at room temperature was previously measured for the intracellular CXCR2 antagonist Sch527123 [59].

Long residence time antagonists are proposed to lead to enhanced clinical efficacy and patience compliance, due to a prolonged receptor blockade, increased selectivity and a decreased dosing frequency [60]. Recently a short residence time antagonist for CCR2 was found to enhance vaccine immunity only after a multi-dose treatment regime, due to its poor pharmacokinetic properties [61]. Increasing the residence time of such ligands could lead to longer-lasting *in vivo* blockade, as was previously also reported for antagonists of the NK1 receptor [62]. To identify whether administration of long residence time antagonists results in more efficacious CCR2 blockade *in vivo*, comparative studies with short residence time antagonists should be performed. Additionally, long residence time antagonists can be used for structure elucidation of CCR2, since attempts to crystallize GPCRs have been proven to be more successful in the presence of long residence time ligands that stabilize the receptor complex [63].

Although several marketed and highly efficacious drugs were determined to slowly dissociate from their target receptor in retrospect [64], it is not solely the receptor residence time that is related to the clinical efficacy and duration of action [65]. Factors such as the association rate of a drug to its receptor, plasma protein binding, pharmacokinetics and rebinding of a drug to its target all contribute to the level of receptor occupancy and the duration of the effect [66-70]. Hence, chemists, pharmacologists and computational biologists should join forces and study the influence of drug binding kinetics on drug action at a molecular as well as a systems level in order to unravel the determinants for clinical success per target and disease [69, 71].

**Final notes**

Altogether the molecular mechanisms of action of orthosteric and allosteric antagonists for CCR2 have been explored and detailed throughout this thesis. In addition, these ligands, with their distinct binding sites, were effective tools to study receptor modulation by physiologically relevant sodium ion concentrations and small molecule amiloride analogues. The discovery of the three different ligand binding sites throughout the entire transmembrane domain of the receptor illustrates that a GPCR behaves as an allosteric machine, rather than as the classically described receptor with a ligand binding site at the extracellular side and a signalling domain at the inside of the cell. In concert with the currently expanding insight in the structure and signalling capacities of GPCRs, the data presented in this thesis allow to better fine-tune the pharmacological modulation of the chemokine receptor CCR2, and GPCRs in general.

## References


1. Bockaert, J., et al., *GPCR interacting proteins (GIPs) in the nervous system: Roles in physiology and pathologies.* Annu Rev Pharmacol Toxicol, 2010. 50: p. 89-109.
2. Favre, N., et al., *Chemokine receptor CCR2 undergoes transportin1-dependent nuclear translocation.* Proteomics, 2008. 8(21): p. 4560-76.
3. Terashima, Y., et al., *Pivotal function for cytoplasmic protein FROUNT in CCR2-mediated monocyte chemotaxis.* Nat Immunol, 2005. 6(8): p. 827-35.
4. Vauquelin, G., et al., *New insights in insurmountable antagonism.* Fundam Clin Pharmacol, 2002. 16(4): p. 263-72.
5. Kenakin, T., S. Jenkinson, and C. Watson, *Determining the potency and molecular mechanism of action of insurmountable antagonists.*J Pharmacol Exp Ther, 2006. 319(2): p. 710-23.
6. Nocker, R.E., et al., *Interleukin-8 in airway inflammation in patients with asthma and chronic obstructive pulmonary disease.* Int Arch Allergy Immunol, 1996. 109(2): p. 183-91.
7. Traves, S.L., et al., *Increased levels of the chemokines GROalpha and MCP-1 in sputum samples from patients with COPD.* Thorax, 2002. 57(7): p. 590-5.
8. Yung, S.C. and P.M. Murphy, *Antimicrobial chemokines.* Front Immunol, 2012. 3: p. 276.
9. Quinones, M.P., et al., *The complex role of the chemokine receptor CCR2 in collagen-induced arthritis: implications for therapeutic targeting of CCR2 in rheumatoid arthritis.* J Mol Med, 2005. 83(9): p. 672-81.
10. Vergunst, C.E., et al., *Modulation of CCR2 in rheumatoid arthritis: a double-blind, randomized, placebo-controlled clinical trial.* Arthritis Rheum, 2008. 58(7): p. 1931-9.
11. Katschke, K.J., Jr., et al., *Differential expression of chemokine receptors on peripheral blood, synovial fluid, and synovial tissue monocytes/macrophages in rheumatoid arthritis.* Arthritis Rheum, 2001. 44(5): p. 1022-32.
12. Lebre, M.C., et al., *Why CCR2 and CCR5 blockade failed and why CCR1 blockade might still be effective in the treatment of rheumatoid arthritis.* PloS One, 2011. 6(7): p. e21772.
13. Proudfoot, A.E., *Is CCR2 the right chemokine receptor to target in rheumatoid arthritis?* Arthritis Rheum, 2008. 58(7): p. 1889-91.
14. Lalezari, J., et al., *Safety, efficacy, and pharmacokinetics of TBR-652, a CCR5/CCR2 antagonist, in HIV-1-infected, treatment-experienced, CCR5 antagonist-naive subjects.* J Acquir Immune Defic Syndrom, 2011. 57(2): p. 118-25.
15. Padi, S.S., et al., *Attenuation of rodent neuropathic pain by an orally active peptide, RAP-103, which potently blocks CCR2- and CCR5-mediated monocyte chemotaxis and inflammation.* Pain, 2012. 153(1): p. 95-106.
16. *Tobira Therapeutics product pipeline as of February 2014* Available from: http://www.tobiratherapeutics.com/discovery.php.
17. Shields, D.C., *Gene conversion among chemokine receptors.* Gene, 2000. 246(1-2): p. 239-45.
18. Peters, J.U., *Polypharmacology - foe or friend?* J Med Chem, 2013. 56(22): p. 8955-71.
19. Carter, P.H., *Progress in the discovery of CC chemokine receptor 2 antagonists, 2009 - 2012.* Exp Opin Ther Pat, 2013. 23(5): p. 549-68.
20. Magnan, R., et al., *Distinct CCK-2 receptor conformations associated with beta-arrestin-2 recruitment or phospholipase-C activation revealed by a biased antagonist.* J Am Chem Soc, 2013. 135(7): p. 2560-73.
21. Kenakin, T. and L.J. Miller, *Seven transmembrane receptors as shapeshifting proteins: the impact of allosteric modulation and functional selectivity on new drug discovery.* Pharmacol Rev, 2010. 62(2): p. 265-304.

22. Kredel, S., et al., *High-content analysis of CCR2 antagonists on human primary monocytes.* J Biomol Screen, 2011. 16(7): p. 683-93.

23. Aiello, R.J., et al., *CCR2 receptor blockade alters blood monocyte subpopulations but does not affect atherosclerotic lesions in apoE(-/-) mice.* Atherosclerosis, 2010. 208(2): p. 370-5.

24. Wang, Y., et al., *CCR2 and CXCR4 regulate peripheral blood monocyte pharmacodynamics and link to efficacy in experimental autoimmune encephalomyelitis.* J Inflamm, 2009. 6: p. 32.

25. Hanefeld, M., et al., *the CCX140-B Diabetes Study Group. Orally-administered chemokine receptor CCR2 antagonist CCX140-B in type 2 diabetes: a pilot double-blind, randomized clinical trial.* J Diabetes Metab, 2012. 3: p. 1-8.

26. Sullivan, T., et al., *CCR2 antagonist CCX140-B provides renal and glycemic benefits in diabetic transgenic human CCR2 knockin mice.* Am J Physiol Renal Physiol, 2013. 305(9): p. F1288-97.

27. Dairaghi, D., et al., *Heteroaryl sulfonamides and ccr2/ccr9*, 2008, Google Patents.

28. Volpe, S., et al., *CCR2 acts as scavenger for CCL2 during monocyte chemotaxis.* PloS One, 2012. 7(5): p. e37208.

29. Ajram, L., et al., *Internalization of the chemokine receptor CCR4 can be evoked by orthosteric and allosteric receptor antagonists.* Eur J Pharmacol, 2014. 729: p 75-85.

30. Staus, D.P., et al., *Regulation of beta2-adrenergic receptor function by conformationally selective single-domain intrabodies.* Mol Pharmacol, 2014. 85(3): p. 472-81.

31. O'Callaghan, K., A. Kuliopulos, and L. Covic, *Turning receptors on and off with intracellular pepducins: new insights into G-protein-coupled receptor drug development.* J Biol Chem, 2012. 287(16): p. 12787-96.

32. Salchow, K., et al., *A common intracellular allosteric binding site for antagonists of the CXCR2 receptor.* Br J Pharmacol, 2010. 159(7): p. 1429-39.

33. Andrews, G., C. Jones, and K.A. Wreggett, *An intracellular allosteric site for a specific class of antagonists of the CC chemokine G protein-coupled receptors CCR4 and CCR5.* Mol Pharmacol, 2008. 73(3): p. 855-67.

34. Dowal, L., et al., *Identification of an antithrombotic allosteric modulator that acts through helix 8 of PAR1.* Proc Natl Acad Sci U S A, 2011. 108(7): p. 2951-6.

35. Nicholls, D.J., et al., *Identification of a putative intracellular allosteric antagonist binding-site in the CXC chemokine receptors 1 and 2.* Mol Pharmacol, 2008. 74(5): p. 1193-202.

36. Buntinx, M., et al., *Pharmacological profile of JNJ-27141491 [(S)-3-[3,4-difluorophenyl)-propyl]-5-isoxazol-5-yl-2-thioxo-2,3-dihydro-1H-imida zole-4-carboxyl acid methyl ester], as a noncompetitive and orally active antagonist of the human chemokine receptor CCR2.* J Pharmacol Exp Ther, 2008. 327(1): p. 1-9.

37. Dasse, O.A., et al., *Novel, Acidic CCR2 Receptor Antagonists: Lead Optimization.* Lett Drug Des Discov, 2007. 4: p. 263-271.

38. Peace, S., et al., *Identification of a sulfonamide series of CCR2 antagonists.* Bioorg Med Chem Lett, 2010. 20(13): p. 3961-4.

39. Zhang, C., et al., *High-resolution crystal structure of human protease-activated receptor 1.* Nature, 2012. 492(7429): p. 387-92.

40. Kredel, S., et al., *CXCR2 inverse agonism detected by arrestin redistribution.* J Biomol Screen, 2009. 14(9): p. 1076-91.

41. Nair, P., et al., *Safety and efficacy of a CXCR2 antagonist in patients with severe asthma and sputum neutrophils: a randomized, placebo-controlled clinical trial.* Clin Exp Allergy, 2012. 42(7): p. 1097-103.

42. Greasley, P.J. and J.C. Clapham, *Inverse agonism or neutral antagonism at G-protein coupled receptors: a medicinal chemistry challenge worth pursuing?* Eur J Pharmacol, 2006. 553(1-3): p. 1-9.

43. Maack, C., et al., *Different intrinsic activities of bucindolol, carvedilol and metoprolol in human failing myocardium.* Br J Pharmacol, 2000. 130(5): p. 1131-9.

44. Kenakin, T., *Efficacy as a vector: the relative prevalence and paucity of inverse agonism.* Mol Pharmacol, 2004. 65(1): p. 2-11.

45. Tchernychev, B., et al., *Discovery of a CXCR4 agonist pepducin that mobilizes bone marrow hematopoietic cells.* Proc Natl Acad Sci U S A, 2010. 107(51): p. 22255-9.

46. Quoyer, J., et al., *Pepducin targeting the C-X-C chemokine receptor type 4 acts as a biased agonist favoring activation of the inhibitory G protein.* Proc Natl Acad Sci U S A, 2013. 110(52): p. 5088-97.

47. Kruse, A.C., et al., *Activation and allosteric modulation of a muscarinic acetylcholine receptor.* Nature, 2013. 504(7478): p. 101-6.

48. Wacker, D., et al., *Structural features for functional selectivity at serotonin receptors.* Science, 2013. 340(6132): p. 615-9.

49. Rasmussen, S.G., et al., *Crystal structure of the beta2 adrenergic receptor-Gs protein complex.* Nature, 2011. 477(7366): p. 549-55.

50. Hall, S.E., et al., *Elucidation of binding sites of dual antagonists in the human chemokine receptors CCR2 and CCR5.* Mol Pharmacol, 2009. 75(6): p. 1325-36.

51. Lane, J.R., P.M. Sexton, and A. Christopoulos, *Bridging the gap: bitopic ligands of G-protein-coupled receptors.* Trends Pharmacol Sci, 2013. 34(1): p. 59-66.

52. Han, K.H., et al., *Role of the first extracellular loop in the functional activation of CCR2. The first extracellular loop contains distinct domains necessary for both agonist binding and transmembrane signaling.* J Biol Chem, 1999. 274(45): p. 32055-62.

53. Peeters, M.C., et al., *Importance of the extracellular loops in G protein-coupled receptors for ligand recognition and receptor activation.* Trends Pharmacol Sci, 2011. 32(1): p. 35-42.

54. Okamoto, M., et al., *A novel C-C chemokine receptor 2 antagonist prevents progression of albuminuria and atherosclerosis in mouse models.* Biol Pharm Bull, 2012. 35(11): p. 2069-74.

55. Yokochi, S., et al., *An anti-inflammatory drug, propagermanium, may target GPI-anchored proteins associated with an MCP-1 receptor, CCR2.* J Interferon Cytokine Res, 2001. 21(6): p. 389-98.

56. Laborde, E., et al., *Discovery, optimization, and pharmacological characterization of novel heteroaroylphenylureas antagonists of C-C chemokine ligand 2 function.* J Med Chem, 2011. 54(6): p. 1667-81.

57. Watson, C., et al., *The CCR5 receptor-based mechanism of action of 873140, a potent allosteric noncompetitive HIV entry inhibitor.* Mol Pharmacol, 2005. 67(4): p. 1268-82.

58. Casilli, F., et al., *Inhibition of interleukin-8 (CXCL8/IL-8) responses by repertaxin, a new inhibitor of the chemokine receptors CXCR1 and CXCR2.* Biochem Pharmacol, 2005. 69(3): p. 385-94.

59. Gonsiorek, W., et al., *Pharmacological characterization of Sch527123, a potent allosteric CXCR1/CXCR2 antagonist.* J Pharmacol Exp Ther, 2007. 322(2): p. 477-85.

60. Tummino, P.J. and R.A. Copeland, *Residence time of receptor-ligand complexes and its effect on biological function.* Biochemistry, 2008. 47(20): p. 5481-92.

61. Mitchell, L.A., et al., *Optimized dosing of a CCR2 antagonist for amplification of vaccine immunity.* Int Immunopharmacol, 2013. 15(2): p. 357-63.

62. Lindstrom, E., et al., *Neurokinin 1 receptor antagonists: correlation between in vitro receptor interaction and in vivo efficacy.* J Pharmacol Exp Ther, 2007. 322(3): p. 1286-93.

63. Venkatakrishnan, A.J., et al., *Molecular signatures of G-protein-coupled receptors.* Nature, 2013. 494(7436): p. 185-94.

64. Guo, D., et al., *Drug-Target Residence Time-A Case for G Protein-Coupled Receptors.* Med Res Rev, 2014. 34(4):856-92.

65. Sykes, D.A., et al., *The Influence of receptor kinetics on the onset and duration of action and the therapeutic index of NVA237 and tiotropium.* J Pharmacol Exp Ther, 2012. 343(2): p. 520-8.

66. Vauquelin, G. and S.J. Charlton, *Long-lasting target binding and rebinding as mechanisms to prolong in vivo drug action.* Br J Pharmacol, 2010. 161(3): p. 488-508.

67. Dahl, G. and T. Akerud, *Pharmacokinetics and the drug-target residence time concept.* Drug Discov Today, 2013. 18(15-16): p. 697-707.

68. Copeland, R.A., *The dynamics of drug-target interactions: drug-target residence time and its impact on efficacy and safety.* Expert Opin Drug Discov, 2010. 5(4): p. 305-10.

69. Yin, N., J. Pei, and L. Lai, *A comprehensive analysis of the influence of drug binding kinetics on drug action at molecular and systems levels.* Mol Biosyst, 2013. 9(6): p. 1381-9.

70. Peletier, L.A., N. Benson, and P.H. van der Graaf, *Impact of plasma-protein binding on receptor occupancy: an analytical description.* J Theor Biol, 2009. 256(2): p. 253-62.

71. Ploeger, B.A., P.H. van der Graaf, and M. Danhof, *Incorporating receptor theory in mechanism-based pharmacokinetic-pharmacodynamic (PK-PD) modeling.* Drug Metab Pharmacokinet, 2009. 24(1): p. 3-15.

# Summary

This thesis has provided novel insights in the molecular mechanism of action of antagonists for the chemokine receptor CCR2. CCR2 belongs to the protein family of G protein-coupled receptors (GPCRs). It is involved in several inflammatory diseases and therefore many small molecule antagonists targeting this receptor have been developed over the years. Unfortunately all clinical candidates tested so far appeared to lack efficacy in man, which stresses the need for a better understanding of their mechanism of action.

**Chapter 1** introduces the main subjects that were discussed in this thesis. Prior to our study of CCR2, the entire family of chemokine receptors and its endogenous chemokines were introduced and discussed in **Chapter 2**. Chemokine receptors are widely expressed on a variety of immune cells and play a crucial role in normal physiology as well as in inflammatory and infectious diseases. The existence of 23 chemokine receptors and 48 chemokine ligands guarantees a tight control and fine-tuning of the immune system. In this chapter the multiple regulatory mechanisms of chemokine signalling at a systemic, cellular, and molecular level were discussed. In particular, this chapter was focused on the impact of biased signalling at the receptor level, an emerging concept in molecular pharmacology. An improved understanding of these mechanisms may provide a framework for more effective drug discovery and development at a target class that is so relevant for immune function.

A selection of reference CCR2 antagonists was studied in a variety of pharmacological binding and functional assays as described in **Chapter 3**. All these antagonists displaced the endogenous agonist $^{125}$I-CCL2 from CCR2 with nanomolar affinity. Two antagonists, INCB3344 and CCR2-RA, were radiolabeled to study the binding site in greater detail. It was discovered that [$^{3}$H]-INCB3344 and [$^{3}$H]-CCR2-RA bind to distinct binding sites at CCR2, the latter being the first allosteric radioligand for CCR2. Besides the binding properties of the antagonists, CCR2 inhibition was examined in multiple functional assays, including a novel label-free whole-cell assay. INCB3344 competitively inhibited CCL2-induced G protein activation, whereas CCR2-RA showed a noncompetitive (insurmountable) or allosteric mode of inhibition. These findings demonstrated that the CCR2 antagonists described in this chapter can be classified into two groups with different binding sites and thereby different modes of inhibition.

In **Chapter 4** the binding site of the allosteric antagonist CCR2-RA-[R] was identified. A chimeric CCR2/CCR5 receptor approach was used to obtain insight into the binding site of the allosteric antagonists, and additionally eight single point mutations were introduced in CCR2 to further characterize the putative binding pocket. All constructs were studied in radioligand binding as well as functional IP turnover assays, providing evidence for an intracellular binding site for CCR2-RA-[R]. The most important residues for binding were found to be the highly conserved tyrosine $Y^{7.53}$ and phenylalanine $F^{8.50}$ of the $NPxxYX_{(5,6)}F$ motif, as well as $V^{6.36}$

at the bottom of TM-VI and $K^{8.49}$ in helix-VIII. In addition, the antagonists JNJ-27141491 and SD-24 were identified to bind at the same binding pocket as CCR2-RA-[R], albeit with distinct orientations. This chapter demonstrated for the first time the presence of an allosteric intracellular binding site for CCR2 antagonists.

In **Chapter 5**, yet another binding pocket was revealed via which amiloride analogues and sodium ions were discovered to modulate CCR2. In radioligand binding studies the amiloride analogue HMA allosterically inhibited binding of the agonist $^{125}$I-CCL2, the orthosteric antagonist [$^{3}$H]-INCB3344 and the intracellular antagonist [$^{3}$H]-CCR2-RA-[R]. Differently, sodium ions only allosterically inhibited $^{125}$I-CCL2 binding, while they enhanced binding of [$^{3}$H]-CCR2-RA-[R]. Three residues located in the core of the transmembrane domain, $D^{2.50}$, $W^{6.48}$ and $H^{7.45}$, turned out to be important for modulation of the antagonist radioligands, since mutation of these residues abolished or diminished the allosteric effects induced by HMA and sodium ions. Upon induced-fit docking of HMA in a homology model of CCR2, its interactions with $D^{2.50}$, $W^{6.48}$ and $H^{7.45}$ were visualized, and additional surrounding residues of this binding pocket were predicted.

**Chapter 6** was focused on the design of high-affinity and long-residence-time orthosteric CCR2 antagonists, which share the same binding site as INCB3344. A new competition association assay was developed for CCR2, which allowed investigation of the relationship between the structure of the ligand and its receptor residence time (i.e., structure–kinetic relationship (SKR)) next to a traditional structure–affinity relationship (SAR). By applying combined knowledge of SAR and SKR, the hit-to-lead process of cyclopentylamines as CCR2 antagonists was re-evaluated. Affinity-based optimization yielded a compound with good binding ($K_i$ = 6.8 nM) but very short residence time (2.4 min). However, when the optimization was also based on residence time, the hit-to-lead process yielded a new high-affinity CCR2 antagonist (3.6 nM), with a residence time of 135 min.

In summary this thesis revealed novel *ins* and *outs* of ligand binding to CCR2, presenting three separate binding pockets via which this receptor can be pharmacologically modulated. Different routes towards insurmountable antagonism of CCR2 were described, either via noncompetitive or via long residence time antagonists, as concluded in **Chapter 7**. These results may allow a more rational design of future antagonists, and are equally important to understand the outcomes of studies with existing CCR2 antagonists. In concert with the currently expanding insight in the structure and signalling capacities of GPCRs, the data presented in this thesis allow to better fine-tune the pharmacological modulation of the chemokine receptor CCR2, and GPCRs in general.

# Samenvatting

In dit proefschrift zijn verschillende benaderingen onderzocht die leiden tot inhibitie van de chemokine receptor CCR2, een receptor die behoort tot de klasse van G-eiwit gekoppelde receptoren (GPCRs). CCR2 is betrokken bij diverse ziektebeelden, en daarom is er een groot aantal antagonisten voor deze receptor ontwikkeld gedurende de afgelopen jaren. Desondanks is er nog geen enkel geneesmiddel gericht tegen CCR2 op de markt gebracht, omdat geen van alle antagonisten effectief is gebleken in klinische studies. Om deze situatie te kunnen verbeteren is een beter begrip van het werkingsmechanisme van CCR2 antagonisten noodzakelijk, waarmee de doelstelling van het onderzoek in dit proefschrift is geformuleerd.

In **Hoofdstuk 1** werden de belangrijkste begrippen en onderwerpen van dit onderzoek geintroduceerd. Vervolgens werd de familie van chemokines en chemokine receptoren uitvoeriger toegelicht en besproken in **Hoofdstuk 2**. In totaal bestaan er 23 verschillende chemokine receptoren, die door één of meerdere van de 48 chemokine liganden kunnen worden geactiveerd. In dit hoofdstuk werden de veelzijdige regulatiemechanismen van chemokine signalering op een systemisch, een cellulair en een moleculair niveau beschreven. De nadruk lag hierbij op 'biased signalling' dat plaatsvindt op moleculair niveau, een fenomeen dat momenteel van grote interesse is in de moleculaire farmacologie. Een beter begrip van al deze factoren tezamen zal bijdragen aan de ontwikkeling van effectievere geneesmiddelen gericht op chemokine receptoren.

In **Hoofdstuk 3** werd een selectie van CCR2 antagonisten bekend uit de literatuur bestudeerd in diverse farmacologische radioligand binding studies en functionele studies. Al deze antagonisten verdrongen de endogene agonist $^{125}$I-CCL2 van CCR2 met nanomolaire affiniteit. Twee antagonisten, INCB3344 en CCR2-RA, werden voorzien van een radioactief label zodat de binding van deze moleculen gedetailleerd kon worden bestudeerd. [$^{3}$H]-INCB3344 en [$^{3}$H]-CCR2-RA bleken op twee verschillende plekken aan de receptor te binden, aangezien deze antagonisten elkaar niet verdrongen van de receptor. Vervolgens werd inhibitie van CCR2 bestudeerd in functionele studies. INCB3344 inhibeerde CCL2-geinduceerde G eiwit activatie op een competitieve manier, terwijl CCR2-RA een niet-competitief en allosteer karakter vertoonde in deze studies. Deze resultaten toonden aan dat de CCR2 antagonisten die in dit hoofdstuk beschreven werden, geclassificeerd kunnen worden in twee groepen met een verschillende bindingsplek en een verschillend werkingsmechanisme.

In **Hoofdstuk 4** werd de zoektocht naar de bindingsplek van de allostere antagonisten CCR2-RA-[R], JNJ-27141491 en SD-24 beschreven. Allereerst werd een benadering met chimere CCR2/CCR5 receptoren gebruikt om inzicht te krijgen in de locatie van de bindingsplaats, waarna acht puntmutaties werden geintroduceerd in de receptor om deze bindingsplaats verder te karakteriseren. De receptorconstructen werden bestudeerd in radioligand binding

studies en functionele studies, die beiden bewijs leverden voor de aanwezigheid van een intracellulaire bindingsplek voor CCR2-RA-[R], JNJ-27141491 en SD-24. De meest belangrijke aminozuren voor de binding van deze liganden waren de zeer geconserveerde tyrosine $Y^{7.53}$ en de fenylalanine $F^{8.50}$ in het $NPxxYX_{(5,6)}F$ motief, samen met de valine $V^{6.36}$ aan de onderkant van TM-VI en de lysine $K^{8.49}$ in helix-VIII. Door middel van deze resultaten werd voor het eerst de aanwezigheid van een allostere intracellulaire bindingsplek voor CCR2 antagonisten aangetoond.

In **Hoofdstuk 5** werd de ontdekking van een derde bindingsplaats in de CCR2 receptor beschreven, waardoor amiloride-derivaten en natrium-ionen de receptor kunnen moduleren. In radioligand binding studies werd aangetoond dat het amiloride-derivaat HMA de binding van de agonist $^{125}$I-CCL2, de orthostere antagonist [$^{3}$H]-INCB3344 en de intracellulaire antagonist [$^{3}$H]-CCR2-RA-[R] op allostere wijze remde. In diezelfde studies werd ontdekt dat natrium ionen enkel de agonist $^{125}$I-CCL2 remden, terwijl de binding van [$^{3}$H]-CCR2-RA-[R] op allostere wijze werd verhoogd. Drie aminozuren die zich in het hart van de receptor bevinden, $D^{2.50}$, $W^{6.48}$ en $H^{7.45}$, bleken belangrijk te zijn voor deze allostere modulatie, omdat mutatie van deze aminozuren het effect van HMA en de natrium-ionen deed verminderen of verdwijnen. Door middel van dit onderzoek werd aangetoond dat CCR2 ten minste drie bindingsplaatsen voor synthetische liganden van de CCR2 receptor heeft.

**Hoofdstuk 6** was gericht op het ontwerp van orthostere CCR2 antagonisten met een hoge affiniteit en lange verblijfstijd op de receptor. Deze antagonisten deelden de CCR2 bindingsplaats van INCB3344. Een competitie associatie studie werd opgezet voor CCR2, die het mogelijk maakte om de relatie tussen de structuur van het ligand en zijn verblijfstijd op de receptor te onderzoeken (structuur–kinetiek relatie (SKR)), alsmede de traditionele structuur–affiniteit relatie (SAR). Door de opgedane kennis van SAR en SKR te combineren, werd het optimalisatieproces van cyclopentylamine CCR2 antagonisten opnieuw geëvalueerd. Optimalisatie op basis van affiniteit resulteerde in een antagonist met hoge affiniteit ($K_i$ = 6.8 nM) maar zeer korte verblijfstijd (2.4 min). Daarentegen, wanneer de optimalisatie geschiedde op basis van de verblijfstijd, leidde dit tot de ontdekking van een nieuwe CCR2 antagonist met hoge affiniteit ($K_i$ = 3.6 nM) en een verblijfstijd van 135 minuten.

Samengevat biedt dit proefschrift nieuw *in*zicht en *uit*zicht op de binding en werking van liganden voor de CCR2 receptor. Er zijn drie verschillende bindingsplaatsen voor liganden van deze receptor ontdekt en gelokaliseerd, waardoor CCR2 op verschillende wijzen farmacologisch kan worden gemoduleerd. De conclusies van deze bevindingen en het toekomstperspectief voor dit onderzoek zijn beschreven in **Hoofdstuk 7**. Deze resultaten kunnen leiden tot een rationeler ontwerp van toekomstige antagonisten, en zijn even zo

belangrijk om uitkomsten van studies met huidige CCR2 antagonisten te interpreteren. In samenhang met de huidige ontwikkeling van de kennis over de structuur en signaleringscapaciteiten van GPCRs, biedt dit werk mogelijkheden om de farmacologische modulatie van de CCR2 receptor op precieze wijze te reguleren, alsmede van GPCRs in het algemeen.

# List of publications

Vilums M, Zweemer AJM, Dekkers S, Askar Y, de Vries H, Saunders J, Stamos D, Brussee J, Heitman LH, IJzerman AP. *Design and Synthesis of Novel Small Molecule CCR2 Antagonists: Evaluation of 4-Aminopiperidine Derivatives*. Manuscript in preparation.

Vilums M, Zweemer AJM, Barmare F, van der Gracht AMF, Bleeker DCT, Yu Z, de Vries H, Gross R, Clemens J, Krenitsky P, Brussee J, Stamos D, Saunders J, Heitman LH, IJzerman AP. *When Structure–Affinity Relationships Meet Structure–Kinetics Relationships: 3-((Inden-1-yl)amino)-1-isopropyl-cyclopentane-1-carboxamides as CCR2 Antagonist*. Manuscript in preparation.

Zweemer AJM, Hammerl D, Massink A, Veenhuizen M, Lenselink EB, de Vries H, Heitman LH, IJzerman AP. *Allosteric modulation of the chemokine receptor CCR2 by amiloride analogues and sodium ions*. Manuscript in preparation.

Zweemer AJM, Bunnik J, Veenhuizen M, Miraglia F, Lenselink EB, Vilums M, de Vries H, Gibert A, Thiele S, Rosenkilde MM, IJzerman AP, Heitman LH. *Discovery and mapping of an intracellular antagonist binding site at the chemokine receptor CCR2*, Mol Pharmacol, 86(4), 2014, 358-368.

Zweemer AJM, Toraskar J, Heitman LH, IJzerman AP. *Bias in chemokine receptor signalling*, Trends Immunol., 35(6), 2014, 243-252.

Vilums M*, Zweemer AJM*, Yu Z, de Vries H, Gross R, Krenitsky P, Clemens J, Barmare F, Brussee H, Stamos D, Saunders J, Heitman LH, IJzerman AP. *Structure-kinetics relationships – an overlooked parameter in hit-to-lead optimization: a case of cyclopentylamines as CCR2 antagonists*, J Med Chem, 56(19), 2013, 7706-7714. *these authors contributed equally

Zweemer AJM, Nederpelt I, Vrieling H, Hafith S, Doornbos MLJ, de Vries H, Abt J, Gross R, Stamos D, Saunders J, Smit MJ, IJzerman AP, Heitman LH. *Multiple binding sites for small molecule antagonists at the chemokine receptor CCR2*, Mol Pharmacol, 84(4), 2013, 551-561.

Sims AH*, Zweemer AJM*, Nagumo Y, Faratian D, Muir M, Dodds M, Um I, Kay C, Hasmann M, Harrison DJ, Langdon SP. *Defining the molecular response to trastuzumab, pertuzumab and combination therapy in ovarian cancer*, Br J Cancer, 106(11), 2012, 1779-1789. *these authors contributed equally

Gao ZG, Verzijl D, Zweemer AJM, Ye K, Göblyös A, IJzerman AP, Jacobson KA. *Functionally biased modulation of $A_3$ adenosine receptor agonist efficacy and potency by imidazoquinolinamine allosteric enhancers*, Biochem Pharmacol, 82(6), 2011, 658-668.

Faratian D, Zweemer AJM, Nagumo Y, Sims AH, Muir M, Dodds M, Mullen P, Um I, Kay C, Hasmann M, Harrison DJ, Langdon SP. *Trastuzumab and pertuzumab produce changes in morphology and estrogen receptor signaling in ovarian cancer xenografts revealing new treatment strategies*, Clin Cancer Res, 17(13), 2011, 4451-4461.

Heitman LH, Göblyös A, Zweemer AJM, Bakker R, Mulder-Krieger T, van Veldhoven JP, de Vries H, Brussee J, IJzerman AP. *A series of 2,4-disubstituted quinolines as a new class of allosteric enhancers of the adenosine $A_3$ receptor*, J Med Chem, 52(4), 2009, 926-931.

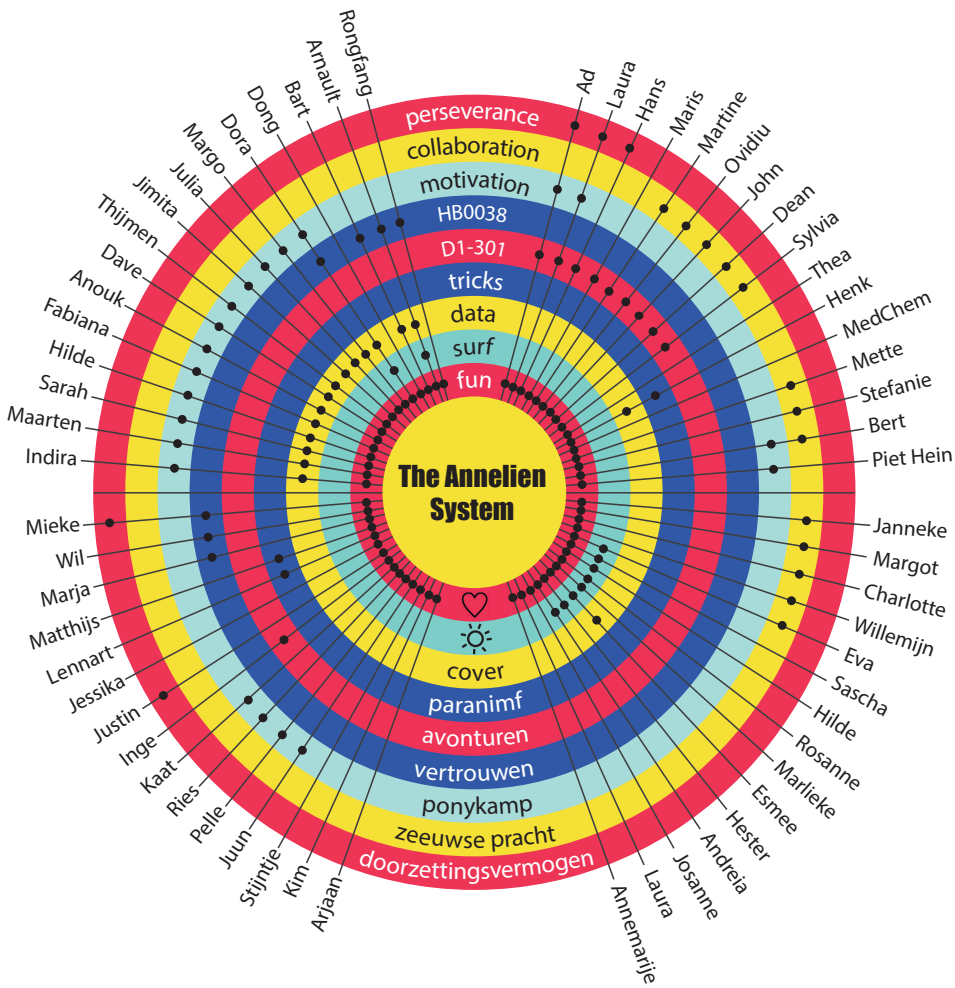
Heitman LH, van Veldhoven JP, Zweemer AJM, Ye K, Brussee J, IJzerman AP. *False positives in a reporter gene assay: identification and synthesis of substituted N-pyridin-2-ylbenzamides as competitive inhibitors of firefly luciferase*, J Med Chem, 51(15), 2008, 4724-4729.

# Curriculum Vitae

Annelien Zweemer was born in Goes, the Netherlands, on September 8th 1985. After graduating from high school at the Pontes College in Goes, she moved to Leiden in 2003 to study Bio-Pharmaceutical Sciences at Leiden University. During her degree she performed two research internships at the Division of Medicinal Chemistry, under supervision of Dr. Laura Heitman and Prof. Ad IJzerman. Her work on allosteric modulators for the adenosine $A_3$ receptor was awarded the Suzanne Hovinga award for the best thesis of Bio-Pharmaceutical and Biomedical Sciences at Leiden University in 2008. Subsequently she moved to Edinburgh, UK, to perform a third internship at the Breakthrough Breast Cancer Research Unit under supervision of Dr. Simon Langdon. She studied the effect of antibody therapy for ovarian cancer, and was awarded the S.E. De Jong prize for the best thesis in Pharmacology at Leiden University in 2009. In that same year she finished her MSc. degree *cum laude*.

In 2010, Annelien started her PhD study at Leiden University within the Division of Medicinal Chemistry, under supervision of Dr. Laura Heitman and Prof. Ad IJzerman. This research was part of the TI-Pharma initiative "Target residence time in translational drug research: the CCR2 chemokine receptor as a case in point" (Project number D1-301), in collaboration with Vertex Pharmaceuticals (San Diego, CA, USA) and the Vrije Universiteit Amsterdam (Amsterdam, The Netherlands). Throughout her PhD studies she presented work described in this thesis at numerous national and international conferences. In 2010 she won the NVF presentation award at the FIGON Dutch Medicines Days in Lunteren. In 2013 she was awarded the 1st poster prize at the LACDR Spring Symposium in Leiden, the 1st poster prize at the TI Pharma Spring Symposium in Utrecht and the 3rd poster prize during the FIGON Dutch Medicine Days in Ede. Annelien is currently working as a postdoctoral researcher in the department of Biological Engineering, headed by Prof. Douglas Lauffenburger, at Massachusetts Institute of Technology in Cambridge, MA.

# Acknowledgements


The Annelien System
perseverance
collaboration
motivation
HB0038
D1-301
tricks
data
surf
fun
cover
paranimf
avonturen
vertrouwen
ponykamp
zeeuwse pracht
doorzettingsvermogen
Rongfang
Arnault
Bart
Dong
Dora
Margo
Julia
Jimita
Thijmen
Dave
Anouk
Fabiana
Hilde
Sarah
Maarten
Indira
Mieke
Wil
Marja
Matthijs
Lennart
Jessika
Justin
Inge
Kaat
Ries
Pelle
Juun
Stijntje
Kim
Arjaan
Ad
Laura
Hans
Maris
Martine
Ovidiu
John
Dean
Sylvia
Thea
Henk
MedChem
Mette
Stefanie
Bert
Piet Hein
Janneke
Margot
Charlotte
Willemijn
Eva
Sascha
Hilde
Rosanne
Marlieke
Esmee
Hester
Andreia
Josanne
Laura
Annemarije

Throughout the past four years I have met, learned from, and collaborated with many different people. I am very grateful for all of your contributions; you kept the system running and enabled the realization of this thesis.

Een groot deel van het werk uit dit proefschrift is uit handen gekomen van het team aan studenten dat mij de afgelopen jaren heeft vergezeld. Bedankt voor jullie inzet, ideeën en energie! Henk, jouw vakkennis, precisie en geduld waren onmisbaar voor het slagen van dit project. Ik heb genoten van onze samenwerking in de afgelopen jaren. Maris, thank you for being the most honest, supportive and ironic co-PhD fellow I could have wished for. All other (ex) colleagues and students from Medicinal Chemistry have been equally important for the great time I've had inside and outside the lab; keep up the spirit!

I would like to thank TI Pharma for enabling this research project in collaboration with Vertex Pharmaceuticals and the Vrije Universiteit Amsterdam. Dean, John and Sylvia, without Vertex' efforts to provide me two great radioligands this thesis would not have existed. In addition, I very much appreciate all the helpful discussions, your drive, and the excellent meetings in San Diego. Martine and Ovidiu, many thanks for being my walking chemokine encyclopedia. With all your helpful comments I was able to smoothly set up the assays in Leiden. Mette and Stefanie, thank you very much for the pleasant and fruitful collaboration that resulted in the work described in Chapter 4. Dit proefschrift draait om de *ins*, die alleen in waarde kunnen toenemen door de juiste *outs*: Esmee, heel erg bedankt voor het ontwerp van de cover!

Laura, mede door jouw aanstekelijke enthousiasme ben ik aan dit avontuur begonnen, en heb ik het tot een goed einde weten te brengen. Ik ben heel blij dat je mij de mogelijkheid hebt gegeven om de student met de langste verblijftijd op de 'LH' receptor te worden. Ad, sinds ik in 2006 voet zette binnen de afdeling heb ik veel mogen leren, proberen en creëren onder jouw toeziend oog. Jouw kennis, betrokkenheid, kritische blik en droge humor waardeer ik enorm. Ik kijk terug op een prachtige eerste reis door de wondere wereld van de wetenschap.

Tot slot, mijn lieve vrienden en familie, ik ben ongelofelijk trots en gelukkig met jullie allen om mij heen. *Als er liefde is, is er geen ver meer en geen dichtbij.*